Functional analysis of NaOCl-sensitive thiol-switches and their impact on the bacillithiol redox potential in *Staphylococcus aureus*

Inaugural-Dissertation

to obtain the academic degree

Doctor rerum naturalium (Dr. rer. nat.)

submitted to the Department of Biology, Chemistry, Pharmacy
of **Freie Universität Berlin**

by

NICO LINZNER

from Greiz, Germany

year of submission: 2020

1st reviewer: Prof. Dr. rer. nat. Haike Antelmann
Institute of Biology-Microbiology, Freie Universität Berlin

2nd reviewer: Prof. Dr. rer. nat. Markus Wahl
Institute of Structural Biochemistry, Freie Universität Berlin

Disputation on 05th November 2020

Table of contents

Zusammenfassung der Dissertation

Das grampositive Bakterium *Staphylococcus aureus* kolonisiert asymptomatisch ca. 30 % der menschlichen Bevölkerung. Jedoch ist *S. aureus* auch ein wichtiger humanpathogener Infektionserreger und verursacht viele lebensbedrohliche, invasive und systemische Erkrankungen. *S. aureus* hat zahlreiche Antibiotikaresistenzen erworben und ist gut an seinem Wirt angepasst, wodurch es dem Bakterium ermöglicht wird, das Immunsystem des Wirts zu umgehen. Unter Infektionsbedingungen oder in seiner ökologischen Nische ist *S. aureus* verschiedenen reaktiven Sauerstoff- und Chlor-Spezies (ROS, RCS) ausgesetzt, wie zum Beispiel H_2O_2 und HOCl, die von Makrophagen, Neutrophilen oder konkurrierenden Bakterien produziert werden. Daher hat *S. aureus* viele Mechanismen zur Abwehr gegen oxidativem Stress entwickelt, wie z. B. antioxidative Enzyme oder niedermolekulare Thiolverbindungen.

Eukaryoten und gramnegative Bakterien verwenden das Tripeptid Glutathion (GSH) und Actinomyceten nutzen Mycothiol (MSH) als niedermolekulare Thiolverbindungen. Allerdings fehlen *S. aureus* die Gene für die Biosynthese von GSH und MSH. Stattdessen nutzt *S. aureus* Bacillithiol (BSH) und Coenzym A (CoASH) als alternative niedermolekulare Thiolverbindungen. Diese Metabolite spielen eine essentielle Rolle bei der Entgiftung von ROS und RCS sowie bei der Aufrechterhaltung der reduzierten Redox-Homöostase in der Zelle bei verschiedenen Arten von Stress. Ein Überblick über die Biosynthese und Funktionen von BSH in *Bacillus subtilis* und *S. aureus* wird im **Kapitel 1** gegeben.

Niedermolekulare Thiolverbindungen spielen eine wichtige Rolle in der Redox-Homöostase aller Zellen. Deshalb ist die Untersuchung des zellulären Redoxpotentials ein Schwerpunkt in der Forschung der Redoxbiologie. In den letzten Jahrzehnten wurden neue genetisch-kodierte Redox-Biosensoren entwickelt, basierend auf dem redox-sensitiven grün-fluoreszierenden Protein (roGFP2). Dadurch konnte die Messung dynamischer Veränderungen des zellulären Redoxpotentials in Echtzeit durchgeführt werden. Dabei werden Redoxine, wie z. B. Glutaredoxin (Grx), Mycoredoxin (Mrx) oder Bacilliredoxin (Brx), an roGFP2 gekoppelt, um in hoher räumlich-zeitlicher Auflösung Veränderungen des Redoxpotentials in Eukaryoten und Prokaryoten zu messen. Die Anwendungen einiger roGFP2-fusionierter Biosensoren in pathogenen Bakterien unter oxidativen Stress und Infektionsbedingungen sind im **Kapitel 2** zusammengefasst**.**

Bei oxidativen Stress und Infektionen können BSH und CoASH Proteine durch *S*-Thiolierungen posttranslational modifizieren. Diese gemischten Protein-Disulfide werden in *S. aureus* als *S*-Bacillithiolierungen oder CoA-Thiolierungen bezeichnet. Durch *S*-Thiolierungen wird die Aktivität von Proteinen reguliert und ein Schutz der Proteine vor Überoxidation zur irreversiblen Cystein-Sulfonsäure vermittelt. *S*-Bacillithiolierungen können durch Bacilliredoxine (Brx) reduziert werden, wodurch Brx selbst *S*-bacillithioliert wird. Brx kann durch ein weiteres BSH-Molekül reduziert werden, wobei Bacillithiol-Disulfid (BSSB)

entsteht. Lange Zeit wurde angenommen, dass die NADPH-abhängige Flavin-Oxidoreduktase YpdA als BSSB-Reduktase fungiert. Die Untersuchung der physiologischen Rolle von YpdA und des Brx/BSH/YpdA-Weges in *S. aureus* unter oxidativen Stress und Infektionsbedingungen wird in **Kapitel 3** als ein Hauptteil der Promotionsarbeit beschrieben. Wir konnten zeigen, dass YpdA *in vitro* und *in vivo* als BSSB-Reduktase fungiert. *In vitro* hängt die enzymatische Aktivität von YpdA vom konservierten Cystein-14 ab. Mittels genetisch-kodierter Brx-roGFP2 und Tpx-roGFP2 Biosensoren und HPLC-Metabolomanalysen konnte ich zeigen, dass die *S. aureus* Δ*ypdA*-Mutante deutlich höhere BSSB-Mengen aufweist und bei der Regeneration des reduzierten BSH-Redoxpotentials (E_{BSH}) beeinträchtigt ist. Somit besitzt YpdA eine wichtige Funktion bei der Aufrechterhaltung der Redox-Homöostase und zur Regeneration des reduzierten E_{BSH} nach oxidativem Stress. Phänotyp-Analysen zeigten, dass YpdA wichtig ist für das Überleben von *S. aureus* nach oxidativem Stress und unter Infektionsbedingungen und damit in die Virulenz involviert ist. Zusätzlich konnte gezeigt werden, dass YpdA zusammen mit BSH und BrxA im BrxA/BSH/YpdA-Redoxweg interagiert. Zusätzlich ist BrxA von Bedeutung für die Fitness von *S. aureus* unter oxidativem Stress und Infektionsbedingungen.

S. aureus kann schnell Antibiotikaresistenzen erwerben, wodurch sich unter anderem Methicillin-resistente *Staphylococcus aureus* (MRSA) Stämme entwickelt haben. Um *S. aureus*-Infektionen erfolgreich bekämpfen zu können, ist die Entwicklung neuer antimikrobieller Substanzen notwendig. Chinone sind aufgrund ihrer beiden Wirk-mechanismen als Elektrophile und Oxidantien starke antimikrobielle Substanzen. In der vorliegenden Dissertation habe ich weiterhin in **Kapitel 4** die antimikrobielle Wirkung und den Wirkmechanismus des natürlichen 1,4-Naphthochinons Lapachol in *S. aureus* untersucht. In Phänotyp-Analysen mittels Wachstums- und Überlebensversuchen zeigte Lapachol eine Wachstums-inhibierende und letale Wirkung in *S. aureus*. Dabei ist die antimikrobielle Wirkung von Lapachol in *S. aureus* von Sauerstoff abhängig, da die toxische Wirkung von Lapachol in Überlebensversuchen unter mikroaerophillen Bedingungen im Vergleich zu aeroben Bedingungen deutlich vermindert war. Durch RNA-Seq wurde gezeigt, dass Lapachol sowohl eine Chinon-spezifische Antwort als auch eine oxidative Stressantwort in *S. aureus* auslöst. Des Weiteren konnte durch die Brx-roGFP2 und Tpx-roGFP2 Biosensoren gezeigt werden, dass *S. aureus* ein oxidiertes E_{BSH} und eine erhöhte intrazelluläre H_2O_2-Menge nach Lapachol-Stress aufweist, was den oxidativen Wirkmechanismus der ROS-Produktion bestätigt. Lapachol-induziertes ROS bewirkt die *S*-Bacillithiolierung von GapDH *in vitro* und in *S. aureus in vivo*. Das aerobe Wachstum von *S. aureus* konnte durch N-Acteylcystein nach Lapachol-Stress verbessert werden. Phänotyp-Untersuchungen zeigten wichtige Funktionen der H_2O_2-entgiftenden Katalase (KatA) und des BrxA/BSH/YpdA-Redoxweges im Wachstum und Überleben von *S. aureus* nach Lapachol-Stress. Außerdem konnte keine Proteinaggregation

in vitro und *in vivo* nach Lapachol-Stress nachgewiesen werden, was die Wirkung von Lapachol über *S*-Alkylierung und Aggregation von Proteinen widerlegt.

Zusammenfassend wurden in der Dissertation neue Erkenntnisse zur Aufrechterhaltung der BSH-Redoxbalance in *S. aureus* unter oxidativen Stress, Infektionsbedingungen und Antibiotika-Stress erzielt. Dabei spielt YpdA eine entscheidende Rolle und ist ein Teil des BrxA/BSH/YpdA-Redoxweges, der an der Virulenz von *S. aureus* beteiligt ist. Des Weiteren konnten wir ebenfalls eine Rolle des BrxA/BSH/YpdA-Weges beim Schutz von *S. aureus* unter Lapachol-Stress, welcher ROS-Produktion und oxidativen Stress in *S. aureus* verursacht, zeigen. Zukünftig könnte YpdA ein neues Ziel für die Entwicklung von Antibiotika sein und Lapachol und dessen Derivate als neue antimikrobielle Substanzen angewendet werden, um MRSA-Infektionen zu bekämpfen.

Summary of the dissertation

The Gram-positive bacterium *Staphylococcus aureus* colonises asymptomatically ca. 30% of the human population. However, *S. aureus* is also a major human pathogen and can cause a wide range of live-threatening diseases, such as soft tissue infections, systemic and invasive diseases. In addition, *S. aureus* has acquired resistance to multiple antibiotics. The pathogen is well adapted to its host, which enables the bacterium to evade the host immune system. Under infections or in its ecological niche, *S. aureus* is exposed to reactive oxygen species and reactive chlorine species (ROS, RCS), such as H_2O_2 and HOCl, which are produced by macrophages, neutrophils or competitive bacteria. Therefore, *S. aureus* has evolved mechanisms to defend itself against oxidative stress, including antioxidant enzymes or low molecular weight (LMW) thiols.

Eukaryotes and Gram-negative bacteria utilize the tripeptide glutathione (GSH), while Actinomycetes use mycothiol (MSH) as their major LMW thiol. However, *S. aureus* lacks GSH and MSH biosynthetic genes. Instead, *S. aureus* uses bacillithiol (BSH) and coenzyme A (CoASH) as an alternative LMW thiol. These small molecules play an essential role in detoxification of ROS and RCS as well as in maintenance of the reduced redox homeostasis inside the cell under different kinds of stress. An overview of the large functional diversity of BSH in *Bacillus subtilis* and *S. aureus* is presented in **chapter 1**.

LMW thiols are important for the redox homeostasis. Thus, redox biology research often focuses on the function of LMW thiols on the cellular redox potential. During the last decades, genetically encoded redox-sensitive green fluorescent protein (roGFP2)-fused biosensors were established as tools for real-time monitoring of dynamic changes of the redox potential. Glutaredoxins (Grx), mycoredoxins (Mrx) and bacilliredoxins (Brx) were fused to roGFP2 to monitor changes of the redox potential in high spatiotemporal resolution in eukaryotes and bacteria. The applications of several roGFP2-fused biosensors in pathogenic bacteria under oxidative stress and infection conditions are summarized in **chapter 2**.

Under oxidative stress and infections, BSH and CoASH can function as redox modifications of protein thiols, leading to *S*-thiolations. These mixed protein disulfides are termed as *S*-bacillithiolations or CoAlations. *S*-thiolations function in redox regulation of proteins and protect proteins against overoxidation to sulfonic acids. *S*-bacillithiolations can be reduced by bacilliredoxins (Brx), resulting in *S*-bacillithiolated Brx, which are reduced by another molecule of BSH, leading to bacillithiol disulfide (BSSB). For a long time, it was postulated that the NADPH-dependent flavin oxidoreductase YpdA might function as a BSSB reductase. Thus, the investigation of the physiological role of YpdA and the Brx/BSH/YpdA redox pathway under oxidative stress and infections in *S. aureus* was a subject of this PhD thesis and is presented in **chapter 3**. Our results demonstrated that YpdA acts as the BSSB reductase *in vitro* and *in vivo*. The enzymatic activity of YpdA was shown to depend on the

conserved Cys14 residue. Using genetically encoded Brx-roGFP2 and Tpx-roGFP2 biosensors and HPLC metabolomics, we revealed that the *S. aureus* Δ*ypdA* mutant has significantly higher BSSB levels and is impaired in the regeneration of the reduced BSH redox potential (E_{BSH}). These results indicated that YpdA is important to maintain the redox homeostasis and to restore the reduced E_{BSH} after oxidative stress. Phenotype analyses showed that YpdA improves the survival after oxidative stress and under infection conditions and thus, it is involved in the virulence of *S. aureus*. In addition, we demonstrated that YpdA acts together with BSH and BrxA in the BrxA/BSH/YpdA redox pathway. Moreover, we showed that BrxA contributes also to the fitness of *S. aureus* under oxidative stress and infections.

S. aureus rapidly acquires resistance to multiple antibiotics, resulting in methicillin-resistant *Staphylococcus aureus* (MRSA) strains. To combat *S. aureus* infections, the development of new antimicrobial compounds is required. Quinones are potent antimicrobial substances because of their bivalent mode of action as electrophiles and oxidants. In this doctoral thesis, we investigated the antimicrobial effect and mode of action of the plant-derived 1,4-naphthoquinone lapachol in *S. aureus* **(chapter 4)**. Phenotype analyses, using growth and survival assays, demonstrated that lapachol is growth-inhibitory and lethal for *S. aureus*. The antimicrobial effect of lapachol in *S. aureus* depends strongly on oxygen availability, since the toxicity of lapachol was decreased in survival assays under microaerophilic conditions compared to aerobic conditions. As revealed by RNA-seq, lapachol induces a strong quinone-specific and oxidative stress response in *S. aureus*. Furthermore, applications of the Brx-roGFP2 and Tpx-roGFP2 biosensors showed that *S. aureus* exhibits an increased E_{BSH} and enhanced intracellular H_2O_2 levels after lapachol stress, indicating ROS-production by lapachol. ROS-induction by lapachol can induce *S*-bacillithiolations of GapDH in *S aureus in vitro* and *in vivo*. Moreover, the addition of the ROS scavenger N-acetyl cysteine to lapachol-stressed *S. aureus* cells improves the survival of the bacteria. The H_2O_2-scavenging catalase (KatA) and the BrxA/BSH/YpdA redox pathway were further shown to be essential for survival under lapachol treatment. In addition, no protein aggregation has been detected *in vitro* and *in vivo* after lapachol stress, supporting that lapachol does not act via the *S*-alkylating mode.

In conclusion, the results of this PhD thesis provided new insights in the maintenance of the BSH redox homeostasis in *S. aureus* under oxidative stress, infection conditions and antibiotics treatment. The BSSB reductase YpdA was shown to play a crucial role in redox homeostasis and is a part of the BrxA/BSH/YpdA redox pathway, which contributes to the virulence of *S. aureus*. Furthermore, the BrxA/BSH/YpdA redox pathway has been shown to protect *S. aureus* against ROS, produced in the oxidative mode of lapachol stress. In the future, YpdA could be a novel drug target. Also, lapachol and its derivatives could be applied as new antimicrobials to combat life-threatening MRSA infections.

List of publications

1)Tung QN, **Linzner N**, Loi VV, Antelmann H. Biosynthesis and functions of bacillithiol in *Firmicutes*. Book chapter no. 20 “Biosynthesis and function of bacillithiol in *Firmicutes*”, Book title “Glutathione”, Editor Leopold Flohe, CRC Press, Taylor & Francis Group, 2018. **(Review Article)**

2) Tung QN, **Linzner N**, Loi VV, Antelmann H. Application of genetically encoded redox biosensors to measure dynamic changes in the glutathione, bacillithiol and mycothiol redox potentials in pathogenic bacteria. *Free Radic Biol Med* 128: 84-96, 2018. **(Review Article)**

3) Linzner N, Loi VV, Fritsch VN, Tung QN, Stenzel S, Wirtz M, Hell R, Hamilton C, Tedin K, Fulde M, Antelmann H. *Staphylococcus aureus* uses the bacilliredoxin (BrxAB)/ bacillithiol disulfide reductase (YpdA) redox pathway to defend against oxidative stress under infections. *Front. Microbiol* 10: 1355, 2019. **(Original Article)**

4) Linzner N*, Fritsch VN*, Busche T, Tung QN, Loi VV, Bernhardt J, Kalinowski J, Antelmann H. The plant-derived naphthoquinone lapachol induces an oxidative stress response in *Staphylococcus aureus*. *Free Radic Biol Med,* Revision re-submitted on 29th June 2020 **(Original Article)**

* *Shared first authorships.*

Declaration of personal contribution to the publications

1) Tung *et al*., 2018: Biosynthesis and function of bacillithiol in *Firmicutes*

I contributed together with Quach Ngoc Tung to the writing of the **sections 20.6 and 20.7** about the functions of bacillithiol in metal homeostasis and virulence and to **sections 20.8 and 20.9** about the role of bacillithiol in *S*-bacillithiolation and its reversal by bacilliredoxins of this review article. I also helped to draft the **figures 6, 7 and 8** related to these parts.

2) Tung *et al*., 2018: Application of genetically encoded redox biosensors to measure dynamic changes in the glutathione, bacillithiol and mycothiol redox potentials in pathogenic bacteria.

I contributed to write the **section 2.1** about the dynamic roGFP2-based biosensors to measure redox changes in Gram-negative bacteria.

3) Linzner *et al*., 2019: *Staphylococcus aureus* uses the bacilliredoxin (BrxAB)/ bacillithiol disulfide reductase (YpdA) redox pathway to defend against oxidative stress under infections.

I contributed to the concept of the paper and performed most experiments for this study. I prepared the samples for quantifications of LMW thiols and disulfides by HPLC **(Fig. 3, S3)**. I measured all kinetics of Brx- and Tpx-roGFP2 biosensor oxidations in comparative studies and among the growth curves *in vivo* and calculated the BSH redox potentials of the different *S. aureus* strains **(Fig. 4, S4-5, S6B, D, S8A, B, and Tab. S4-6)**. I performed the anti-BSH Western blot analyses **(Fig. 5)**. Furthermore, I was involved in performance of the phenotype analyses after NaOCl and H_2O_2 stress **(Fig. 6, 7)** and contributed with the infection assay of the complemented strains **(Fig. 8B, D)** to this study. I conducted the multiple alignments of BrxA, BrxB and YpdA proteins **(Fig. S1)**. I drafted most of the figures and wrote the paper together with Haike Antelmann.

4) Linzner *et al*., 2020: The plant-derived naphthoquinone lapachol induces an oxidative stress response in *Staphylococcus aureus*.

My contribution included the analyses of the antimicrobial effect of lapachol on *S. aureus* **(Fig. 1)** and the determination of the MIC **(Table S4)**. I conducted the measurements of the Brx- and Tpx-roGFP2 biosensors **(Fig. 4A, B)**. Furthermore, I performed the anti-BSH Western blots **(Fig. 6)** and the analyses of GapDH aggregation *in vitro* after lapachol stress **(Fig. S1A)**. I drafted most of the figures and wrote the manuscript together with Haike Antelmann.

Introduction and general conclusion

1. The relevance of *Staphylococcus aureus* as a major human pathogen

In 1880, staphylococci were first described by the Scottish surgeon Sir Alex Ogston as *Micrococcus*, which were isolated from pus of surgical abscesses and described as “the masses looked like bunches of grapes” [158, 221]. The term *Staphylococcus* descends from the Greek and is composed of *staphyle* (“bunch of grapes”) and *kokkos* (“corn, berry”) [49, 158]. Later, the German Friedrich Julius Rosenbach isolated two strains and renamed one of them as *Staphylococcus aureus* (*S. aureus*) (Latin for “golden”) [49, 224, 262] because of the characteristic pigmentation of this species by the carotenoid staphyloxanthin [189, 190, 231]. *S. aureus* is a Gram-positive, catalase-positive, oxidase-negative, facultative anaerobe, non-motile, non-spore forming, spherical bacterium with a diameter of 0.5 to 1.0 µm [49]. It belongs taxonomically to the phylum Firmicutes. The bacterium is able to grow with high salt concentrations (10-15% NaCl) and at temperatures between 10°C and 45°C with an optimum at 30-37°C [49]. *S. aureus* can be distinguished from other staphylococci by the existence of the extracellular protein coagulase [49], which forms a complex with prothrombin in the plasma to stimulate the clotting reaction [108, 242].

S. aureus colonizes permanently ~20 to 30% of the healthy human population as an asymptomatic commensal [146]. The anterior nares are the ecological niche in humans of *S. aureus*, while an intact skin of humans is only colonized temporary [2, 6, 312, 320]. A healthy human with an intact immune system has just a low risk to get sick. However, as a carrier of *S. aureus* this risk is increased [6]. Children (<2 years), the elderly (>65 years) and in particular immunodeficient patients in hospitals, which have a catheter or had a surgery, are at high risk to get a local or invasive disease, if they are infected by *S. aureus* [6, 21, 75]. Thus, staphylococcal colonization is a critical step of the *S. aureus* pathogenesis. After colonization, *S. aureus* can get into wounds or scratches on damaged skin and can cause local soft skin or tissue infection, like carbuncle, impetigo bullosa, boils or wound infections [6]. Due to a wound infection, *S. aureus* can enter the bloodstream (bacteraemia), spreads out in the body and can further cause life-threatening invasive diseases, such as septicaemia, endocarditis, osteomyelitis or necrotizing pneumonia [2, 6, 297]. Moreover, *S. aureus* is able to cause shock syndromes by toxins, like staphylococcal scalded skin syndrome (SSSS), toxic shock syndrome (TSS) or foodborne gastroenteritis [6]. In addition, *S. aureus* is able to persist in its host by forming “small colony variants” (SCVs) [247] or can produce biofilms in catheter or on implants [7, 45]. Without any suitable treatment, the consequences of *S. aureus* infections can be fatal.

The ability of *S. aureus* to cause a wide range of diseases in several tissues and niches of the human body is based on the possession of a diverse and great equipment of virulence

factors. Among others, *S. aureus* exhibits many cell wall-bound and surface-associated proteins, which can interact and bind to components of the extracellular matrix (ECM), such as fibrinogen, fibronectin or collagen [33, 76]. These proteins can be divided into two main classes: covalently cell wall-attached proteins, termed as “microbial surface component recognizing adhesive matrix molecules” (MSCRAMMs) [76, 86] and non-covalently linked surface proteins with specific cell wall domains, named as “secretable expanded repertoire adhesive molecules” (SERAMs) [33, 57]. Examples for MSCRAMMs are the fibronectin-binding proteins (FnbPA/B), clumping factors (ClfA/B) or collagen-binding adhesins (Cna) [86]. The extracellular adherence protein (Eap), the ECM binding protein (Emp) and the extracellular fibrinogen binding protein (Efb) belong to the class of SERAMs [33]. Furthermore, *S. aureus* secretes several toxins, which can form pores and cause lysis of host cells. These include the leucocidins (LukAB, LukED, LukSF), α-haemolysin (Hla) and phenol-soluble modulins (PSM) [15, 240, 289]. To coordinate a controlled expression of the virulence factors, *S. aureus* possesses a network of global regulatory systems and transcriptional regulators, such as the quorum sensing systems Agr (accessory gene regulator) and SaeRS (staphylococcal exoprotein expression), the sigma factor SigB or the transcriptional regulator SarA (staphylococcal accessory regulator) [23, 34]. Exemplarily, SigB regulates approximately 250 genes of the general stress response after alkaline stress, heat shock and oxidative stress as well as several virulence factors [151, 227, 231]. Thus, *S. aureus* is well adapted to colonize and disseminate inside the host and to evade the human immune system.

The composition of the virulent determinants is very variable and can change rapidly in *S. aureus* strains. This flexibility is ensured by a large amount of mobile genetic elements (MGE), which represent approximately 15-20% of the *S. aureus* accessory genome [162, 163]. MGEs are defined as certain pieces of DNA, which are able to be transmitted by horizontal gene transfer (HGT) within a genome or between organisms [161, 163]. The staphylococcal MGEs are composed of bacteriophages, pathogenicity islands (SaPI), plasmids, transposons and staphylococcal cassette chromosomes (SCC). They often encode for non-essential genes, including virulence factors or resistance cassettes [161, 163]. Remarkably, it has been found that virulence factors are mostly transferred by phages or SaPI, while resistance genes are often associated with SCC, plasmids or transposons [163]. Typical virulence factors, which were acquired from *S. aureus* by bacteriophages or SaPIs, are toxins, like exotoxin A, leucocidins or the toxic shock syndrome toxin (TSST), and proteins, such as chemotaxis inhibitory protein (CHIP) or staphylokinase (Sak) [161, 163]. The best known SCC is the SCC*mec*, which encodes genes for resistance against the β-lactam antibiotic methicillin (*mec* operon) [129, 130, 141, 163]. Among others, this SCC exhibits the gene *mecA,* which encodes for the penicillin-binding protein 2’ (PBP2’), a hallmark of so-called methicillin-resistant

Staphylococcus aureus (MRSA) strains [287, 304]. In contrast to usual PBPs, PBP2' binds with a significantly lower affinity to β-lactam antibiotics [104, 255, 304].

In 1960's, MRSA were first described [134]. Nowadays, they are a widely distributed threat in the human community as well as in hospitals [21]. MRSA strains can be classified into three groups: community-acquired (CA-MRSA), hospital-acquired (HA-MRSA) and livestock-associated MRSA (LA-MRSA) [21, 161]. CA-MRSA cause mainly infections of people, which did not have any close proximity to the health care system. In contrast, HA-MRSA are often associated with infections in hospitals, like post-surgery or elderly [21, 47, 161]. In addition, LA-MRSA are originated from pig farms, where they colonize asymptomatically pigs and acquire multiple antibiotic resistances (SCC*mec* and tetracycline) due to the intensive application of antibiotics in animal farming [161, 326]. Thus, farm-associated people can be infected with these LA-MRSA. Furthermore, CA- and HA-MRSA are different in regards to their virulence factors. While CA-MRSA isolates have a small SCC*mec* (type V or VI) and carry often the Panton-Valentine leucocidin (PVL), the HA-MRSA strains exhibit a large SCC*mec* (type I, II or III) and are rare connected to PVL [161]. Moreover, Busche *et al*. (2018) could show that zoonotic LA-MRSA of the clonal complex 398 have reduced SigB and higher Agr activities [26]. This different regulation results in increased α-/β-haemolyses, decreased biofilm formation and lower staphyloxanthin levels as revealed by comparative secretome and phenotype analyses [26]. Usually, MRSA isolates are susceptible to glycopeptide antibiotics, such as vancomycin. However, some MRSA isolates have acquired the *vanA* gene from a co-colonized vancomycin-resistant *Enterococcus* (VRE) strain due to HGT of a transposon [161, 283, 317, 327]. These strains are termed as vancomycin-resistant *Staphylococcus aureus* (VRSA). In the present work, the experiments were performed with the early HA-MRSA isolate *S. aureus* COL [60, 87].

In 2017, approximately 120,000 cases of bloodstream infections, including about 20,000 deaths, were caused by MRSA in the United States [148]. In Europe 2015, it was estimated that there were about 150,000 cases and approximately 7,000 deaths in health care caused by MRSA, which is the second most common cause overall infections with antibiotic-resistant bacteria [29].

In conclusion, the success of *S. aureus* as a major human pathogen is attributed to its ability to resist environmental stress conditions (like salt or high temperature), its ability to acquire rapidly many antibiotic resistances and its flexible equipment of many different virulence factors. Thus, *S. aureus* was included as one of six ESKAPE pathogens by the "European Centre of Disease Prevention and Control" [232]. Due to the current MRSA as well as VRSA strains and expected further increased acquisition of antibiotic resistances, it is necessary to find new therapy strategies including novel drugs and drug targets to combat

infections with multi antibiotic resistant *S. aureus* strains. Therefore, the research on human pathogenic bacteria, like *S. aureus*, is inevitable in the future.

2. Responses of *S. aureus* under oxidative stress and infection conditions

S. aureus has acquired many virulence determinants and can cause many diseases (see section 1). During infections, *S. aureus* has to cope with different reactive species from several endogenous and exogenous sources. This kind of stress is termed as oxidative stress. Oxidative stress is defined in the literature as "an imbalance between oxidants and antioxidants in favour of the oxidants, leading to a disruption of redox signalling and control and/or molecular damage" [282]. The following section focuses on the origins of reactive species, gives an overview of the different reactive species and their mode of action. Furthermore, it reviews the defence mechanism of *S. aureus* against oxidative stress in detail.

2.1 Significance and origins of reactive species

Reactive species play an important role in signalling (oxidative eustress), but they can also cause damage (oxidative distress) [281]. During oxidative eustress, reactive species function in low concentrations as second messenger molecules in eukaryotes to regulate signalling pathways [74, 280]. In oxidative distress, reactive species exist in higher concentrations and can damage biological macromolecules [126, 127, 281]. Since the present work focused on the research on the role of oxidative stress to kill MRSA and the defence mechanisms of *S. aureus* to combat oxidative stress, the following section addresses oxidative damage by reactive species.

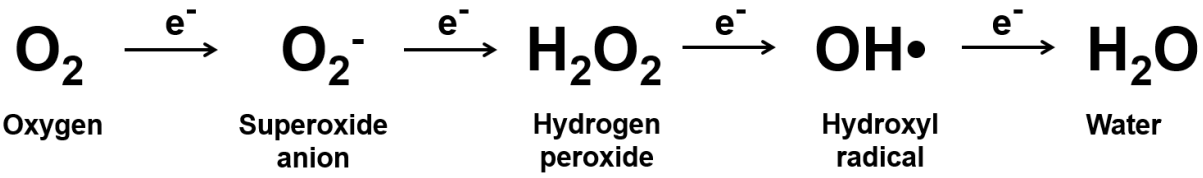

Fig. 1: One-electron reductions from oxygen to water. ROS, such as superoxide anion (O_2^-), hydrogen peroxide (H_2O_2) and the hydroxyl radical (OH•), can be generated by one-electron transfer to oxygen during respiration. The figure is adapted from reference [181].

The term oxidative stress comprises different types of reactive species. The so-called reactive oxygen species (ROS) are the best-known type of oxidative stress. ROS include free radicals as well as chemically stable compounds, such as superoxide anion (O_2^-), hydrogen peroxide (H_2O_2) or the highly-reactive hydroxyl radical (OH•) [126, 127, 281]. In all aerobic respiring organisms, endogenous ROS are generated as unwanted toxic by-products of the respiration during one-electron-reduction steps of molecular oxygen **(Fig.1)** [126, 127, 281]. Thereby, the electrons are transferred from univalent electron donors, like flavins of

dehydrogenases or respiratory quinones, to oxygen, leading to ROS formation [127]. For *Escherichia coli*, it has been shown that the NADH dehydrogenase II (NDH-II) of the respiratory chain is the source for endogenous O_2^- and H_2O_2 production [196]. Furthermore, the accidental autoxidation of non-respiratory reduced flavoenzymes leads to O_2^- and H_2O_2 generation [126, 127, 192].

During colonization of the anterior nares and the upper respiratory tract, *S. aureus* co-colonizes its ecological niches together with many other bacterial species, including lactic acid bacteria, such as *Streptococcus pneumoniae* [17, 172]. These lactic acid bacteria generate high amounts of H_2O_2 up to a millimolar range due to their aerobic metabolism by the enzymes lactate and pyruvate oxidases. This allows *S. pneumoniae* to kill competitive bacteria in the upper respiratory tract [170, 239, 290, 305]. It has been shown that the generated H_2O_2 of pneumococci kills *S. aureus in vitro* [253]. This fact is supported by the finding that the staphylococcal catalase, a H_2O_2-detoxifying enzyme, is important for *S. aureus* survival in the presence of *S. pneumoniae in vitro* and in a murine model of nasal colonization [228]. In contrast, a rat animal model revealed that the *S. aureus* density did not decrease by H_2O_2-producing *S. pneumoniae in vivo* [187]. Thus, further studies are required to analyse the interaction between *S. aureus* and *S. pneumoniae*.

Furthermore, *S. aureus* is exposed to ROS inside phagosomes of activated macrophages or neutrophils [71, 323]. A hallmark of the human innate immune system to defend against invading pathogens is the so-called oxidative burst. Thereby, the NADPH oxidase (NOX2) produces O_2^- by reduction of oxygen with NADPH [9, 323]. During the maturation of the phagolysosome and to maintain the charge of the phagosomal membrane, the vacuolar ATPase transfers H^+ protons in the phagosome, resulting in a strong decrease of the phagosomal pH to 5-6 [71, 101, 323]. Due to the acidification, O_2^- converts rapidly to H_2O_2 [71, 323]. In the final step, the myeloperoxidase (MPO) utilizes H_2O_2 and chloride to synthesize the strong oxidant hypochlorous acid (HOCl) [323]. This oxidant belongs to the reactive chlorine species (RCS) and is the main reason for bacterial killing by macrophages and neutrophils [323].

In addition to ROS and RCS, reactive nitrogen species (RNS) also play a role during the oxidative burst. After an inflammatory stimulus, the inducible nitric oxide synthase (iNOS) produces nitric oxide (NO•) and L-citrulline from L-arginine and oxygen [18, 55, 71, 318]. NO• can react with O_2^- to the highly reactive RNS peroxynitrite ($ONOO^-$) [71, 292]. RNS are able to kill pathogens, like *S. aureus* [185].

Due to the modes of action of ROS and RCS (see section 2.2) as well as during metabolism, many compounds with an electron-deficient carbon centre are produced, which further lead to oxidative damage [4, 69, 188, 263]. Such substances are termed as reactive

electrophile species (RES) and include α-β-unsaturated aldehydes (formaldehyde, methylglyoxal), epoxides or quinones [4, 69, 188, 263].

Finally, antimicrobial compounds can act as electrophile and/or can generate ROS as part of their modes of action. It has been shown that some antibiotics induce O_2^- and OH• generation inside bacteria [12, 59, 90, 147, 315]. For example, norfloxacin or a high dose of vancomycin increase OH• levels in *S. aureus* [147]. Moreover, for a long time, garlic is applied to combat bacterial infections, because it exhibits antibacterial properties [257]. Thereby, its active compound allicin (thio-2-propene-1-sulfinic acid *S*-allyl ester) acts mainly as a thiol-reactive compound and belongs to the class of reactive sulfur species (RSS) [5, 20, 180, 248].

In conclusion, under infection conditions, *S. aureus* has to deal with a wide range of reactive species, such as ROS, RCS, RES, RNS or RSS, which are produced during respiration, by competitive bacteria, neutrophils or antibacterial compounds **(Fig. 2)**. These reactive species can damage all biological macromolecules, such as proteins, carbohydrates, lipids, metal cofactors or DNA. The mode of action of selected ROS, RCS and RES species is described in more detail in the following section.

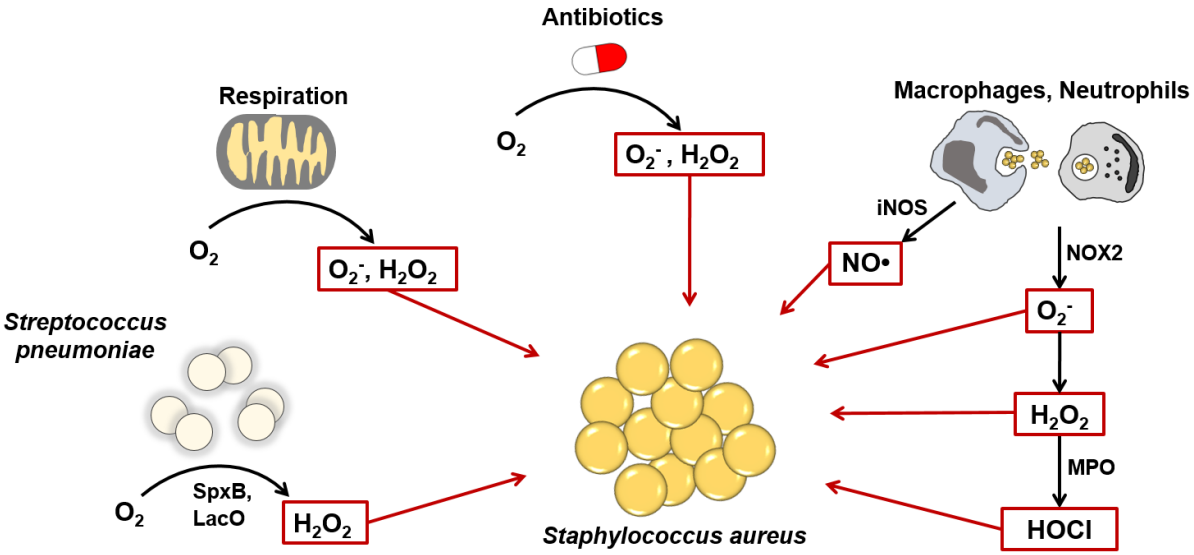

Fig. 2: Exogenous and endogenous sources of ROS, RNS and RCS during infections with *S. aureus*. During aerobic respiration, ROS, like O_2^- or H_2O_2, can arise as by-products in the respiratory chain of *S. aureus* or the host. *S. aureus* co-colonizes the upper respiratory tract with bacteria, such as *Streptococcus pneumoniae*, which can produce a large quantity of H_2O_2 by lactate oxidase (LacO) or pyruvate oxidase (SpxB) under aerobic conditions. Antibiotics, used to combat *S. aureus* infections, can generate ROS. A hallmark of the innate immune system is the oxidative burst by macrophages and neutrophils. Thereby, the NADPH oxidase (NOX2) generates O_2^-, which can be converted to H_2O_2 by superoxide dismutase (SOD). The myeloperoxidase (MPO) uses H_2O_2 together with Cl^- to produce the strong oxidant hypochlorous acid (HOCl). In addition, the inducible nitrite oxide synthase (iNOS) generates nitric oxide (NO•). All ROS, RNS and RCS can damage biological macromolecules in *S. aureus*. This figure is adapted from [292].

2.2 Modes of action of reactive oxygen and reactive chlorine species (ROS, RCS)

The presenting section reviews the basics of the chemistry and the reactions with biological macromolecules of ROS and RCS. An important factor to describe the reactivity of an oxidant is the second order rate constant *k*, which is used to depict the proportionality between the reaction rate and the reactants of a reaction [1, 14]. Thus, *k* is indirectly a determinant of the velocity of a chemical reaction and states how fast a chemical reaction can potentially proceed [1, 14].

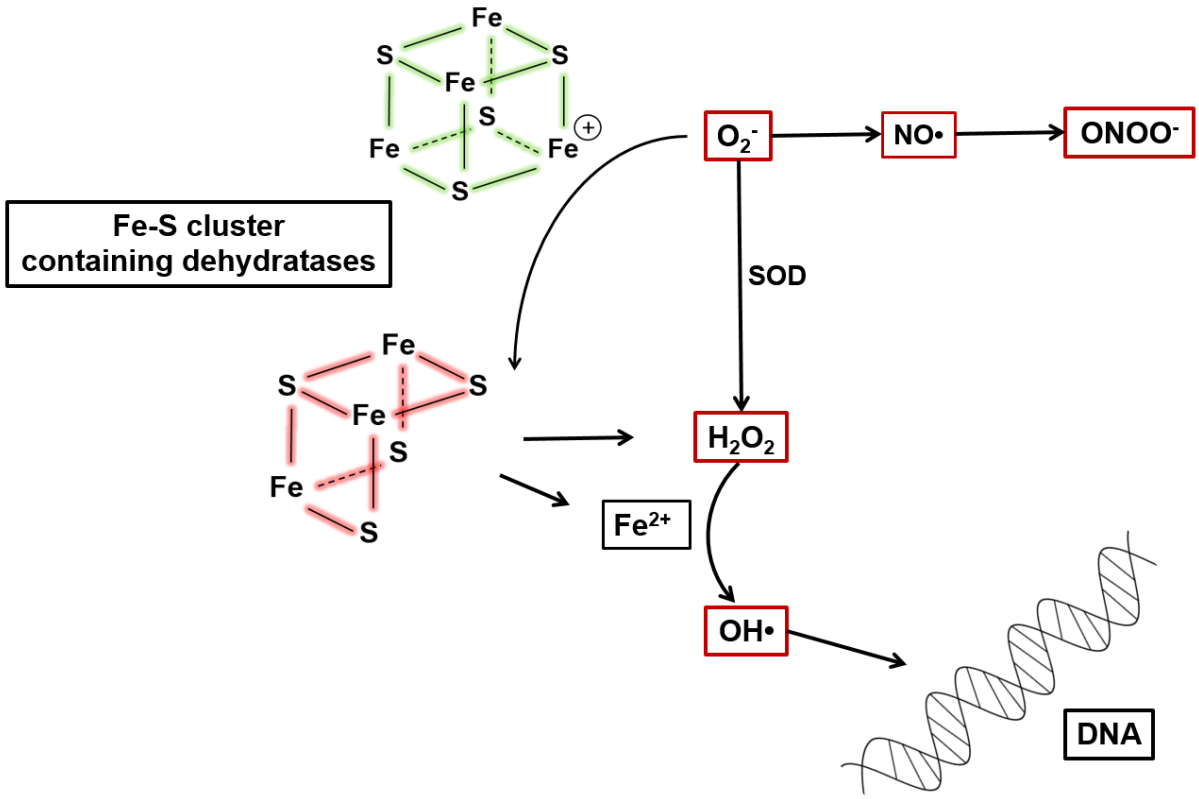

Fig. 3: Modes of action of superoxide (O_2^-). O_2^- can react with an iron residue of the iron-sulfur-cluster of dehydratases. Thereby, Fe^{2+} is released and the Fe-S cluster is unfunctional. Moreover, the superoxide dismutase (SOD) can detoxify O_2^- to hydrogen peroxide (H_2O_2), which can react with the released free Fe^{2+} to generate hydroxyl radicals (OH•) via Fenton chemistry. Among others, OH• leads to damage of the DNA. In addition, O_2^- reacts rapidly with nitric oxide (NO•), resulting in peroxynitrite ($ONOO^-$). This figure is adapted from references [126, 127].

Respiration and the oxidative burst are the main sources of ROS, which have high potential to damage biological macromolecules. Although, these oxidants are classified as ROS, they are completely different in regard to their reactivity and chemistry. O_2^- has a reduced ability to oxidize electron-rich molecules because of its anionic charge [126, 321]. Members of the dehydratases, such as aconitase, are composed of a four-iron-four-sulfur cluster ($[4Fe\text{-}4S]^{2+}$) in their catalytic centre **(Fig. 3)** [72, 126]. The catalytic centre has an uncoordinated iron atom in the resting state of the enzyme. Therefore, this active site iron exhibits a positive charge [72, 126]. Thus, the active site of dehydratases is an attractive target for O_2^- with a second order rate constant (*k*) up to 10^6 M^{-1} s^{-1}, leading to the inactivation of the enzyme and

the release of iron (Fe^{2+}) [73, 126]. Moreover, O_2^- can react rapidly with NO•, to form $ONOO^-$ (k=1.6x10^{10} M^{-1} s^{-1}) [292, 323]. Furthermore, short-chain sugars are a target of O_2^-, resulting in the α-β-unsaturated RES methylglyoxal [222]. In biological systems, O_2^- can be detoxified by the enzyme superoxide dismutase (SOD), yielding in H_2O_2 formation [193, 194].

H_2O_2 is uncharged and possesses a stable oxygen-oxygen-bond (O-O), which decreases its reactivity to biomolecules [126, 321-323]. Therefore, H_2O_2 acts as a nucleophile and is a weak one-electron oxidant [268, 322]. Thus, a high energy is required to break the bond to activate the reactivity. That can be facilitated by d-orbitals of transition metals, like iron [126]. Due to this fact, H_2O_2 has similar reactivity properties, like O_2^-, to the active site iron of Fe-S clusters (k=10^3 M^{-1} s^{-1}) and can cause inactivation of $[4Fe\text{-}4S]^{2+}$-containing dehydratases [73, 126]. Furthermore, H_2O_2 plays a key role in Fenton chemistry [70, 100, 126]. It is likely that the released Fe^{2+} from iron-sulfur clusters by O_2^- reacts with H_2O_2, leading to OH• formation [100, 126]. The OH• is highly reactive (k=10^9 M^{-1} s^{-1}) because it has no charge and no stable bond [126, 321]. It reacts intensively with bases or the backbone of the DNA, resulting in oxidation of bases or double strand breaks [27]. Based on the chemical properties of the sulfur atom of cysteines and methionines as well as due to the polarizability of the O-O bond, H_2O_2 can also act as an electrophile and can oxidize proteins [107, 126, 323]. The reactivity of a cysteine depends strongly on its localisation in the protein and its pK_a, which is affected by amino acids in close proximity [4, 107, 243]. At a physiological pH of 7.4, the characteristic pK_a of a cysteine sulfhydryl is 8.6 [4, 107]. Under these conditions, H_2O_2 has a slow reactivity to free cysteines (k=2.9 M^{-1} s^{-1}) [126, 324]. Catalytic cysteines at the active site of enzymes are often surrounded by amino acids, which can deprive protons from the cysteine. This localization can lead to alterations of the thiol pK_a, resulting in a change of the protonation equilibrium [107, 243]. Thus, the free thiol (Cys-SH, oxidation state: -2) is changed to the deprotonated thiolate anion (Cys-S^-, oxidation state: -1) [107, 243]. Consequently, the pK_a can drop until 3.5 [94, 107]. Therefore, the reactivity of H_2O_2 to the cysteine thiolate form increases significantly (k=20 M^{-1} s^{-1}) **(Fig. 4)** [126, 324]. For specific catalytic cysteines, like the active site cysteines in OxyR of *E. coli*, the oxidation rate constant by H_2O_2 was determined as 10^7 M^{-1} s^{-1} [8].

Due to oxidation, cysteines can form a huge variety of post-translational modifications **(Fig. 4)** [4, 107]. The oxidation of thiolate anions by H_2O_2 causes firstly an unstable cysteine sulfenic acid intermediate (R-SOH, oxidation state: 0) [4, 107]. Due to further oxidation, the cysteinyl residue of the protein will be “overoxidized” to the irreversible forms of cysteine sulfinic acid (R-SO_2H, oxidation state: +2) and cysteine sulfonic acid (R-SO_3H, oxidation state: +4) [4, 107]. Finally, the protein loses its function [107, 123]. To prevent the overoxidation, the cysteine sulfenic acid can react with another thiol group, leading to reversible inter- or intramolecular protein disulfide formation (RSSR; oxidation state: -1) [4, 107]. Moreover, the

reaction of cysteine sulfenic acid with low molecular weight (LMW) thiols (like glutathione, mycothiol, bacillithiol) protects proteins against overoxidation, resulting in mixed protein disulfides (*S*-thiolations; see section 3 for more details) [4, 181].

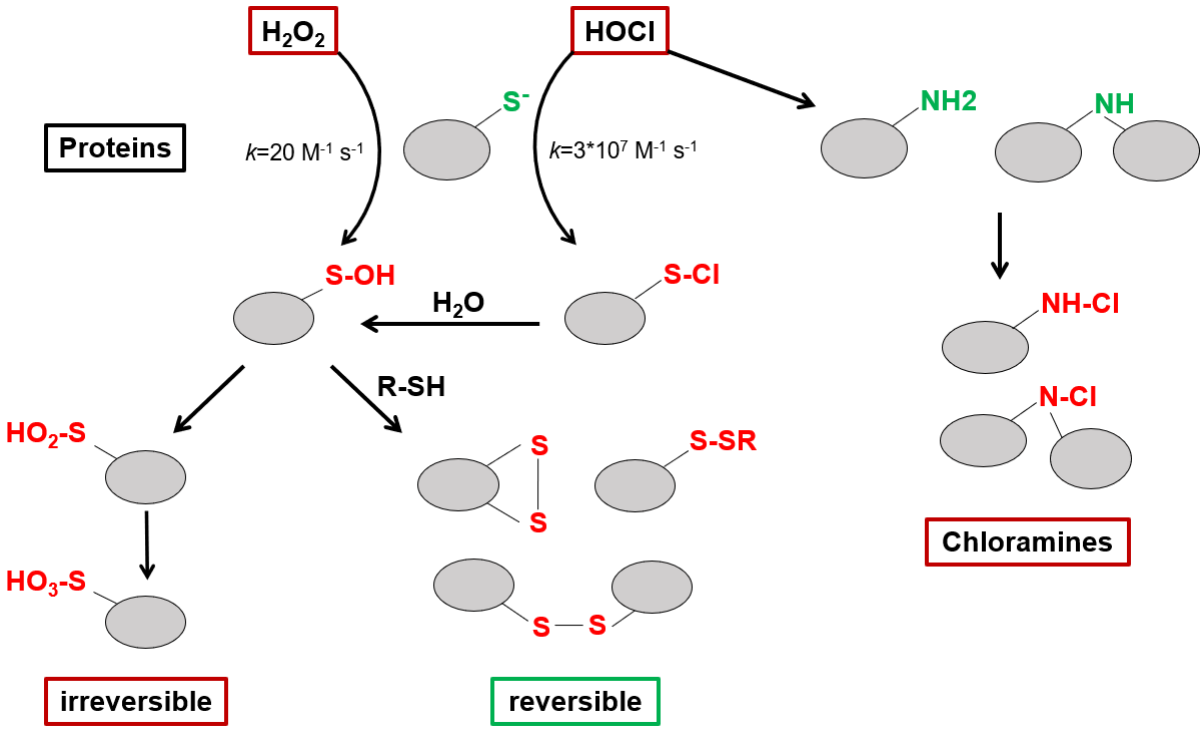

Fig. 4: Selected modes of action of H_2O_2 and HOCl with proteins. H_2O_2 can oxidize thiolate groups of proteins (k=20 M^{-1} s^{-1}), leading to cysteine sulfenic acid formation (S-OH). This reaction is several magnitudes faster with HOCl (k=3x10^7 M^{-1} s^{-1}), leading firstly to a chlorination, which is converted in aqueous solution to S-OH. Further oxidation of S-OH results in irreversible cysteine modifications such as sulfinic (R-SO_2H) and sulfonic acid (R-SO_3H). In addition, S-OH can react with other thiol groups of proteins or LMW thiols (R-SH), leading to reversible inter- and intramolecular disulfide formation (S-S) as well as *S*-thiolations of proteins (S-SR). Furthermore, HOCl can also oxidize primary or secondary amines of proteins to form chloramines (R-NH-Cl; R-N-Cl). This figure is adapted from references [4, 95, 181].

During the oxidative burst, neutrophils generate HOCl (see section 2.1 for more details). HOCl is a strong two-electron oxidant, which reacts with almost all biological macromolecules [48]. The major target of HOCl is the nucleophilic thiol group of cysteines, methionines and low molecular weight (LMW) thiols [48, 230]. Thereby, HOCl (k=3x10^7 M^{-1} s^{-1}) has a significantly higher reactivity compared to H_2O_2 **(Fig. 4)** [48, 230]. Recently, the second order rate constant of k=6x10^7 M^{-1} s^{-1} has been determined for the reaction between HOCl and the major LMW thiol of *S. aureus* bacillithiol (BSH) [54]. These reactions occur in a few milliseconds. Therefore, the lifetime of HOCl *in vivo* is also estimated in this order [48]. Initially, the reaction of cysteine and HOCl leads to chlorination, resulting in an unstable sulfenyl chloride (R-SCl) intermediate [48, 106]. In aqueous solution, that intermediate is converted to R-SOH [48, 106]. Similar to H_2O_2 stress, R-SOH can be further oxidized to R-SO_2H and R-SO_3H, yielding in overoxidation and dysfunction of proteins [48, 106]. Moreover, HOCl can generate chloramines (RCH_2NHCl) by reaction with primary or

secondary amines **(Fig. 4)** [48, 106]. Chloramines are able to oxidize sulfur containing amino acids, however, the reactivity is lesser than with HOCl (k=205 to 479 M^{-1} s^{-1}) [48, 106, 241]. Taken together, ROS and RCS can cause a wide range of oxidative damage and lead to different modifications on biological molecules.

2.3 Modes of action of quinones as reactive electrophile species (RES) and oxidants

Quinones are chemically defined as “diketones derived from aromatic compounds” [24] and they are widely distributed compounds in nature from bacteria to insects and humans [58, 201, 220, 269]. Quinones are divided up into three structural groups: benzoquinones, naphthoquinones and anthraquinones [218]. Some quinones play important roles in essential processes, like ubi- or menaquinones, within the respiratory chain [58, 218, 313]. Here, they donate electrons and transfer them from one respiratory chain complex to another [58, 218, 313]. In addition, it is well established that many quinones have antimicrobial activities, whereby some organisms produce quinones for protection against bacteria [42, 269].

The toxicity of quinones is exerted by two mechanisms: an electrophilic and an oxidative mode of action [19, 201, 220]. Quinones can have carbon-nitrogen (C=N) and carbon-oxygen (C=O) double bonds at the ring structure, leading to electron-deficient carbon atoms and a partial positive charge [19, 201, 220]. Thus, they can react as electrophiles with nucleophilic thiol groups of cysteines and can form thiol-*S*-alkylations via 1,4-Michael-addition, resulting in aggregation and depletion of thiol containing proteins as well as LMW thiols [19, 159, 201, 220].

During their oxidative mode of action, quinones are reduced to semiquinone radicals by an one-electron reduction or to hydroquinones by a two-electron reduction pathway [19, 201, 220]. In the presence of oxygen, the semiquinone radical is reoxidized, which produces ROS, like O_2^- [19, 201, 220]. This process is named as redox cycling [97]. O_2^- can be converted spontaneously or by the enzyme superoxide dismutase to H_2O_2, which can react with deprotonated cysteine residues of proteins (see section 2.2) [4, 19, 201, 220]. Chemical features and physiological conditions, including pH, the chemical structure of a quinone or the pre- and absence of oxygen, determine how a quinone mainly acts [24, 270, 285]. The current study includes the analyses of the mode of action of the naphthoquinone lapachol in *S. aureus* (see section 2.5 for more details).

In conclusion, the bivalent quinones mode of action makes them to a reactive species with a high toxic potential.

2.4 Defence mechanisms of *S. aureus* to combat oxidative stress and quinones

During infections, the major human pathogen *S. aureus* is exposed to different reactive species, including ROS, RCS, RNS and RES (see section 2.1 to 2.3 for more details). *S. aureus* has evolved a diverse range of determinants and mechanisms to defend against and respond to reactive species **(Fig. 5)** [85]. In general, the defence mechanisms against oxidative stress in *S. aureus* can be divided into two sections. On the one hand, there are determinants to detoxify reactive species and to protect or repair oxidative damage [85]. On the other hand, there is a network of global and specific regulators to sense oxidative stress and to regulate the oxidative stress response in *S. aureus* [85].

S. aureus possesses different specific enzymes to detoxify reactive species. The superoxide dismutase (SOD) catalyses the detoxification of O_2^- to oxygen and H_2O_2 [193, 194]. *S. aureus* has two SODs, the manganese-containing SodA and the Fe-containing SodM [41, 306]. H_2O_2 can be further converted to oxygen and water by a catalase [143]. In *S. aureus*, the gene *katA* encodes for the iron-dependent catalase KatA [120, 266]. Moreover, *S. aureus* uses different peroxiredoxins to detoxify H_2O_2, such as alkyl hydroperoxide reductase AhpCF, bacterioferritin comigratory protein (Bcp) or the thiol peroxidase Tpx [120, 325]. These different enzymes confer the strong resistance to H_2O_2 of *S. aureus* [316]. In addition, KatA and AhpCF are important for nasal colonization of *S. aureus* [44]. The RNS NO• can be detoxified by the enzyme flavohemoglobin (Hmp) in *S. aureus*. Hmp can convert NO• in the presence of oxygen and NADPH to nitrate [84, 88, 105]. Staphylococcal Hmp confers resistance to nitrosative stress and is required for full virulence in mice with a functional iNOS [88, 256]. Thus far, specific enzymes, which can detoxify HOCl and OH•, could not be identified because of their high reactivity with all biomolecules (see section 2.2). However, cells are able to decrease their toxicity by non-enzymatic antioxidants or can prevent Fenton reaction by detoxifying H_2O_2 by KatA and peroxiredoxins (see above). Moreover, iron-storage proteins sequester free iron. Therefore, *S. aureus* uses ferritin (FtnA) or the Dps-homolog metallo-regulated gene (MrgA) [120].

Furthermore, *S. aureus* has also non-enzymatic antioxidants, including pigments and the so-called low molecular weight (LMW) thiols, to render reactive species harmless. *S. aureus* produces the membrane-bound golden C_{30}-triterpenoid staphyloxanthin [189, 190, 231]. Carotenoids, like staphyloxanthin, are able to quench reactive species because of their conjugated double bonds [39, 150]. Thereby, staphyloxanthin functions as an antioxidant and can protect *S. aureus* against singlet oxygen, OH•, $ONOO^-$, HOCl and H_2O_2 [39, 46, 173]. Moreover, it improves the survival of *S. aureus* during neutrophil killing [39, 173]. LMW thiols are small, highly reactive, non-protein molecules with a thiol group and function as cellular redox buffers [64, 311]. They are important to maintain a reduced redox balance in organisms [311]. *S. aureus* uses bacillithiol (BSH) and coenzyme A (CoASH) as its LMW thiols (see

section 3 for more details) [209, 216, 244]. Under ROS and HOCl stress, LMW thiols are oxidized to their corresponding thiol disulfide (BSSB, $CoAS_2$) or can protect proteins against overoxidation to sulfinic or sulfonic acid, leading to a mixed protein disulfide formation (*S*-bacillithiolations; *S*-CoAlations) [4, 181, 311]. In addition, *S. aureus* has a bacillithiol disulfide reductase (YpdA) and a CoA disulfide reductase (Cdr) to diminish bacillithiol (BSSB) and CoA disulfides ($CoAS_2$) (see section 3 for more detail) [52, 165, 199]. Besides from *S*-thiolations of proteins, proteins can also form inter- and intramolecular disulfides as a reversible post-translational modification after oxidative stress [4]. To regenerate such disulfides, *S. aureus* uses the ubiquitous thioredoxin redox system. Thereby, thioredoxin (TrxA) can reduce the protein disulfides [116]. Afterwards, the thioredoxin reductase (TrxB) recovers oxidized TrxA back to its reduced state under consumption of NADPH [116].

One main target of O_2^- and H_2O_2 is the iron-sulfur cluster (Fe-S cluster) of dehydratases [126]. *S. aureus* can repair damaged Fe-S clusters by the di-iron protein ScdA [226]. The transcription of *scdA* is strongly upregulated after H_2O_2 stress [32]. HOCl causes protein unfolding and aggregation [95]. Therefore, *S. aureus* induces the expression of chaperones and proteases to prevent protein aggregation or to degrade irreversible damaged or unfolded proteins caused by HOCl [78, 79, 95, 284]. Heat shock proteins and proteases in *S. aureus* include among others DnaJ, DnaK-GrpE, Clp proteases and GroESL [78, 79, 284]. The induction of the expression of chaperons and proteases belongs to the signature of the oxidative stress response in *S. aureus* and could be detected after HOCl, AGXX®, allicin, methylhydroquinone (MHQ) and lapachol stress in the transcriptome [80, 164, 177, 178, 180]. AGXX® is a surface-coating compound, which is constituted of the two transition metals silver (Ag) and ruthenium (Ru). These metals interact as a micro galvanic cell, resulting in ROS formation, such as H_2O_2 or OH• [40, 96].

During the staphylococcal oxidative stress response, many transcriptional regulators participate to sense oxidative stress and to induce the expression of genes, which are involved in detoxification of reactive species. The most important regulator after oxidative stress is the peroxide stress regulator PerR. The iron-containing PerR acts as a repressor of its controlled genes under non-stress conditions [120, 135]. Under oxidative stress, H_2O_2 reacts with iron and OH• is generated, which leads to oxidation of the iron-coordinating histidines [135, 155]. Finally, this oxidation results in the release of iron and the regulator loses its DNA binding activity [135, 155]. Therefore, the expression of genes for the oxidative stress resistance (*katA*, *ahpCF*, *trxB, bcp*) and iron-storage proteins (*ftnA*, *mrgA*) is induced [120]. Moreover, iron seems to play a main role in the regulation of the PerR regulon. The ferric uptake regulator Fur can induce iron-dependent the transcription of *katA* [121] and influences the expression of *ftnA*, *ahpC* and *mrgA* independently from PerR [203].

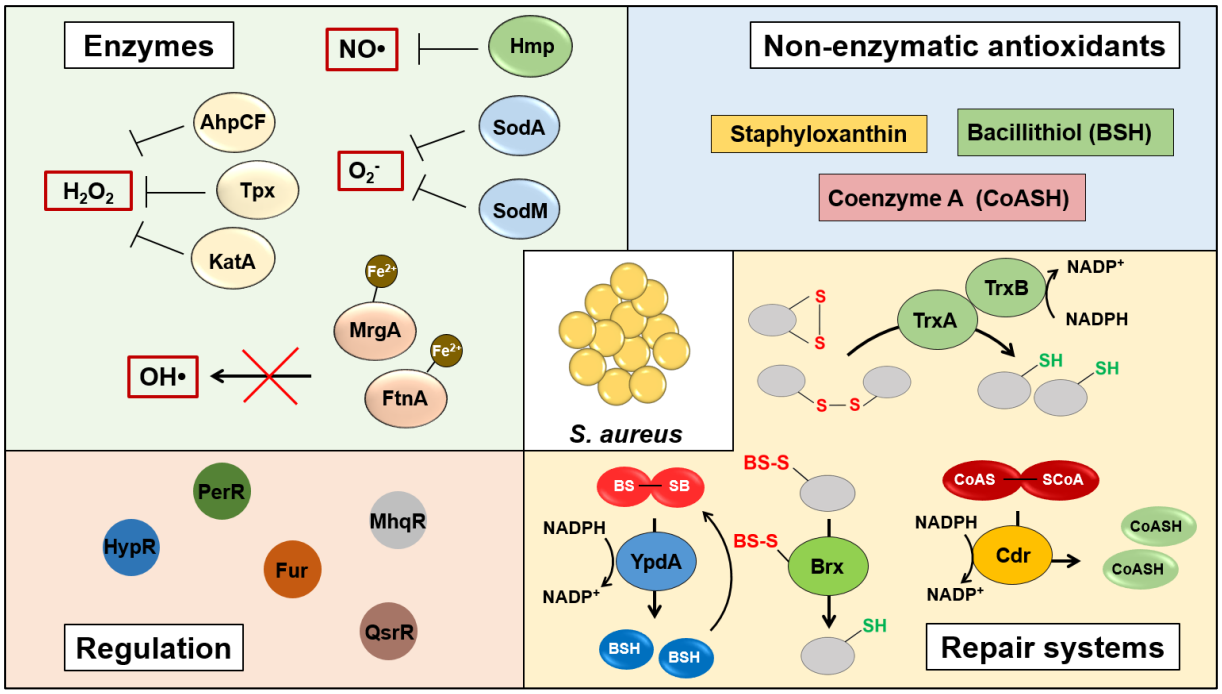

Fig. 5: Schematic overview about selected determinants of staphylococcal defence mechanisms against oxidative and quinone stress. Reactive species can be detoxified by specific enzymes, such as superoxide dismutases (SodA, SodM), catalase (KatA), alkyl hydroperoxide reductase (AhpCF), thiol peroxidase (Tpx) or flavohemoglobin (Hmp). In addition, iron-binding proteins (MrgA, FtnA) can sequester free iron to prevent OH• generation via Fenton chemistry. The non-enzymatic antioxidants, like the golden pigment staphyloxanthin and the LMW thiols bacillithiol and coenzyme A are also involved in detoxification of reactive species or in protection of proteins against oxidative damages. Transcriptional regulators, such as HypR, PerR, Fur, MhqR or QsrR, are important to sense ROS and quinone stress and to induce the specific stress response in *S. aureus*. Furthermore, *S. aureus* possesses also different systems to repair oxidative damages of proteins. Intra- and intermolecular disulfides can be reduced by the thioredoxin system (TrxA/B). Bacilliredoxins (Brx) can diminish *S*-bacillithiolated proteins, leading to *S*-bacillithiolated Brx (Brx-SSB), which can be reduced by BSH, resulting in bacillithiol disulfide (BSSB) formation. The NADPH-dependent disulfide reductases YpdA and Cdr convert BSSB and coenzyme A disulfide ($CoAS_2$) to the reduced LMW thiols BSH and CoASH, respectively. This figure is adapted from reference [85].

Recently, Loi *et al*. (2018) could identify a hypochlorite-specific transcriptional repressor HypR in *S. aureus*, which controls the NADPH-dependent flavin disulfide reductase MerA [178]. Under HOCl stress, HypR forms an intermolecular disulfide between cysteines 33 and 99, leading to the dissociation of HypR from the DNA and induction of the *hypR-merA* operon [178]. The Δ*merA* mutant was significantly more sensitive to HOCl exposure in growth and survival assays and showed a decreased survival under macrophage infection conditions [178]. However, an overexpression of MerA in the Δ*hypR* mutant did not increase the survival of *S. aureus* under infection conditions [178]. The specific substrate of MerA after HOCl stress remains to be elucidated. Nevertheless, it has been shown that MerA can detoxify allicin [180].

Furthermore, *S. aureus* has also defence mechanisms to overcome quinone stress, including the quinone-sensing and response repressor (QsrR) and the methylhydroquinone-specific repressor (MhqR) [80, 136]. QsrR is a redox-sensitive regulator and controls a nitroreductase, a NADH-dependent flavinmononucleotide reductase and a

glyoxalase/bleomycin resistance protein [136]. In contrast, MhqR regulates the expression of the *mhqRED* operon, which includes a phospholipase/carboxylesterase (MhqD) and a ring-cleavage dioxygenase (MhqE) [80]. All these enzymes are predicted to participate in the decomposition of quinones. The Δ*qsrR* mutant was more resistant to 1,4-benzoquinone, methyl-*p*-benzoquinone and MHQ compared to the parental wild-type strain [80, 136]. In addition, the Δ*mhqR* mutant shows higher resistance to MHQ stress than the wild type [80]. Importantly, Fritsch *et al.* (2019) revealed that the MhqR regulon confers resistance to quinone-like antimicrobials and fluoroquinolones, such as norfloxacin, ciprofloxacin, rifampicin or the blue-coloured phenazine of *Pseudomonas aeruginosa* pyocyanin [80]. However, the Δ*mhqR* mutant was more sensitive to the plant-derived naphthoquinone lapachol, indicating that the MhqR operon does not confer resistance to lapachol [80]. Lapachols mode of action and which defence mechanisms of *S. aureus* are involved to confer resistance to lapachol stress were investigated in this PhD thesis (see section 2.5 and **chapter 4** for more details) [164].

In summary, *S. aureus* possesses a vast amount of defence mechanisms to resist against diverse kinds of reactive species, including ROS, RCS, RNS or RES **(Fig. 5)**. Furthermore, the expression of the oxidative stress and quinone response is controlled by specific transcriptional regulators.

2.5 The oxidative mode of action of the naphthoquinone lapachol

S. aureus is a major human pathogen and acquires rapidly antibiotic resistances, resulting in current MRSA and VRSA strains (see section 1 for more detail). Thus, it is necessary to find new drug targets or to develop new antimicrobial compounds to combat *S. aureus* infections. Quinones are potent antimicrobial substances because of their bivalent mode of action (see section 2.3 for more detail). The plant-derived lapachol is a fully substituted 2-hydroxy-3-(3-methyl-2-butenyl)-1,4-naphthoquinone. It was originally isolated from the lapacho tree *Tabebuia impetiginosa* and is described in the literature to have cytotoxic, antiparasitic and antimicrobial properties [62, 122, 250]. Thereby, lapachol has growth-retarding effects on several cancer cell lines and the Balb/c murine peritoneal macrophage cell line [238, 259, 293]. Moreover, previous studies showed that lapachol is more toxic against Gram-positive bacteria than Gram-negative bacteria [229, 235, 288]. In addition, Kumagai *et al*. (1997) and Goulart *et al*. (2003) showed that lapachol can be reduced to its semiquinone anion, which interacts with oxygen, leading to ROS formation *in vitro* [91, 152]. However, no studies have investigated the mode of action in pathogenic bacteria and their defence mechanisms. Recently, it was shown that the staphylococcal flavohemoglobin Hmp has an enhanced affinity to reduce 2-hydroxy-1,4-naphthoquinones [204].

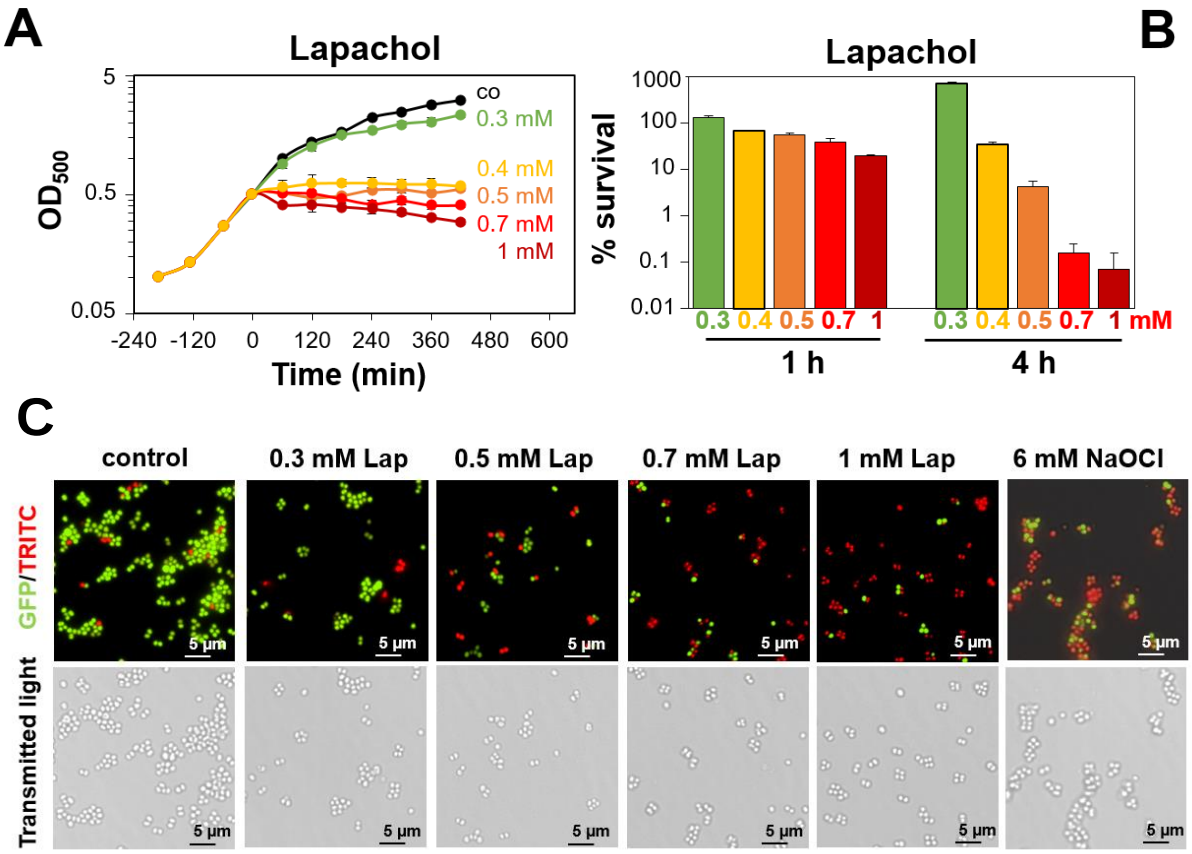

Fig. 6: Lapachol has a strong antimicrobial effect on *S. aureus*. (A) While *S. aureus* can grow after sub-lethal concentration of 0.3 mM lapachol, 0.4 mM inhibits the growth of the human pathogen. **(B)** Survival rates after several concentrations of lapachol show the strong antimicrobial effect of the naphthoquinone on *S. aureus*. The exposure of 1 mM lapachol for four hours leads to a decrease of the survival rate to less than 0.1%. **(C)** LIVE/DEAD™ viability assay with *S. aureus* COL WT after different concentrations of lapachol stress. *S. aureus* was exposed to 0.3 to 1 mM lapachol (Lap) stress. Afterwards the cells were labelled with SYTO9 and propidium iodide and visualized with a fluorescence microscope. As a positive control for dead cells, 6 mM sodium hypochlorite (NaOCl) was used. Living *S. aureus* cells are shown in green, dead cells fluoresce in red. Only a few cells are green after 0.7 and 1 mM lapachol, indicating lapachol has a strong toxic effect on *S. aureus*. The growth and survival assays were performed together with Verena N. Fritsch. The figure is from the manuscript of chapter 4 [164].

As one major part of this PhD thesis, the antimicrobial effect of lapachol on *S. aureus* and its mode of action in *S. aureus* was investigated **(Fig. 6) (chapter 4)** [164]. Firstly, I performed together with Verena N. Fritsch growth and survival assays of the HA-MRSA strain *S. aureus* COL after exposure to different concentrations of lapachol under aerobic conditions. While *S. aureus* could grow after 0.3 mM lapachol treatment, 0.4 mM lapachol inhibited the growth and killed *S. aureus* **(Fig. 6A)**. Importantly, the survival rate of *S. aureus* was lower than 0.1% after 4h of 1 mM lapachol stress **(Fig. 6B)** [164]. In addition, I analysed the cell viability using the LIVE/DEAD™ assay **(Fig. 6C)**. Thereby, living cells are visible in green (SYTO9-labelled) and dead bacteria are shown in red (propium iodide-labelled) using a fluorescence microscope. Only a few *S. aureus* cells fluoresced in green after 1 mM lapachol

stress. These results revealed that lapachol has a strong antimicrobial effect on the major human pathogen *S. aureus* [164].

Furthermore, I determined the minimal inhibitory concentration (MIC) of lapachol on *S. aureus* using 96-well plates. The MIC was between 0.625 and 1.25 mM lapachol [164], which agrees with the previously determined MIC of 128-256 µg/ml (≈ 0.528-1.057 mM) lapachol towards *S. aureus* [223]. However, this MIC is significantly higher than the lethal concentrations, revealed by growth and survival assays. It might be that different growth conditions, which result in differences in the oxygen supply, are responsible for this discrepancy. Additionally, survival assays under microaerophilic conditions demonstrated that lapachol is less toxic (1 mM: >80% survival after 4 h) compared to aerobic conditions (1 mM: <0.1% survival after 4 h) [164], indicating that the oxygen supply has a significant impact on the toxicity of lapachol.

Next, the mode of action of lapachol, leading to the cell death of *S. aureus*, was studied. Therefore, a RNA-seq analysis of *S. aureus* transcriptome after lapachol stress was performed. The transcriptome revealed that lapachol induces a strong quinone-specific and oxidative stress response in *S. aureus*, including upregulation of the QsrR, MhqR, HrcA, CtsR and PerR regulons as well as the increased transcription of most of the BSH genes **(Fig. 7)** [164]. The HrcA and CtsR regulons include heat shock proteins and proteases, such as DnaJ, DnaK-GrpE, the proteases ClpP, ClpB and ClpC as well as GroESL [78, 79, 284]. These chaperons and proteases are required to degrade irreversibly damaged proteins and to prevent protein aggregation [78, 79, 284]. Furthermore, lapachol causes an upregulation of the PerR regulon. This regulon includes genes encoding for enzymes, which are important to detoxify ROS and to recover from disulfide stress, such as KatA, AhpCF, Tpx or TrxB [120]. In addition, lapachol also induces the quinone-specific QsrR and MhqR regulons [164]. The two repressors QsrR and MhqR control the transcription of genes encoding for enzymes, which are predicted to be involved in quinone detoxification [80, 136]. However, Fritsch *et al.* (2019) revealed that the *mhqRED* operon does not confer resistance to lapachol [80].

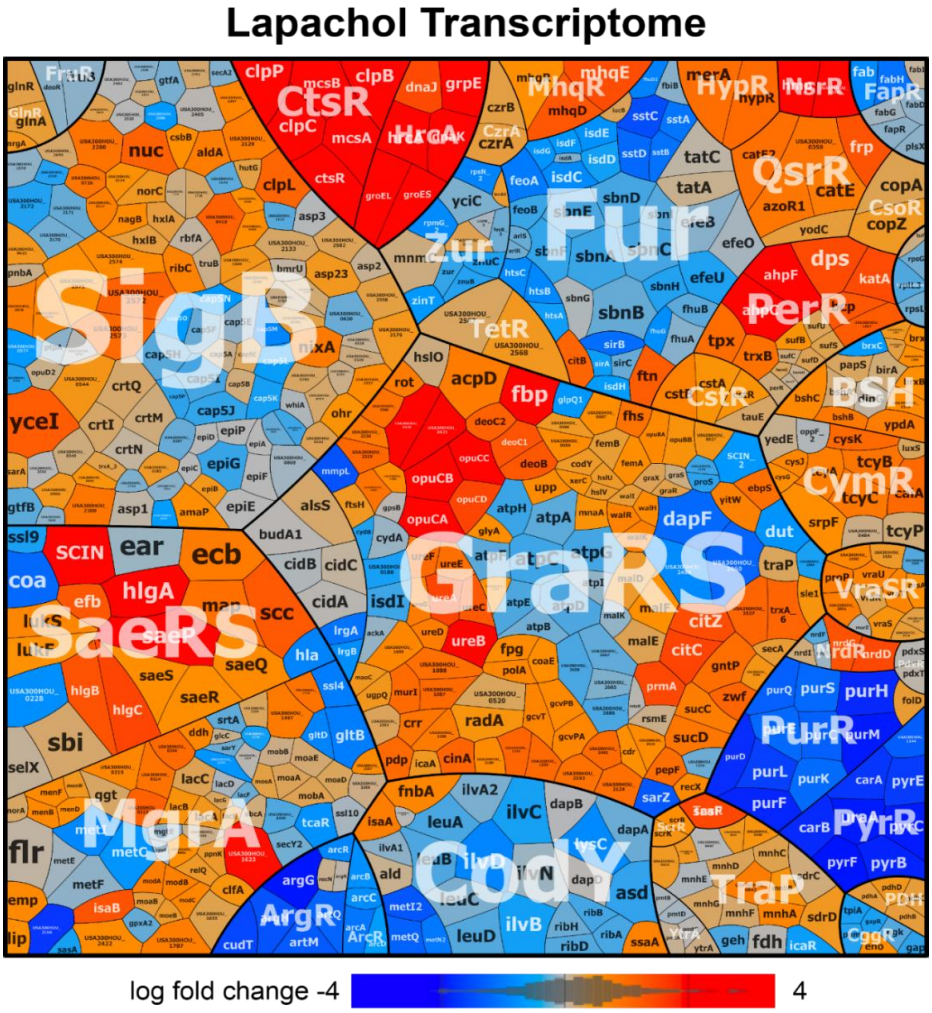

Fig. 7: Lapachol induces a quinone-specific and oxidative stress response in *S. aureus* as revealed by RNA-seq analyses. The lapachol transcriptome is shown as a Voronoi tree map, which contains up- and downregulated genes clustered in regulons after lapachol stress compared to control conditions. Upregulated genes and regulons are coloured in red, whereas downregulated genes and regulons are shown in blue. Lapachol induces the transcription of the HrcA, CtsR, MhqR, QsrR and PerR regulons as well as the BSH-related genes in *S. aureus*. The RNA-seq analyses was performed by Tobias Busche and Jörn Kalinowski from the Center for Biotechnology in Bielefeld. The figure is from the manuscript of chapter 4 [164].

As depicted in section 2.3, quinones can act in two ways, as electrophiles and as oxidants. As electrophiles, quinones are able to react with nucleophilic thiol groups of cysteines and can form thiol-*S*-alkylations via 1,4-Michael-addition, leading to protein aggregations, like it has been shown for benzoquinones [19, 159, 201, 220]. However, I did not detect any protein aggregation of the glyceraldehyde-3-phosphate dehydrogenase (GapDH) *in vitro* even after 7.5 mM lapachol **(chapter 4)** using specific anti-GapDH Western blots and SDS PAGE [164]. Also *in vivo*, lapachol did not induce any protein aggregation in *S. aureus* as revealed by analysis of insoluble protein fractions after lapachol stress with SDS PAGE by Vu Van Loi [164]. Additionally, the redox-state of the transcriptional repressor HypR was analysed after exposure to lapachol. HypR possesses three cysteines and senses thiol stress via formation of an intermolecular disulfide-linked dimer between the cysteine residues 33 and 99 [178]. The

His-tagged HypR dimer was detected after lapachol stress in non-reducing Western blots using an anti-His-tag antibody, however, HypR could be reduced in reducing Western blots. These results indicate that HypR was not irreversibly aggregated in the presence of lapachol. These findings support the assumption that lapachol as a fully substituted quinone might act presumably mainly as a redox cycler [24, 285]. Thus, it was assumed that lapachol acts primarily as an oxidant than as an electrophile.

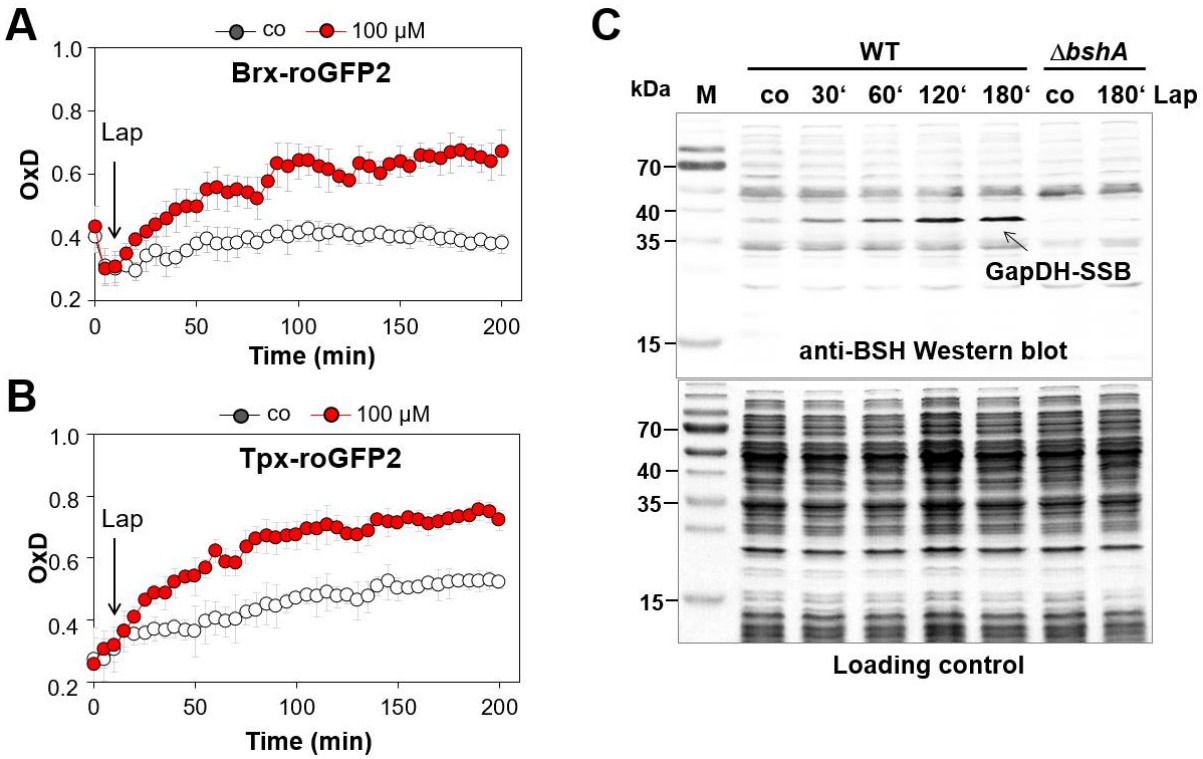

Fig. 8: Lapachol causes an increase of the BSH redox potential (E_{BSH}), enhances the intracellular H_2O_2 levels and provokes *S*-bacillithiolations in *S. aureus*. (A) The Brx-roGFP2 biosensor is oxidized after lapachol stress, indicating that lapachol causes an enhanced E_{BSH}. **(B)** *S. aureus* exhibits higher intracellular H_2O_2 levels after lapachol stress as revealed by the Tpx-roGFP2 biosensor oxidation after exposure to lapachol. (C) BSH-specific Western blot analyses demonstrated that lapachol causes an increased *S*-bacillithiolation of the staphylococcal GapDH. Figures are from the manuscript of chapter 4 [164].

To analyse the oxidative mode of action of lapachol, I did apply the genetically encoded roGFP2-fused redox biosensors Brx- and Tpx-roGFP2 (introduction is given in section 4) [164]. Brx-roGFP2 was used to monitor changes in the BSH redox potential (E_{BSH}) **(Fig. 8A)**, whereas Tpx-roGFP2 was applied to detect changes of the endogenous H_2O_2 levels in *S. aureus* after exposure to lapachol **(Fig. 8B)**. Both biosensors were significantly more oxidized in the presence of lapachol stress, indicating that lapachol increases the intracellular H_2O_2 levels in *S. aureus* and further rises the E_{BSH} **(Fig. 8A, B)** [164]. Moreover, the addition of the ROS scavenger N-acetyl cysteine (NAC) could significantly increase the survival of *S. aureus* after

lethal lapachol stress, confirming further that lapachol generates ROS [164]. These results support that lapachol acts by its oxidative mode of action and produces ROS in *S. aureus*.

Certain determinants of the staphylococcal oxidative stress response (see section 2.4 for more details) might be involved to defend against ROS produced by lapachol. One of them is BSH (see section 3.2 for more details), which protects proteins against overoxidation, leading to *S*-bacillithiolations [31, 181]. Therefore, I analysed the *S*-bacillithiolation pattern of GapDH *in vitro* and *in vivo* in *S. aureus* after lapachol stress. Previously, it has been shown that GapDH is the most abundant *S*-bacillithiolated protein after HOCl stress in *S. aureus*, which can be detected as the major protein band using a specific anti-BSH Western blot [123]. Here, I could demonstrate that lapachol provokes an increased *S*-bacillithiolated GapDH band **(Fig. 8C)** [164]. Additionally, *S*-bacillithiolation of purified GapDH was also detected after treatment with lapachol [164]. These results revealed that lapachol induces *S*-bacillithiolations of GapDH *in vitro* and *in vivo* in *S. aureus.*

Next, the phenotype of the Δ*katA* mutant after exposure to lapachol was investigated to analyse the ROS production by lapachol. As revealed in growth and survival assays, the Δ*katA* mutant was significantly more sensitive to lapachol stress compared to the wild type. These phenotypes could be restored by complementation with *katA*. This result approves that lapachol produces ROS in its oxidative mode of action and KatA is important to detoxify the produced ROS [164]. Additionally, Quach Ngoc Tung showed that lapachol-treated cells exhibit a higher H_2O_2 detoxification capacity compared to non-stressed cells as revealed by the FOX assay, confirming the induction of the PerR regulon by lapachol and thus the enhanced expression of *katA* [164]. Furthermore, I demonstrated that lapachol causes *S*-bacillithiolations of proteins **(see Fig. 8C)**. Recently, it has been shown that bacilliredoxins and the BSSB reductase YpdA are necessary to reduce *S*-bacillithiolated proteins and to regenerate reduced BSH (see section 3 for more details) [123, 165, 199]. Therefore, Verena N. Fritsch performed phenotype analyses of the Δ*bshA*, Δ*brxAB* and Δ*ypdA* mutants [164]. All these mutants were significantly attenuated in growth and survival after exposure to lapachol stress. These phenotypes could be also restored by complementation with *bshA*, *brxA* and *ypdA* [164]. These findings demonstrated that BSH and the BSH redox pathway (BrxAB, YpdA) are important to reduce *S*-bacillithiolated proteins after lapachol stress **(Fig. 9)**.

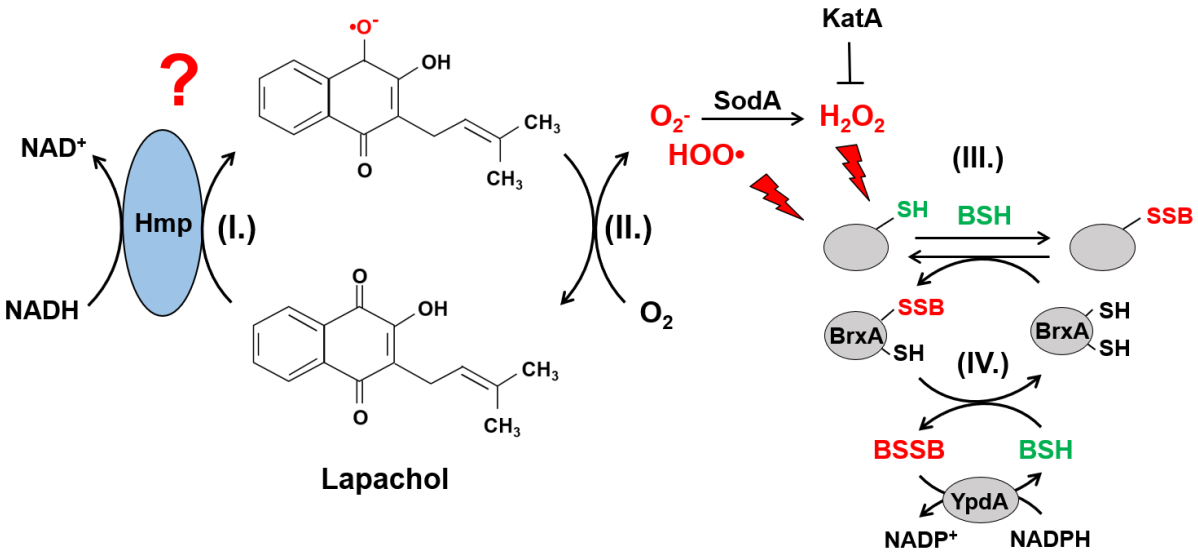

Fig. 9: Proposed model of the redox-active mode of action of lapachol in *S. aureus*.
(I.) Lapachol can act as a redox cycler. Thereby, Lapachol can probably be reduced to its radical anion by an one electron reduction under NADH consumption. Due to its enhanced affinity for reduction of 2-methyl-1,4-naphthoquinones and its strong upregulation after lapachol stress in the transcriptome, the flavohemoglobin Hmp might be a candidate for the reduction of lapachol in *S. aureus* [204]. **(II.)** The radical anion of lapachol can be reduced by oxygen to form ROS, such as superoxide anion (O_2^-) or peroxyl radical (HOO•). The reactive oxygen species O_2^- is converted to H_2O_2 by superoxide dismutase (SodA). H_2O_2 can be detoxified by catalase (KatA). **(III.)** HOO• and H_2O_2 can react with thiol groups of proteins to form cysteine sulfenyl acid intermediate (S-OH). The LMW thiol BSH forms mixed disulfides with proteins to protect them against overoxidation, leading to *S*-bacillithiolations (-SSB) **(IV.)** The BSH/BrxA/YpdA redox pathway is required to recover *S*-bacillithiolated proteins. The *S*-bacillithiolation is reduced by the bacilliredoxin BrxA, resulting in BrxA-SSB formation. BSH can regenerate reduced BrxA, leading to bacillithiol disulfide (BSSB). The NADPH-dependent BSSB reductase YpdA converts BSSB to regenerate BSH. This figure is adapted from reference [164].

In conclusion, the study could show that the naphthoquinone lapachol has a strong antimicrobial effect on the human pathogen *S. aureus* and that lapachol acts mainly via its oxidative mode of action. Thereby, lapachol induces a quinone-specific and oxidative stress response, increases the E_{BSH} and causes *S*-bacillithiolations in *S. aureus*. Furthermore, KatA and the BSH redox pathway are involved in the defence against oxidative stress generated by the redox cycle of lapachol **(Fig. 9)**. ROS scavenger (NAC) and microaerophilic growth conditions reduce strongly the antimicrobial effect of lapachol on *S. aureus*. No evidence could be detected that lapachol does induce protein aggregation. Thus, these findings support the supposition that fully substituted quinones, like lapachol, might act preferred as a redox cycler than as an electrophile. 1,4-naphthoquinone possesses a benzene ring on one side of the quinoid ring, which attenuates the nucleophilic 1,4-Michael addition. As a consequence, 1,4-naphthoquinones react with thiol groups at their carbon residues at positions 2 and 3 [24, 285]. If the quinones are substituted at these positions of the quinoid ring, the *S*-alkylation ability of quinones is reduced [24, 285].

3. The impact of low molecular weight (LMW) thiols in the bacterial defence against oxidative stress

LMW thiols are small non-protein molecules, which have a thiol as their functional group. They play a crucial role to maintain the redox homeostasis in eukaryotes and prokaryotes [181, 311]. Until now, 12 different types of LMW thiols are known, ten of them exist in bacteria [215, 311]. The following section reviews the different types and functions of LMW thiols in bacteria. In particular, it highlights the role of bacillithiol (BSH) as the major LMW thiol in Firmicutes and reveals the physiological role of the BSH redox pathway, including bacilliredoxins and YpdA, under oxidative stress and infection conditions. Moreover, it provides an insight into the role of coenzyme A (CoASH) as an alternative LMW thiol in *S. aureus*.

3.1 Biosynthesis and functions of LMW thiols in bacteria

A wide range of LMW thiols is known. Some human parasites, such as *Trichomonas vaginalisor*, use the ubiquitous amino acid cysteine (CysSH) as their major thiol redox buffer [319]. CysSH can also be used by bacteria as an alternative thiol in the absence of their main LMW thiol **(Fig. 10)** [35, 36]. The tropical parasites Leishmania and Trypanosomes have trypanothione ($T(SH)_2$) as a unique LMW thiol [67, 149]. Moreover, a few marine invertebrates as well as Leishmania possess Ovothiol (OSH) to resist oxidative stress [149, 303, 311].

The best known LMW thiol is the tripeptide glutathione (GSH) **(Fig. 10)**. GSH was discovered by Sir Fredrick Hopkins in the 1920's [118, 119]. It is composed of the three amino acids glutamic acid, glycine and cysteine, which are linked to γ-L-glutamyl-L-cysteinylglycine [119, 191]. Most eukaryotes, including humans, animals and plants, and many microorganisms, including most of the Gram-negative bacteria, produce GSH in a millimolar range from 0.1 up to 10 mM [65, 66, 195]. In addition, some pathogenic Gram-positive bacteria, such as *Listeria monocytogenes*, *Streptococcus agalactiae* or *S. pneumoniae*, are able to produce or to import GSH [89, 133, 246]. Moreover, *E. coli* produces also glutathionylspermidine (GSP) as an alternative LMW thiol [38]. Interestingly, it has been shown that some Halobacteria and lactic acid bacteria of the genus *Leuconostoc* use the precursor of GSH synthesis γ-glutamylcysteine (γ-Glu-Cys) as their main LMW thiol [144, 213]. The glutathione amide (GASH) is used as a redox buffer by anaerobic sulfur bacteria [11]. In *E. coli*, the tripeptide GSH is synthetized by a two-step pathway: In the first step, glutamic acid is linked to cysteine by the glutamate-cysteine ligase (GshA), yielding γ-Glu-Cys. Afterwards, the GSH synthetase (GshB) adds glycine to γ-Glu-Cys [191]. GSH plays an important role in the maintenance of the redox balance and is involved in the detoxification of metals, xenobiotics and reactive species, such as HOCl, monochloramine, H_2O_2, OH•, NO• or methylglyoxal [181, 191, 311]. Under infection conditions, GSH is important for survival and virulence of the human

pathogens *S. pneumoniae*, *L. monocytogenes* and *Salmonella enterica* serovar Typhimurium [246, 254, 286]. Under oxidative stress, GSH can protect proteins against irreversible damages. Thereby, it forms GSH mixed protein disulfides, named as *S*-glutathiolations [181, 191, 311]. Furthermore, it can protect against environmental stress, such as osmotic stress or under acidic conditions [191].

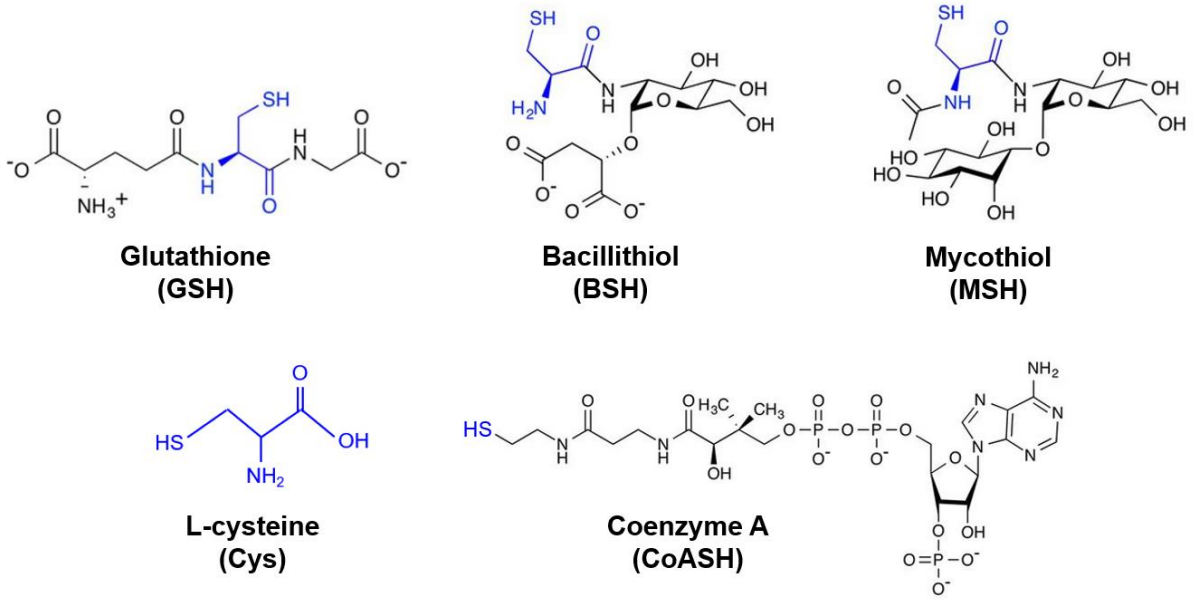

Fig. 10: Structures of bacterial low molecular weight (LMW) thiols. Bacteria use different LMW thiols, which are structurally divers. However, all LMW thiols unite the thiol group, which is derived from cysteine (shown in blue). Most Gram-negative bacteria use glutathione (GSH) as their major LMW thiol. The major LMW thiol of Firmicutes is bacillithiol (BSH). Bacteria of the phylum Actinomycetes, like *Mycobacterium* or *Corynebacterium*, produce mycothiol (MSH). In absence of their major LMW thiol, some bacteria utilize L-cysteine (Cys). *S. aureus* and some *Bacillus* spec. can use coenzyme A (CoASH) as an alternative LMW thiol. This figure is adapted from references [31, 215, 311].

However, not all bacteria can use or synthesize GSH. Species of the phylum Actinomycetes, such as Corynebacteria, Mycobacteria or *Streptomycetes*, utilize several millimolar of mycothiol (MSH) as their major LMW thiol **(Fig. 10)** [137, 181, 210]. MSH was first described in the early 1990's [211, 264, 291]. This thiol redox buffer exhibits the chemical structure of a N-acetyl-cysteine-N-glucosamine-*myo*-inositol (NAc-Cys-GlcN-*myo*-ino) [137, 181, 210]. The MSH biosynthesis is composed of five steps. First of all, 1-*O*-(2-acetamido-2-deoxy-α-D-glucopyranosyl)-D-*myo*-inositol-3-phosphate (GlcNAc-Ins-P) is formed by linkage of *myo*-inositol-1-P and UDP-N-GlcNAc, which is catalysed by the glycosyltransferase MshA. Next, the phosphatase MshA2 removes the phosphate and further MshB deacetylates GlcNAc-Ins to GlcN-Ins. This serves as a substrate for the cysteine ligase MshC, which adds cysteine, leading to Cys-GlcN-Ins generation. Finally, the cysteine residue is acetylated by the acetyltransferase MshD, resulting in MSH [137, 210]. Similar to GSH, MSH is crucial for resistance against ROS, HOCl, RNS, RES and antibiotics [25, 35, 181, 210, 251, 252]. It is involved to increase the fitness of industrial *Corynebacterium glutamicum* strains and confers

further resistance to H_2O_2, ethanol, alkylating agents, acids, aromatic compounds and toxic heavy metals [174, 175, 181, 210]. Moreover, *Mycobacterium tuberculosis* requires MSH for growth under laboratory conditions [267]. Under H_2O_2 and HOCl stress, MSH prevents an overoxidation of proteins to rescue their functions, resulting in *S*-mycothiolations of important metabolic enzymes, such as GapDH [35, 110, 111, 181]. In addition, Mycobacteria as well as some fungi can use the 2-thiolhistidine ergothioneine (ESH) as further thiol redox buffer [128, 273].

However, Gram-positive bacteria of the phylum Firmicutes, such as *B. subtilis* or *S. aureus*, produce none of the named LMW thiols. In contrast, they synthesize bacillithiol (BSH) as their major LMW thiol and coenzyme A (CoASH) as an alternative LMW thiol **(Fig. 10)** (see sections 3.2 & 3.3 for more details) [31, 181]. Recently, it has been shown that the BSH-derivative N-metyl-bacillithiol (N-Me-BSH) is the main LMW thiols in phototrophic bacteria, of the family *Chlorobiaceae* [112, 215].

In summary, ten different LMW thiols are known in bacteria, from which the best-studied and most prevalent redox buffers are GSH, MSH and BSH. These molecules are crucial to maintain the redox balance, to prevent irreversible protein damages after oxidative stress and to detoxify reactive species. Thus, LMW thiols of bacteria play an important role in fitness, virulence and resistance against several types of stress.

3.2 Bacillithiol (BSH) as the major LMW thiol in Firmicutes

Since BSH was discovered in the low GC (guanosine and cytosine) Gram-positive bacteria of the phylum Firmicutes in 2007 [156, 217], many studies investigate the properties, functions and impacts of BSH in the bacterial physiology.

3.2.1 Discovery, biophysical properties and biosynthesis of BSH

Neither GSH nor MSH were identified in Firmicutes [65, 209]. For a long time, it seemed that CoASH and CysSH function as the major LMW thiols in such bacteria. Actually in *S. aureus* and *Bacillus* spec., CoASH and CysSH were found in millimolar concentrations [209, 216, 217]. In 2007, the groups of Al Claiborne and John Helmann could both discover BSH independently of each other [156, 217]. Besides from CoASH, an unknown 398 Da thiol was identified during the investigation of the thiol content of *B. anthracis* [217]. In addition, Lee *et al*. (2007) could show that the oxidation of the organic peroxide sensor OhrR of *B. subtilis* leads to mixed disulfide formation between the regulator and three different thiols: CoASH, CysSH and a new 398 Da thiol [156]. In 2009, Newton *et al*. elucidated the chemical structure of the novel thiol as an α-anomeric glycoside of L-cysteinyl-D-glucosamine with L-malic acid and termed it as bacillithol, because of the wide distribution among *Bacillus* species [31, 216].

Moreover, BSH was also found in *S. aureus*, *S. carnosus*, *Deinococcus radiodurans* and recently in the Gram-negative bacterium *Thermus thermophilus* [37, 216, 219]. The chemical structure of BSH is similar to MSH. Instead of the *myo*-inositol in MSH, BSH contains L-malic acid. Moreover, the cysteine is not acetylated in BSH [125, 216].

BSH exhibits unique biophysical properties. At a physiological pH (in *B. subitilis*: 7.7 [145]), BSH occurs as a dianion, because the amino group of the cysteinyl residue is protonated by the linked glucosamine and the thiol group is deprotonated [274]. Due to the link of malate acid, which is negatively charged, the BSH thiolate form is stabilised [237, 274]. Thus, the thiol group of BSH (7.97) has a lower pK_a value than in other LMW thiols, such as CysSH (8.38), CoASH (9.83), MSH (8.76) or GSH (8.93) [237, 274, 276]. Therefore, the calculated pH-dependent proportion of the reactive thiolate anion form is the highest in BSH under physiological pH conditions [274, 276]. In Firmicutes, that portion (BSH thiolate: 21.9%) is significantly higher than the thiolate portions of CysSH (14.6%) and CoASH (0.7%) [274]. GSH and MSH have also lower thiolate portions (for both <10%) than BSH at physiological pH [274, 276]. Moreover, BSH possesses the highest redox potential ($E^{0'}$ = -221 mV) among all LMW thiols. Nevertheless, it is comparable to the $E^{0'}$ of other LMW thiols [237, 274, 276]. In addition, in *B. subtilis* and *S. aureus*, it was determined that BSH is the most abundant LMW thiol relative to CysSH and CoASH and exists in a range of 1 to 5 mM in these bacteria [31, 244, 274]. During this PhD thesis, we could determine that *S. aureus* COL has around 1.7 µmol BSH/g raw dry weight (rdw) in RPMI medium (at OD_{500} of 0.9) under control conditions [165]. In conclusion, BSH is the predominant nucleophilic LMW thiol in Firmicutes [31, 237].

The biosynthetic pathway of BSH includes three steps catalysed by the enzymes BshA, BshB and BshC **(Fig. 11)** [31, 83].

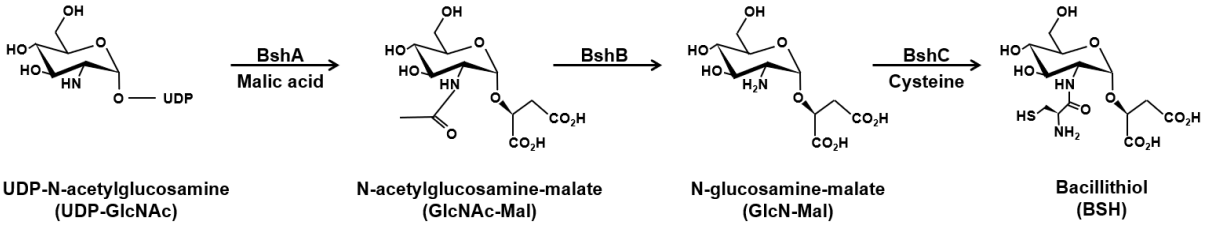

Fig. 11: The three-step biosynthesis pathway of BSH in *S. aureus*. At first, malic acid is conjugated to GlcNAc by the glycosyltransferase BshA. The N-acetylhydrolase BshB catalyses the deacetylation of GlcNAc and finally the cysteine ligase BshC links L-cysteine and GlcN-Mal to result BSH. This figure is adapted from references [31, 237].

Due to the structural similarity between BSH and MSH, the genes for the enzymes of the first (*bshA*) and the second (*bshB1*) pathway steps were found by sequence homology to MSH biosynthesis genes [31, 83]. In addition, the BshC could be identified by phylogenomic profile analyses [31, 83]. First, the glycosyltransferase BshA catalyses the linkage of UDP-GlcNAc and L-malic acid (Mal), yielding Glc-NAc-Mal [31, 83]. Afterwards, Glc-NAc-Mal is

deacetylated by the N-acetylhydrolase BshB [31, 83]. In several *Bacillus* species, it was found that these bacteria have two enzymes with N-acetylhydrolase activity (BshB1 and BshB2) [68, 83]. In contrast, the human pathogen *S. aureus* possesses only one deacetylase BshB. Furthermore, the staphylococcal BshB has also BSH conjugate amidase activity (Bca) (see section 3.2.2 for more details) [249]. Finally, L-cysteine is added to GlcN-Mal by the cysteine ligase BshC, resulting in BSH [31, 83]. All enzymes are essential for the BSH synthesis in *B. subtilis* and in *S. aureus*, because deletions in genes encoding for *bshA*, *bshB* or *bshC*, resulting in strains, which are unable to produce BSH [83, 249]. In *B. subtilis*, the transcriptional regulator Spx functions as an activator of the BSH biosynthesis genes [81]. It has been shown that the BSH level is significantly decreased in a *spx* null mutant compared to the WT [81]. In the last few years, it has been revealed that the BSH synthesis genes are enhanced transcribed after HOCl, MHQ, allicin, AGXX® and lapachol stress in *S. aureus* [80, 164, 177, 178, 180].

In summary, BSH functions as the major LMW thiols in low GC Gram-positive bacteria, such as *B. subtilis* and *S. aureus*. Furthermore, the enzymes BshA, BshB and BshC catalyse the biosynthesis of BSH in a three-step pathway.

3.2.2 Functions of BSH in Firmicutes

In particular for GSH and MSH, it has been shown that these LMW thiols play a crucial role in detoxification of different stress. Thus, they confer resistance to a wide range of reactive species, including ROS, RES, HOCl or antibiotics [137, 181, 191, 210]. Similar, BSH has a huge diversity of functions in GC low Gram-positive bacteria **(Fig. 12)** [31, 181, 237]. The major LMW thiol of Firmicutes is required to detoxify H_2O_2, HOCl, hydrogen sulfide (H_2S), allicin, alkylating agents (monobromobimane, N-ethylmaleimide), electrophiles (diamide, methylglyoxal) or antibiotics, like fosfomycin [31, 36, 83, 180, 181]. Thereby, a main function of BSH is the prevention of protein overoxidation under oxidative stress conditions, whereby it forms mixed disulfides with proteins, termed as *S*-bacillithiolation [31, 181]. Furthermore, it is involved to confer resistance against high salt stress, acidic stress, toxins or heavy metal stress [83, 212, 249]. The LMW thiol BSH is also important to protect *S. aureus* against oxidative stress produced by the surface coating antimicrobial compound AGXX® or by the 1,4-naphthoquinone lapachol [164, 177]. In addition, BSH is important for survival of *S. aureus* under infection conditions [244, 245].

In bacteria, the gaseous H_2S is produced in cysteine metabolism during transsulfuration [138, 233, 234, 277]. However, it is also toxic and can form per- and polysulfides, which are termed as reactive sulfur species (RSS) [200]. These RSS react with cysteinyl residues of proteins, leading to *S*-sulfhydration of proteins and decrease of its enzymatic activity [200, 234]. To protect proteins against *S*-sulfhydrations, BSH can react with H_2S to form bacillithiol

persulfide (BSSH) in *S. aureus* [234, 278]. The Fe(II)-containing persulfide dioxygenase (CstB) oxidizes BSSH, resulting in reduced BSH and thiosulfate (TS) [278]. In addition, allicin, the active compound of garlic, can react with BSH to yield *S*-allylmercaptobacillithiol (BSSA) or allicin can cause *S*-thioallylation of proteins [180]. *S*-thioallylated proteins and BSSA can be reduced by the BSH redox pathway (see section 3.2.3 for more details) [180].

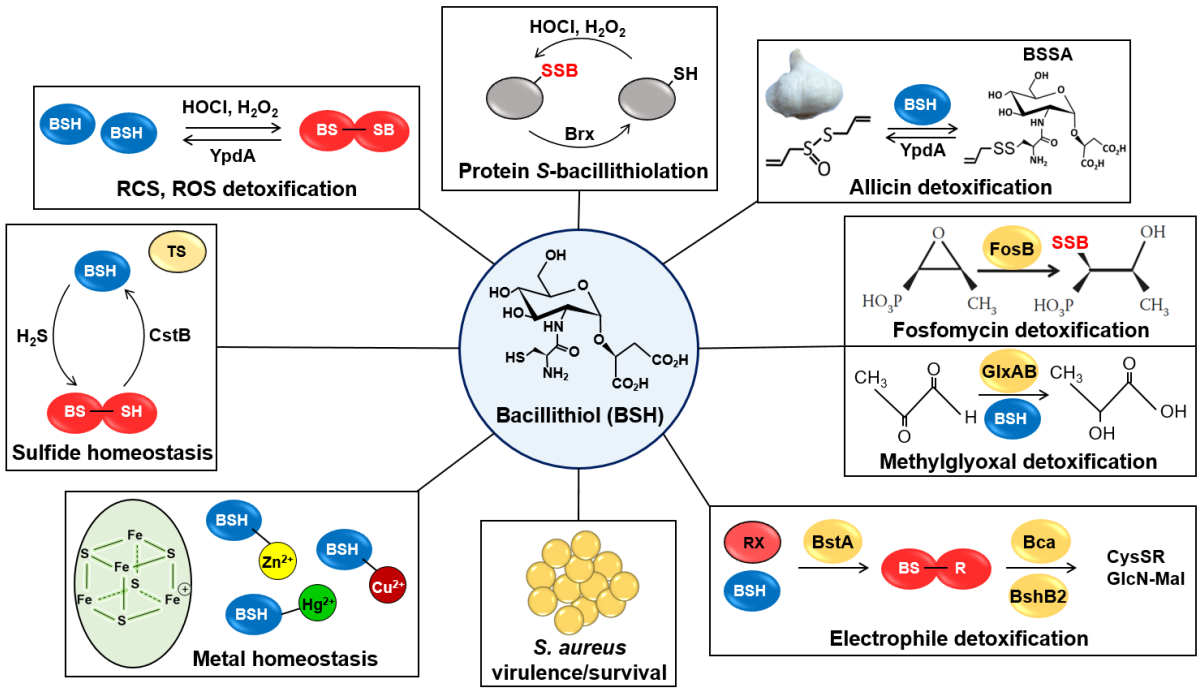

Fig. 12: Bacillithiol (BSH) has many different functions in bacteria. BSH is structurally an α-anomeric glycoside of L-cysteinyl-D-glucosamine. Under HOCl and H_2O_2 stress, BSH is oxidized to its corresponding thiol disulfide (BSSB). That can be recycled back to BSH by the BSSB reductase YpdA. In addition, BSH can protect proteins against overoxidation, leading to *S*-bacillithiolations (-SSB), which can be reduced by bacilliredoxins (Brx). BSH can detoxify the active compound of garlic allicin, resulting in *S*-allylmercaptobacillithiol (BSSA), which can be recycled by YpdA. The bacillithiol transferase FosB uses BSH as a co-factor to detoxify fosfomycin. BSH is also involved in detoxification of methylglyoxal (MG), whereby the glyoxalases I and II (GlxAB) convert MG together with BSH to D-lactate. Furthermore, BSH can be added to electrophiles or toxins by BSH-*S*-transferase BstA, resulting in BSH-conjugates (BS-R). The BSH-*S*-conjugate amidase Bca converts BS-R to GlcN-Mal and N-acetylcysteine-*S*-toxin (CySR). The virulence and the survival of *S. aureus* under infections is significantly increased by BSH. Several bacteria use BSH as a buffer of heavy metals, like Hg^{2+}, Zn^{2+} or Cu^{2+}. Moreover, it is supposed that BSH is involved in iron-sulfur cluster assembly. In addition, BSH can react with hydrogen sulfide (H_2S), leading to bacillithiol persulfide (BSSH) formation. BSSH can be recycled to reduced BSH and thiosulfate (TS) by the persulfide dioxygenase (CstB). This figure is adapted from references [31, 125, 301].

Furthermore, BSH is also involved in the detoxification of alkylating agents and toxins. Thereby, it is proposed that the bacillithiol-*S*-transferase (BstA) conjugates BSH specifically to toxic electrophiles, resulting in BSH-conjugates (BS-R) [31, 77, 214, 236]. The substrate specificity *in vivo* remains to be elucidated, but BstA can add BSH to the alkylating monochlorobimane (mBCl) *in vitro* [214, 236]. Afterwards, BS-R is converted to GlcN-Mal and N-acetylcysteine-*S*-toxin (CySR) by the bacillithiol-*S*-conjugate amidase (Bca) [68, 212, 249]. Interestingly, the N-acetylhydrolase BshB of the BSH biosynthesis pathway has a bivalent

function and can act as a Bca in *Bacillus* spec. and *S. aureus* [68, 212, 249]. GlcN-Mal is again used by BshC for BSH synthesis [68, 212, 249]. In addition, the staphylococcal BstA is also able to conjugate BSH to the antibiotics cerulenin and rifamycin [249].

The bactericidal antibiotic fosfomycin is an inhibitor of the cell wall synthesis and has been applied to combat MRSA infections [198]. However, *S. aureus* as well as *Bacillus* spec. use BSH and the thiol-*S*-transferase FosB to resist fosfomycin treatments [63, 244, 275, 295]. Thereby, FosB acts as a second bacillithiol-*S*-transferase and catalyzes the conjugation of BSH to the epoxide ring of fosfomycin [153, 258, 275, 296]. The similar fosfomycin-sensitive phenotypes of the Δ*bshA* and Δ*fosB* mutants demonstrate that BSH and FosB interact together to confer fosfomycin resistance [83, 244].

During the glycolysis, methylglyoxal (MG) can arise as a toxic electrophilic by-product [43]. In *B. subtilis*, it has been shown that the MG detoxification can proceed in a BSH-dependent manner. Thereby, BSH reacts spontaneously with MG to form the BS-hemithioacetal [30, 31]. Next, the glyoxalase I (GlxA) converts BS-hemithioacetal to *S*-lactosyl-BSH, which is used by glyoxalase II (GlxB). GlxB forms D-lactate and regenerates BSH [30, 31]. In summary, BSH plays a major role in detoxification of electrophiles and antibiotics in Firmicutes.

Apart from that, BSH is also involved to maintain the metal homeostasis and can protect against metal toxicity in BSH producing bacteria. Mutants, lacking BSH, are hypersensitive to different metal stress, such as Cd, Cu or Cr [249]. BSH is able to bind Zn(II) and can act as Zn(II) buffer in *B. subtilis* [184]. Furthermore, it can reduce the toxicity of Zn(II) and Cd(II) in CadA- and CzcD-deficient mutants, which lack Zn(II) and Cd(II) efflux systems [184]. Moreover, the copper chaperone CopZ interacts together with BSH to bind Cu(I), whereby BSH is involved in copper homeostasis [142]. In *T. thermophilus*, Hg(II) is sequestered by BSH, leading to increased Hg(II) resistance [219]. It has been revealed that Δ*bshA* and Δ*bshC* mutants are more sensitive to Hg(II) stress [219]. In addition, BSH has also a role in Fe-S cluster assembly in *S. aureus*, because BSH-deficient strains have similar phenotypes than mutants lacking the Fe-S cluster carrier protein Nfu [261]. Several activities of Fe-S cluster containing proteins, such as asconitase (AcnA) or isopropylmalate isomerase (LeuCD), were decreased in a Δ*bshA* mutant strain [261]. For *S. aureus*, it was proposed that BSH might function in Fe-S cluster carriage to the apo-proteins together with Nfu and SufA [261].

In *B. subtilis*, it has been determined that the redox ratio between reduced BSH and oxidized bacillithiol disulfide (BSSB) is higher than 100:1 [274]. Under oxidative stress, BSH can react with H_2O_2 or HOCl to render these oxidants ineffective, leading to BSSB formation and a decrease of the BSH/BSSB redox ratio [37, 54, 125, 181]. Additionally, HOCl also oxidized BSH to higher oxidation species, like BSH sulfinic acid (BSO_2H), BSH sulfonic acid (BSO_3H) or BSH sulfonamide ($BS O_2N$) [54].

One of the major functions of BSH is the protection of proteins against irreversible damages due to oxidative stress. Under H_2O_2 and HOCl stress, BSH can react with unstable cysteine sulfenic acid intermediates (R-SOH) of proteins, leading to *S*-bacillithiolations and inactivation of the enzymatic activity [123-125]. Moreover, *S*-bacillithiolations have also been identified after AGXX® and lapachol stress to protect proteins against ROS produced by these compounds (see section 2.5 and **chapter 4** for more details) [164, 177]. These *S*-bacillithiolations are reversible post-translational modifications [181]. Specific glutaredoxin-like proteins, named as bacilliredoxins (BrxA, BrxB), are required to reduce *S*-bacillithiolated proteins and to regenerate their activity (see section 3.2.3 for more details) [82, 123]. Thus, BSH is one of the determinants in redox regulation in Firmicutes. Under oxidative stress, the maintenance of the activity of metabolic key enzymes is important to ensure a functional metabolism. Many *S*-bacillithiolated proteins were identified in several *Bacillus* species and *S. carnosus* [36, 37, 125]. Briefly, the most abundant *S*-bacillithiolated protein in *Bacillus* species is MetE, a methionine synthetase [37]. This and further *S*-bacillithiolations of YxjG and SerA lead to methionine starvation in *B. subtilis* [36]. The transcriptional peroxide regulator OhrR is *S*-bacillithiolated after HOCl and organic hydroperoxide stress in *B. subitilis*, resulting in induction of the peroxiredoxin OhrA expression [36, 156]. Moreover, Chi *et al*. (2013) could identify 54 *S*-bacillithiolated proteins, including among others the translation elongation factor EF-Tu, several enzymes of the amino acids biosynthesis (AroA, AroE, SerA, LuxS) and the bacilliredoxins (YphP, YtxJ) [37]. The copper chaperone CopZ is also *S*-bacillithiolated in *B. subtilis* [142].

Furthermore, one of the most abundant targets of *S*-thiolations is the glyceraldehyde-3-phosphate dehydrogenase (GapDH) [125, 181]. *S*-glutathiolations, *S*-mycothiolations and *S*-bacillithiolations of GapDH have been detected in several organisms [109, 111, 123]. For example, GapDH is the most abundant *S*-mycothiolated protein after HOCl stress in *C. diphtheriae* [111]. During glycolysis, GapDH converts glyceraldehyde-3-phosphate (G3P) to 1,3-bisphosphoglycerate, resulting in NADH generation [109]. In *S. aureus*, the cysteine residue 151 (Cys151) acts as the active site of GapDH, which is deprotonated by the neighboring histidine residue 178 [123, 205]. Therefore, the active site possesses a nucleophilic thiol group. Thus, the Cys151 is more susceptible to oxidation by H_2O_2 (k=100 M^{-1} s^{-1}) and HOCl, leading to inactivation of GapDH [109, 123, 171, 205]. In different bacteria, GapDH is a preferred target of oxidation by HOCl and H_2O_2 stress [35-37, 111, 123]. Weber *et al*. (2004) and Imber *et al*. (2018) could demonstrate that GapDH is oxidized at position Cys151 by H_2O_2 and HOCl in *S. aureus in vivo* [123, 316]. To protect this key enzyme of the glycolysis against overoxidation, BSH reacts with the oxidized active site of GapDH, leading to *S*-bacillithiolation [4, 181]. Thereby, GapDH is the most abundant *S*-bacillithiolated protein in *S. aureus* after exposure to HOCl revealed by OxICAT analyses [123]. Using BSH-

specific Western blots, *S*-bacillithiolated GapDH can be used as a hallmark of the bacillithiolation pattern in *S. aureus* after different types of stress, including AGXX®, HOCl and lapachol [123, 164, 177]. Further targets of *S*-bacillithiolations in *S. aureus* after HOCl stress are the aldehyde dehydrogenase AldA, the Mn-dependent pyrophosphatase PpaC, the ribosomal protein RpmJ and inosine-5'-monophosphate dehydrogenase GuaB [123, 124]. These results reveal that *S*-bacillithiolations play a major role in protection and redox-regulation of metabolism under oxidative stress in Firmicutes.

In conclusion, BSH has many different functions in Firmicutes, including detoxification of ROS, HOCl, antibiotics, toxic metals, alkylating agents and electrophiles **(Fig. 12)**. Furthermore, it is involved in maintenance of the redox and metal homeostasis in BSH-producing bacteria. In *S. aureus*, BSH plays an important role in survival under infection conditions. The most important activity of BSH is the ability to react with proteins, resulting in reversible *S*-bacillithiolations under oxidative stress. Thus, BSH can protect enzymes against overoxidation and functions in redox-regulation. However, *S*-bacillithiolated proteins loss their enzymatic activity. Therefore, a specific redox pathway is required to reduce *S*-bacillithiolated proteins and to restore their function. For that, Firmicutes possess the BSH redox pathway, including bacilliredoxins (BrxA, BrxB) and the BSSB reductase YpdA (see sections 3.2.3, 3.2.4 and **chapter 3** for more details).

3.2.3 Regeneration of *S*-bacillithiolated proteins by bacilliredoxins

Under oxidative stress, proteins can be protected against overoxidation by *S*-thiolations, which are reversible thiol switch mechanisms [4, 181]. *S*-glutathiolated, *S*-mycothiolated or *S*-bacillithiolated proteins can be reduced by specific redox systems because enzymes lose their activity by *S*-thiolations [181]. In general, these redox systems are composed of a so-called redoxin and a NADPH-dependent thiol disulfide reductase [117]. Redoxins are small enzymes with a redox-active disulfide site, which can specifically reduce *S*-thiolated proteins [117]. For reduction of *S*-glutathiolations, eukaryotes and Gram-negative bacteria have glutaredoxins (Grx), which were first described in *E. coli* [114, 115]. Grx are distinguished in regard to the structure of their active site in dithiol Grx (CPTC motif) and later discovered monothiol Grx (CGPS motif) [160]. Three dithiol Grx (Grx1, Grx2, Grx3) and one monothiol Grx (Grx4) were identified in *E. coli* [160]. During reduction of *S*-glutathiolated proteins, Grx is glutathiolated (Grx-SSG). A further molecule of GSH can diminish the Grx-SSG, leading to glutathione disulfide (GSSG) formation. The NADPH-dependent GSSG reductase (Gor) regenerates reduced GSH **(Fig. 13)** [3, 181]. Both Grx and Gor are important to protect eukaryotes and bacteria against oxidative stress and metal stress [28, 93, 183, 208, 246, 265].

Similarly, the reduction of *S*-mycothiolated proteins requires the MSH redox pathway, including mycoredoxins (Mrx) and the mycothiol disulfide (MSSM) reductase (Mtr) in Actinomycetes. Briefly, the mycothiol of *S*-mycothiolated proteins is transferred to Mrx, resulting in Mrx-SSM formation that is reduced by MSH, yielding MSSM, which is recycled back to MSH by Mtr under NADPH consumption **(Fig. 13)** [181]. The Mrx1 of Mycobacteria has a CGYC motif [310]. Mrx1 and Mtr are involved to confer resistance against metals, antibiotics and oxidative stress in Actinomycetes [225, 279, 310]. In addition, the thioredoxin system can also function in de-mycothiolation of a protein in absence of the Mrx1/MSH/Mtr redox pathway [111].

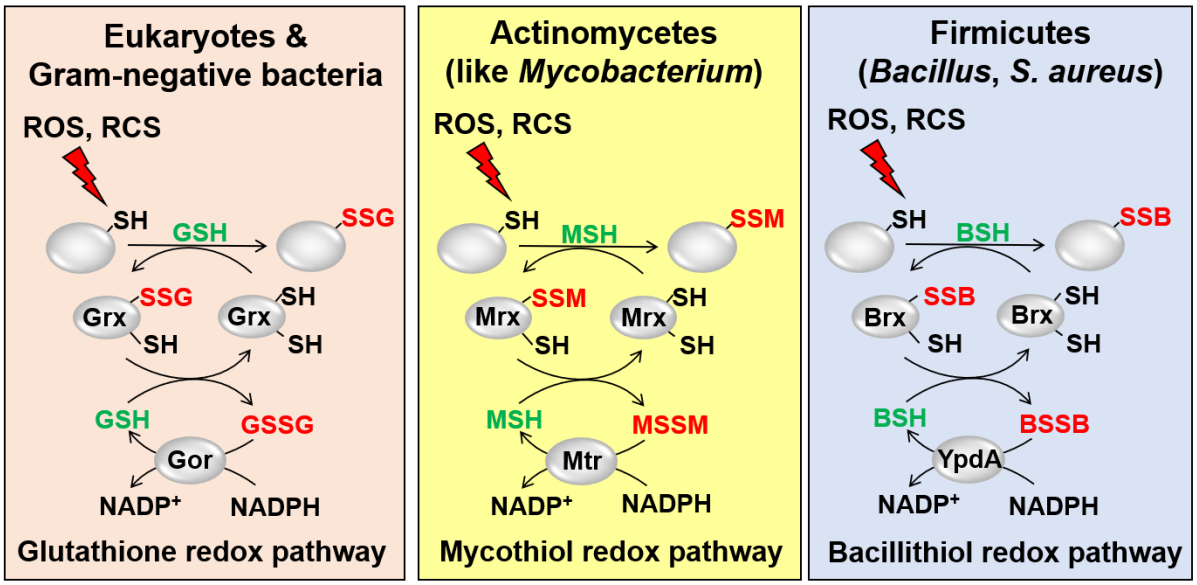

Fig. 13: Redox pathways are required to reduce *S*-thiolated proteins and to regenerate reduced LMW thiols after oxidative stress. Eukaryotes and Gram-negative bacteria use the GSH redox pathway, Actinomycetes possess the MSH redox pathway and BSH-producing Firmicutes have the BSH redox pathway. Under ROS or RCS stress, LMW thiols (GSH, MSH, BSH) can protect proteins against overoxidation, leading to mixed protein disulfides termed as *S*-thiolations (*S*-glutathiolations (-SSG), *S*-mycothiolations (-SSM), *S*-bacillithiolations (-SSB)). Redoxins (Grx, Mrx, Brx) can reduce *S*-thiolated proteins, whereby the LMW thiol is transferred to the redoxin, resulting in Grx-SSG, Mrx-SSM or Brx-SSB. A second molecule of the respective LMW thiol diminishes the *S*-thiolated redoxin, leading to thiol disulfide formation (GSSG, MSSM, BSSB). Finally, a NADPH-dependent thiol disulfide reductase (Gor, Mtr, YpdA) recycles the reduced LMW thiol (GSH, MSH, BSH). This figure is adapted from reference [181].

In BSH-producing bacteria, like *Bacillus* spec. and *S. aureus*, the BSH redox pathway functions in de-bacillithiolation of *S*-bacillithiolated proteins **(Fig. 13)**. Using a genomic profiling analysis, Gaballa *et al*. identified four genes with putative thioredoxin and thioredoxin reductase activity, which co-occurred with the BSH biosynthesis genes in *B. subtilis* [83]. These include the two di-thiol thioredoxin-like proteins YphP and YqiW, the monothiol thioredoxin-like protein YtxJ and a thioredoxin reductase-like protein YpdA [83]. YphP and YqiW are paralogs with 53% identity and belong to the DUF1094 protein family [53, 83]. Both paralogs possess an unusual CGC motif at the active site [53, 83]. A structural analysis of YphP suggests that it functions as a disulfide isomerase [53]. In contrast, YtxJ is a member of

the thioredoxin family, has its active site cysteine within the TCPIS motif and was suggested to function as a monothiol Grx-like protein [83]. In addition, it was assumed that YphP, YqiW and YtxJ act analogous to Grx and Mrx. Therefore, these proteins were renamed as bacilliredoxins BrxA (YphP), BrxB (YqiW) and BrxC (YtxJ), respectively [82, 83]. While the exact enzymatic function in de-bacillithiolation of BrxC remains unclear, the roles of BrxA and BrxB have been characterized in *B. subtilis* and *S. aureus* [82, 123, 165]. Both BrxA and BrxB can reduce *S*-bacillithiolated MetE and OhrR, leading to *S*-bacillithiolation of Brx in *B. subitilis* (Brx-SSB) [82]. Thereby, the presence of the amino-terminal cysteine is essential for the function of Brx [82]. Brx attacks the *S*-bacillithiolation of proteins by its amino-terminal cysteine of the active site, by which the BSH is transferred to the amino-terminal cysteine **(Fig. 14)** [82].

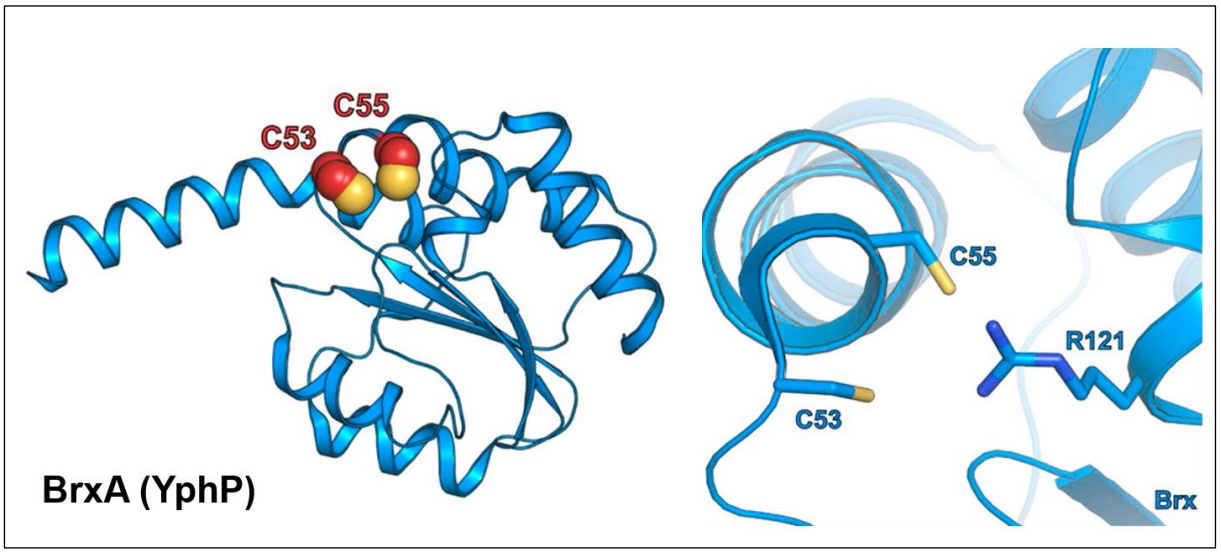

Fig. 14: Structure of bacilliredoxin A (BrxA, formerly YphP) of *B. subtilis*. BrxA has an unusual CGC motif with the amino-terminal active cysteine at position 53 (C53) and the resolving cysteine at position 55 (C55). The figure is from reference [125].

Afterwards, Brx-SSB can be reduced by the resolving cysteine of Brx and a second molecule of BSH, resulting in bacillithiol disulfide (BSSB) formation **(Fig. 13)** [31, 125]. For a long time, it was postulated that the thioredoxin reductase-like protein YpdA might function as a BSSB reductase, but the experimental evidence was missing. Recently, the evidence for the enzymatic function of YpdA as a BSSB reductase *in vitro* and in *S. aureus in vivo* could be provided (see section 3.2.4 and **chapter 3** for more details) **(Fig. 13)** [165, 199].

In *S. aureus*, BrxA and BrxB homolog proteins were identified with 54% and 68% sequence identity, respectively, to the BrxA and BrxB of *B. subtilis* [179]. The staphylococcal BrxA can reduce *S*-bacillithiolated GapDH after oxidative stress *in vitro* [123]. Therefore, the glycolytic activity of GapDH could be restored to around 70%. This is strongly dependent on the presence of the amino-terminal cysteine at position 54, because the BrxAC54A mutant protein was only able to restore the activity of GapDH to 25% [123].

In the present PhD thesis, a major part was the characterization of the physiological role of BrxA and BrxB in *S. aureus* COL under oxidative stress and infection conditions **(chapter 3)** [165]. Northern blot analyses showed that *brxA* and *brxB* expression is enhanced after thiol-specific stress, such as HOCl or diamide [165]. Furthermore, I prepared samples for HPLC metabolomics and performed Brx-roGFP2 biosensor measurements. I could show that the deletions of BrxA and BrxB do not affect the BSH/BSSB redox ratio and that the two Brx do not contribute to the regeneration of the BSH redox potential (E_{BSH}) after HOCl stress [165]. In addition, Quach Ngoc Tung confirmed that BrxA is sufficient to reduce *S*-bacillithiolated GapDH *in vitro* using biochemical NADPH consumption assays and BSH-specific Western blots [165].

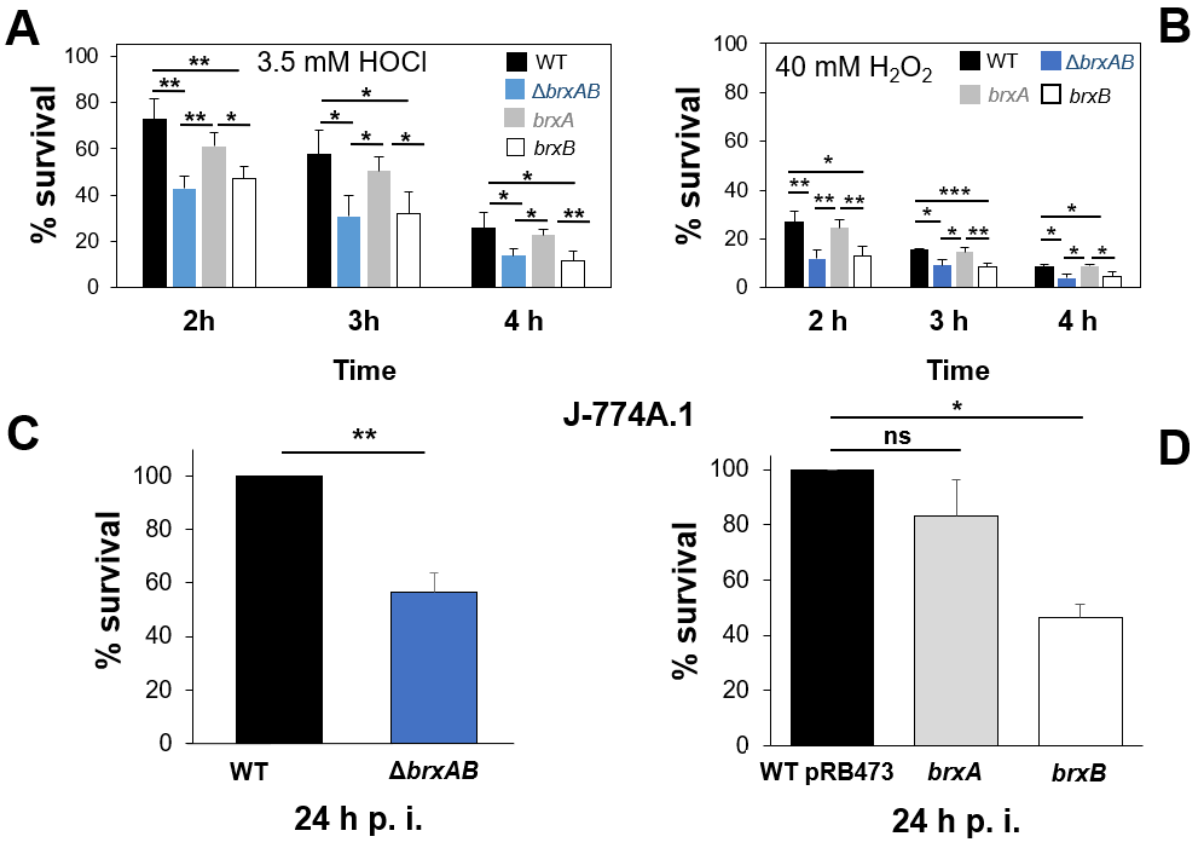

Fig. 15: BrxA is important for survival under oxidative stress and infection conditions. (A, B) After lethal HOCl and H_2O_2 stress, the Δ*brxAB* double mutant showed significantly decreased survival rates compared to the wild type (WT). These phenotypes could be restored by complementation with *brxA*, but not with *brxB*. **(C, D)** The Δ*brxAB* mutant is more sensitive in survival than the WT under murine macrophages (J-774A.1) infections. While the *brxA* complemented strain could restore this phenotype back to 80% of the WT level, the *brxB* complemented strain was unable to restore the phenotype. The growth and survival assays were performed together with Verena N. Fritsch. The macrophage infection assays were done together with Vu Van Loi. The figures are from the publication of chapter 3 [165].

In phenotype analyses, I showed together with Verena N. Fritsch that the Δ*brxAB* double mutant was more sensitive to HOCl stress in growth and survival compared to the parental wild-type strain (WT) **(Fig. 15A)**. Furthermore, the survival rate of the Δ*brxAB* mutant was significantly decreased after lethal H_2O_2 stress compared to the WT **(Fig. 15B)**. In addition,

Vu Van Loi and I revealed that the Δ*brxAB* mutant was attenuated in survival under macrophage infections **(chapter 3) (Fig. 15C)** [165]. All these sensitive phenotypes of the Δ*brxAB* double mutant could be restored back to the WT level by complementation with *brxA*, but not with *brxB* **(Fig. 15A, B, D)**. These results indicate that BrxA might has a more important role to confer resistance of *S. aureus* under oxidative stress and infection conditions than BrxB [165].

Recently, it has been revealed that BrxA and BrxB are involved in de-thioallylation of proteins after allicin stress in *S. aureus* [180]. Therefore, Brx can reduce *S*-thioallylated proteins, leading to *S*-thioallylation of Brx and regeneration of the enzymatic activity of the previous *S*-thioallylated protein [180]. Phenotype analyses showed that the decreased growth after allicin stress of the Δ*brxAB* mutant could be complemented by *brxA* and *brxB*, respectively [180]. Moreover, in biochemical de-thioallylation assays, BrxA was just able to restore the glycolytic activity of GapDH to around 25% [180]. Potentially, BrxB can regenerate the GapDH activity after *S*-thioallylation stronger than BrxA, however, the experimental evidence is missing yet.

In conclusion, BrxA and BrxB are thioredoxin-like proteins, which are required to reduce *S*-bacillithiolated and *S*-thioallylated proteins, leading to Brx-SSB or *S*-thioallylation of Brx. Thereby, they can partially restore the enzymatic activity of a previous *S*-bacillithiolated protein, by which they contribute to improve the bacterial fitness under oxidative stress and infection conditions.

3.2.4 The role of YpdA as BSSB reductase in fitness and virulence of *S. aureus*

To protect the proteins against overoxidation and to rescue their function, the LMW thiol BSH can react with proteins, leading to *S*-bacillithiolations. These bacillithiolations can be reduced by Brx, resulting in Brx-SSB, which is diminished by BSH, yielding BSSB [31]. In Gram-negative bacteria and Actinomycetes, Gor and Mtr can convert GSSG or MSSM back to the reduced LMW thiol GSH or MSH, respectively. However, in Firmicutes, the experimental evidence for the activity of an enzyme, which can function as a BSSB reductase remained to be elucidated [181]. Since 2010, it was postulated that the NADPH-dependent pyridine nucleotide disulfide oxidoreductase YpdA acts as a BSSB reductase, because genomic profiling analyses revealed that YpdA co-occurs with the genes of the BSH biosynthesis [83]. YpdA is a member of the FAD/NAD(P)-binding domain superfamily (IPR036188) [83].

As a major part of this doctoral thesis, the function and physiological role of YpdA in *S. aureus* COL under oxidative stress and infection conditions were analysed **(chapter 3)** [165]. Simultaneously, the group of Ambrose Cheung characterized this enzyme [199]. Previously, it has been shown that *ypdA* is enhanced transcribed after HOCl, MHQ, allicin,

AGXX®, NO• or diamide stress in *S. aureus* in RNA-seq analyses [80, 113, 177, 178, 180, 244], indicating that YpdA might be involved in the oxidative stress response. The transcript of *ypdA* is monocistronic [165, 199]. Northern blot analyses were used to investigate the transcription levels of *ypdA* after different oxidative and electrophilic stress, including diamide, H_2O_2, HOCl, formaldehyde, methylglyoxal and MHQ. Disulfide stress, like diamide or HOCl, induced an increased transcription of *ypdA* [165]. In addition, the Cheung lab could also demonstrate that YpdA expression is enhanced by oxidative, nitrosative and electrophilic stress as revealed by YpdA-specific Western blot [199]. Interestingly, a transcriptional induction after 10 mM H_2O_2 stress in RPMI was not detected in our study [165], however, the other study showed an enhanced expression of YpdA after 20 mM H_2O_2 in TSB medium [199]. Maybe, the 10 mM H_2O_2 stress was not sufficient to induce an enhanced *ypdA* transcription.

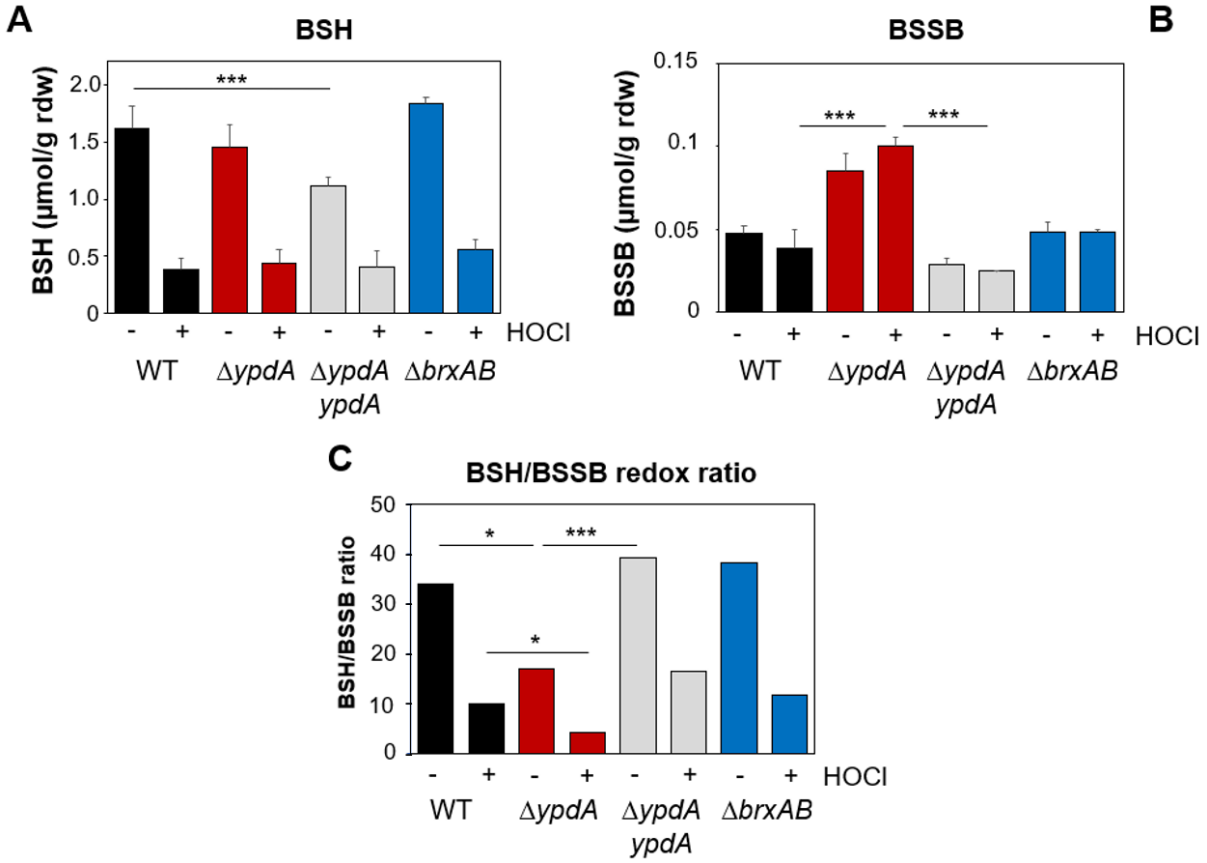

Fig. 16: The *S. aureus* Δ*ypdA* mutant shows significantly higher BSSB levels and a decreased BSH/BSSB redox ratio before and after HOCl stress. (A, B) The *S. aureus* COL wild type (WT) and the Δ*ypdA* as well as Δ*brxAB* mutants exhibit approximately the same BSH levels under non-stress conditions. HOCl causes a strong depletion of the reduced BSH pool, but no increased BSSB levels. Importantly, the Δ*ypdA* mutant has the largest BSSB levels before and after stress compared to the WT, Δ*brxAB* mutant and the *ypdA* complemented strain. **(C)** The BSH/BSSB redox ratio is significantly decreased in the Δ*ypdA* mutant. These findings revealed that YpdA is crucial to reduce BSSB and to maintain the redox homeostasis. The HPLC measurements of the metabolomics were done by Markus Wirtz and Rüdiger Hell. The figures are modified from the publication of chapter 3 [165].

Next, the function of YpdA in *S. aureus in vivo* was investigated. Therefore, I prepared together with Quach Ngoc Tung the samples to quantify the intracellular thiols and disulfides

before and after stress using HPLC metabolomics **(Fig. 16)** [165]. Thereby, around 1.5 to 1.8 µmol BSH/g rdw in the WT and the Δ*ypdA* mutant were detected. After HOCl stress, there is a strong 5-fold depletion of the reduced BSH pool **(Fig. 16A)** [165]. However, an increased BSSB level after HOCl stress compared to the control condition was not observed, suggesting that BSH is used for *S*-bacillithiolations of proteins. Importantly, the Δ*ypdA* mutant has significantly higher BSSB levels before and after HOCl stress than the WT. That phenotype could be restored by the *ypdA* complemented strain **(Fig. 16B) (chapter 3)** [165]. Thus, the Δ*ypdA* mutant shows a strong decreased BSH/BSSB redox ratio compared to the WT and the complemented strain **(Fig. 16C)** [165].

Mikheyeva *et al*. were also able to demonstrate that the Δ*ypdA* mutant exhibits significantly higher BSSB levels and a decreased BSH/BSSB redox ratio compared to the WT and the *ypdA* complemented strain after 20 mM H_2O_2 stress [199]. In addition, they revealed that a YpdA overexpression strain has a lower amount of BSSB and a higher redox ratio than the WT [199]. However, there was just a 2-fold depletion of the reduced BSH levels after H_2O_2 stress in comparison to the control condition [199], indicating that H_2O_2 provokes less *S*-bacillithiolations than HOCl. It is known that HOCl reacts several magnitudes faster with cysteinyl residues of proteins than H_2O_2 [230, 324]. Furthermore, I detected higher redox ratios than the other study [165, 199]. This might be caused by using different cultivation conditions and distinct *S. aureus* strains. While our study used the HA-MRSA strain *S. aureus* COL [165], Mikheyeva *et al*. performed their experiments with a *bshC*-repaired *S. aureus* SH1000 strain [199], which is naturally BSH-negative because of a mutation in the *bshC* gene [212, 245].

In addition, I also showed that YpdA is specific for the reduction of BSSB but does not affect the amount of cystine. The Δ*ypdA* mutant exhibited nearly the same cystine levels before and after HOCl stress in comparison to the WT [165]. Nevertheless, both studies could clearly show that YpdA is crucial for regeneration of the reduced BSH pool by reduction of BSSB levels and is important to maintain the redox homeostasis.

Additionally, I applied the genetically encoded Brx- and Tpx-roGFP2 biosensors to monitor changes in the BSH redox potential (E_{BSH}) and in the intra-bacterial H_2O_2 levels after oxidative stress **(chapter 3)** [165]. The deletion of *ypdA* did not change the E_{BSH} during the growth in LB medium **(Fig. 17A)**. However, the Δ*ypdA* mutant was strongly impaired in regeneration of its reduced E_{BSH} after HOCl and H_2O_2 stress compared to the WT **(Fig. 17B, C)** [165]. Furthermore, the intracellular H_2O_2 levels could not be reduced in the Δ*ypdA* mutant after 100 mM H_2O_2 stress as revealed by Tpx-roGFP2 measurements. In contrast, the WT was able to diminish its intra-bacterial amounts of H_2O_2 after stress induction **(Fig. 17D)** [165]. These findings demonstrated that YpdA plays a major role in regeneration of the reduced E_{BSH} after oxidative stress and affects the reduction of intracellular H_2O_2 levels in *S. aureus*.

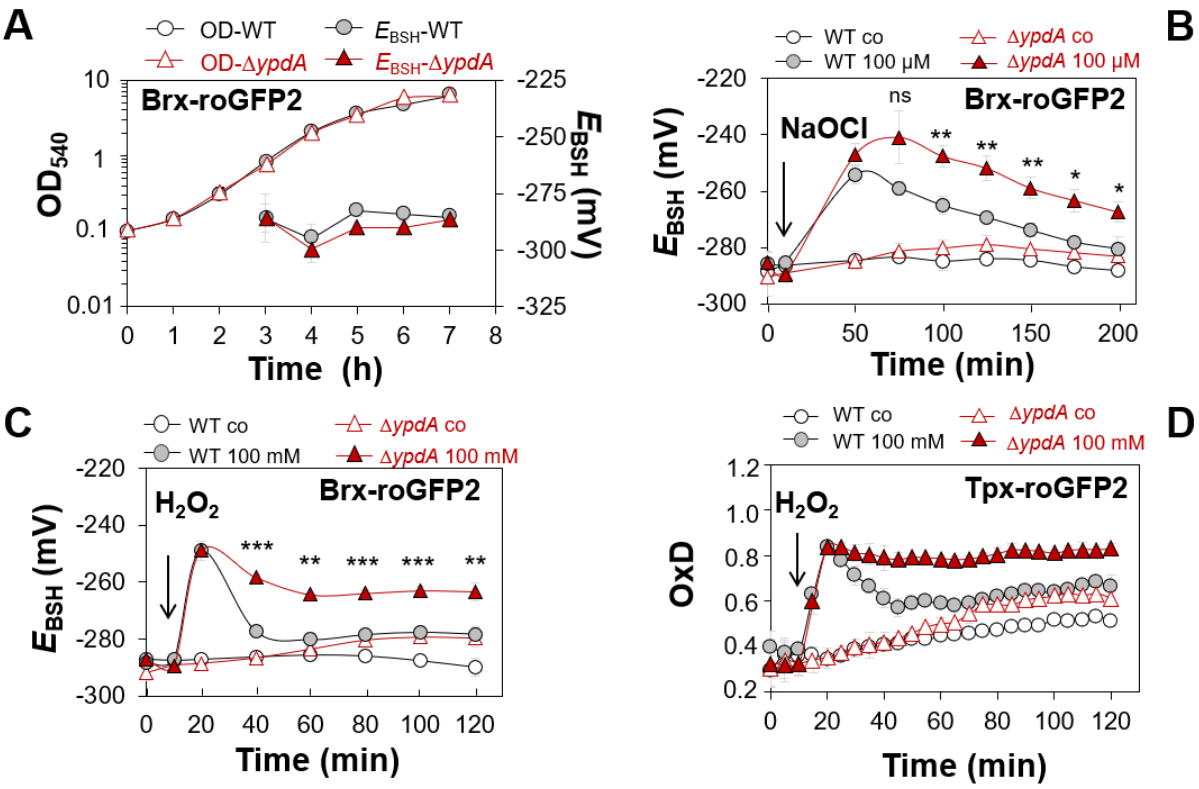

Fig. 17: YpdA is important to regenerate the reduced BSH redox potential (E_{BSH}) and affects the detoxification of H_2O_2 in *S. aureus*. (A) The deletion of *ypdA* influences not the E_{BSH} among the growth in LB medium. **(B, C)** While the *S. aureus* COL wild type (WT) is able to regenerate the E_{BSH} after exposure to HOCl and H_2O_2 stress, the Δ*ypdA* mutant is attenuated to restore its reduced E_{BSH}, indicating that YpdA is important to regenerate the reduced E_{BSH} after oxidative stress. **(D)** Tpx-roGFP2 biosensor measurements revealed that the Δ*ypdA* mutant exhibits significantly higher intracellular H_2O_2 levels than the WT after 100 mM H_2O_2 stress. This result suggests that YpdA affects the detoxification of H_2O_2 in *S. aureus*. The figures are from the accepted publication of chapter 3 [165].

Furthermore, our study and Mikheyeva *et al*. were interested to characterize the enzymatic activity of YpdA. First, both studies could show that YpdA contains the flavin adenine dinucleotide (FAD) cofactor, because the purified YpdA protein extract has a characteristic yellow colour and the UV-visible absorption spectrum exhibits the typically absorbance maxima at 375 and 450 nm [165, 199]. Using biochemically NADPH coupled assays, both studies demonstrated that YpdA consumes NADPH as a cofactor [165, 199]. In addition, YpdA can also utilize NADH as a cofactor [199]. The use of NADPH is dependent on the Rossman fold domain (in YpdA: $\underline{G}_{10}\underline{GG}PC_{14}\underline{G}$), because the YpdAG10A mutant protein did not utilize the cofactors NADPH or NADH [199], however, a YpdAC14A mutant protein can still use NADPH as a cofactor [165]. Moreover, one aim of this study was to show that YpdA can use BSSB as a substrate, because the experimental evidence was still missing. Therefore, Quach Ngoc Tung added different thiol disulfides (GSSG, $CoAS_2$, BSSB) as possible substrates for YpdA and measured the NADPH consumption as a change in the absorbance at 340 nm [165]. While no increase of the NADPH consumption after addition of GSSG or $CoAS_2$ was observed, an enhanced NADPH consumption in the presence of BSSB was detected **(Fig. 18A)** [165].

However, the YpdAC14A mutant protein could not use BSSB as a substrate because no increase of the NADPH consumption was detectable [165]. These findings indicate that YpdA uses NAD(P)H and FAD as cofactors and BSSB as its substrate, which is dependent on the conserved cysteine at position 14 **(Fig. 18B)** [165]. Previously, it has been shown that the Cys14 of YpdA is oxidized during NaOCl stress in the *S. aureus* proteome as revealed by OxICAT analyses, supporting the function of Cys14 as active site of YpdA [123]. In future studies, the exact reaction mechanism of BSSB reduction by YpdA remains to be elucidated. In conclusion, this study provide the evidence that YpdA functions as the BSSB reductase under NADPH consumption *in vitro*. In *S. aureus*, YpdA is essential to recycle BSSB back to reduced BSH, to regenerate the E_{BSH} after oxidative stress and to maintain the redox homeostasis *in vivo*.

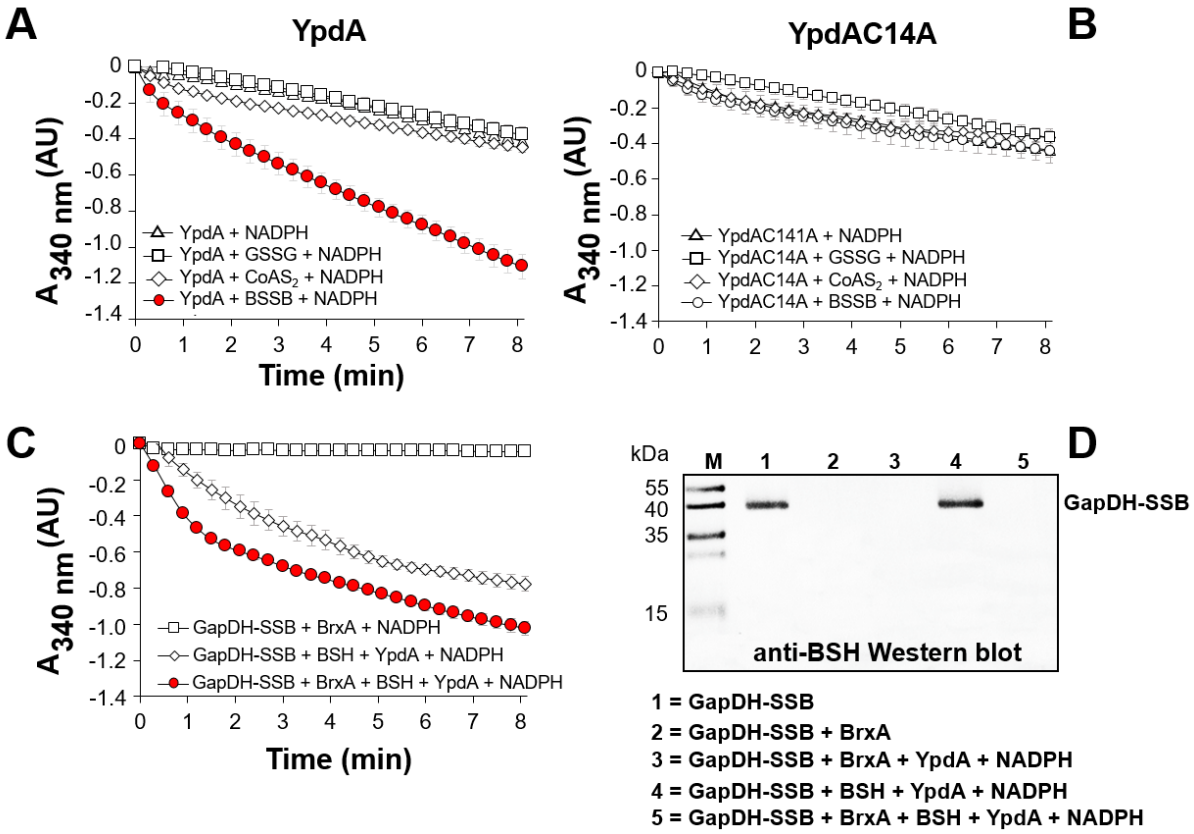

Fig. 18: YpdA functions as a BSSB reductase *in vitro* and acts together with BrxA and BSH in the BrxA/BSH/YpdA redox pathway. (A) Measurements in changes of the absorbance at 340 nm in biochemical NADPH-coupled assays revealed that purified YpdA consumes NADPH. While an increased NADPH consumption is detectable in presence of BSSB, no enhanced NADPH consumption is observed in presence of GSSG or $CoAS_2$. **(B)** The YpdAC14A mutant protein is still able to consume NADPH alone. However, it is impaired to utilize BSSB, indicating that C14 is crucial for the activity of YpdA in BSSB reduction. **(C)** The fastest NADPH consumption was measured during de-bacillithiolation of GapDH-SSB in presence of the complete BrxA/BSH/YpdA redox pathway. **(D)** As shown by anti-BSH Western blot analysis, BrxA is required for reduction of *S*-bacillithiolated GapDH. While BrxA is sufficient to diminish GapDH-SSB, YpdA and BSH alone cannot de-bacillithiolate GapDH. These experiments were performed by Quach Ngoc Tung. The figures are from the paper of chapter 3 [165].

Furthermore, Quach Ngoc Tung showed that YpdA interacts together with BSH and BrxA in the BrxA/BSH/YpdA redox pathway **(Fig. 18C, D)** [165]. As revealed by biochemical NADPH-coupled assays and BSH-specific Western blots, BrxA is required to reduce GapDH-SSB, yielding BrxA-SSB **(Fig. 18C, D)**. Afterwards, BSH reduces BrxA-SSB to form BSSB. The latter is used by YpdA to regenerate BSH **(Fig. 18C)** [165].

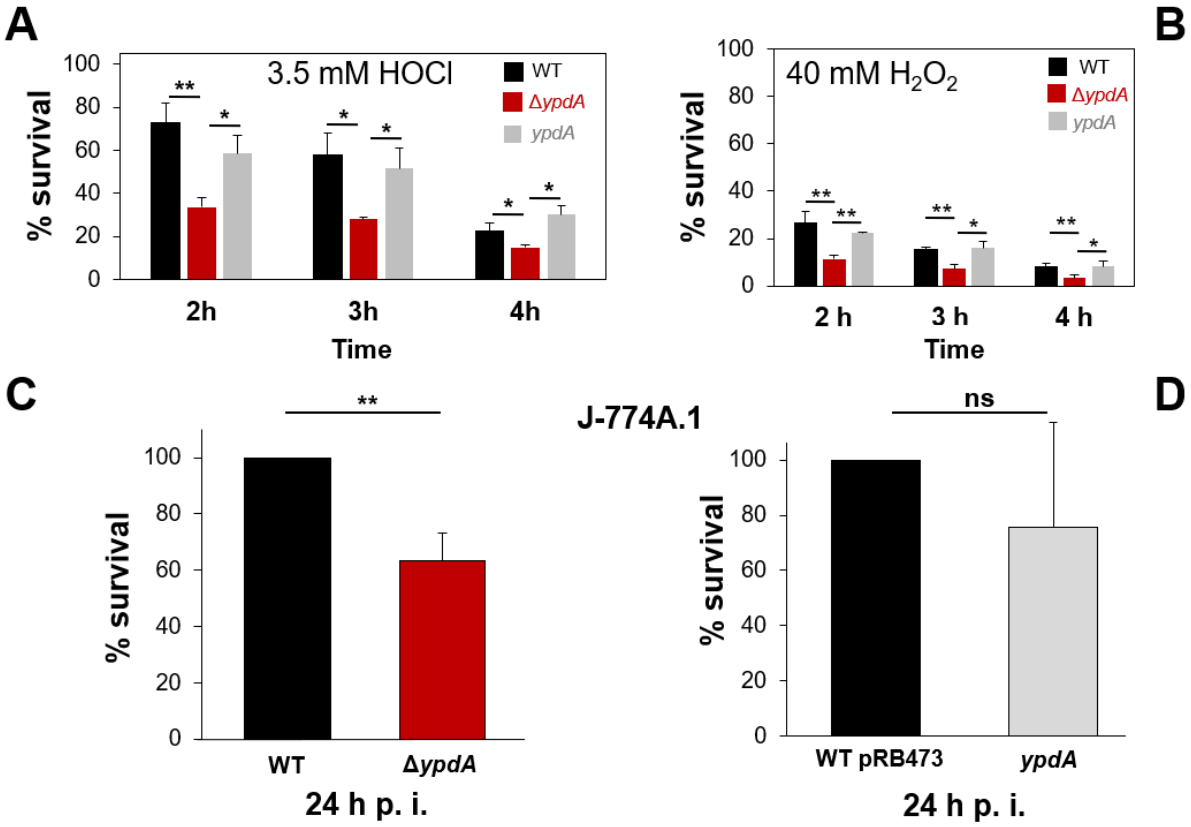

Fig. 19: YpdA has a crucial role in survival under oxidative stress conditions and in virulence of *S. aureus*. (A, B) The Δ*ypdA* mutant was significantly more attenuated in survival after lethal HOCl and H_2O_2 stress compared to the WT and the *ypdA* complemented strain. **(C, D)** Under murine macrophage (J-774A.1) infections, the Δ*ypdA* mutant showed a decreased survival rate than the WT. The *ypdA* complemented strain was able to restore this phenotype back to around 80% of the WT level. The growth and survival assays were performed together with Verena N. Fritsch. The macrophage infection assays were done together with Vu Van Loi. The figures are from the publication of chapter 3 [165].

Next, the physiological role of YpdA in *S. aureus* under oxidative stress and infection conditions was analysed. I performed together with Verena N. Fritsch growth and survival assays. These analyses showed that the Δ*ypdA* mutant was significantly more sensitive to HOCl stress than the WT **(chapter 3) (Fig. 19A)** [165]. Moreover, a lethal concentration of 40 mM H_2O_2 provoked a stronger decrease in survival of the Δ*ypdA* mutant compared to the WT **(Fig. 19B)**. These phenotypes could be restored back to the WT level by complementation with *ypdA* **(Fig. 19A; B)** [165]. Moreover, the Δ*brxAB* Δ*ypdA* triple mutant strain has no additive effect on the phenotypes, but it exhibits nearly the same phenotypes as the Δ*brxAB* double or the Δ*ypdA* single mutant after lethal H_2O_2 and HOCl stress. In addition, the triple mutant strain

is also attenuated in regeneration of its reduced E_{BSH} after exposure to HOCl [165]. These results revealed again that YpdA is a part of the BrxA/BSH/YpdA redox pathway in *S. aureus*.

In addition, Mikheyeva *et al*. demonstrated that overexpression of YpdA could improve the bacterial fitness after HOCl, H_2O_2, diamide and methylglyoxal stress [199]. Furthermore, Vu Van Loi and I determined the survival rates of the *S. aureus* COL WT, the Δ*ypdA* mutant and the *ypdA* complemented strains after 24 h under murine macrophage infections **(Fig. 19C)** [165]. Thereby, the survival of the Δ*ypdA* mutant was significantly decreased compared to the WT. The *ypdA* complemented strain could restore this phenotype to around 80% of the WT level **(Fig. 19D)** [165]. Additionally, the Δ*ypdA* mutant had a lower survival rate in human whole blood as well as in human neutrophils [199]. In contrast, the YpdA overexpression strain exhibits increased survival rates in whole blood and in neutrophils compared to the WT [199]. Taken together, these phenotype analyses underline that YpdA improves the survival under infection conditions and thus, it contributes to the virulence of *S. aureus*.

Apart from the reduction of BSSB, YpdA can also use *S*-allylmercaptobacillithiol (BSSA) as a substrate [180]. Allicin causes *S*-thioallylation of proteins, which can be reduced by BrxA, resulting in BrxA-SSA formation. Similar to *S*-bacillithiolations, BSH can diminish BrxA-SSA, leading to BSSA generation. Finally, YpdA converts, dependent on the cysteine at position 14, BSSA to BSH and allyl thiol [180]. In addition, the Δ*ypdA* mutant was more sensitive to allicin stress than the WT. This phenotype could be restored by complementation with *ypdA* [180].

In conclusion, our study and Mikheyeva *et al*. could provide the experimental evidence that YpdA functions as a BSSB reductase *in vitro* and *in vivo* [165, 199]. In *S. aureus*, YpdA plays an important role in maintenance of the reduced E_{BSH} and the redox homeostasis after oxidative stress and improves the survival under oxidative stress and infection conditions.

3.3 Coenzyme A (CoA) as an alternative LMW thiol in bacteria

A lot of metabolic enzymes require cofactors for their enzymatic activity. It was estimated that around 4% of all cellular enzymes use coenzyme A (CoASH) as a cofactor [154]. This cofactor was discovered in the 1940s by Fritz Lipmann and colleagues and was named coenzyme A due to its ability to function as a heat-stable enzymatic cofactor for acetylations [166-169]. CoASH occurs ubiquitously in all living organisms and is an essential cofactor [92].

In general, CoASH consists of a nucleotide (3'-phosphorylated ADP), vitamin B5 (pantothenic acid) and an amino acid (cysteine) [10, 13]. The biosynthesis pathway includes several steps [13], whereby the pantothenate kinase (CoaA) is involved in the regulation of the CoASH biosynthesis. Purified CoaA of rat kidney cells was inhibited by CoASH feedback regulation *in vitro* [139]. In *E. coli*, it has been shown that CoaA is the primary step of CoASH biosynthesis regulation by feedback inhibition [131, 260]. In contrast, CoaA is insensitive

against feedback inhibition by CoASH in *S. aureus* and *Bacillus anthracis*, which could explain that some bacteria can produce significant higher CoASH levels than other bacteria [157, 217]. In the human pathogens *B. anthracis*, *S. aureus* or *Borellia burgdorferi*, CoASH levels in a millimolar range were determined [22, 209, 217, 244]. *S. aureus* COL has approximately 0.89 ± 0.5 µmol CoASH per g dry weight [244].

The combination of a thiol group and a nucleotide ensures that CoASH functions in a wide range of metabolic pathways and redox regulation **(Fig. 20)** [13, 92]. In metabolism, it acts as an acyl carrier and can activate carbonyl molecules [13, 92]. Furthermore, CoASH can be linked to several carboxylic acids, which generates many metabolically active thioester derivatives, such as acetyl CoA, malonyl CoA or 3-hydroxy-3-methylglutaryl CoA (HMG-CoA) [92, 294]. These thioesters are involved in many biochemical reactions of central metabolic pathways, including the citric acid cycle, fatty acid and amino acid metabolism or peptidoglycan biosynthesis [92, 294]. Furthermore, acetyl-CoA is the most abundant CoASH derivative (79.8%) in exponentially growing *E. coli* cells, whereas only 13.8% of the CoA pool exist as free CoASH [132].

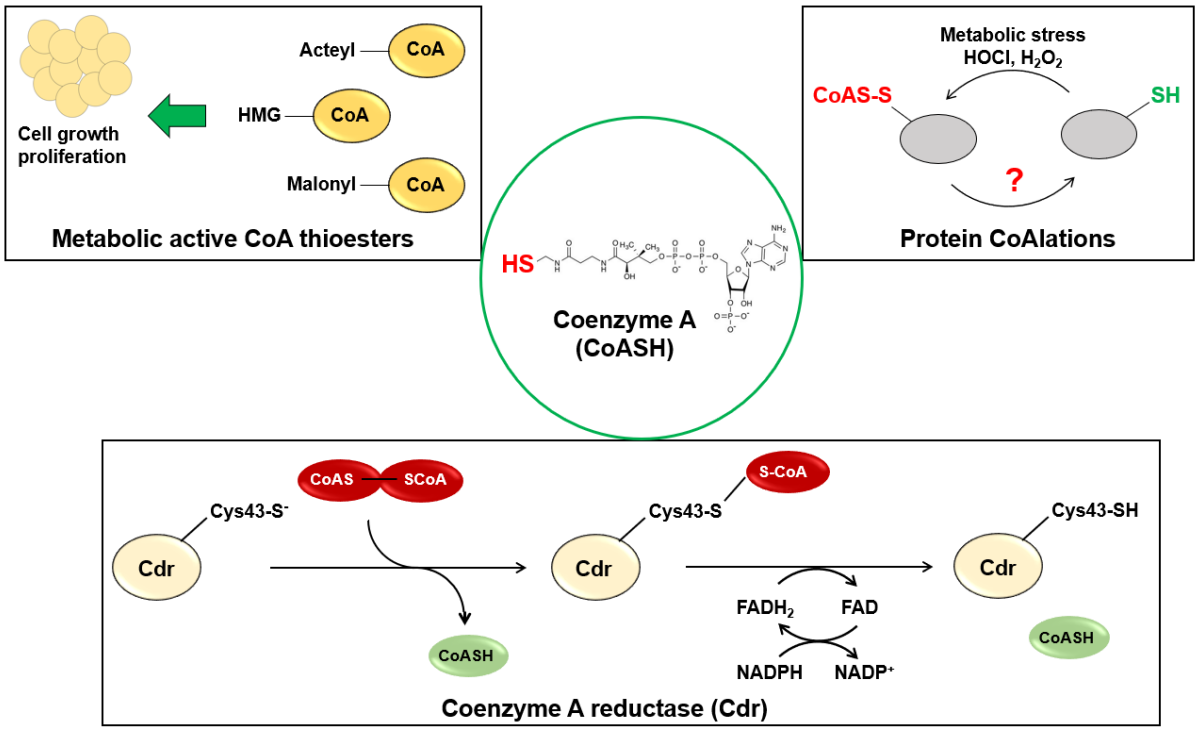

Fig. 20: Cellular functions of Coenzyme A (CoASH) and its derivatives and the catalytic mechanism of the coenzyme A disulfide reductase Cdr. Metabolic active CoA thioester derivatives activate many carbonyl molecules and act as cofactors in metabolic pathways such as citric acid pathway. Under metabolic stress and oxidative stress conditions, CoASH functions as a LMW thiol and can protect proteins against overoxidation, leading to protein CoAlations (R-SCoA). It remains to be elucidated, how CoAlations can be reduced *in vivo*. Cdr is a NADPH-dependent flavin oxidoreductase, which can recycle CoASH by reduction of coenzyme A disulfide (CoAS-SCoA, $CoAS_2$). Firstly, the catalytic cysteine at position 43 attacks $CoAS_2$, resulting in the release of one CoASH molecule and CoAlation of Cdr. $FADH_2$ and NADPH regenerate Cdr and a second molecule of CoASH is released. This figure is adapted from references [92, 309].

In redox regulation, CoASH functions as a LMW thiol in human pathogenic bacteria and in the anaerobic archaeon *Pyrococcus horikoshii* [22, 103, 209, 217]. For a long time, it was less known about the physiological role of CoASH in redox regulation. In *B. subtilis*, it can form protein mixed disulfides with OhrR under peroxide stress, leading to the detachment of the repressor from the DNA and protection against overoxidation [156]. However, the CoAlated OhrR was less abundant than the *S*-bacillithiolated OhrR [156]. Just in 2017, Tsuchiya *et al.* named post-translational modifications of proteins by covalent attachments of CoASH as CoAlations **(Fig. 20)** [298]. Using CoA specific Western blots and mass spectrometry, CoAlations are detectable after oxidative (H_2O_2, HOCl, diamide) and metabolic stress in mammalian tissues and in bacteria [298, 299]. It was identified that over 12% of proteins are CoAlations after diamide stress in *S. aureus*, including key enzymes of metabolic pathways (GapDH, AldA, GuaB), protein synthesis, oxidative stress response and transcriptional regulators (PerR, CtsR) [299]. Similar to *S*-bacillithiolations, CoAlations can prevent irreversible inhibition of the staphylococcal GapDH by H_2O_2 *in vitro*. Thereby, the GapDH activity is 90% decreased and can be fully restored by treatment with DTT [299].

To regenerate CoAlated proteins, thioredoxin might function in reduction of CoAlations. However, the discovery of specific “CoAredoxins” remains to be elucidated [92]. Under oxidative stress CoASH is also oxidized to CoASH disulfide ($CoAS_2$), which can be reduced to CoASH by the coenzyme A disulfide reductase (Cdr) in *S. aureus* [51, 52]. Thereby, it is proposed that Cdr attacks $CoAS_2$ with its catalytic Cys43, leading to the release of one molecule CoASH and mixed enzyme-substrate disulfide formation **(Fig. 20)** [182, 186, 309]. The CoAlated Cdr is reduced by its cofactors $FADH_2$ and NADPH and the second molecule of CoASH is released. The tyrosine at position 361 is predicted to be involved in catalysis of the deprotonation of the catalytic Cys43 [186].

Only a few studies were performed to analyse the function of Cdr in bacteria. *B. burgdorferi* uses CoASH as its major LMW thiol [22]. The Cdr of *B. burgdorferi* was predicted to function in H_2O_2 detoxification, whereby CoASH reacts with H_2O_2, leading to $CoAS_2$ formation. That can be recycled to CoASH by Cdr *in vitro* [22]. However, an *in vivo* analysis revealed that a Δ*cdr* mutant is not affected after H_2O_2 stress [61]. In addition, the *Borrelia* oxidative stress response regulator BosR seems to be involved in regulation of Cdr expression [22]. Eggers *et al*. could demonstrate that a *B. burgdorferi* Δ*cdr* mutant strain is more sensitive to 5 mM *t*-butyl-hydroperoxide compared to the WT and the *cdr* complemented strain [61]. Moreover, the Δ*cdr* mutant was attenuated in growth under aerobic (15% O_2, 6% CO_2) and anaerobic (<1% O_2, 9-13% CO_2) conditions [61]. Under infection conditions, Cdr is important for survival of the spirochetes in fed nymphs of the tick *Ixodes scapularis*, but not in unfed nymphs of ticks [61]. Furthermore, mice were not infected with *B. burgdorferi* by tick nymphs, if the nymphs are colonized with the Δ*cdr* mutant strain [61]. These results indicate that Cdr is

crucial for infection of mammalians by the human pathogen *B. burgdorferi*. In the archaeon *P*. *horikoshii*, a gene, which encodes for Cdr, was discovered and its function in $CoAS_2$ reduction was analysed *in vitro*, but no experiments were done to analyse the function *in vivo* [103]. Although, the structure and function of the staphylococcal Cdr *in vitro* are elucidated [51, 52, 186], the physiological role *in vivo* and the impact of Cdr under metabolic and oxidative stress as well as infection conditions are not yet completely understood. Further studies should aim to elucidate the function of the staphylococcal Cdr *in vivo*. Nevertheless, investigations to develop specific inhibitors against Cdr are already done [309, 314].

4. Development and principles of redox-active biosensors and their applications in the major human pathogen *S. aureus*

Many human pathogenic bacteria, including *S. aureus*, have acquired multiple antibiotic resistances and have evolved strategies to overcome the oxidative burst of macrophages and neutrophils. Thereby, one of the crucial factors for bacteria is to maintain their redox homeostasis. However, conventional redox measurements, like HPLC metabolomics, have some limitations due to the disruption of the living cells [197]. Thus, it is not possible to analyse dynamic changes in the redox homeostasis. In addition, the use of fluorescent dyes to detect LMW thiols or ROS inside cells are error-prone and they do not provide information about the redox state [197]. Therefore, a tool was required, which allows a non-disruptive and ratiometric approach to measure redox changes insight the cells in high spatiotemporal resolution and to investigate the cellular redox state [197]. The group of James Remington developed and characterised redox-sensitive green fluorescent proteins (roGFPs) [56, 102]. The scientists used the *Aequorea victoria* green fluorescent protein (GFP) and engineered two redox-active Cys residues in GFP by replacing serine at position 147 and glutamine at position 204. In addition, the Cys48 and serine 65 were replaced by serine and threonine, respectively, to obtain roGFP2 **(Fig. 21)** [56, 102], which was used for the applied biosensors in this PhD thesis.

The application of roGFP2 probes allows ratiometric measurements [197, 271]. Thereby, the oxidation of roGFP2 leads to a disulfide bond between the Cys147 and Cys204, whereas a reduction dissolves the disulfide bond **(Fig. 21)**. The absence or presence of the disulfide bond results in protonation and conformational changes of the chromophore [197, 271]. The roGFP2 molecule exhibits two excitation maxima at 405 nm and 488 nm, whose fluorescence intensities are dependent on the oxidation state of the disulfide bond. By oxidation, the excitation maximum at 405 nm increases and the excitation maximum at 488 nm decreases. This is exactly vice versa under reduced conditions **(Fig. 21)** [197, 271]. By using fully oxidized and reduced control samples and the Nernst equation, the degree of oxidation (OxD) of the desired sample can be measured and calculated. Importantly, the protonation of

the roGFP2 chromophore is not affected by a physiological pH range inside cells. Additionally, Trx cannot interact with roGFP2 due to steric hindrance [197, 271]. roGFP2 equilibrates to the predominated thiol/thiol disulfide redox couple of the cell (e.g. 2 GSH/GSSG, 2 MSH/MSSM, 2 BSH/BSSB) [197, 271]. However, the presence of redoxins (Grx, Mrx, Brx) affects this equilibration, because redoxins can catalyse the thiol disulfide exchange reaction between the LMW thiol and roGFP2 [98, 271]. Thus, the redoxins Grx1, Mrx1 and BrxA were fused to roGFP2 via an amino acid linker, which shifts the equilibrium towards the predominated thiol/thiol disulfide redox couple [16, 98, 179]. Such biosensors were applied in several studies, for example in plants, eukaryotic parasites or bacteria [16, 140, 272, 300, 302, 307, 308].

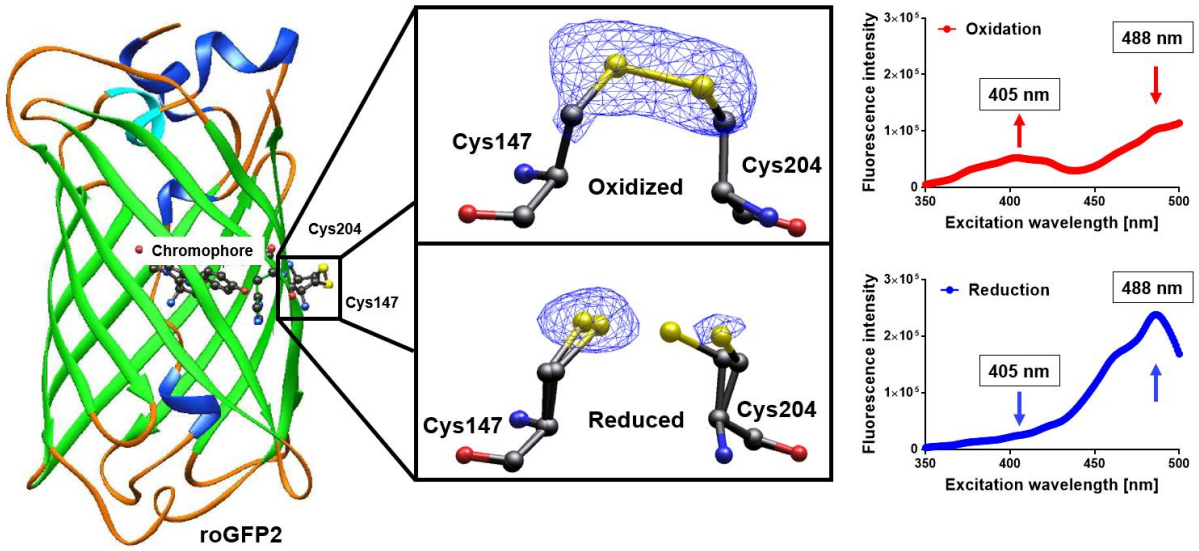

Fig. 21: Principle of ratiometric measurements with redox-sensitive green fluorescent protein 2 (roGFP2). The group of James Remington engineered two redox active cysteines at positions 147(Cys147) and 204 (Cys204) in GFP and replaced Cys48 and serine 65 by serine and threonine, respectively, to obtain roGFP2, which exhibits two excitation maxima at 405 and 488 nm. During oxidation, the two Cys form an intramolecular disulfide bond, leading to a conformational change of the chromophore. Thereby, the excitation maximum at 405 nm increases, whereas the excitation maximum at 488 nm decreases. Under reduced conditions, the two Cys form not a disulfide bond, which causes a decrease of the 405 nm excitation maximum and an increase of the 488 nm excitation maximum. The figures were taken and modified from references [102, 179].

Due to the focus of this work on the human pathogen *S. aureus* COL, which uses BSH as its major LMW thiol, the principle of the Brx-roGFP2 biosensor is explained, which was developed in our working group previously [176, 179]. This genetically encoded biosensor is composed of the staphylococcal BrxA and roGFP2, which are linked via a 30 amino acid linker [176, 179]. BrxA can react with BSSB, leading to *S*-bacillithiolated BrxA. Due to the close proximity between BrxA and roGFP2, the *S*-bacillithiolation is transferred via a thiol disulfide exchange reaction to roGFP2, resulting in disulfide formation between the Cys147 and Cys204 of roGFP2 **(Fig. 22A)** [176, 179]. That causes the already mentioned change in the conformation of the chromophore of roGFP2 and due to the ratiometric properties of roGFP2,

the OxD of the biosensor and the BSH redox potential (E_{BSH}) of *S. aureus* can be measured [176, 179]. The Brx-roGFP2 biosensor responds rapidly and specifically to physiological BSSB levels in *S. aureus*. The functionality of the biosensor depends on the redox-active Cys54 [179]. In *S. aureus*, the Brx-roGFP2 biosensor was applied to monitor in real-time changes of the E_{BSH} among the growth and after oxidative stress. It has been shown that *S. aureus* is able to regenerate its reduced E_{BSH} after oxidative stress [179].

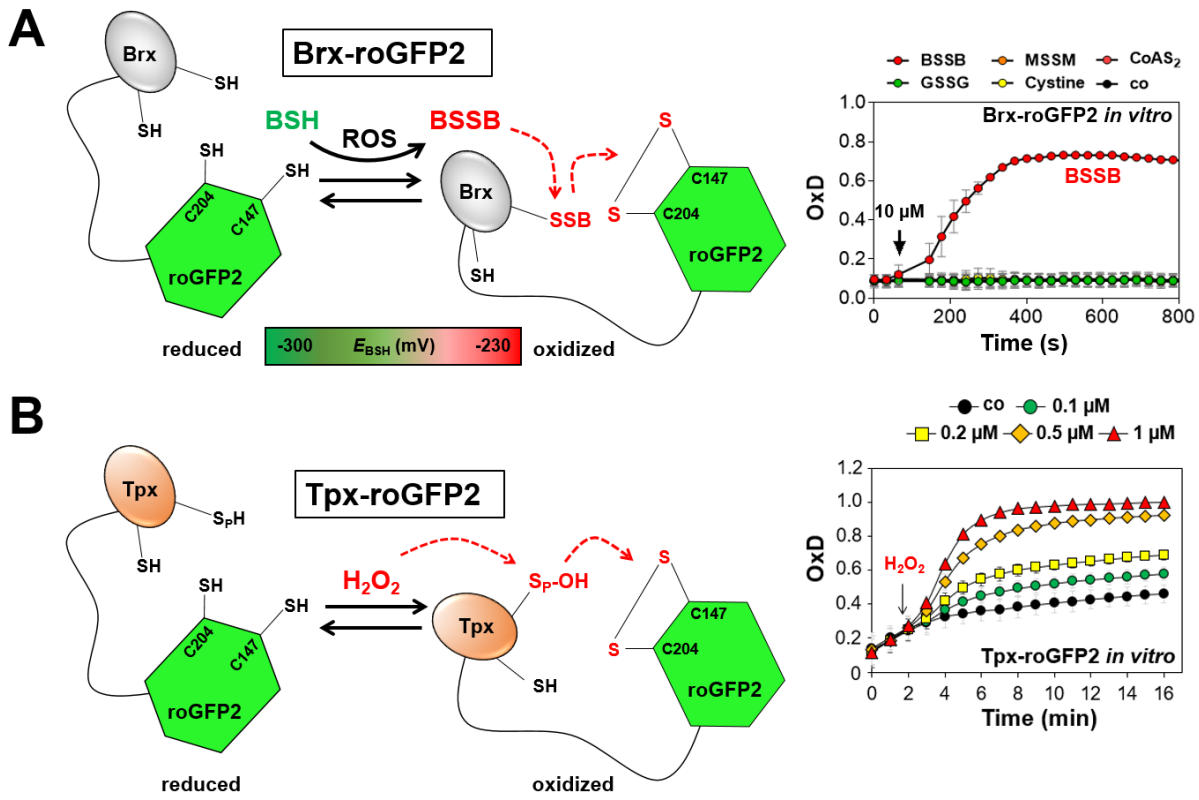

Fig. 22: Principles of Brx- and Tpx-roGFP2 biosensors. (A) Brx-roGFP2 consists of staphylococcal BrxA and roGFP2, whereby roGFP2 equilibrates with the 2 BSH/BSSB redox couple. Under oxidative stress, BSH is converted to BSSB, which can be detected by BrxA, leading to BrxA-SSB formation. Due to the close proximity of BrxA to roGFP2, the *S*-bacillithiolation is transferred to roGFP2 via a thiol disulfide exchange reaction, resulting in intramolecular disulfide bond formation and change of the chromophore of roGFP2. The Brx-roGFP2 biosensor reacts rapidly to 10 µM BSSB, but not to any other thiol disulfide *in vitro* [176, 179]. **(B)** Tpx-roGFP2 is composed of the staphylococcal thiol peroxidase Tpx, which is fused to roGFP2. After H_2O_2 stress, the peroxidative Cys (S_P) attacks H_2O_2, leading to sulfenic acid intermediate (S_P-OH), which is transferred to roGFP2. Tpx-roGFP2 reacts fast and specific to H_2O_2 *in vitro*. The figure is adapted from references [165, 179].

Using the Brx-roGFP2 biosensor, Loi *et al.* (2018, 2019) could show that the surface coating compound AGXX® and allicin cause an increased E_{BSH} in *S. aureus* [177, 180]. In addition, the Brx-roGFP2 biosensor was applied to analyse if antibiotics can produce ROS. However, the E_{BSH} of *S. aureus* was not changed after treatment with several antibiotics, including vancomycin, erythromycin and ciprofloxacin [179]. In contrast, some studies could show that antibiotics generate ROS [12, 59, 90, 147, 315]. Maybe, the ROS generation is to less for detection by this biosensor. During this PhD thesis, I used the biosensor to analyse

the role of YpdA and BrxAB in the regeneration of the E_{BSH} after H_2O_2 and HOCl stress (see sections 3.2.3, 3.2.4 and **chapter 3** for more details) [165] and to detect ROS generation by the 1,4-naphthoquinone lapachol (see section 2.5 and **chapter 4** for more details) [164].

For ROS, in particular H_2O_2, several biosensors have been developed. By fusion of peroxiredoxins (Orp1, Tsa2), it is possible to monitor dynamic changes of the intracellular H_2O_2 levels in eukaryotic as well as in prokaryotic cells [50, 99, 202]. In the present work, we have engineered the novel H_2O_2-specific biosensor Tpx-roGFP2, which consists of the staphylococcal thiol peroxidase Tpx and roGFP2 **(Fig. 22B)** [165]. This biosensor allows ratiometric measurements to monitor changes of the intra-bacterial H_2O_2 levels during growth and under oxidative stress conditions in *S. aureus*. **(chapter 3)** [165]. The H_2O_2 is attacked by the peroxidative Cys60 leading to a Cys-SOH residue, which is transferred to roGFP2. We could show that Tpx-roGFP2 responds fast and highly specific to H_2O_2. Only 1 µM H_2O_2 is sufficient to fully oxidize this biosensor *in vitro* **(Fig. 22B)** [165]. Using the Tpx-roGFP2 biosensor, we could demonstrate that YpdA affects indirectly the H_2O_2 detoxification in *S. aureus* (see section 3.2.4 and **chapter 3** for more details) [165]. Furthermore, we revealed that lapachol induces ROS production (section 2.5 and **chapter 4**) [164]. Future studies could use the Tpx-roGFP2 biosensor to detect ROS after antibiotic treatments due to the higher specificity to ROS, like H_2O_2, compared to Brx-roGFP2 [165, 179]. Moreover, both biosensors could be applied to monitor changes of the E_{BSH} and the intracellular H_2O_2 levels in *S. aureus* under infection conditions. Interestingly, it has been revealed that genetically encoded biosensors can be applied for real-time monitoring of HOCl production in phagocytosing neutrophils [50]. However, the working group of Lars Leichert could demonstrate that HOCl, produced by neutrophils, caused unspecific oxidation of Grx1-roGFP2, Orp1-roGFP2 and roGFP2 *in vitro* and under infections of *E. coli in vivo* [50, 206, 207]. Thus, for the application under infection conditions, it should be proofed, if the measured results with the Brx- and Tpx-roGFP2 biosensors deliver a specific information.

In conclusion, genetically encoded redox biosensors are useful tools in redox biology with a wide range of applications to investigate the redox state of organisms under different conditions.

5. Conclusion and future perspectives

S. aureus is a major human pathogen, which can cause many diseases. Under infections, *S. aureus* has to deal with different ROS and RCS, which are produced by macrophages and neutrophils. Therefore, *S. aureus* has evolved several factors to defend against oxidative stress, including LMW thiols. *S. aureus* uses BSH as its major LMW thiol, which plays an essential role in detoxification of ROS and RCS. Moreover, BSH is important to maintain the reduced redox state of the cell. Under oxidative stress, BSH can protect proteins against overoxidation, leading to *S*-bacillithiolations. *S*-bacillithiolated proteins can be reduced by bacilliredoxins (Brx), resulting in *S*-bacillithiolated Brx, which are diminished by another molecule of BSH, yielding BSSB.

In this PhD thesis, we could provide experimental evidence that the NADPH-dependent thiol disulfide oxidoreductase YpdA acts as the BSSB reductase *in vitro* and in *S. aureus in vivo*. Thereby, YpdA is important to maintain the redox homeostasis and to regenerate the reduced E_{BSH} after oxidative stress. Furthermore, YpdA improves the survival under infection conditions and thus, it is involved in the virulence of *S. aureus*. In addition, we revealed that YpdA acts together with BSH and BrxA in the BrxA/BSH/YpdA redox pathway. Moreover, BrxA contributes to the fitness of *S. aureus* under oxidative stress and infections.

Additionally, we have clearly shown that the 1,4-naphthoquinone lapachol acts mainly as a redox cycler. Thereby, lapachol induces ROS production and causes an oxidative shift of the E_{BSH}, *S*-bacillithiolations and thiol-oxidation of the redox-sensor HypR in *S. aureus*. In contrast, lapachol does not lead to protein aggregation *in vitro* and *in vivo*. We could also show that KatA and the BrxA/BSH/YpdA redox pathway are required to defend towards ROS generated by the naphthoquinone lapachol. Finally, we have engineered and applied the novel H_2O_2-specific Tpx-roGFP2 biosensor, which allows measurements of intra-bacterial H_2O_2 levels in *S. aureus*.

In conclusion, the present work characterized the physiological role of the BrxA/BSH/YpdA redox pathway in *S. aureus* under oxidative stress and infections. The elucidation of the exact mechanism of YpdA to reduce BSSB could be an aim of future studies. Due to its important role, BrxA and YpdA could be candidates as drug targets for the development of new drugs to combat MRSA infections in the future. Additionally, the Tpx-roGFP2 biosensor could be used for real-time monitoring of dynamic changes of the intracellular H_2O_2 levels in *S. aureus* under infection conditions or antibiotic treatments.

References

1. Adam, G, Läuger, P, Stark, G. Physikalische Chemie und Biophysik. *Springer Verlag*, Heidelberg, 2009.
2. Aires De Sousa, M, De Lencastre, H. Bridges from hospitals to the laboratory: genetic portraits of methicillin-resistant *Staphylococcus aureus* clones. *FEMS Immunol. Med. Microbiol. 40*(2): 101-111, 2004.
3. Antelmann, H. Oxidative stress responses and redox signalling mechanisms in *Bacillus subtilis* and *Staphylococcus aureus*. *Academic Press*2015.
4. Antelmann, H, Helmann, JD. Thiol-based redox switches and gene regulation. *Antioxid. Redox Signal. 14*(6): 1049-1063, 2011.
5. Arbach, M, Santana, TM, Moxham, H, Tinson, R, Anwar, A, Groom, M, Hamilton, CJ. Antimicrobial garlic-derived diallyl polysulfanes: Interactions with biological thiols in *Bacillus subtilis*. *Biochim Biophys Acta Gen Subj 1863*(6): 1050-1058, 2019.
6. Archer, GL. *Staphylococcus aureus*: a well-armed pathogen. *Clin. Infect. Dis. 26*(5): 1179-1181, 1998.
7. Arciola, CR, Campoccia, D, Speziale, P, Montanaro, L, Costerton, JW. Biofilm formation in *Staphylococcus* implant infections. A review of molecular mechanisms and implications for biofilm-resistant materials. *Biomaterials 33*(26): 5967-5982, 2012.
8. Åslund, F, Zheng, M, Beckwith, J, Storz, G. Regulation of the OxyR transcription factor by hydrogen peroxide and the cellular thiol-disulfide status. *Proc. Natl. Acad. Sci. U. S. A. 96*(11): 6161-6165, 1999.
9. Babior, BM, Kipnes, RS, Curnutte, JT. Biological defense mechanisms. The production by leukocytes of superoxide, a potential bactericidal agent. *J. Clin. Invest. 52*(3): 741-744, 1973.
10. Baddiley, J, Thain, EM, Novelli, GD, Lipmann, F. Structure of coenzyme A. *Nature 171*(4341): 76, 1953.
11. Bartsch, RG, Newton, GL, Sherrill, C, Fahey, RC. Glutathione amide and its perthiol in anaerobic sulfur bacteria. *J. Bacteriol. 178*(15): 4742-4746, 1996.
12. Becerra, MC, Albesa, I. Oxidative stress induced by ciprofloxacin in *Staphylococcus aureus*. *Biochem. Biophys. Res. Commun. 297*(4): 1003-1007, 2002.
13. Begley, TP, Kinsland, C, Strauss, E. The biosynthesis of coenzyme A in bacteria. *Vitam. Horm. 61*157-171, 2001.
14. Berger, C, Bockenheimer, A. Lebensdauerabschätzung an Kunststoffrohren mittels Zeitstand-Innendruckversuch. *Materialwiss Werkst 38*(5): 418-422, 2007.
15. Berube, BJ, Bubeck Wardenburg, J. *Staphylococcus aureus* alpha-toxin: nearly a century of intrigue. *Toxins (Basel) 5*(6): 1140-1166, 2013.
16. Bhaskar, A, Chawla, M, Mehta, M, Parikh, P, Chandra, P, Bhave, D, Kumar, D, Carroll, KS, Singh, A. Reengineering redox sensitive GFP to measure mycothiol redox potential of *Mycobacterium tuberculosis* during infection. *PLoS Pathog. 10*(1): e1003902, 2014.
17. Bogaert, D, De Groot, R, Hermans, PWM. *Streptococcus pneumoniae* colonisation: the key to pneumococcal disease. *Lancet Infect. Dis. 4*(3): 144-154, 2004.
18. Bogdan, C, Rollinghoff, M, Diefenbach, A. The role of nitric oxide in innate immunity. *Immunol. Rev. 173*17-26, 2000.
19. Bolton, JL, Trush, MA, Penning, TM, Dryhurst, G, Monks, TJ. Role of quinones in toxicology. *Chem. Res. Toxicol. 13*(3): 135-160, 2000.
20. Borlinghaus, J, Albrecht, F, Gruhlke, MC, Nwachukwu, ID, Slusarenko, AJ. Allicin: chemistry and biological properties. *Molecules 19*(8): 12591-12618, 2014.
21. Boucher, HW, Corey, GR. Epidemiology of methicillin-resistant *Staphylococcus aureus*. *Clin. Infect. Dis. 46 Suppl 5*S344-349, 2008.
22. Boylan, JA, Hummel, CS, Benoit, S, Garcia-Lara, J, Treglown-Downey, J, Crane, EJ, 3rd, Gherardini, FC. *Borrelia burgdorferi* bb0728 encodes a coenzyme A disulphide reductase whose function suggests a role in intracellular redox and the oxidative stress response. *Mol. Microbiol. 59*(2): 475-486, 2006.
23. Bronner, S, Monteil, H, Prevost, G. Regulation of virulence determinants in *Staphylococcus aureus*: complexity and applications. *FEMS Microbiol. Rev. 28*(2): 183-200, 2004.
24. Brunmark, A, Cadenas, E. Redox and addition chemistry of quinoid compounds and its biological implications. *Free Radic. Biol. Med. 7*(4): 435-477, 1989.
25. Buchmeier, NA, Newton, GL, Koledin, T, Fahey, RC. Association of mycothiol with protection of *Mycobacterium tuberculosis* from toxic oxidants and antibiotics. *Mol. Microbiol. 47*(6): 1723-1732, 2003.

26. Busche, T, Hillion, M, Van Loi, V, Berg, D, Walther, B, Semmler, T, Strommenger, B, Witte, W, Cuny, C, Mellmann, A, Holmes, MA, Kalinowski, J, Adrian, L, Bernhardt, J, Antelmann, H. Comparative secretome analyses of human and zoonotic *Staphylococcus aureus* isolates CC8, CC22, and CC398. *Mol. Cell. Proteomics 17*(12): 2412-2433, 2018.
27. Cadet, J, Delatour, T, Douki, T, Gasparutto, D, Pouget, J-P, Ravanat, J-L, Sauvaigo, S. Hydroxyl radicals and DNA base damage. *Mutat. Res. 424*(1-2): 9-21, 1999.
28. Carmel-Harel, O, Storz, G. Roles of the glutathione- and thioredoxin-dependent reduction systems in the *Escherichia coli* and saccharomyces cerevisiae responses to oxidative stress. *Annu. Rev. Microbiol. 54*439-461, 2000.
29. Cassini, A, Hogberg, LD, Plachouras, D, Quattrocchi, A, Hoxha, A, Simonsen, GS, Colomb-Cotinat, M, Kretzschmar, ME, Devleesschauwer, B, Cecchini, M, Ouakrim, DA, Oliveira, TC, Struelens, MJ, Suetens, C, Monnet, DL. Attributable deaths and disability-adjusted life-years caused by infections with antibiotic-resistant bacteria in the EU and the European Economic Area in 2015: a population-level modelling analysis. *Lancet Infect. Dis. 19*(1): 56-66, 2019.
30. Chandrangsu, P, Dusi, R, Hamilton, CJ, Helmann, JD. Methylglyoxal resistance in *Bacillus subtilis*: contributions of bacillithiol-dependent and independent pathways. *Mol. Microbiol. 91*(4): 706-715, 2014.
31. Chandrangsu, P, Loi, VV, Antelmann, H, Helmann, JD. The Role of Bacillithiol in Gram-Positive Firmicutes. *Antioxid. Redox Signal. 28*(6): 445-462, 2018.
32. Chang, W, Small, DA, Toghrol, F, Bentley, WE. Global transcriptome analysis of *Staphylococcus aureus* response to hydrogen peroxide. *J. Bacteriol. 188*(4): 1648-1659, 2006.
33. Chavakis, T, Preissner, KT, Herrmann, M. The anti-inflammatory activities of *Staphylococcus aureus*. *Trends Immunol. 28*(9): 408-418, 2007.
34. Cheung, AL, Bayer, AS, Zhang, G, Gresham, H, Xiong, YQ. Regulation of virulence determinants *in vitro* and *in vivo* in *Staphylococcus aureus*. *FEMS Immunol. Med. Microbiol. 40*(1): 1-9, 2004.
35. Chi, BK, Busche, T, Van Laer, K, Basell, K, Becher, D, Clermont, L, Seibold, GM, Persicke, M, Kalinowski, J, Messens, J, Antelmann, H. Protein *S*-mycothiolation functions as redox-switch and thiol protection mechanism in *Corynebacterium glutamicum* under hypochlorite stress. *Antioxid. Redox Signal. 20*(4): 589-605, 2014.
36. Chi, BK, Gronau, K, Mader, U, Hessling, B, Becher, D, Antelmann, H. *S*-bacillithiolation protects against hypochlorite stress in *Bacillus subtilis* as revealed by transcriptomics and redox proteomics. *Mol. Cell. Proteomics 10*(11): M111 009506, 2011.
37. Chi, BK, Roberts, AA, Huyen, TT, Basell, K, Becher, D, Albrecht, D, Hamilton, CJ, Antelmann, H. *S*-bacillithiolation protects conserved and essential proteins against hypochlorite stress in firmicutes bacteria. *Antioxid. Redox Signal. 18*(11): 1273-1295, 2013.
38. Chiang, BY, Chen, TC, Pai, CH, Chou, CC, Chen, HH, Ko, TP, Hsu, WH, Chang, CY, Wu, WF, Wang, AH, Lin, CH. Protein *S*-thiolation by glutathionylspermidine (Gsp): the role of *Escherichia coli* Gsp synthetase/amidase in redox regulation. *J. Biol. Chem. 285*(33): 25345-25353, 2010.
39. Clauditz, A, Resch, A, Wieland, KP, Peschel, A, Gotz, F. Staphyloxanthin plays a role in the fitness of *Staphylococcus aureus* and its ability to cope with oxidative stress. *Infect. Immun. 74*(8): 4950-4953, 2006.
40. Clauss-Lendzian, E, Vaishampayan, A, De Jong, A, Landau, U, Meyer, C, Kok, J, Grohmann, E. Stress response of a clinical *Enterococcus faecalis* isolate subjected to a novel antimicrobial surface coating. *Microbiol. Res. 207*53-64, 2018.
41. Clements, MO, Watson, SP, Foster, SJ. Characterization of the major superoxide dismutase of *Staphylococcus aureus* and its role in starvation survival, stress resistance, and pathogenicity. *J. Bacteriol. 181*(13): 3898-3903, 1999.
42. Colwell, CA, Mccall, M. Studies on the mechanism of antibacterial action of 2-methyl-1,4-naphthoquinone. *Science 101*(2632): 592-594, 1945.
43. Cooper, RA. Metabolism of methylglyoxal in microorganisms. *Annu. Rev. Microbiol. 38*49-68, 1984.
44. Cosgrove, K, Coutts, G, Jonsson, IM, Tarkowski, A, Kokai-Kun, JF, Mond, JJ, Foster, SJ. Catalase (KatA) and alkyl hydroperoxide reductase (AhpC) have compensatory roles in peroxide stress resistance and are required for survival, persistence, and nasal colonization in *Staphylococcus aureus*. *J. Bacteriol. 189*(3): 1025-1035, 2007.
45. Costerton, JW, Stewart, PS, Greenberg, EP. Bacterial biofilms: a common cause of persistent infections. *Science 284*(5418): 1318-1322, 1999.
46. Dahl, TA, Midden, WR, Hartman, PE. Comparison of killing of Gram-negative and Gram-positive bacteria by pure singlet oxygen. *J. Bacteriol. 171*(4): 2188-2194, 1989.

47. David, MZ, Daum, RS. Community-associated methicillin-resistant *Staphylococcus aureus*: epidemiology and clinical consequences of an emerging epidemic. *Clin. Microbiol. Rev. 23*(3): 616-687, 2010.
48. Davies, MJ, Hawkins, CL, Pattison, DI, Rees, MD. Mammalian heme peroxidases: from molecular mechanisms to health implications. *Antioxid. Redox Signal. 10*(7): 1199-1234, 2008.
49. De Vos, P, Garrity, MG, Jones, D, Krieg, RN, Ludwig, W, Rainey, AF, Schleifer, K-H, Whitman, BW. Bergey's Manual of Systematic Bacteriology: The *Firmicutes*. 2 ed., *Springer*, New York, 2009.
50. Degrossoli, A, Müller, A, Xie, K, Schneider, JF, Bader, V, Winklhofer, KF, Meyer, AJ, Leichert, LI. Neutrophil-generated HOCl leads to non-specific thiol oxidation in phagocytized bacteria. *Elife. 7*, 2018.
51. Delcardayre, SB, Davies, JE. *Staphylococcus aureus* coenzyme A disulfide reductase, a new subfamily of pyridine nucleotide-disulfide oxidoreductase. Sequence, expression, and analysis of *cdr*. *J. Biol. Chem. 273*(10): 5752-5757, 1998.
52. Delcardayre, SB, Stock, KP, Newton, GL, Fahey, RC, Davies, JE. Coenzyme A disulfide reductase, the primary low molecular weight disulfide reductase from *Staphylococcus aureus.* Purification and characterization of the native enzyme. *J. Biol. Chem. 273*(10): 5744-5751, 1998.
53. Derewenda, U, Boczek, T, Gorres, KL, Yu, M, Hung, LW, Cooper, D, Joachimiak, A, Raines, RT, Derewenda, ZS. Structure and function of *Bacillus subtilis* YphP, a prokaryotic disulfide isomerase with a CXC catalytic motif. *Biochemistry 48*(36): 8664-8671, 2009.
54. Dickerhof, N, Paton, L, Kettle, AJ. Oxidation of bacillithiol by myeloperoxidase-derived oxidants. *Free Radic. Biol. Med.*, 2020.
55. Ding, AH, Nathan, CF, Stuehr, DJ. Release of reactive nitrogen intermediates and reactive oxygen intermediates from mouse peritoneal macrophages. Comparison of activating cytokines and evidence for independent production. *J. Immunol. 141*(7): 2407-2412, 1988.
56. Dooley, CT, Dore, TM, Hanson, GT, Jackson, WC, Remington, SJ, Tsien, RY. Imaging dynamic redox changes in mammalian cells with green fluorescent protein indicators. *J. Biol. Chem. 279*(21): 22284-22293, 2004.
57. Dreisbach, A, Van Dijl, JM, Buist, G. The cell surface proteome of *Staphylococcus aureus*. *Proteomics 11*(15): 3154-3168, 2011.
58. Dunphy, PJ, Brodie, AF. [233] The structure and function of quinones in respiratory metabolism. *Methods Enzymol. 18*407-461, 1971.
59. Dwyer, DJ, Kohanski, MA, Hayete, B, Collins, JJ. Gyrase inhibitors induce an oxidative damage cellular death pathway in *Escherichia coli*. *Mol. Syst. Biol. 3*91, 2007.
60. Dyke, KG, Jevons, MP, Parker, MT. Penicillinase production and intrinsic resistance to penicillins in *Staphylococcus aures*. *Lancet 1*(7442): 835-838, 1966.
61. Eggers, CH, Caimano, MJ, Malizia, RA, Kariu, T, Cusack, B, Desrosiers, DC, Hazlett, KR, Claiborne, A, Pal, U, Radolf, JD. The coenzyme A disulphide reductase of *Borrelia burgdorferi* is important for rapid growth throughout the enzootic cycle and essential for infection of the mammalian host. *Mol. Microbiol. 82*(3): 679-697, 2011.
62. Epifano, F, Genovese, S, Fiorito, S, Mathieu, V, Kiss, R. Lapachol and its congeners as anticancer agents: a review. *Phytochem. Rev. 13*(1): 37-49, 2013.
63. Etienne, J, Gerbaud, G, Fleurette, J, Courvalin, P. Characterization of staphylococcal plasmids hybridizing with the fosfomycin resistance gene *fosB*. *FEMS Microbiol. Lett. 84*(1): 119-122, 1991.
64. Ezraty, B, Gennaris, A, Barras, F, Collet, JF. Oxidative stress, protein damage and repair in bacteria. *Nat. Rev. Microbiol. 15*(7): 385-396, 2017.
65. Fahey, RC, Brown, WC, Adams, WB, Worsham, MB. Occurrence of glutathione in bacteria. *J. Bacteriol. 133*(3): 1126-1129, 1978.
66. Fahey, RC, Sundquist, AR. Evolution of glutathione metabolism. *John Wiley & Sons, Inc.*, New York, 1991.
67. Fairlamb, AH, Blackburn, P, Ulrich, P, Chait, BT, Cerami, A. Trypanothione: a novel bis(glutathionyl)spermidine cofactor for glutathione reductase in trypanosomatids. *Science 227*(4693): 1485-1487, 1985.
68. Fang, Z, Roberts, AA, Weidman, K, Sharma, SV, Claiborne, A, Hamilton, CJ, Dos Santos, PC. Cross-functionalities of *Bacillus* deacetylases involved in bacillithiol biosynthesis and bacillithiol-*S*-conjugate detoxification pathways. *Biochem. J. 454*(2): 239-247, 2013.
69. Farmer, EE, Davoine, C. Reactive electrophile species. *Curr. Opin. Plant Biol. 10*(4): 380-386, 2007.

70. Fenton, HJH. LXXIII.—Oxidation of tartaric acid in presence of iron. *J. Chem. Soc. Trans. 65*899-910, 1894.
71. Flannagan, RS, Heit, B, Heinrichs, DE. Antimicrobial Mechanisms of Macrophages and the Immune Evasion Strategies of *Staphylococcus aureus*. *Pathogens 4*(4): 826-868, 2015.
72. Flint, DH, Emptage, MH, Finnegan, MG, Fu, W, Johnson, MK. The role and properties of the iron-sulfur cluster in *Escherichia coli* dihydroxy-acid dehydratase. *J. Biol. Chem. 268*(20): 14732-14742, 1993.
73. Flint, DH, Tuminello, JF, Emptage, MH. The inactivation of Fe-S cluster containing hydro-lyases by superoxide. *J. Biol. Chem. 268*(30): 22369-22376, 1993.
74. Forman, HJ, Maiorino, M, Ursini, F. Signaling functions of reactive oxygen species. *Biochemistry 49*(5): 835-842, 2010.
75. Foster, TJ. The *Staphylococcus aureus* "superbug". *J. Clin. Invest. 114*(12): 1693-1696, 2004.
76. Foster, TJ, Geoghegan, JA, Ganesh, VK, Hook, M. Adhesion, invasion and evasion: the many functions of the surface proteins of *Staphylococcus aureus*. *Nat. Rev. Microbiol. 12*(1): 49-62, 2014.
77. Francis, JW, Royer, CJ, Cook, PD. Structure and function of the bacillithiol-*S*-transferase BstA from *Staphylococcus aureus*. *Protein Sci. 27*(4): 898-902, 2018.
78. Frees, D, Gerth, U, Ingmer, H. Clp chaperones and proteases are central in stress survival, virulence and antibiotic resistance of *Staphylococcus aureus*. *Int. J. Med. Microbiol. 304*(2): 142-149, 2014.
79. Frees, D, Savijoki, K, Varmanen, P, Ingmer, H. Clp ATPases and ClpP proteolytic complexes regulate vital biological processes in low GC, Gram-positive bacteria. *Mol. Microbiol. 63*(5): 1285-1295, 2007.
80. Fritsch, VN, Loi, VV, Busche, T, Sommer, A, Tedin, K, Nurnberg, DJ, Kalinowski, J, Bernhardt, J, Fulde, M, Antelmann, H. The MarR-type repressor MhqR confers quinone and antimicrobial resistance in *Staphylococcus aureus*. *Antioxid. Redox Signal. 31*(16): 1235-1252, 2019.
81. Gaballa, A, Antelmann, H, Hamilton, CJ, Helmann, JD. Regulation of *Bacillus subtilis* bacillithiol biosynthesis operons by Spx. *Microbiology 159*(Pt 10): 2025-2035, 2013.
82. Gaballa, A, Chi, BK, Roberts, AA, Becher, D, Hamilton, CJ, Antelmann, H, Helmann, JD. Redox regulation in *Bacillus subtilis*: The bacilliredoxins BrxA(YphP) and BrxB(YqiW) function in de-bacillithiolation of *S*-bacillithiolated OhrR and MetE. *Antioxid. Redox Signal. 21*(3): 357-367, 2014.
83. Gaballa, A, Newton, GL, Antelmann, H, Parsonage, D, Upton, H, Rawat, M, Claiborne, A, Fahey, RC, Helmann, JD. Biosynthesis and functions of bacillithiol, a major low-molecular-weight thiol in Bacilli. *Proc. Natl. Acad. Sci. U. S. A. 107*(14): 6482-6486, 2010.
84. Gardner, PR, Gardner, AM, Martin, LA, Salzman, AL. Nitric oxide dioxygenase: an enzymic function for flavohemoglobin. *Proc. Natl. Acad. Sci. U. S. A. 95*(18): 10378-10383, 1998.
85. Gaupp, R, Ledala, N, Somerville, GA. Staphylococcal response to oxidative stress. *Front Cell Infect Microbiol 2*33, 2012.
86. Geoghegan, JA, Foster, TJ. Cell wall-anchored surface proteins of *Staphylococcus aureus*: Many proteins, multiple functions. *Curr. Top. Microbiol. Immunol. 409*95-120, 2017.
87. Gill, SR, Fouts, DE, Archer, GL, Mongodin, EF, Deboy, RT, Ravel, J, Paulsen, IT, Kolonay, JF, Brinkac, L, Beanan, M, Dodson, RJ, Daugherty, SC, Madupu, R, Angiuoli, SV, Durkin, AS, Haft, DH, Vamathevan, J, Khouri, H, Utterback, T, Lee, C, Dimitrov, G, Jiang, L, Qin, H, Weidman, J, Tran, K, Kang, K, Hance, IR, Nelson, KE, Fraser, CM. Insights on evolution of virulence and resistance from the complete genome analysis of an early methicillin-resistant *Staphylococcus aureus* strain and a biofilm-producing methicillin-resistant *Staphylococcus epidermidis* strain. *J. Bacteriol. 187*(7): 2426-2438, 2005.
88. Goncalves, VL, Nobre, LS, Vicente, JB, Teixeira, M, Saraiva, LM. Flavohemoglobin requires microaerophilic conditions for nitrosative protection of *Staphylococcus aureus*. *FEBS Lett. 580*(7): 1817-1821, 2006.
89. Gopal, S, Borovok, I, Ofer, A, Yanku, M, Cohen, G, Goebel, W, Kreft, J, Aharonowitz, Y. A multidomain fusion protein in *Listeria monocytogenes* catalyzes the two primary activities for glutathione biosynthesis. *J. Bacteriol. 187*(11): 3839-3847, 2005.
90. Goswami, M, Mangoli, SH, Jawali, N. Involvement of reactive oxygen species in the action of ciprofloxacin against *Escherichia coli*. *Antimicrob. Agents Chemother. 50*(3): 949-954, 2006.
91. Goulart, MLOF, Falkowski, P, Ossowski, T, Liwo, A. Electrochemical study of oxygen interaction with lapachol and its radical anions. *Bioelectrochem 59*(1-2): 85-87, 2003.
92. Gout, I. Coenzyme A: a protective thiol in bacterial antioxidant defence. *Biochem. Soc. Trans. 47*(1): 469-476, 2019.

93. Grant, CM, Collinson, LP, Roe, JH, Dawes, IW. Yeast glutathione reductase is required for protection against oxidative stress and is a target gene for yAP-1 transcriptional regulation. *Mol. Microbiol. 21*(1): 171-179, 1996.
94. Grauschopf, U, Winther, JR, Korber, P, Zander, T, Dallinger, P, Bardwell, JCA. Why is DsbA such an oxidizing disulfide catalyst? *Cell 83*(6): 947-955, 1995.
95. Gray, MJ, Wholey, WY, Jakob, U. Bacterial responses to reactive chlorine species. *Annu. Rev. Microbiol. 67*141-160, 2013.
96. Guridi, A, Diederich, AK, Aguila-Arcos, S, Garcia-Moreno, M, Blasi, R, Broszat, M, Schmieder, W, Clauss-Lendzian, E, Sakinc-Gueler, T, Andrade, R, Alkorta, I, Meyer, C, Landau, U, Grohmann, E. New antimicrobial contact catalyst killing antibiotic resistant clinical and waterborne pathogens. *Mater. Sci. Eng. C Mater. Biol. Appl. 50*1-11, 2015.
97. Gutierrez, PL. The metabolism of quinone-containing alkylating agents: free radical production and measurement. *Front. Biosci. 5*D629-638, 2000.
98. Gutscher, M, Pauleau, AL, Marty, L, Brach, T, Wabnitz, GH, Samstag, Y, Meyer, AJ, Dick, TP. Real-time imaging of the intracellular glutathione redox potential. *Nat. Methods 5*(6): 553-559, 2008.
99. Gutscher, M, Sobotta, MC, Wabnitz, GH, Ballikaya, S, Meyer, AJ, Samstag, Y, Dick, TP. Proximity-based Protein Thiol Oxidation by H2O2-scavenging Peroxidases. *J. Biol. Chem. 284*(46): 31532-31540, 2009.
100. Haber, F, Weiss, J. The catalytic decomposition of hydrogen peroxide by iron salts. *Proc. R. Soc. A. - Math. Phys. 147*(861): 332-351, 1934.
101. Hackam, DJ, Rotstein, OD, Zhang, WJ, Demaurex, N, Woodside, M, Tsai, O, Grinstein, S. Regulation of phagosomal acidification. Differential targeting of Na+/H+ exchangers, Na+/K+-ATPases, and vacuolar-type H+-atpases. *J. Biol. Chem. 272*(47): 29810-29820, 1997.
102. Hanson, GT, Aggeler, R, Oglesbee, D, Cannon, M, Capaldi, RA, Tsien, RY, Remington, SJ. Investigating mitochondrial redox potential with redox-sensitive green fluorescent protein indicators. *J. Biol. Chem. 279*(13): 13044-13053, 2004.
103. Harris, DR, Ward, DE, Feasel, JM, Lancaster, KM, Murphy, RD, Mallet, TC, Crane, EJ, 3rd. Discovery and characterization of a coenzyme A disulfide reductase from *Pyrococcus horikoshii*. Implications for this disulfide metabolism of anaerobic hyperthermophiles. *FEBS J. 272*(5): 1189-1200, 2005.
104. Hartman, BJ, Tomasz, A. Low-affinity penicillin-binding protein associated with beta-lactam resistance in *Staphylococcus aureus*. *J. Bacteriol. 158*(2): 513-516, 1984.
105. Hausladen, A, Gow, A, Stamler, JS. Flavohemoglobin denitrosylase catalyzes the reaction of a nitroxyl equivalent with molecular oxygen. *Proc. Natl. Acad. Sci. U. S. A. 98*(18): 10108-10112, 2001.
106. Hawkins, CL, Pattison, DI, Davies, MJ. Hypochlorite-induced oxidation of amino acids, peptides and proteins. *Amino Acids 25*(3-4): 259-274, 2003.
107. Held, JM, Gibson, BW. Regulatory control or oxidative damage? Proteomic approaches to interrogate the role of cysteine oxidation status in biological processes. *Mol. Cell. Proteomics 11*(4): R111 013037, 2012.
108. Hemker, HC, Bas, BM, Muller, AD. Activation of a pro-enzyme by a stoichiometric reaction with another protein. The reaction between prothrombin and staphylocoagulase. *Biochim. Biophys. Acta 379*(1): 180-188, 1975.
109. Hildebrandt, T, Knuesting, J, Berndt, C, Morgan, B, Scheibe, R. Cytosolic thiol switches regulating basic cellular functions: GAPDH as an information hub? *Biol. Chem. 396*(5): 523-537, 2015.
110. Hillion, M, Bernhardt, J, Busche, T, Rossius, M, Maass, S, Becher, D, Rawat, M, Wirtz, M, Hell, R, Ruckert, C, Kalinowski, J, Antelmann, H. Monitoring global protein thiol-oxidation and protein *S*-mycothiolation in *Mycobacterium smegmatis* under hypochlorite stress. *Sci. Rep. 7*(1): 1195, 2017.
111. Hillion, M, Imber, M, Pedre, B, Bernhardt, J, Saleh, M, Loi, VV, Maass, S, Becher, D, Astolfi Rosado, L, Adrian, L, Weise, C, Hell, R, Wirtz, M, Messens, J, Antelmann, H. The glyceraldehyde-3-phosphate dehydrogenase GapDH of *Corynebacterium diphtheriae* is redox-controlled by protein *S*-mycothiolation under oxidative stress. *Sci. Rep. 7*(1): 5020, 2017.
112. Hiras, J, Sharma, SV, Raman, V, Tinson, RaJ, Arbach, M, Rodrigues, DF, Norambuena, J, Hamilton, CJ, Hanson, TE. Physiological studies of *Chlorobiaceae* suggest that bacillithiol derivatives are the most widespread thiols in bacteria. *mBio. 9*(6), 2018.

113. Hochgräe, F, Wolf, C, Fuchs, S, Liebeke, M, Lalk, M, Engelmann, S, Hecker, M. Nitric oxide stress induces different responses but mediates comparable protein thiol protection in *Bacillus subtilis* and *Staphylococcus aureus*. *J. Bacteriol. 190*(14): 4997-5008, 2008.
114. Holmgren, A. Hydrogen donor system for *Escherichia coli* ribonucleoside-diphosphate reductase dependent upon glutathione. *Proc. Natl. Acad. Sci. U. S. A. 73*(7): 2275-2279, 1976.
115. Holmgren, A. Glutathione-dependent synthesis of deoxyribonucleotides. Purification and characterization of glutaredoxin from *Escherichia coli*. *J. Biol. Chem. 254*(9): 3664-3671, 1979.
116. Holmgren, A. Thioredoxin. *Annu. Rev. Biochem. 54*237-271, 1985.
117. Holmgren, A. Thioredoxin and glutaredoxin systems. *J. Biol. Chem. 264*(24): 13963-13966, 1989.
118. Hopkins, FG. On an autoxidisable constituent of the cell. *Biochem. J. 15*(2): 286-305, 1921.
119. Hopkins, FG. On glutathione: a reinvestigation. *J. Biol. Chem. 84*(1): 269-320, 1929.
120. Horsburgh, MJ, Clements, MO, Crossley, H, Ingham, E, Foster, SJ. PerR controls oxidative stress resistance and iron storage proteins and is required for virulence in *Staphylococcus aureus*. *Infect. Immun. 69*(6): 3744-3754, 2001.
121. Horsburgh, MJ, Ingham, E, Foster, SJ. In *Staphylococcus aureus,* Fur is an interactive regulator with PerR, contributes to virulence, and Is necessary for oxidative stress resistance through positive regulation of catalase and iron homeostasis. *J. Bacteriol. 183*(2): 468-475, 2001.
122. Hussain, H, Green, IR. Lapachol and lapachone analogs: a journey of two decades of patent research(1997-2016). *Expert Opin. Ther. Pat. 27*(10): 1111-1121, 2017.
123. Imber, M, Huyen, NTT, Pietrzyk-Brzezinska, AJ, Loi, VV, Hillion, M, Bernhardt, J, Tharichen, L, Kolsek, K, Saleh, M, Hamilton, CJ, Adrian, L, Gräter, F, Wahl, MC, Antelmann, H. Protein *S*-bacillithiolation functions in thiol protection and redox regulation of the glyceraldehyde-3-phosphate dehydrogenase Gap in *Staphylococcus aureus* under hypochlorite stress. *Antioxid. Redox Signal. 28*(6): 410-430, 2018.
124. Imber, M, Loi, VV, Reznikov, S, Fritsch, VN, Pietrzyk-Brzezinska, AJ, Prehn, J, Hamilton, C, Wahl, MC, Bronowska, AK, Antelmann, H. The aldehyde dehydrogenase AldA contributes to the hypochlorite defense and is redox-controlled by protein *S*-bacillithiolation in *Staphylococcus aureus*. *Redox Biol 15*557-568, 2018.
125. Imber, M, Pietrzyk-Brzezinska, AJ, Antelmann, H. Redox regulation by reversible protein *S*-thiolation in Gram-positive bacteria. *Redox Biol 20*130-145, 2019.
126. Imlay, JA. Pathways of oxidative damage. *Annu. Rev. Microbiol. 57*395-418, 2003.
127. Imlay, JA. The molecular mechanisms and physiological consequences of oxidative stress: lessons from a model bacterium. *Nat. Rev. Microbiol. 11*(7): 443-454, 2013.
128. Ishikawa, Y, Israel, SE, Melville, DB. Participation of an intermediate sulfoxide in the enzymatic thiolation of the imidazole ring of hercynine to form ergothioneine. *J. Biol. Chem. 249*(14): 4420-4427, 1974.
129. Ito, T, Katayama, Y, Asada, K, Mori, N, Tsutsumimoto, K, Tiensasitorn, C, Hiramatsu, K. Structural comparison of three types of staphylococcal cassette chromosome *mec* integrated in the chromosome in methicillin-resistant *Staphylococcus aureus*. *Antimicrob. Agents Chemother. 45*(5): 1323-1336, 2001.
130. Ito, T, Katayama, Y, Hiramatsu, K. Cloning and nucleotide sequence determination of the entire *mec* DNA of pre-methicillin-resistant *Staphylococcus aureus* N315. *Antimicrob. Agents Chemother. 43*(6): 1449-1458, 1999.
131. Jackowski, S, Rock, CO. Regulation of coenzyme A biosynthesis. *J. Bacteriol. 148*(3): 926-932, 1981.
132. Jackowski, S, Rock, CO. Consequences of reduced intracellular coenzyme A content in *Escherichia coli*. *J. Bacteriol. 166*(3): 866-871, 1986.
133. Janowiak, BE, Griffith, OW. Glutathione synthesis in *Streptococcus agalactiae*. One protein accounts for gamma-glutamylcysteine synthetase and glutathione synthetase activities. *J. Biol. Chem. 280*(12): 11829-11839, 2005.
134. Jevons, MP, Coe, AW, Parker, MT. Methicillin resistance in staphylococci. *Lancet 1*(7287): 904-907, 1963.
135. Ji, CJ, Kim, JH, Won, YB, Lee, YE, Choi, TW, Ju, SY, Youn, H, Helmann, JD, Lee, JW. *Staphylococcus aureus* PerR is a hypersensitive hydrogen peroxide sensor using iron-mediated histidine oxidation. *J. Biol. Chem. 290*(33): 20374-20386, 2015.
136. Ji, Q, Zhang, L, Jones, MB, Sun, F, Deng, X, Liang, H, Cho, H, Brugarolas, P, Gao, YN, Peterson, SN, Lan, L, Bae, T, He, C. Molecular mechanism of quinone signaling mediated

through *S*-quinonization of a YodB family repressor QsrR. *Proc. Natl. Acad. Sci. U. S. A. 110*(13): 5010-5015, 2013.
137. Jothivasan, VK, Hamilton, CJ. Mycothiol: synthesis, biosynthesis and biological functions of the major low molecular weight thiol in actinomycetes. *Nat. Prod. Rep. 25*(6): 1091-1117, 2008.
138. Kabil, O, Banerjee, R. Characterization of patient mutations in human persulfide dioxygenase (ETHE1) involved in H_2S catabolism. *J. Biol. Chem. 287*(53): 44561-44567, 2012.
139. Karasawa, T, Yoshida, K, Furukawa, K, Hosoki, K. Feedback inhibition of pantothenate kinase by coenzyme A and possible role of the enzyme for the regulation of cellular coenzyme A level. *J. Biochem. 71*(6): 1065-1067, 1972.
140. Kasozi, D, Mohring, F, Rahlfs, S, Meyer, AJ, Becker, K. Real-time imaging of the intracellular glutathione redox potential in the malaria parasite *Plasmodium falciparum*. *PLoS Pathog. 9*(12): e1003782, 2013.
141. Katayama, Y, Ito, T, Hiramatsu, K. A new class of genetic element, *Staphylococcus* cassette chromosome *mec*, encodes methicillin resistance in *Staphylococcus aureus*. *Antimicrob. Agents Chemother. 44*(6): 1549-1555, 2000.
142. Kay, KL, Hamilton, CJ, Le Brun, NE. Mass spectrometry of *B. subtilis* CopZ: Cu(i)-binding and interactions with bacillithiol. *Metallomics 8*(7): 709-719, 2016.
143. Keilin, D, Hartree, EF. On the mechanism of the decomposition of hydrogen peroxide by catalase. *Proc R Soc B 124*(837): 397-405, 1997.
144. Kim, EK, Cha, CJ, Cho, YJ, Cho, YB, Roe, JH. Synthesis of gamma-glutamylcysteine as a major low-molecular-weight thiol in lactic acid bacteria *Leuconostoc* spp. *Biochem. Biophys. Res. Commun. 369*(4): 1047-1051, 2008.
145. Kitko, RD, Cleeton, RL, Armentrout, EI, Lee, GE, Noguchi, K, Berkmen, MB, Jones, BD, Slonczewski, JL. Cytoplasmic acidification and the benzoate transcriptome in *Bacillus subtilis*. *PLoS One 4*(12): e8255, 2009.
146. Kluytmans, J, Van Belkum, A, Verbrugh, H. Nasal carriage of *Staphylococcus aureus*: epidemiology, underlying mechanisms, and associated risks. *Clin. Microbiol. Rev. 10*(3): 505-520, 1997.
147. Kohanski, MA, Dwyer, DJ, Hayete, B, Lawrence, CA, Collins, JJ. A common mechanism of cellular death induced by bactericidal antibiotics. *Cell 130*(5): 797-810, 2007.
148. Kourtis, AP, Hatfield, K, Baggs, J, Mu, Y, See, I, Epson, E, Nadle, J, Kainer, MA, Dumyati, G, Petit, S, Ray, SM, Ham, D, Capers, C, Ewing, H, Coffin, N, Mcdonald, LC, Jernigan, J, Cardo, D. Vital signs: Epidemiology and recent trends in methicillin-resistant and in methicillin-susceptible *Staphylococcus aureus* bloodstream infections - United States. *MMWR Morb. Mortal. Wkly. Rep. 68*(9): 214-219, 2019.
149. Krauth-Siegel, RL, Comini, MA. Redox control in trypanosomatids, parasitic protozoa with trypanothione-based thiol metabolism. *Biochim. Biophys. Acta 1780*(11): 1236-1248, 2008.
150. Krinsky, NI. Antioxidant functions of carotenoids. *Free Radic. Biol. Med. 7*(6): 617-635, 1989.
151. Kullik, I, Giachino, P, Fuchs, T. Deletion of the Alternative Sigma Factor çB in Staphylococcus aureus Reveals Its Function as a Global Regulator of Virulence Genes. *J. Bacteriol. 180*(18): 4814-4820, 1998.
152. Kumagai, Y, Tsurutani, Y, Shinyashiki, M, Homma-Takeda, S, Nakai, Y, Yoshikawa, T, Shimojo, N. Bioactivation of lapachol responsible for DNA scission by NADPH-cytochrome P450 reductase. *Environ. Toxicol. Pharmacol. 3*(4): 245-250, 1997.
153. Lamers, AP, Keithly, ME, Kim, K, Cook, PD, Stec, DF, Hines, KM, Sulikowski, GA, Armstrong, RN. Synthesis of bacillithiol and the catalytic selectivity of FosB-type fosfomycin resistance proteins. *Org Lett 14*(20): 5207-5209, 2012.
154. Lee, CH, Chen, AF. Immobilized coenzymes and derivatives. *Academic Press*, New York, 1982.
155. Lee, JW, Helmann, JD. The PerR transcription factor senses H_2O_2 by metal-catalysed histidine oxidation. *Nature 440*(7082): 363-367, 2006.
156. Lee, JW, Soonsanga, S, Helmann, JD. A complex thiolate switch regulates the *Bacillus subtilis* organic peroxide sensor OhrR. *Proc. Natl. Acad. Sci. U. S. A. 104*(21): 8743-8748, 2007.
157. Leonardi, R, Chohnan, S, Zhang, YM, Virga, KG, Lee, RE, Rock, CO, Jackowski, S. A pantothenate kinase from *Staphylococcus aureus* refractory to feedback regulation by coenzyme A. *J. Biol. Chem. 280*(5): 3314-3322, 2005.
158. Licitra, G. Etymologia: *Staphylococcus*. *Emerg. Infect. Dis. 19*(9): 1553, 2013.
159. Liebeke, M, Pother, DC, Van Duy, N, Albrecht, D, Becher, D, Hochgrafe, F, Lalk, M, Hecker, M, Antelmann, H. Depletion of thiol-containing proteins in response to quinones in *Bacillus subtilis*. *Mol. Microbiol. 69*(6): 1513-1529, 2008.

160. Lillig, CH, Berndt, C, Holmgren, A. Glutaredoxin systems. *Biochim. Biophys. Acta 1780*(11): 1304-1317, 2008.
161. Lindsay, JA. Genomic variation and evolution of *Staphylococcus aureus*. *Int. J. Med. Microbiol. 300*(2-3): 98-103, 2010.
162. Lindsay, JA. *Staphylococcus aureus* genomics and the impact of horizontal gene transfer. *Int. J. Med. Microbiol. 304*(2): 103-109, 2014.
163. Lindsay, JA, Holden, MT. Understanding the rise of the superbug: investigation of the evolution and genomic variation of *Staphylococcus aureus*. *Funct Integr Genomics 6*(3): 186-201, 2006.
164. Linzner, N, Fritsch, VN, Busche, T, Tung, QN, Loi, VV, Bernhardt, J, Kalinowski, J, Antelmann, H. The plant-derived naphthoquinone lapachol causes an oxidative stress response in *Staphylococcus aureus*. *Free Radic. Biol. Med.*, 2020: Revision re-submitted on 29th June 2020
165. Linzner, N, Loi, VV, Fritsch, VN, Tung, QN, Stenzel, S, Wirtz, M, Hell, R, Hamilton, CJ, Tedin, K, Fulde, M, Antelmann, H. *Staphylococcus aureus* uses the bacilliredoxin (BrxAB)/bacillithiol disulfide reductase (YpdA) redox pathway to defend against oxidative stress under infections. *Front. Microbiol. 10*1355, 2019.
166. Lipmann, F. Acetylation of sulfanilamide by liver homogenates and extracts. *J. Biol. Chem. 160*(1): 173-190, 1945.
167. Lipmann, F. On chemistry and function of coenzyme A. *Bacteriol. Rev. 17*(1): 1-16, 1953.
168. Lipmann, F, Kaplan, NO. A common factor in the enzymatic acetylation of sulfanilamide and of choline. *J. Biol. Chem. 162*(3): 743-744, 1946.
169. Lipmann, F, Kaplan, NO, Novelli, GD, Tuttle, LC, Guirard, BM. Coenzyme for acetylation, a pantothenic acid derivative. *J. Biol. Chem. 167*(3): 869, 1947.
170. Lisher, JP, Tsui, HT, Ramos-Montanez, S, Hentchel, KL, Martin, JE, Trinidad, JC, Winkler, ME, Giedroc, DP. Biological and Chemical Adaptation to Endogenous Hydrogen Peroxide Production in *Streptococcus pneumoniae* D39. *mSphere 2*(1), 2017.
171. Little, C, O'brien, PJ. Mechanism of peroxide-inactivation of the sulphydryl enzyme glyceraldehyde-3-phosphate dehydrogenase. *Eur. J. Biochem. 10*(3): 533-538, 1969.
172. Liu, CM, Price, LB, Hungate, BA, Abraham, AG, Larsen, LA, Christensen, K, Stegger, M, Skov, R, Andersen, PS. *Staphylococcus aureus* and the ecology of the nasal microbiome. *Sci Adv 1*(5): e1400216, 2015.
173. Liu, GY, Essex, A, Buchanan, JT, Datta, V, Hoffman, HM, Bastian, JF, Fierer, J, Nizet, V. *Staphylococcus aureus* golden pigment impairs neutrophil killing and promotes virulence through its antioxidant activity. *J. Exp. Med. 202*(2): 209-215, 2005.
174. Liu, YB, Chen, C, Chaudhry, MT, Si, MR, Zhang, L, Wang, Y, Shen, XH. Enhancing *Corynebacterium glutamicum* robustness by over-expressing a gene, *mshA*, for mycothiol glycosyltransferase. *Biotechnol. Lett. 36*(7): 1453-1459, 2014.
175. Liu, YB, Long, MX, Yin, YJ, Si, MR, Zhang, L, Lu, ZQ, Wang, Y, Shen, XH. Physiological roles of mycothiol in detoxification and tolerance to multiple poisonous chemicals in *Corynebacterium glutamicum*. *Arch. Microbiol. 195*(6): 419-429, 2013.
176. Loi, VV, Antelmann, H. Method for measurement of bacillithiol redox potential changes using the Brx-roGFP2 redox biosensor in *Staphylococcus aureus*. *MethodsX 7*100900, 2020.
177. Loi, VV, Busche, T, Preuß, T, Kalinowski, J, Bernhardt, J, Antelmann, H. The AGXX® antimicrobial coating causes a thiol-specific oxidative stress response and protein *S*-bacillithiolation in *Staphylococcus aureus*. *Front. Microbiol. 9*3037, 2018.
178. Loi, VV, Busche, T, Tedin, K, Bernhardt, J, Wollenhaupt, J, Huyen, NTT, Weise, C, Kalinowski, J, Wahl, MC, Fulde, M, Antelmann, H. Redox-sensing under hypochlorite stress and infection conditions by the Rrf2-family repressor HypR in *Staphylococcus aureus*. *Antioxid. Redox Signal. 29*(7): 615-636, 2018.
179. Loi, VV, Harms, M, Müller, M, Huyen, NTT, Hamilton, CJ, Hochgräfe, F, Pane-Farre, J, Antelmann, H. Real-time imaging of the bacillithiol redox potential in the human pathogen *Staphylococcus aureus* using a genetically encoded bacilliredoxin-fused redox biosensor. *Antioxid. Redox Signal. 26*(15): 835-848, 2017.
180. Loi, VV, Huyen, NTT, Busche, T, Tung, QN, Gruhlke, MCH, Kalinowski, J, Bernhardt, J, Slusarenko, AJ, Antelmann, H. *Staphylococcus aureus* responds to allicin by global *S*-thioallylation - Role of the Brx/BSH/YpdA pathway and the disulfide reductase MerA to overcome allicin stress. *Free Radic. Biol. Med. 139*55-69, 2019.
181. Loi, VV, Rossius, M, Antelmann, H. Redox regulation by reversible protein *S*-thiolation in bacteria. *Front. Microbiol. 6*187, 2015.

182. Luba, J, Charrier, V, Claiborne, A. Coenzyme A-disulfide reductase from *Staphylococcus aureus*: evidence for asymmetric behavior on interaction with pyridine nucleotides. *Biochemistry 38*(9): 2725-2737, 1999.
183. Luikenhuis, S, Perrone, G, Dawes, IW, Grant, CM. The yeast *Saccharomyces cerevisiae* contains two glutaredoxin genes that are required for protection against reactive oxygen species. *Mol. Biol. Cell 9*(5): 1081-1091, 1998.
184. Ma, Z, Chandrangsu, P, Helmann, TC, Romsang, A, Gaballa, A, Helmann, JD. Bacillithiol is a major buffer of the labile zinc pool in *Bacillus subtilis*. *Mol. Microbiol. 94*(4): 756-770, 2014.
185. Malawista, SE, Montgomery, RR, Van Blaricom, G. Evidence for reactive nitrogen intermediates in killing of staphylococci by human neutrophil cytoplasts. A new microbicidal pathway for polymorphonuclear leukocytes. *J. Clin. Invest. 90*(2): 631-636, 1992.
186. Mallett, TC, Wallen, JR, Karplus, PA, Sakai, H, Tsukihara, T, Claiborne, A. Structure of coenzyme A-disulfide reductase from *Staphylococcus aureus* at 1.54 Å resolution. *Biochemistry 45*(38): 11278-11289, 2006.
187. Margolis, E. Hydrogen peroxide-mediated interference competition by *Streptococcus pneumoniae* has no significant effect on *Staphylococcus aureus* nasal colonization of neonatal rats. *J. Bacteriol. 191*(2): 571-575, 2009.
188. Marnett, LJ, Riggins, JN, West, JD. Endogenous generation of reactive oxidants and electrophiles and their reactions with DNA and protein. *J. Clin. Invest. 111*(5): 583-593, 2003.
189. Marshall, JH, Wilmoth, GJ. Pigments of *Staphylococcus aureus*, a series of triterpenoid carotenoids. *J. Bacteriol. 147*(3): 900-913, 1981.
190. Marshall, JH, Wilmoth, GJ. Proposed pathway of triterpenoid carotenoid biosynthesis in *Staphylococcus aureus*: evidence from a study of mutants. *J. Bacteriol. 147*(3): 914-919, 1981.
191. Masip, L, Veeravalli, K, Georgiou, G. The many faces of glutathione in bacteria. *Antioxid. Redox Signal. 8*(5-6): 753-762, 2006.
192. Massey, V. Activation of molecular oxygen by flavins and flavoproteins. *J. Biol. Chem. 269*(36): 22459-22462, 1994.
193. Mccord, JM, Fridovich, I. The reduction of cytochrome c by milk xanthine oxidase. *J. Biol. Chem. 243*(21): 5753-5760, 1968.
194. Mccord, JM, Fridovich, I. Superoxide dismutase. An enzymic function for erythrocuprein (hemocuprein). *J. Biol. Chem. 244*(22): 6049-6055, 1969.
195. Meister, A. Glutathione metabolism and its selective modification. *J. Biol. Chem. 263*(33): 17205-17208, 1988.
196. Messner, KR, Imlay, JA. The identification of primary sites of superoxide and hydrogen peroxide formation in the aerobic respiratory chain and sulfite reductase complex of *Escherichia coli*. *J. Biol. Chem. 274*(15): 10119-10128, 1999.
197. Meyer, AJ, Dick, TP. Fluorescent protein-based redox probes. *Antioxid. Redox Signal. 13*(5): 621-650, 2010.
198. Michalopoulos, AS, Livaditis, IG, Gougoutas, V. The revival of fosfomycin. *Int. J. Infect. Dis. 15*(11): e732-739, 2011.
199. Mikheyeva, IV, Thomas, JM, Kolar, SL, Corvaglia, AR, Gaiotaa, N, Leo, S, Francois, P, Liu, GY, Rawat, M, Cheung, AL. YpdA, a putative bacillithiol disulfide reductase, contributes to cellular redox homeostasis and virulence in *Staphylococcus aureus*. *Mol. Microbiol. 111*(4): 1039-1056, 2019.
200. Mishanina, TV, Libiad, M, Banerjee, R. Biogenesis of reactive sulfur species for signaling by hydrogen sulfide oxidation pathways. *Nat. Chem. Biol. 11*(7): 457-464, 2015.
201. Monks, TJ, Hanzlik, RP, Cohen, GM, Ross, D, Graham, DG. Quinone chemistry and toxicity. *Toxicol. Appl. Pharmacol. 112*(1): 2-16, 1992.
202. Morgan, B, Van Laer, K, Owusu, TN, Ezerina, D, Pastor-Flores, D, Amponsah, PS, Tursch, A, Dick, TP. Real-time monitoring of basal H_2O_2 levels with peroxiredoxin-based probes. *Nat. Chem. Biol. 12*(6): 437-443, 2016.
203. Morrissey, JA, Cockayne, A, Brummell, K, Williams, P. The staphylococcal ferritins are differentially regulated in response to iron and manganese and via PerR and Fur. *Infect. Immun. 72*(2): 972-979, 2004.
204. Moussaoui, M, Miseviciene, L, Anusevicius, Z, Maroziene, A, Lederer, F, Baciou, L, Cenas, N. Quinones and nitroaromatic compounds as subversive substrates of *Staphylococcus aureus* flavohemoglobin. *Free Radic. Biol. Med. 123*107-115, 2018.
205. Mukherjee, S, Dutta, D, Saha, B, Das, AK. Crystal structure of glyceraldehyde-3-phosphate dehydrogenase 1 from methicillin-resistant *Staphylococcus aureus* MRSA252 provides novel insights into substrate binding and catalytic mechanism. *J. Mol. Biol. 401*(5): 949-968, 2010.

206. Müller, A, Schneider, JF, Degrossoli, A, Lupilova, N, Dick, TP, Leichert, LI. Fluorescence spectroscopy of roGFP2-based redox probes responding to various physiologically relevant oxidant species *in vitro*. *Data Brief 11*617-627, 2017.
207. Müller, A, Schneider, JF, Degrossoli, A, Lupilova, N, Dick, TP, Leichert, LI. Systematic *in vitro* assessment of responses of roGFP2-based probes to physiologically relevant oxidant species. *Free Radic. Biol. Med. 106*329-338, 2017.
208. Muller, EG. A glutathione reductase mutant of yeast accumulates high levels of oxidized glutathione and requires thioredoxin for growth. *Mol. Biol. Cell 7*(11): 1805-1813, 1996.
209. Newton, GL, Arnold, K, Price, MS, Sherrill, C, Delcardayre, SB, Aharonowitz, Y, Cohen, G, Davies, J, Fahey, RC, Davis, C. Distribution of thiols in microorganisms: mycothiol is a major thiol in most Actinomycetes. *J. Bacteriol. 178*(7): 1990-1995, 1996.
210. Newton, GL, Buchmeier, N, Fahey, RC. Biosynthesis and functions of mycothiol, the unique protective thiol of Actinobacteria. *Microbiol. Mol. Biol. Rev. 72*(3): 471-494, 2008.
211. Newton, GL, Fahey, RC, Cohen, G, Aharonowitz, Y. Low-molecular-weight thiols in *Streptomycetes* and their potential role as antioxidants. *J. Bacteriol. 175*(9): 2734-2742, 1993.
212. Newton, GL, Fahey, RC, Rawat, M. Detoxification of toxins by bacillithiol in *Staphylococcus aureus*. *Microbiology 158*(Pt 4): 1117-1126, 2012.
213. Newton, GL, Javor, B. gamma-glutamylcysteine and thiosulfate are the major low-molecular-weight thiols in halobacteria. *J. Bacteriol. 161*(1): 438-441, 1985.
214. Newton, GL, Leung, SS, Wakabayashi, JI, Rawat, M, Fahey, RC. The DinB superfamily includes novel mycothiol, bacillithiol, and glutathione *S*-transferases. *Biochemistry 50*(49): 10751-10760, 2011.
215. Newton, GL, Rawat, M. N-methyl-bacillithiol, a novel thiol from anaerobic bacteria. *mBio 10*(1), 2019.
216. Newton, GL, Rawat, M, La Clair, JJ, Jothivasan, VK, Budiarto, T, Hamilton, CJ, Claiborne, A, Helmann, JD, Fahey, RC. Bacillithiol is an antioxidant thiol produced in bacilli. *Nat. Chem. Biol. 5*(9): 625-627, 2009.
217. Nicely, NI, Parsonage, D, Paige, C, Newton, GL, Fahey, RC, Leonardi, R, Jackowski, S, Mallett, TC, Claiborne, A. Structure of the type III pantothenate kinase from *Bacillus anthracis* at 2.0 Å resolution: implications for coenzyme A-dependent redox biology. *Biochemistry 46*(11): 3234-3245, 2007.
218. Nohl, H, Jordan, W, Youngman, RJ. Quinones in biology: Functions in electron transfer and oxygen activation. *Free Radic. Biol. Med. 2*(1): 211-279, 1986.
219. Norambuena, J, Wang, Y, Hanson, T, Boyd, JM, Barkay, T. Low-molecular-weight thiols and thioredoxins are important players in Hg(II) resistance in *Thermus thermophilus* HB27. *Appl. Environ. Microbiol. 84*(2), 2018.
220. O'brien, PJ. Molecular mechanisms of quinone cytotoxicity. *Chem. Biol. Interact. 80*(1): 1-41, 1991.
221. Ogston, A. Über Abszesse. *Arch. Klin. Chir. 25*588-600, 1880.
222. Okado-Matsumoto, A, Fridovich, I. The role of alpha,beta -dicarbonyl compounds in the toxicity of short chain sugars. *J. Biol. Chem. 275*(45): 34853-34857, 2000.
223. Oliveira, CGT, Miranda, FF, Ferreira, VF, Freitas, CC, Rabello, RF, Carballido, JM, Corrêa, LCD. Synthesis and antimicrobial evaluation of 3-hydrazino-naphthoquinones as analogs of lapachol. *J. Braz. Chem. Soc. 12*(3): 339-345, 2001.
224. Oliveira, D, Borges, A, Simões, M. *Staphylococcus aureus* toxins and their molecular activity in infectious diseases. *Toxins (Basel) 10*(6): 252, 2018.
225. Ordonez, E, Van Belle, K, Roos, G, De Galan, S, Letek, M, Gil, JA, Wyns, L, Mateos, LM, Messens, J. Arsenate reductase, mycothiol, and mycoredoxin concert thiol/disulfide exchange. *J. Biol. Chem. 284*(22): 15107-15116, 2009.
226. Overton, TW, Justino, MC, Li, Y, Baptista, JM, Melo, AM, Cole, JA, Saraiva, LM. Widespread distribution in pathogenic bacteria of di-iron proteins that repair oxidative and nitrosative damage to iron-sulfur centers. *J. Bacteriol. 190*(6): 2004-2013, 2008.
227. Pané-Farré, J, Jonas, B, Förstner, K, Engelmann, S, Hecker, M. The sigmaB regulon in *Staphylococcus aureus* and its regulation. *Int. J. Med. Microbiol. 296*(4-5): 237-258, 2006.
228. Park, B, Nizet, V, Liu, GY. Role of *Staphylococcus aureus* catalase in niche competition against *Streptococcus pneumoniae*. *J. Bacteriol. 190*(7): 2275-2278, 2008.
229. Park, BS, Kim, JR, Lee, SE, Kim, KS, Takeoka, GR, Ahn, YJ, Kim, JH. Selective growth-inhibiting effects of compounds identified in *Tabebuia impetiginosa* inner bark on human intestinal bacteria. *J. Agric. Food Chem. 53*(4): 1152-1157, 2005.

230. Pattison, DI, Davies, MJ. Absolute rate constants for the reaction of hypochlorous acid with protein side chains and peptide bonds. *Chem. Res. Toxicol. 14*(10): 1453-1464, 2001.
231. Pelz, A, Wieland, KP, Putzbach, K, Hentschel, P, Albert, K, Götz, F. Structure and biosynthesis of staphyloxanthin from *Staphylococcus aureus*. *J. Biol. Chem. 280*(37): 32493-32498, 2005.
232. Pendleton, JN, Gorman, SP, Gilmore, BF. Clinical relevance of the ESKAPE pathogens. *Expert Rev. Anti Infect. Ther. 11*(3): 297-308, 2013.
233. Peng, H, Shen, J, Edmonds, KA, Luebke, JL, Hickey, AK, Palmer, LD, Chang, FJ, Bruce, KA, Kehl-Fie, TE, Skaar, EP, Giedroc, DP. Sulfide homeostasis and nitroxyl intersect via formation of reactive sulfur species in *Staphylococcus aureus*. *mSphere 2*(3), 2017.
234. Peng, H, Zhang, Y, Palmer, LD, Kehl-Fie, TE, Skaar, EP, Trinidad, JC, Giedroc, DP. Hydrogen sulfide and reactive sulfur species impact proteome *S*-sulfhydration and global virulence regulation in *Staphylococcus aureus*. *ACS Infect Dis 3*(10): 744-755, 2017.
235. Pereira, EM, Machado Tde, B, Leal, IC, Jesus, DM, Damaso, CR, Pinto, AV, Giambiagi-Demarval, M, Kuster, RM, Santos, KR. *Tabebuia avellanedae* naphthoquinones: activity against methicillin-resistant staphylococcal strains, cytotoxic activity and *in vivo* dermal irritability analysis. *Ann. Clin. Microbiol. Antimicrob. 5*5, 2006.
236. Perera, VR, Newton, GL, Parnell, JM, Komives, EA, Pogliano, K. Purification and characterization of the *Staphylococcus aureus* bacillithiol transferase BstA. *Biochim. Biophys. Acta 1840*(9): 2851-2861, 2014.
237. Perera, VR, Newton, GL, Pogliano, K. Bacillithiol: a key protective thiol in *Staphylococcus aureus*. *Expert Rev. Anti Infect. Ther. 13*(9): 1089-1107, 2015.
238. Perez-Sacau, E, Diaz-Penate, RG, Estevez-Braun, A, Ravelo, AG, Garcia-Castellano, JM, Pardo, L, Campillo, M. Synthesis and pharmacophore modeling of naphthoquinone derivatives with cytotoxic activity in human promyelocytic leukemia HL-60 cell line. *J. Med. Chem. 50*(4): 696-706, 2007.
239. Pericone, CD, Bae, D, Shchepetov, M, Mccool, T, Weiser, JN. Short-sequence tandem and nontandem DNA repeats and endogenous hydrogen peroxide production contribute to genetic instability of *Streptococcus pneumoniae*. *J. Bacteriol. 184*(16): 4392-4399, 2002.
240. Peschel, A, Otto, M. Phenol-soluble modulins and staphylococcal infection. *Nat. Rev. Microbiol. 11*(10): 667-673, 2013.
241. Peskin, AV, Winterbourn, CC. Kinetics of the reactions of hypochlorous acid and amino acid chloramines with thiols, methionine, and ascorbate. *Free Radic. Biol. Med. 30*(5): 572-579, 2001.
242. Phonimdaeng, P, O'reilly, M, Nowlan, P, Bramley, AJ, Foster, TJ. The coagulase of *Staphylococcus aureus* 8325-4. Sequence analysis and virulence of site-specific coagulase-deficient mutants. *Mol. Microbiol. 4*(3): 393-404, 1990.
243. Poole, LB. The basics of thiols and cysteines in redox biology and chemistry. *Free Radic. Biol. Med. 80*148-157, 2015.
244. Posada, AC, Kolar, SL, Dusi, RG, Francois, P, Roberts, AA, Hamilton, CJ, Liu, GY, Cheung, A. Importance of bacillithiol in the oxidative stress response of *Staphylococcus aureus*. *Infect. Immun. 82*(1): 316-332, 2014.
245. Pöther, DC, Gierok, P, Harms, M, Mostertz, J, Hochgräfe, F, Antelmann, H, Hamilton, CJ, Borovok, I, Lalk, M, Aharonowitz, Y, Hecker, M. Distribution and infection-related functions of bacillithiol in *Staphylococcus aureus*. *Int. J. Med. Microbiol. 303*(3): 114-123, 2013.
246. Potter, AJ, Trappetti, C, Paton, JC. *Streptococcus pneumoniae* uses glutathione to defend against oxidative stress and metal ion toxicity. *J. Bacteriol. 194*(22): 6248-6254, 2012.
247. Proctor, RA, Von Eiff, C, Kahl, BC, Becker, K, Mcnamara, P, Herrmann, M, Peters, G. Small colony variants: a pathogenic form of bacteria that facilitates persistent and recurrent infections. *Nat. Rev. Microbiol. 4*(4): 295-305, 2006.
248. Rabinkov, A, Miron, T, Konstantinovski, L, Wilchek, M, Mirelman, D, Weiner, L. The mode of action of allicin: trapping of radicals and interaction with thiol containing proteins. *BBA - General Subjects 1379*(2): 233-244, 1998.
249. Rajkarnikar, A, Strankman, A, Duran, S, Vargas, D, Roberts, AA, Barretto, K, Upton, H, Hamilton, CJ, Rawat, M. Analysis of mutants disrupted in bacillithiol metabolism in *Staphylococcus aureus*. *Biochem. Biophys. Res. Commun. 436*(2): 128-133, 2013.
250. Ravelo, A, Estévez-Braun, A, Pérez-Sacau, E. The chemistry and biology of lapachol and related natural products α and β-lapachones. Stud. Nat. Prod. Chem., *Elsevier*2003, pp. 719-760.

251. Rawat, M, Johnson, C, Cadiz, V, Av-Gay, Y. Comparative analysis of mutants in the mycothiol biosynthesis pathway in *Mycobacterium smegmatis*. *Biochem. Biophys. Res. Commun. 363*(1): 71-76, 2007.
252. Rawat, M, Newton, GL, Ko, M, Martinez, GJ, Fahey, RC, Av-Gay, Y. Mycothiol-deficient *Mycobacterium smegmatis* mutants are hypersensitive to alkylating agents, free radicals, and antibiotics. *Antimicrob. Agents Chemother. 46*(11): 3348-3355, 2002.
253. Regev-Yochay, G, Trzcinski, K, Thompson, CM, Malley, R, Lipsitch, M. Interference between *Streptococcus pneumoniae* and *Staphylococcus aureus*: *In vitro* hydrogen peroxide-mediated killing by *Streptococcus pneumoniae*. *J. Bacteriol. 188*(13): 4996-5001, 2006.
254. Reniere, ML, Whiteley, AT, Hamilton, KL, John, SM, Lauer, P, Brennan, RG, Portnoy, DA. Glutathione activates virulence gene expression of an intracellular pathogen. *Nature 517*(7533): 170-173, 2015.
255. Reynolds, PE, Brown, DF. Penicillin-binding proteins of beta-lactam-resistant strains of *Staphylococcus aureus*. Effect of growth conditions. *FEBS Lett. 192*(1): 28-32, 1985.
256. Richardson, AR, Dunman, PM, Fang, FC. The nitrosative stress response of *Staphylococcus aureus* is required for resistance to innate immunity. *Mol. Microbiol. 61*(4): 927-939, 2006.
257. Rivlin, RS. Historical perspective on the use of garlic. *J. Nutr. 131*(3s): 951S-954S, 2001.
258. Roberts, AA, Sharma, SV, Strankman, AW, Duran, SR, Rawat, M, Hamilton, CJ. Mechanistic studies of FosB: a divalent-metal-dependent bacillithiol-*S*-transferase that mediates fosfomycin resistance in *Staphylococcus aureus*. *Biochem. J. 451*(1): 69-79, 2013.
259. Rocha, MN, Nogueira, PM, Demicheli, C, De Oliveira, LG, Da Silva, MM, Frezard, F, Melo, MN, Soares, RP. Cytotoxicity and *in vitro* antileishmanial activity of antimony (V), bismuth (V), and tin (IV) complexes of lapachol. *Bioinorg. Chem. Appl. 2013*961783, 2013.
260. Rock, CO, Park, HW, Jackowski, S. Role of feedback regulation of pantothenate kinase (CoaA) in control of coenzyme A levels in *Escherichia coli*. *J. Bacteriol. 185*(11): 3410-3415, 2003.
261. Rosario-Cruz, Z, Chahal, HK, Mike, LA, Skaar, EP, Boyd, JM. Bacillithiol has a role in Fe-S-cluster biogenesis in *Staphylococcus aureus*. *Mol. Microbiol. 98*(2): 218-242, 2015.
262. Rosenbach, F. Mikroorganismen bei den Wundinfections-Krankheiten des Menschen Wiesbaden. *JF Bergmann's Verlag*1884.
263. Rudolph, TK, Freeman, BA. Transduction of redox signaling by electrophile-protein reactions. *Sci Signal 2*(90): re7, 2009.
264. Sakuda, S, Zhou, ZY, Yamada, Y. Structure of a novel disulfide of 2-(N-acetylcysteinyl)amido-2-deoxy-alpha-D-glucopyranosyl-*myo*-inositol produced by *Streptomyces* sp. *Biosci. Biotechnol. Biochem. 58*(7): 1347-1348, 1994.
265. Sanchez-Riego, AM, Lopez-Maury, L, Florencio, FJ. Glutaredoxins are essential for stress adaptation in the cyanobacterium *Synechocystis* sp. PCC 6803. *Front Plant Sci 4*428, 2013.
266. Sanz, R, Mari, NI, Ruiz-Santa-Quiteria, JA, Orden, JA, Cid, D, Diez, RM, Silhadi, KS, Amils, R, De La Fuente, R. Catalase deficiency in *Staphylococcus aureus* subsp. *anaerobius* is associated with natural loss-of-function mutations within the structural gene. *Microbiology 146 (Pt 2)*465-475, 2000.
267. Sareen, D, Newton, GL, Fahey, RC, Buchmeier, NA. Mycothiol is essential for growth of *Mycobacterium tuberculosis* Erdman. *J. Bacteriol. 185*(22): 6736-6740, 2003.
268. Sawyer, DT, Sobkowiak, A, Matsushita, T. Metal [MLx; M = Fe, Cu, Co, Mn]/hydroperoxide-induced activation of dioxygen for the oxygenation of hydrocarbons: Oxygenated Fenton chemistry. *Acc. Chem. Res 29*(9): 409-416, 1996.
269. Schildknecht, H. Die Wehrchemie von Land- und Wasserkäfern. *Angew. Chem. 82*(1): 17-25, 1970.
270. Schultz, TW, Sinks, GD, Cronin, MTD. Quinone-induced toxicity to Tetrahymena: structure-activity relationships. *Aquat. Toxicol. 39*(3-4): 267-278, 1997.
271. Schwarzländer, M, Dick, TP, Meyer, AJ, Morgan, B. Dissecting redox biology using fluorescent protein sensors. *Antioxid. Redox Signal. 24*(13): 680-712, 2016.
272. Schwarzländer, M, Fricker, MD, Müller, C, Marty, L, Brach, T, Novak, J, Sweetlove, LJ, Hell, R, Meyer, AJ. Confocal imaging of glutathione redox potential in living plant cells. *J. Microsc. 231*(2): 299-316, 2008.
273. Seebeck, FP. I*n vitro* reconstitution of mycobacterial ergothioneine biosynthesis. *J. Am. Chem. Soc. 132*(19): 6632-6633, 2010.
274. Sharma, SV, Arbach, M, Roberts, AA, Macdonald, CJ, Groom, M, Hamilton, CJ. Biophysical features of bacillithiol, the glutathione surrogate of *Bacillus subtilis* and other firmicutes. *ChemBioChem 14*(16): 2160-2168, 2013.

275. Sharma, SV, Jothivasan, VK, Newton, GL, Upton, H, Wakabayashi, JI, Kane, MG, Roberts, AA, Rawat, M, La Clair, JJ, Hamilton, CJ. Chemical and Chemoenzymatic syntheses of bacillithiol: a unique low-molecular-weight thiol amongst low G + C Gram-positive bacteria. *Angew. Chem. Int. Ed. Engl. 50*(31): 7101-7104, 2011.
276. Sharma, SV, Van Laer, K, Messens, J, Hamilton, CJ. Thiol Redox and pKa Properties of Mycothiol, the Predominant Low-Molecular-Weight Thiol Cofactor in the Actinomycetes. *ChemBioChem 17*(18): 1689-1692, 2016.
277. Shatalin, K, Shatalina, E, Mironov, A, Nudler, E. H_2S: a universal defense against antibiotics in bacteria. *Science 334*(6058): 986-990, 2011.
278. Shen, J, Keithly, ME, Armstrong, RN, Higgins, KA, Edmonds, KA, Giedroc, DP. *Staphylococcus aureus* CstB Is a novel multidomain persulfide dioxygenase-sulfurtransferase involved in hydrogen sulfide detoxification. *Biochemistry 54*(29): 4542-4554, 2015.
279. Si, M, Zhao, C, Zhang, B, Wei, D, Chen, K, Yang, X, Xiao, H, Shen, X. Overexpression of mycothiol disulfide reductase enhances *Corynebacterium glutamicum* robustness by modulating cellular redox homeostasis and antioxidant proteins under oxidative Stress. *Sci. Rep. 6*29491, 2016.
280. Sies, H. Hydrogen peroxide as a central redox signaling molecule in physiological oxidative stress: Oxidative eustress. *Redox Biol 11*613-619, 2017.
281. Sies, H, Berndt, C, Jones, DP. Oxidative Stress. *Annu. Rev. Biochem. 86*715-748, 2017.
282. Sies, H, Jones, DP. Encyclopedia of stress 2ed., *Elsevier*, Amsterdam, 2007.
283. Sigurdardottir, B, Berg, JV, Hu, J, Alamu, J, Mcnutt, LA, Diekema, DJ, Herwaldt, LA. Descriptive epidemiology and case-control study of patients colonized with vancomycin-resistant *Enterococcus* and methicillin-resistant *Staphylococcus aureus*. *Infect. Control Hosp. Epidemiol. 27*(9): 913-919, 2006.
284. Singh, VK, Syring, M, Singh, A, Singhal, K, Dalecki, A, Johansson, T. An insight into the significance of the DnaK heat shock system in *Staphylococcus aureus*. *Int. J. Med. Microbiol. 302*(6): 242-252, 2012.
285. Smith, MT. Quinones as mutagens, carcinogens, and anticancer agents: introduction and overview. *J. Toxicol. Environ. Health 16*(5): 665-672, 1985.
286. Song, M, Husain, M, Jones-Carson, J, Liu, L, Henard, CA, Vazquez-Torres, A. Low-molecular-weight thiol-dependent antioxidant and antinitrosative defences in *Salmonella* pathogenesis. *Mol. Microbiol. 87*(3): 609-622, 2013.
287. Song, MD, Wachi, M, Doi, M, Ishino, F, Matsuhashi, M. Evolution of an inducible penicillin-target protein in methicillin-resistant *Staphylococcus aureus* by gene fusion. *FEBS Lett. 221*(1): 167-171, 1987.
288. Souza, MA, Johann, S, Lima, LA, Campos, FF, Mendes, IC, Beraldo, H, Souza-Fagundes, EM, Cisalpino, PS, Rosa, CA, Alves, TM, De Sa, NP, Zani, CL. The antimicrobial activity of lapachol and its thiosemicarbazone and semicarbazone derivatives. *Mem. Inst. Oswaldo Cruz 108*(3), 2013.
289. Spaan, AN, Van Strijp, JaG, Torres, VJ. Leukocidins: staphylococcal bi-component pore-forming toxins find their receptors. *Nat. Rev. Microbiol. 15*(7): 435-447, 2017.
290. Spellerberg, B, Cundell, DR, Sandros, J, Pearce, BJ, Idanpaan-Heikkila, I, Rosenow, C, Masure, HR. Pyruvate oxidase, as a determinant of virulence in *Streptococcus pneumoniae*. *Mol. Microbiol. 19*(4): 803-813, 1996.
291. Spies, HS, Steenkamp, DJ. Thiols of intracellular pathogens. Identification of ovothiol A in *Leishmania donovani* and structural analysis of a novel thiol from *Mycobacterium bovis*. *Eur. J. Biochem. 224*(1): 203-213, 1994.
292. Storz, G, Imlay, JA. Oxidative stress. *Curr. Opin. Microbiol. 2*(2): 188-194, 1999.
293. Sunassee, SN, Veale, CG, Shunmoogam-Gounden, N, Osoniyi, O, Hendricks, DT, Caira, MR, De La Mare, JA, Edkins, AL, Pinto, AV, Da Silva Junior, EN, Davies-Coleman, MT. Cytotoxicity of lapachol, beta-lapachone and related synthetic 1,4-naphthoquinones against oesophageal cancer cells. *Eur. J. Med. Chem. 62*98-110, 2013.
294. Theodoulou, FL, Sibon, OC, Jackowski, S, Gout, I. Coenzyme A and its derivatives: renaissance of a textbook classic. *Biochem. Soc. Trans. 42*(4): 1025-1032, 2014.
295. Thompson, MK, Keithly, ME, Goodman, MC, Hammer, ND, Cook, PD, Jagessar, KL, Harp, J, Skaar, EP, Armstrong, RN. Structure and function of the genomically encoded fosfomycin resistance enzyme, FosB, from *Staphylococcus aureus*. *Biochemistry 53*(4): 755-765, 2014.
296. Thompson, MK, Keithly, ME, Harp, J, Cook, PD, Jagessar, KL, Sulikowski, GA, Armstrong, RN. Structural and chemical aspects of resistance to the antibiotic fosfomycin conferred by FosB from *Bacillus cereus*. *Biochemistry 52*(41): 7350-7362, 2013.

297. Tong, SY, Davis, JS, Eichenberger, E, Holland, TL, Fowler, VG, Jr. *Staphylococcus aureus* infections: epidemiology, pathophysiology, clinical manifestations, and management. *Clin. Microbiol. Rev. 28*(3): 603-661, 2015.
298. Tsuchiya, Y, Peak-Chew, SY, Newell, C, Miller-Aidoo, S, Mangal, S, Zhyvoloup, A, Bakovic, J, Malanchuk, O, Pereira, GC, Kotiadis, V, Szabadkai, G, Duchen, MR, Campbell, M, Cuenca, SR, Vidal-Puig, A, James, AM, Murphy, MP, Filonenko, V, Skehel, M, Gout, I. Protein CoAlation: a redox-regulated protein modification by coenzyme A in mammalian cells. *Biochem. J. 474*(14): 2489-2508, 2017.
299. Tsuchiya, Y, Zhyvoloup, A, Bakovic, J, Thomas, N, Yu, BYK, Das, S, Orengo, C, Newell, C, Ward, J, Saladino, G, Comitani, F, Gervasio, FL, Malanchuk, OM, Khoruzhenko, AI, Filonenko, V, Peak-Chew, SY, Skehel, M, Gout, I. Protein CoAlation and antioxidant function of coenzyme A in prokaryotic cells. *Biochem. J. 475*(11): 1909-1937, 2018.
300. Tung, QN, Linzner, N, Loi, VV, Antelmann, H. Application of genetically encoded redox biosensors to measure dynamic changes in the glutathione, bacillithiol and mycothiol redox potentials in pathogenic bacteria. *Free Radic. Biol. Med. 128*84-96, 2018.
301. Tung, QN, Linzner, N, Van Loi, V, Antelmann, H. Biosynthesis and functions of bacillithiol in Firmicutes. in: L Flohe (Ed.), Glutathione, *CRC Press*, Boca Raton 2018, pp. 357-366.
302. Tung, QN, Loi, VV, Busche, T, Nerlich, A, Mieth, M, Milse, J, Kalinowski, J, Hocke, AC, Antelmann, H. Stable integration of the Mrx1-roGFP2 biosensor to monitor dynamic changes of the mycothiol redox potential in *Corynebacterium glutamicum*. *Redox Biol 20*514-525, 2019.
303. Turner, E, Klevit, R, Hopkins, PB, Shapiro, BM. Ovothiol: a novel thiohistidine compound from sea urchin eggs that confers NAD(P)H-O_2 oxidoreductase activity on ovoperoxidase. *J. Biol. Chem. 261*(28): 13056-13063, 1986.
304. Ubukata, K, Yamashita, N, Konno, M. Occurrence of a beta-lactam-inducible penicillin-binding protein in methicillin-resistant staphylococci. *Antimicrob. Agents Chemother. 27*(5): 851-857, 1985.
305. Udaka, S, Koukol, J, Vennesland, B. Lactic oxidase of Pneumococcus. *J. Bacteriol. 78*714-725, 1959.
306. Valderas, MW, Hart, ME. Identification and characterization of a second superoxide dismutase gene (*sodM*) from *Staphylococcus aureus*. *J. Bacteriol. 183*(11): 3399-3407, 2001.
307. Van Der Heijden, J, Bosman, ES, Reynolds, LA, Finlay, BB. Direct measurement of oxidative and nitrosative stress dynamics in *Salmonella* inside macrophages. *Proc. Natl. Acad. Sci. U. S. A. 112*(2): 560-565, 2015.
308. Van Der Heijden, J, Vogt, SL, Reynolds, LA, Pena-Diaz, J, Tupin, A, Aussel, L, Finlay, BB. Exploring the redox balance inside Gram-negative bacteria with redox-sensitive GFP. *Free Radic. Biol. Med. 91*34-44, 2016.
309. Van Der Westhuyzen, R, Strauss, E. Michael acceptor-containing coenzyme A analogues as inhibitors of the atypical coenzyme A disulfide reductase from *Staphylococcus aureus*. *J. Am. Chem. Soc. 132*(37): 12853-12855, 2010.
310. Van Laer, K, Buts, L, Foloppe, N, Vertommen, D, Van Belle, K, Wahni, K, Roos, G, Nilsson, L, Mateos, LM, Rawat, M, Van Nuland, NA, Messens, J. Mycoredoxin-1 is one of the missing links in the oxidative stress defence mechanism of Mycobacteria. *Mol. Microbiol. 86*(4): 787-804, 2012.
311. Van Laer, K, Hamilton, CJ, Messens, J. Low-molecular-weight thiols in thiol-disulfide exchange. *Antioxid. Redox Signal. 18*(13): 1642-1653, 2013.
312. Von Eiff, C, Becker, K, Machka, K, Stammer, H, Peters, G. Nasal carriage as a source of *Staphylococcus aureus* bacteremia. . *N. Engl. J. Med. 344*(1): 11-16, 2001.
313. Wakeman, CA, Hammer, ND, Stauff, DL, Attia, AS, Anzaldi, LL, Dikalov, SI, Calcutt, MW, Skaar, EP. Menaquinone biosynthesis potentiates haem toxicity in *Staphylococcus aureus*. *Mol. Microbiol. 86*(6): 1376-1392, 2012.
314. Wallace, BD, Edwards, JS, Wallen, JR, Moolman, WJ, Van Der Westhuyzen, R, Strauss, E, Redinbo, MR, Claiborne, A. Turnover-dependent covalent inactivation of *Staphylococcus aureus* coenzyme A-disulfide reductase by coenzyme A-mimetics: mechanistic and structural insights. *Biochemistry 51*(39): 7699-7711, 2012.
315. Wang, X, Zhao, X. Contribution of oxidative damage to antimicrobial lethality. *Antimicrob. Agents Chemother. 53*(4): 1395-1402, 2009.
316. Weber, H, Engelmann, S, Becher, D, Hecker, M. Oxidative stress triggers thiol oxidation in the glyceraldehyde-3-phosphate dehydrogenase of *Staphylococcus aureus*. *Mol. Microbiol. 52*(1): 133-140, 2004.

317. Weigel, LM, Clewell, DB, Gill, SR, Clark, NC, Mcdougal, LK, Flannagan, SE, Kolonay, JF, Shetty, J, Killgore, GE, Tenover, FC. Genetic analysis of a high-level vancomycin-resistant isolate of *Staphylococcus aureus*. *Science 302*(5650): 1569-1571, 2003.
318. Weinberg, JB, Misukonis, MA, Shami, PJ, Mason, SN, Sauls, DL, Dittman, WA, Wood, ER, Smith, GK, Mcdonald, B, Bachus, KE. Human mononuclear phagocyte inducible nitric oxide synthase (iNOS): analysis of iNOS mRNA, iNOS protein, biopterin, and nitric oxide production by blood monocytes and peritoneal macrophages. *Blood 86*(3): 1184-1195, 1995.
319. Westrop, GD, Georg, I, Coombs, GH. The mercaptopyruvate sulfurtransferase of *Trichomonas vaginalis* links cysteine catabolism to the production of thioredoxin persulfide. *J. Biol. Chem. 284*(48): 33485-33494, 2009.
320. Williams, RE. Healthy carriage of *Staphylococcus aureus*: its prevalence and importance. *Bacteriol. Rev. 27*56-71, 1963.
321. Winterbourn, CC. Reconciling the chemistry and biology of reactive oxygen species. *Nat. Chem. Biol. 4*(5): 278-286, 2008.
322. Winterbourn, CC. The biological chemistry of hydrogen peroxide. *Methods Enzymol. 528*3-25, 2013.
323. Winterbourn, CC, Kettle, AJ. Redox reactions and microbial killing in the neutrophil phagosome. *Antioxid. Redox Signal. 18*(6): 642-660, 2013.
324. Winterbourn, CC, Metodiewa, D. Reactivity of biologically important thiol compounds with superoxide and hydrogen peroxide. *Free Radic. Biol. Med. 27*(3-4): 322-328, 1999.
325. Wolf, C, Hochgräfe, F, Kusch, H, Albrecht, D, Hecker, M, Engelmann, S. Proteomic analysis of antioxidant strategies of *Staphylococcus aureus:* diverse responses to different oxidants. *Proteomics 8*(15): 3139-3153, 2008.
326. Wulf, M, Voss, A. MRSA in livestock animals-an epidemic waiting to happen? *Clin. Microbiol. Infect. 14*(6): 519-521, 2008.
327. Zhu, W, Clark, NC, Mcdougal, LK, Hageman, J, Mcdonald, LC, Patel, JB. Vancomycin-resistant *Staphylococcus aureus* isolates associated with Inc18-like *vanA* plasmids in Michigan. *Antimicrob. Agents Chemother. 52*(2): 452-457, 2008.

Chapter 1

Biosynthesis and functions of bacillithiol in *Firmicutes*

Quach Ngoc Tung[1], Nico Linzner[1], Vu Van Loi[1], Haike Antelmann[1*]

[1]*Freie Universität Berlin, Institute for Biology-Microbiology, D-14195 Berlin, Germany*

*Corresponding author: haike.antelmann@fu-berlin.de

Published in:
Book chapter No. 20, Book title “Glutathione”, CRC Press, Taylor & Francis Group (2018)

DOI: https://doi.org/10.1201/9781351261760

Personal contribution:

I contributed together with Quach Ngoc Tung to the writing of the **sections 20.6 and 20.7** about the functions of bacillithiol in metal homeostasis and virulence and to **sections 20.8 and 20.9** about the role of bacillithiol in *S*-bacillithiolation and its reversal by bacilliredoxins of this review article. I also helped to draft the **figures 6, 7 and 8** related to these parts.

Chapter 2

Application of genetically encoded redox biosensors to measure dynamic changes in the glutathione, bacillithiol and mycothiol redox potentials in pathogenic bacteria

Quach Ngoc Tung[1], Nico Linzner[1], Vu Van Loi[1], Haike Antelmann[1*]

[1]*Freie Universität Berlin, Institute for Biology-Microbiology, D-14195 Berlin, Germany*

*Corresponding author: haike.antelmann@fu-berlin.de

Published in:
Free Radical Biology and Medicine 128: 84-96. (2018)

DOI: https://doi.org/10.1016/j.freeradbiomed.2018.02.018

Personal contribution:
I contributed to write the **section 2.1** about the dynamic roGFP2-based biosensors to measure redox changes in Gram-negative bacteria.

Free Radical Biology and Medicine 128 (2018) 84–96

Contents lists available at ScienceDirect

Free Radical Biology and Medicine

journal homepage: www.elsevier.com/locate/freeradbiomed

Review Article

Application of genetically encoded redox biosensors to measure dynamic changes in the glutathione, bacillithiol and mycothiol redox potentials in pathogenic bacteria

Quach Ngoc Tung, Nico Linzner, Vu Van Loi, Haike Antelmann*

Freie Universität Berlin, Institute for Biology-Microbiology, Königin-Luise-Strasse 12-16, D-14195 Berlin, Germany

ARTICLE INFO

Keywords:
Listeria monocytogenes
Salmonella Typhimurium
Staphylococcus aureus
Mycobacterium tuberculosis
Glutathione
Bacillithiol
Mycothiol
roGFP2/redox biosensors

ABSTRACT

Gram-negative bacteria utilize glutathione (GSH) as their major LMW thiol. However, most Gram-positive bacteria do not encode enzymes for GSH biosynthesis and produce instead alternative LMW thiols, such as bacillithiol (BSH) and mycothiol (MSH). BSH is utilized by *Firmicutes* and MSH is the major LMW thiol of *Actinomycetes*. LMW thiols are required to maintain the reduced state of the cytoplasm, but are also involved in virulence mechanisms in human pathogens, such as *Staphylococcus aureus*, *Mycobacterium tuberculosis*, *Streptococcus pneumoniae*, *Salmonella enterica* subsp. Typhimurium and *Listeria monocytogenes*. Infection conditions often cause perturbations of the intrabacterial redox balance in pathogens, which is further affected under antibiotics treatments. During the last years, novel glutaredoxin-fused roGFP2 biosensors have been engineered in many eukaryotic organisms, including parasites, yeast, plants and human cells for dynamic live-imaging of the GSH redox potential in different compartments. Likewise bacterial roGFP2-based biosensors are now available to measure the dynamic changes in the GSH, BSH and MSH redox potentials in model and pathogenic Gram-negative and Gram-positive bacteria.

In this review, we present an overview of novel functions of the bacterial LMW thiols GSH, MSH and BSH in pathogenic bacteria in virulence regulation. Moreover, recent results about the application of genetically encoded redox biosensors are summarized to study the mechanisms of host-pathogen interactions, persistence and antibiotics resistance. In particularly, we highlight recent biosensor results on the redox changes in the intracellular food-borne pathogen *Salmonella* Typhimurium as well as in the Gram-positive pathogens *S. aureus* and *M. tuberculosis* during infection conditions and under antibiotics treatments. These studies established a link between ROS and antibiotics resistance with the intracellular LMW thiol-redox potential. Future applications should be directed to compare the redox potentials among different clinical isolates of these pathogens in relation to their antibiotics resistance and to screen for new ROS-producing drugs as promising strategy to combat antimicrobial resistance.

1. Functions of low molecular weight thiols in pathogenic bacteria

1.1. Functions of glutathione in virulence and protein S-glutathionylation in pathogenic bacteria

Low molecular weight (LMW) thiols play important roles to maintain the reduced state of the cytoplasm in all organisms [1,2]. Glutathione (GSH) functions as major LMW thiol in Gram-negative bacteria and in few Gram-positives, such as *Streptococci, Listeria, Lactobacilli* and *Clostridia* (Fig. 1). However, some Gram-positive pathogens also use ABC transporters to import GSH either from host cells or from the growth medium, as shown for *Streptococcus pneumoniae* and *Listeria monocytogenes* [3,4]. The biosynthesis and functions of GSH have been widely studied in *Escherichia coli,* which produces millimolar concentrations of GSH [2,5]. GSH maintains protein thiols in its reduced state, functions as a storage form of cysteine and is resistant to metal-catalyzed autooxidation [2]. GSH undergoes autooxidation 7 times slower compared to free Cys. Under oxidative stress, GSH is oxidized to glutathione disulfide (GSSG) which is reduced by the glutathione reductase (Gor) on expense of NADPH (Fig. 2). The GSH/GSSG ratio ranges from 30:1 to 100:1 and the standard thiol-disulfide redox potential of GSH was determined as $E^{0'}$(GSSG/GSH) = − 240 mV at physiological pH values in the cytoplasm of *E. coli* [1,6]. Many detoxification functions of GSH have been studied in *E. coli*. GSH is important

* Corresponding author.
E-mail address: haike.antelmann@fu-berlin.de (H. Antelmann).

https://doi.org/10.1016/j.freeradbiomed.2018.02.018
Received 24 December 2017; Received in revised form 8 February 2018; Accepted 13 February 2018
Available online 15 February 2018

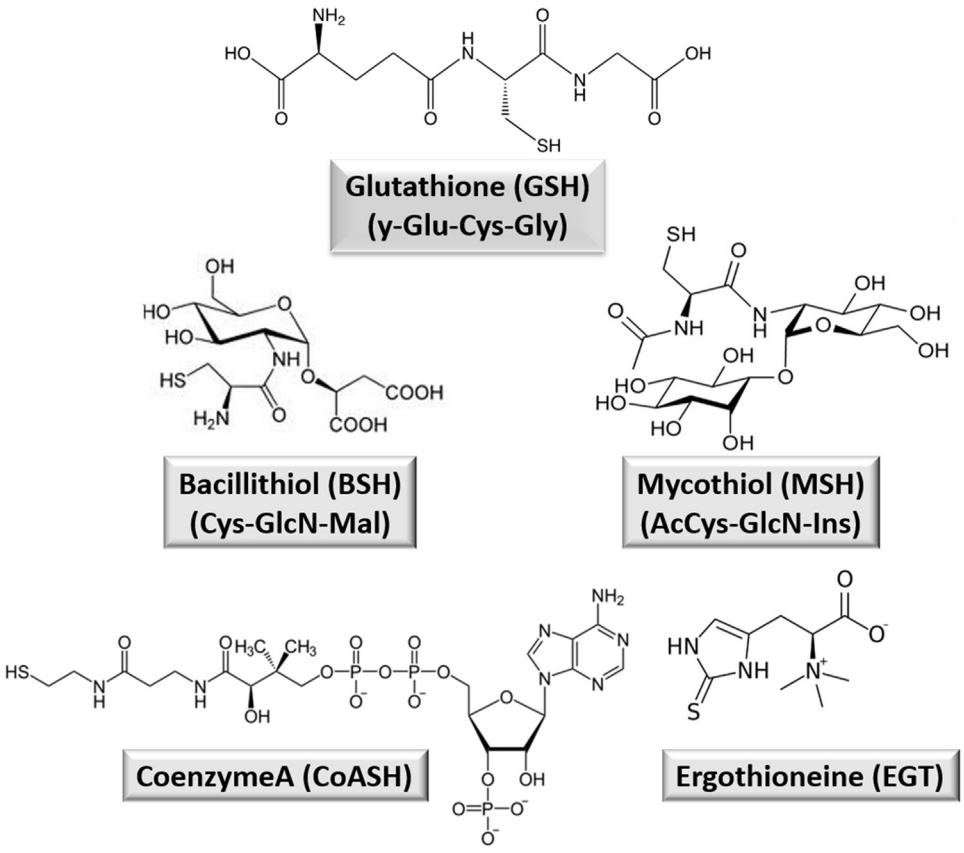

Fig. 1. Structures of major bacterial low molecular weight (LMW) thiols. The major LMW thiols are glutathione (GSH) present in Gram-negative bacteria and few Gram-positive bacteria. Bacillithiol (BSH) is the major LMW thiol in *Firmicutes*, such as *Bacillus* and *Staphylococcus* species. Mycothiol (MSH) is utilized in all *Actinomycetes*, including mycobacteria, corynebacteria and streptomycetes. Coenzyme A (CoASH) also serves as alternative LMW thiol-redox buffer in *S. aureus* and *B. anthracis*. Ergothioneine (EGT) is a histidine-derived alternative LMW thiol in mycobacteria.

for the defense against redox active compounds, xenobiotics, antibiotics, toxic metals and metalloids as reviewed previously [5]. Of note, GSH is an important cofactor of glyoxalases involved in detoxification of the toxic electrophile methyglyoxal as natural byproduct of the glycolysis in *E. coli* [7–10].

Apart from its well-studied detoxification functions, GSH contributes to the virulence of important human pathogens. The involvement of GSH in virulence has been studied in the extracellular facultative anaerobic pathogen *S. pneumoniae* as well as for the intracellular food-borne pathogens *L. monocytogenes* and *Salmonella enterica* subsp. Typhimurium (*S.* Typhimurium) [3,4,11–14]. The glutathione reductase Gor and the GSH-uptake system GshT protect *S. pneumoniae* against oxidative stress and toxic metal ions and are required for colonization and invasion in a mice model of infection [3]. *L. monocytogenes* is a facultative intracellular pathogen that has a saprophytic lifestyle in the soil and a parasitic in the host [15]. Specific evasion strategies enable to escape the phagolysosome and to proliferate inside the host cell cytosol. *L. monocytogenes* utilizes host-derived GSH, but can also synthesize bacterial GSH *via* the GshF fusion protein [14]. Bacterial and host-derived GSH are both important for virulence and expression of virulence factors in *L. monocytogenes*. The virulence mechanism involves activation of the positive regulatory factor A (PrfA) by allerosteric binding of GSH as cofactor to PrfA [13,14] **(**Fig. 3**)**. PrfA is a member of the CRP/FNR family and the master regulator for many virulence factors including the actin assembly factor ActA. ActA mediates actin polymerization and is essential for intracellular spread of the pathogen across host cells [15]. The structure of the PrfA-GSH complex has been recently determined to investigate the mechanisms for activation of PrfA upon GSH binding. GSH binding to a specific tunnel site of PrfA induces conformational changes in the tunnel site of PrfA that stabilizes the helix-turn-helix (HTH) motifs and primes PrfA for binding to the operator DNA [13]. Another structural study of the PrfA-GSH complex suggested that GSH binding induces local conformational changes in PrfA, allowing DNA binding and activation of gene transcription [16]. The GSH level and the reduced cytosol of the host cells further influence the virulence of *L. monocytogenes* [17]. Bacteria cultivated under reducing growth conditions in minimal medium with GSH had a higher PrfA activation state and virulence factor expression resulting in higher virulence in a murine infection model [17]. PrfA controls also listeriolysin O (LLO) as cholesterol-dependent cytolysin (CDC) required for host-cell lysis [15]. Interestingly, LLO was shown to be regulated by *S*-glutathionylation at a conserved Cys residue by host and bacterial derived GSH which inhibits its hemolytic activity to lyse red blood cells [18]. These two examples of PrfA and LLO highlight the important roles of GSH in activation of virulence factors expression and redox regulation in an important intracellular pathogen.

The intracellular pathogen *S.* Typhimurium, which causes gastroenteritis, resides inside a *Salmonella*-containing vacuole (SCV) and injects *Salmonella* pathogenicity island 2 effectors (SP-2) *via* a type-III-secretion system (T3SS) directly into the host cell. *S.* Typhimurium encounters oxidative stress by the phagocyte NADPH oxidase (Nox) that produces Reactive Oxygen Species (ROS) as oxidative burst. Reactive Nitrogen Species (RNS) are generated by the inducible NO synthase (iNOS) inside macrophages and neutrophils **(**Fig. 3**)**. In *S.* Typhimurium, GSH-deficient mutants displayed an increased sensitivity to ROS and RNS and were attenuated in an acute model of salmonellosis in $NRAMP^{R}$ mice that produces a high NO level [11]. Thus, GSH is important for the defense against ROS and RNS produced by Nox and iNOS as shown in the model of salmonellosis [11]. In addition, GSH was shown to be required for efficient transcription of the Spi-2 targets under NO stress. The Spi-2 system interferes with lysosomal trafficking and promotes intracellular replication inside the SCV [19,20]. Spi-2 reduces the contact between *Salmonella*-containing vacuoles (SCV) and NADPH phagocyte oxidase vesicles. Thus, Spi-2 protects *S.* Typhimurium against the oxidative burst inside macrophages by maintaining

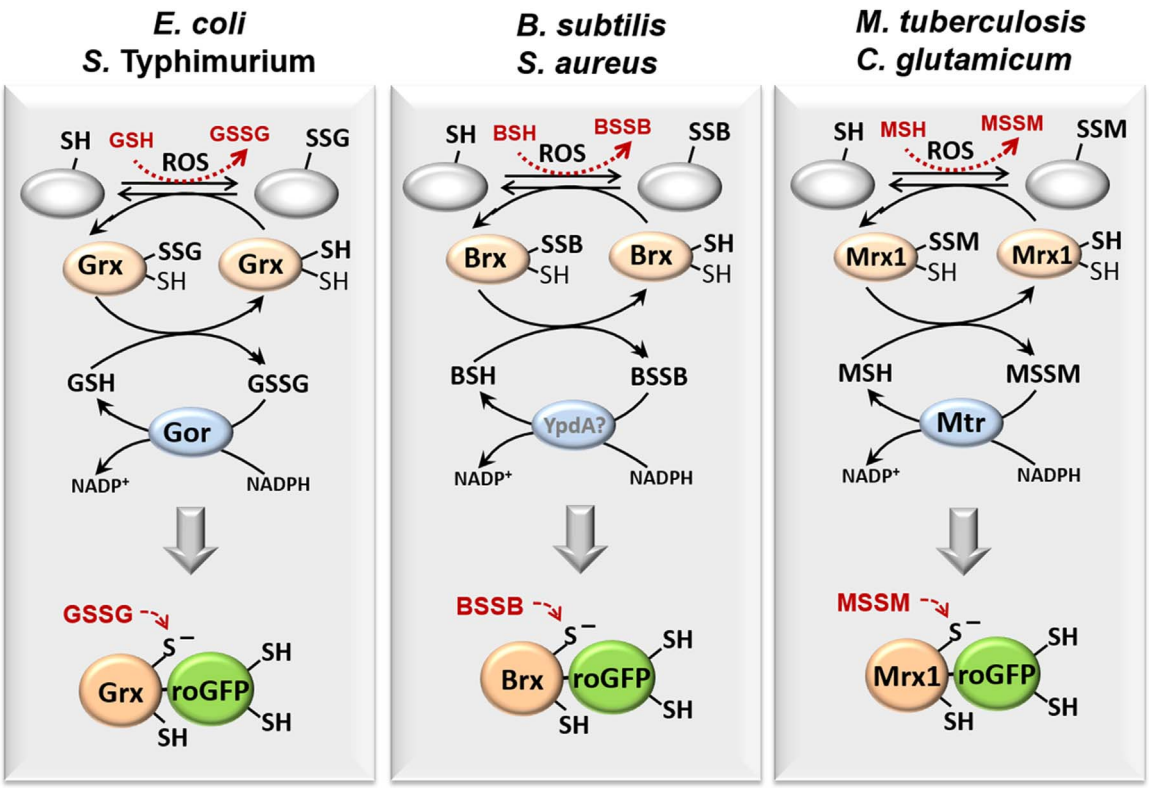

Fig. 2. Reduction of *S*-glutathionylations, *S*-bacillithiolations and *S*-mycothiolations by glutaredoxin, bacilliredoxin and mycoredoxin pathways and design of genetically encoded Grx1-roGFP2, Brx-roGFP2 and Mrx1-roGFP2 biosensors. The *S*-glutathionylated proteins are reduced by glutaredoxins (Grx) leading to a Grx-SSG intermediate that is reduced by GSH and the NADPH-dependent GSSG reductase (Gor). These pathways for reduction of *S*-glutathionylated proteins are present in *E. coli*, *S.* Typhimurium and other Gram-negative bacteria. Analogous bacilliredoxin and mycoredoxin pathways are present in BSH- and MSH-producing Gram-positive bacteria, such as *S. aureus* and *B. subtilis* as BSH producer and *M. tuberculosis* and *C. glutamicum* that utilize MSH. The *S*-bacillithiolated proteins are reduced by bacilliredoxins (Brx) leading to Brx-SSB formation. The regeneration of Brx-SSB could require BSH and perhaps the NADPH-dependent pyridine nucleotide oxidoreductase YpdA. In *Actinomycetes*, mycoredoxin1 (Mrx1) catalyzes reduction of *S*-mycothiolated proteins leading to Mrx1-SSM generation that is recycled by MSH and the NADPH-dependent MSSM reductase Mtr. The genetically-encoded biosensors were used to measure the dynamic changes of the intracellular redox potentials in eukaryotes and Gram-negative bacteria, such as *E. coli* and *S.* Typhimurium (Grx1-roGFP2) as well as in the Gram-positive bacteria *S. aureus* (Brx-roGFP2) and *M. tuberculosis* (Mrx1-roGFP2), respectively.

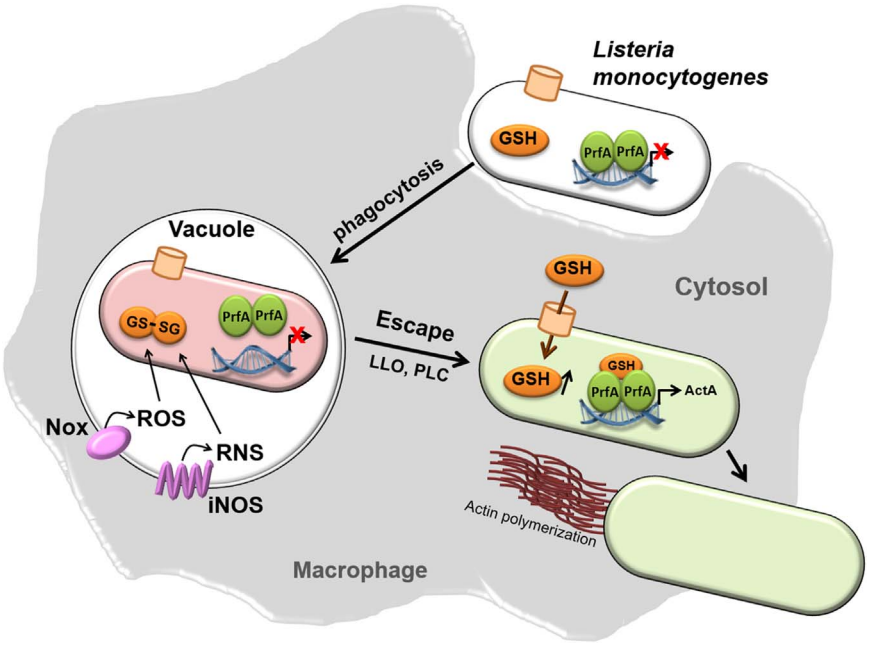

Fig. 3. Functions of GSH in PrfA activation for virulence factor expression in the intracellular pathogen *Listeria monocytogenes*. After phagocytosis by macrophages, the intercellular pathogen *L. monocytogenes* resides in an oxidizing vacuole (red), containing ROS and RNS that are produced by Nox and iNOS. *L. monocytogenes* has the ability to synthesize GSH, but can utilize GSH from host cells. In the oxidizing vacuole, GSH produced by *L. monocytogenes* is oxidized to GSSG, which does not bind the PrfA transcription factor [14]. *L. monocytogenes* escapes into the reducing host cell cytosol, leading to GSH regeneration and uptake of GSH from host cells. PrfA binds GSH and activates transcription of PrfA regulon genes, such as *actA*. ActA expression leads to Actin polymerization that allows movement of *L. monocytogenes* through host cells.
This figure is adapted from Ref. [14].

the intracellular thiol-redox balance [12,21]. The importance of this T3SS Spi-2 for ROS evasion was demonstrated using the roGFP2 biosensor as outlined in the biosensor section [12].

In *Yersinia pestis*, host-derived GSH functions in *S*-glutathionylation of the T3SS effector protein LcrV. *Y. pestis* causes bubonic plaques as extraordinary virulence mechanism and employs a T3SS for secretion of Yop effectors directly into the host cell cytoplasm [22]. These effectors function in pathogen evasion and neutralization of the host immune defense. The T3SS first secretes the LcrV protein, a plaque-protecting antigen that forms the needle cap protein of the T3SS and is essential for plaque pathogenesis [23,24]. LcrV is *S*-glutathionylated at Cys273 by host-derived GSH after its translocation and *S*-glutathionylation of LcrV is important for virulence of *Y. pestis* [25]. *S*-glutathionylated LcrV binds to host ribosomal protein S3 (RPS3), promotes effector secretion and macrophage killing. In addition, *S*-glutathionylation of LcrV contributes to bubonic plague pathogenesis in mice and rat models of infections [25]. In conclusion, GSH was shown to control expression and modification of virulence factors that are secreted by the T3SS in bacterial pathogens. Moreover, GSH is essential for survival under infection conditions in different pathogens, such as *S. pneumoniae, L. monocytogenes* and *S.* Typhimurium.

1.2. Functions of bacillithiol in the virulence and protein S-bacillithiolation in Gram-positive Firmicutes

The Gram-positive *Firmicutes* bacteria, such as *Bacillus* and *Staphylococcus* species utilize bacillithiol (BSH, Cys-GlcN-malate) as their major LMW thiol (Fig. 1) [26,27]. In *B. subtilis* and *S. aureus*, BSH is important for detoxification of many redox-active compounds. BSH-deficient mutants showed growth and survival defects after treatment with ROS, electrophiles, HOCl, toxins, alkylating agents, heavy metals and redox-active antibiotics, such as fosfomycin and rifampicin [28–30]. BSH functions as cofactor for thiol-dependent detoxification enzymes, such as thiol-*S*-transferases (FosB) and glyoxalases (GlxA/B). These thiol-dependent enzymes conjugate BSH to toxic electrophiles, fosfomycin and methylglyoxal for its detoxification [28,31]. BSH has also an impact on metal homeostasis and functions in Zn^{2+}-storage, FeS cluster assembly and copper buffering [32–35]. The standard thiol-redox potential of BSH was calculated as $E^{0'}$(BSSB/BSH) = − 221 mV and the BSH/BSSB ratios were determined as 100:1–400:1 under control conditions in *B. subtilis* cells [35–37]. Under NaOCl stress, the BSSB level is increased indicating a more oxidized BSH redox potential [38]. The NADPH-dependent pyridine nucleotide disulfide reductase YpdA is supposed to functions as BSSB reductase (Fig. 2), but its role in regeneration of BSH has not been demonstrated.

Of note, BSH has an important role for virulence in the major pathogen *S. aureus*. BSH protects *S. aureus* under infection-like conditions in phagocytosis assays using human and murine macrophages [29,30]. The survival of BSH-minus clinical MRSA strains was strongly impaired in human whole-blood survival assays [29]. The exact protective role of BSH inside the host is unknown, but the yellow antioxidant pigment staphyloxanthin was present at lower amounts in the absence of BSH [29]. *S. aureus* isolates carry many mobile genetic elements, such as prophages, pathogenicity islands, transposons and plasmids explaining their high genome diversity. Due to a former transposon or other insertion element, *S. aureus* NCTC8325 derivatives (*e.g.* SH1000) are *bshC* mutants and do not produce BSH [29,30,39]. Thus, also *S. aureus* SH1000 was impaired in survival inside murine macrophages and human epithelial cells and the phenotype could be restored by complementation with plasmid-encoded *bshC* [29,30]. Thus, BSH functions as virulence mechanism in the defense against the host immune system in *S. aureus* clinical isolates. Macrophages and neutrophils produce large quantities of ROS and HOCl as well as bactericidal ammonium chloramines during the oxidative burst [40–42]. Thus, the defense mechanism of BSH could involve regulatory mechanisms by formation of BSH mixed protein disulfides (*S*-bacillithiolations) in *S. aureus* inside neutrophils and macrophages.

To get insights into the targets for *S*-bacillithiolations in *S. aureus* under infection-like conditions, we have studied the quantitative thiol-redox proteome of *S. aureus* USA300 under NaOCl stress using the OxICAT approach [43]. In total, 58 Cys residues with > 10% increased thiol-oxidation could be quantified under NaOCl stress. In addition, five *S*-bacillithiolated were identified in *S. aureus* under NaOCl stress by shotgun proteomics. These *S*-bacillithiolated proteins showed the highest oxidation increase of > 29% in the OxiCAT analysis. The glyceraldehyde-3-phosphate dehydrogenase Gap was identified as most abundant *S*-bacillithiolated protein representing 4% of the total Cys abundance in the proteome. Protein *S*-bacillithiolation functions in redox regulation and protects the active site Cys151 of *S. aureus* Gap under H_2O_2 and NaOCl stress against overoxidation *in vitro* [43]. Future studies should reveal whether *S*-bacillithiolation of Gap or other proteins could provide protection of *S. aureus* under infection conditions inside macrophages and neutrophils. This adaptation to infection conditions in *S. aureus* could involve the metabolic re-configuration of central carbon metabolism as shown in eukaryotic organisms [44,45]. In yeast cells, Gap oxidation has been linked to the re-direction of the glycolytic flux into the pentose phosphate pathway (PPP) to increase NADPH levels. NADPH is used as electron donor for thioredoxin and glutathione reductases to recover from oxidative stress [44,45]. Similar mechanisms could be relevant also for *S. aureus* to enhance survival under infection conditions.

Apart from BSH, *S. aureus* produces also coenzymeA (CoASH) as abundant alternative LMW thiols and essential cofactor in cellular metabolism. Moreover, a CoASH disulfide oxidoreductase (Cdr) is encoded in the genome of *S. aureus* that could be involved in reduction of CoAS disulfides [27]. However, the functions of CoASH and Cdr for the redox regulation of proteins by CoA-thiolations are unknown in *S. aureus*. Recently, CoA-thiolation was shown in mammalian cells as a widespread post-translational redox modification under oxidative stress [46]. Numerous Cys peptides with CoA-thiolation sites were detected in H_2O_2-treated heart cells and in the mitochondria of liver cells from starved rats [46]. The authors developed a monoclonal antibody for enrichment of CoA-thiolated proteins and identified 80 CoA mixed disulfides (58 proteins) in heart cells and 43 CoA-thiolated Cys peptides (33 proteins) in liver cells using mass spectrometry. Many CoA-thiolated proteins function in main metabolic pathways, like the TCA cycle and the beta-oxidation pathway of fatty acids. These pathways involve activated CoA-derivatives, such as acetyl-CoA indicating that CoA metabolism and CoA-thiolation are functionally connected. It was also demonstrated that CoA-thiolation can inactivate enzymes and function in redox regulation of the glycolytic GapDH, the isocitrate dehydrogenase IDH and other metabolic enzymes [46]. Thus, it will be interesting to reveal if GapDH and other *S*-bacillithiolated proteins are also targets for CoA-thiolation in *S. aureus* under NaOCl stress.

The reduction of *S*-bacillithiolated proteins is catalyzed by bacilliredoxins (BrxA and BrxB) that belong to DUF1094 family. Brx proteins possess an unusual CGC motif, but function similar like glutaredoxins in *B. subtilis* and *S. aureus* (Fig. 2) [43,47]. Thus, Brx of *S. aureus* has been used to construct the first Brx-roGFP2-fused biosensor to measure changes in the BSH redox potential in *S. aureus* under oxidative stress and infection conditions inside human macrophages as outlined in the biosensor section.

1.3. Functions of mycothiol in the virulence and protein S-mycothiolation in Actinomycetes

Mycothiol (MSH; NAc-Cys-GlcNAc-myoinositol) is the major LMW thiol in high-GC Gram-positive *Actinomycetes,* including *Streptomycetes*, *Mycobacterium* and *Corynebacterium* species (Fig. 1) [48,49]. Under oxidative stress, MSH is oxidized to MSH disulfide (MSSM) and maintained in a reduced state by the mycothiol disulfide reductase Mtr. MSH is involved in detoxification of numerous compounds, such as ROS,

RES, alkylating agents, toxins, antibiotics (erythromycin, vancomycin, rifampin, azithromycin), heavy metals and toxic metalloids, aromatic compounds, ethanol and glyphosate as studied in different *Actinomycetes* [48,50–53]. In *Streptomyces lincolnensis*, MSH participates in the biosynthesis of the sulfur-containing antibiotics lincomycin [54]. For more details of these many detoxification functions of MSH and MSH-dependent enzymes, the reader is referred to previous and recent reviews [28,55].

Under hypochlorite stress, MSH was shown to form mixed disulfides with protein thiols, termed as protein *S*-mycothiolation [56–58]. Protein *S*-mycothiolation protects protein thiols against the formation of sulfinic and sulfonic acids and regulates protein activities, as demonstrated in *Corynebacterium glutamicum, Corynebacterium diphtheriae* and *Mycobacterium smegmatis*. About 25 *S*-mycothiolated proteins were identified in *C. glutamicum* [56], 26 proteins in *C. diphtheriae* [58] and 58 in *M. smegmatis* under NaOCl stress [57]. Among the S-mycothiolated proteins, several are conserved *S*-thiolated at their active sites Cys residues in different Gram-positive bacteria, including thiol-peroxidases/peroxiredoxins (Tpx, AhpC), ribosomal proteins (RpsM, RplC), the IMP dehydrogenase (GuaB), the myo-inositol-1-phosphate synthase (Ino1), the methionine synthase (MetE) and the glycolytic GapDH [38,56]. The extend of protein *S*-mycothiolation correlates with the different MSH levels in corynebacteria and mycobacteria [59]. While *M. smegmatis* contains 6 μmol/g raw dry weight (rdw) MSH [57], only 0.3 μmol/g rdw were determined in *C. diphtheriae* [58]. Thus, corynebacteria most likely utilize also alternative LMW thiols which remains to be investigated.

Mycobacteria utilize the histidine-derivative ergothioneine (EGT) as another alternative LMW thiol. MSH and EGT are both required for full virulence and redox homeostasis of *Mycobacterium tuberculosis* (*Mtb*) [60,61]. Both LMW thiols contribute also to full peroxide resistance of *M. smegmatis* [62]. EGT levels are even increased in the *mshA* mutant confirming that EGT can compensate for the absence of MSH [63]. Our redox proteomics studies revealed an increased thiol-oxidation level in the *M. smegmatis mshC* mutant which could involve alternative *S*-ergothionylation which remains to be elucidated [57]. However, in contrast to MSH, EGT is actively secreted into the supernatant [62]. Future studies should be directed to study the role of EGT secretion in regulation of EGT levels, modulation of host ROS levels and *S*-thiolation of bacterial and host proteins during infections.

Protein *S*-mycothiolation is redox-regulated by both, the mycoredoxin and thioredoxin pathways as demonstrated for thiol peroxidases (Tpx, Mpx, AhpE), the methionine sulfoxide reductase (MsrA) and the glycolytic GapDH *in vitro* [56,58,64–66]. Reduction of *S*-mycothiolated GapDH occurred much faster by Mrx1 compared to Trx *in vitro* indicating that Mrx1 is probably the main de-mycothiolating enzyme *in vivo* [58]. In addition, *S*-mycothiolation of GapDH is faster compared to its overoxidation *in vitro*. The methionine synthase MetE was further protected by *S*-mycothiolation under acid stress conditions in *C. glutamicum* [67]. These results indicate that *S*-mycothiolation can efficiently protect the active site Cys residues against overoxidation to sulfinic or sulfonic acids and can be reversed by both, the Mrx1 and Trx pathways. Mrx1 was used to construct the first MSH specific genetically encoded biosensor Mrx1-roGFP2 to measure changes in the MSH redox potential.

Apart from *S*-mycothiolation, MSH plays also an important role for growth, survival and antibiotics resistance under infection conditions in the major pathogen *Mtb* [61,68]. *Mtb* is the etiologic agent of tuberculosis (TB) disease resulting in about 2 million human death each year [69]. Due to the slow intracellular growth of *Mtb* inside the phagosomes of macrophages, TB patients have to be treated with antibiotics for several months, resulting in multiple and extreme drug resistant *Mtb* isolates (MDR/XDR) as a major health burden. MSH is involved in the activation of the first-line anti-TB drug isoniazid (INH) in *Mtb* [70]. INH is a pro-drug that is activated by the catalase KatG and MSH resulting in a NAD-INH adduct that finally inhibits InhA of the mycolic acid biosynthesis pathway [71]. Thus, the evolved INH resistant *Mtb* isolates often carry spontaneous mutations in *katG*, *mshA* and in the target gene *inhA* [51]. This requires alternative drug developments to treat emerging resistant *Mtb* isolates. Since MSH is important for virulence of *Mtb*, inhibitors of MSH biosynthesis and recycling have been successfully applied in combination therapies that target MshB, MshC, Mtr and the MSH-*S*-conjugate amidase Mca as new anti-TB drugs [72]. Moreover, ROS-producing compounds have been designed and may have a great potential to tackle anti-tuberculosis drug resistance. In the later sections, we will highlight recent work in drug research showing the power of the genetically encoded Mrx1-roGFP2 biosensor to study the role of MSH in antibiotics resistance, to reveal the involvement of ROS in the killing mode of antibiotics under infection conditions and to develop new combination therapies involving ROS-producing compounds.

2. Dynamic redox potential measurements using roGFP2-based biosensors in pathogens

The development of redox-sensitive green fluorescent proteins (roGFPs) has enabled the ratiometric measurement of the cellular redox potential at high sensitivity and spatiotemporal resolution using live-imaging approaches [73–76]. For construction of roGFPs, two redox-active Cys residues (Cys147 and Cys204) were introduced in the GFP molecule that form a disulfide bond upon oxidation resulting in conformational changes of the chromophore and fluorescence changes [76]. The roGFP2 biosensor has two excitation maxima at 405 and 488 nm, which change upon oxidation resulting in a ratiomeric biosensor response [74,77]. The Cys pair in roGFPs has been shown to equilibrate with the GSH/GSSG redox couple and the probes are widely used to measure the changes in the GSH redox potential in living eukaryotic cells [76]. However, the equilibration of endogenously expressed roGFPs with the GSH/GSSG pair is too slow and limited by the Grx expression levels. The Grx levels vary also in different compartments and are rate-limiting factors in the thiol-disulfide exchange reactions between the probe and the GSH pool.

To facilitate the specific response of roGFP2 with the GSH/GSSG redox couple, human glutaredoxin was fused to roGFP2 to construct the Grx1-roGFP2 biosensor for real-time measurements of the dynamic changes in the GSH redox potential (E_{GSH}) in eukaryotic organisms [75]. The Grx1-roGFP2 biosensor responds much faster within seconds to nanomolar concentrations of GSSG compared to unfused roGFP2 [74,75]. Thus, the Grx1-roGFP2 probe is highly specific and detects small changes in the GSH redox potential in living eukaryotic cells. To date, roGFP2 and Grx1-roGFP2 biosensors have been applied in many eukaryotic organisms and pathogens to study intracellular redox changes in *Arabidopsis thaliana, Caenorhabditis elegans* [75,78,79], yeast cells and the malaria parasite *Plasmodium falciparum* [80]. In particularly, pathogens are well suited to analyze the effect of drugs on the cellular redox metabolism and hence, the biosensors can help to screen for novel ROS-producing drugs. In this part of the review, we will present an overview about the application of roGFP2 biosensors in major human pathogens, including the foodborne intracellular pathogen *S*. Typhimurium, the extracellular Gram-positive pathogen *S. aureus* and in the intracellular major pathogen *M. tuberculosis*. Altogether, the biosensor results have advanced our understanding of the mechanisms of survival and intracellular replication, ROS evasion and persistence as well as antibiotics resistance in many important human pathogens.

2.1. Dynamic roGFP2-based biosensors to measure redox changes in Gram-negative bacteria

The roGFP2 biosensors were first applied in Gram-negative bacteria to measure the redox changes during growth, under oxidant and antibiotics treatment as well as infection conditions. In *E. coli*, plasmid-

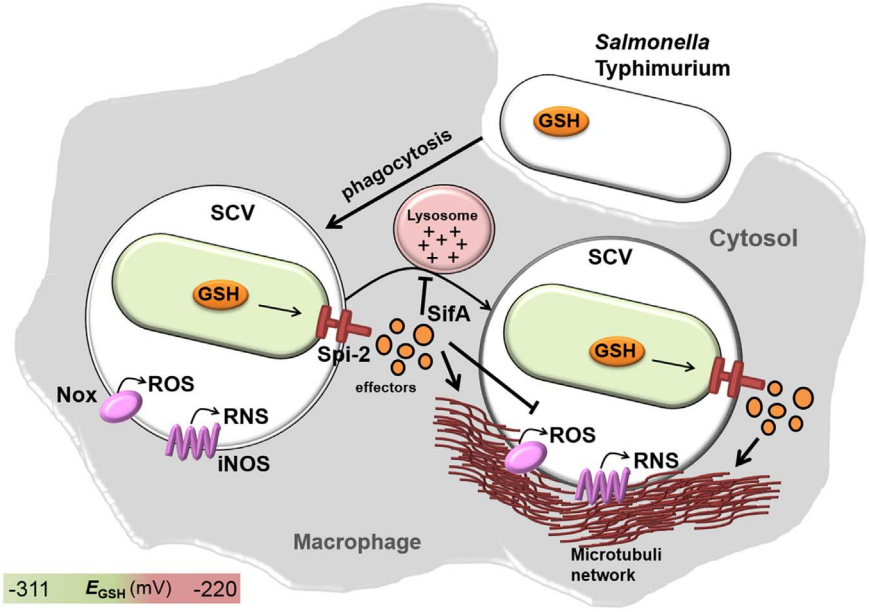

Fig. 4. Mechanisms of ROS evasion allowing intracellular replication of *Salmonella* Typhimurium inside the SCV to escape the host immune defense as revealed by the roGFP2 biosensor. The intracellular pathogen *S*. Typhimurium produces GSH and replicates inside macrophages in a *Salmonella*-containing vacuole (SCV). *S*. Typhimurium escapes ROS in the SCV by the type-III-secretion system Spi-2 that injects effectors directly into the host cell cytoplasm. GSH is required for transcription of the Spi-2 targets under NO stress. *S*. Typhimurium cells are highly reduced (green) inside in the SCV, while those that escape into host cells cytoplasm are oxidized [12]. The Spi-2 effector SifA affects co-localization of SCV and Nox vesicles and controls the vacuole integrity *via* microtubuli formation, which contributes to ROS evasion [12]. The Spi-2 effectors also interfere with lysosomal trafficking, promoting intracellular replication inside the SCV [19,20]. Thus, the Spi-2 system *via* its effector SifA functions in ROS evasion, controls vacuole integrity and maintains the intracellular redox balance of *S*. Typhimurium inside the SCV to allow intracellular replication [12].

encoded roGFP2 was used to observe cellular oxidation in response to different oxidants, toxic heavy metals and metalloids [81,82]. Toxic biocides, pollutants and metalloids are often found as environmental contaminants and originate from anthropogenic and natural sources. Thus, roGFP2 served as diagnostic tool to measure oxidative stress in *E. coli* by toxic environmental contaminants. Low levels of 0.1–1 mM H_2O_2 resulted in a rapid roGFP2 biosensor response. The roGFP2 biosensor showed also a fast response to heavy metals, such as Cd^{2+}, Zn^{2+}, Cu^{2+}, Pb^{2+}, arsenite and selenite as well as biocides and redox-cycling agents (menadione, naphthalene). However, quantification of the biosensor response using the microplate reader was not possible after exposure to toxic heavy metals or metalloids due to instability of the roGFP2 biosensor [81]. To increase roGFP2 stability, *E. coli* cells expressing the roGFP2 biosensor were immobilized in a transparent *k*-carrageenan (KC) matrix for further toxicity measurements [83]. The detection limit to measure a biosensor response was defined as 0.2 µg/l for arsenite and 5.8 ng/l for selenite. These immobilized roGFP2 expressing *E. coli* cells were applied to screen for bioavailability and toxic effects of pollutants [83].

2.1.1. The T3SS Spi-2 contributes to ROS evasion in S. Typhimurium

The first physiological studies in pathogenic Gram-negative bacteria using roGFP2 biosensors were performed in the intracellular pathogen *S*. Typhimurium that replicates inside the SCV [12]. *S*. Typhimurium escapes ROS by the T3SS Spi-2 that injects effectors directly into the host cell cytoplasm (Fig. 4). Thus, the biosensor was used to elucidate whether the T3SS Spi-2 contributes to evasion from the host innate immune defense to escape ROS and RNS. The intrabacterial redox changes were measured in *S*. Typhimurium after infection of HeLa cells and THP-1 cells that produce different ROS levels. In addition, the influences of the Spi-2 system and its effector SifA on ROS evasion strategies were investigated using *ssaR* and *sifA* mutants which are reviewed in this part.

S. Typhimurium encounters an acidic environment inside macrophages. Thus, it was first confirmed that the purified roGFP2 probe is not pH-sensitive *in vitro*. Next, the biosensor response inside *S*. Typhimurium cells was measured after treatment with H_2O_2 and the NO donor SpermineNONOate since *S*. Typhimurium has to cope with ROS and RNS that are produced by Nox and iNOS after phagocytosis. The roGFP2 biosensor responds very fast and reversible to 50–500 µM H_2O_2, but only high concentrations of 25 mM H_2O_2 lead to full oxidation of the probe inside *S*. Typhimurium. However, due to the detoxification by catalases and peroxidases, cells could quickly regenerate the reduced state even after treatment with high H_2O_2 levels. In contrast, exposure to 5–20 mM of the NO-donor resulted in a strongly increased biosensor oxidation with no recovery of the reduced state. These experiments verified that the probe detects intrabacterial redox changes under physiological micromolar ROS and RNS challenge.

To analyze the redox changes in *S*. Typhimurium after infection of host cells, epithelium-like HeLa cells and macrophages-like THP-1 cells were used. Interestingly, *S*. Typhimurium replicating inside THP-1 cells experienced higher levels of redox stress compared to bacteria infected in HeLa cells. The THP-1 cell line is known to produce higher ROS levels and is able to kill the majority of *S*. Typhimurium cells [12]. Moreover, redox stress heterogeneity was observed between different *S*. Typhimurium cells that maybe important to understand persistence and antibiotic resistance mechanisms.

In human and murine macrophages it was further shown that *S*. Typhimurium cells experience more redox stress in the cytosol compared to that residing in the SCV indicating that replication inside the vacuole contributes to ROS evasion. Thus, the role of the T3SS Spi-2 as ROS evasion strategy inside the SCV was investigated in the *ssaR* mutant that lacks the functional Spi-2 system (Fig. 4) [12]. The *ssaR* mutant displayed a higher oxidation level in THP-1 cells compared to the wild type indicating that the Spi-2 system contributes to ROS evasion. Previous studies revealed that Spi-2 effectors affect co-localization of SCV and phagocyte Nox vesicles, which contributes to ROS evasion [12,21]. Among the Spi-2 effectors, SifA was shown to control vacuole integrity as ROS evasion strategy. The biosensor measurements revealed that ROS evasion by the Spi-2 system requires an intact SCV since the *sifA* mutant experienced a higher redox stress [12]. Thus, the Spi-2 system functions *via* its effector SifA in ROS evasion to maintain the reduced state of the cytoplasm and to allow intracellular survival of *S*. Typhimurium [12].

2.1.2. Regulation of H_2O_2 detoxification and ROS-generation by antibiotics and toxic metals

Bacteria have evolved different antioxidant enzymes for ROS detoxification, such as catalases, thiol-dependent peroxidases, peroxiredoxins and superoxide dismutase [84]. The role of many H_2O_2 scavenging enzymes is often unknown in bacteria [85] and hence roGFP2 biosensors can contribute to study the dynamics and activity of ROS-degradation by the different bacterial enzymes. Thus, the roGFP2 biosensor was applied to measure redox changes and the ROS

detoxification capacity after treatment with H_2O_2, toxic heavy metals and antibiotics across different Gram-negative bacteria, including non-pathogenic and pathogenic *E. coli*, *Citrobacter rodentium*, *Yersinia pseudotuberculosis*, *Salmonella enterica* serovar Typhi and *S.* Typhimurium [86]. Using specific mutants in catalases and peroxidases, the kinetics of H_2O_2 detoxification was monitored for each antioxidant enzyme in different bacteria. Although the bacterial species were evolutionary related, the activities of their H_2O_2 detoxification enzymes showed strong variations. This enabled also to measure the ROS detoxification capacity of *S.* Typhimurium during priming with sub-lethal doses of 500 μM H_2O_2 and subsequent challenge with higher doses of 1 mM H_2O_2 compared to naïve cells. The primed bacteria could faster detoxify 1 mM H_2O_2 and recover to the reduced state compared to naïve bacteria [86].

In *S.* Typhimurium, the biosensor further allowed to measure endogenous ROS production in a catalase/peroxidase-negative *hpxf* mutant during different growth phases, media and temperatures. The endogenous ROS levels were highest during the later exponential growth at 37 °C in rich media compared to minimal medium. Thus, optimal growth conditions that allow a maximum growth rate correlate with high oxygen consumption and increased ROS generation. Similar as in the first *E. coli* roGFP2 approach [83], the toxicity of metals was assessed due to ROS production using the biosensor in *S.* Typhimurium [86]. While certain metal ions are required for H_2O_2 detoxification, exposure of *S.* Typhimurium to zinc and nickel contributed to ROS generation by inhibition of ROS detoxification enzymes (zinc) or spontaneous thiol-oxidation (nickel).

Next, biosensor measurements were performed under antibiotics treatment to validate whether ROS are involved in the killing mode of antibiotics, a continuous and controversial debate among microbiologists [87–89]. The oxidation-sensitive *S.* Typhimurium *hpxf* mutant was exposed to different antibiotics classes, including aminoglycosides, quinolones, cephalosporine and β-lactam antibiotics, but no increased biosensor oxidation could be monitored. This indicates that these antibiotics classes do not enhance endogenous ROS as killing mode in the *S.* Typhimurium *hpxf* mutant [86]. In contrast, Shukla and coworkers [90] showed that exposure to ampicillin, amikacin and ciprofloxacin leads to an impaired redox balance and increased biosensor oxidation in *E. coli*. Moreover, hydrogen persulfide (H_2S) was shown to protect *E. coli* against oxidative stress triggered by bactericidal antibiotics which is controlled by two mechanisms. H_2S mediated antibiotic tolerance involves rerouting of the electron flow from the energy-efficient cytochrome bo oxidase (Cyo) to the less-energy efficient cytochrome bd oxidase (CydBD) to maintain the respiratory flux and the redox balance. In addition, H_2S enhances the activities of the antioxidant enzymes catalase and superoxide dismutase which contributes to ROS detoxification under antibiotics treatments [90].

In *S.* Typhimurium, the roGFP2 biosensor was further applied to determine the real-time H_2O_2-influx [91]. The H_2O_2-influx was calculated by multiplication of the membrane permeability coefficient (P), the membrane surface area (A) and the difference between the inner and outer H_2O_2 concentrations (ΔC) as revealed by the degree of biosensor oxidation. The results showed that H_2O_2 first enters the cells by passive diffusion which is suddenly stopped, also termed as “switching point”. This stop in the H_2O_2 influx was caused by changes in the outer membrane permeability, as verified by spheroplasts lacking an outer membrane. The spheroplasts exhibited a significantly faster H_2O_2-influx without the “switching point”. The outer membrane proteins OmpA and OmpC were shown to regulate the H_2O_2 influx by opening and closing of their beta barrel structures [91].

Altogether, the roGFP2 biosensor has been widely used to measure the intrabacterial redox changes in several Gram-negative bacteria during the growth and under treatment with ROS and redox-active compounds, such as toxic metals and antibiotics as well as during infection and intracellular replication. The results revealed surprising differences in the H_2O_2 detoxification kinetics by antioxidant enzymes, such as catalases and peroxidases across closely related bacteria. Different antibiotics did not caused increased ROS-formation in a *S.* Typhimurium ROS-sensitive mutant [86], while Shukla and coworkers [90] revealed enhanced roGFP2 oxidation by antibiotics in *E. coli* cells. These different studies using the same roGFP2 biosensors further contribute to the controversial debate about the involvement of ROS in the killing mode of antibiotics. Moreover, roGFP2 biosensor measurements revealed that H_2O_2-influx is regulated by switching point due to OMPs that can open and close their beta-barrel. Of particular importance are further the roGFP2 biosensor measurements of *S.* Typhimurium inside the SCV. It was shown that the type-III-secretion system Spi-2 is required for ROS evasion and this depends on an intact vacuole. The bacteria were protected against ROS inside the SCV while bacteria that escaped into the host cell cytoplasm were more oxidized by ROS.

However, as critical remark, it has to be mentioned that the authors used only uncoupled roGFP2 for all measurements of the intrabacterial redox potential in *S.* Typhimurium. The unfused roGFP2 biosensor suffers from its low specificity for the GSH/GSSG redox couple and the limited availability of endogenous Grx. Thus, whether the roGFP2 probe specifically responds to GSH redox potential changes or other redox signals is not known. Future studies should be performed using the Grx1-roGFP2 biosensor which is highly specific to measure ratiometric changes in the GSH redox potential [75]. It will be also interesting to apply the Grx1-roGFP2 biosensor to study the mechanisms of ROS evasion in other GSH-utilizing intracellular pathogens, such as *L. monocytogenes* and *Legionella pneumophila*.

2.2. Dynamic measurement of the BSH redox potential (E_{BSH}) using the Brx-roGFP2 biosensor in the human pathogen S. aureus

We have recently fused bacilliredoxin (Brx) of *S. aureus* to roGFP2 to construct the first genetically encoded Brx-roGFP2 biosensor for dynamic measurement of the intracellular BSH redox potential (E_{BSH}) in *S. aureus* [92]. The BSH redox potential changes were determined during the growth, under ROS and NaOCl stress, during infection inside THP-1 macrophages and antibiotics treatments in two clinical MRSA isolates COL and USA300. In both MRSA strains, BSH enhances the survival during phagocytosis with human and murine macrophage-like cell lines [29,30]. Brx-roGFP2 is highly specific for physiological levels of 10–100 μM BSSB which depends on the Brx active site Cys *in vitro*. Thus, Brx-roGFP2 facilitates rapid equilibration of the biosensor with the BSH/BSSB couple to determine the changes in the BSH redox potential inside *S. aureus*.

First, an increased biosensor oxidation was measured in *S. aureus* COL and USA300 in rich medium during the stationary phase compared to the log phase. The dynamic range of Brx-roGFP2 was higher in COL compared to USA300, which may depends on their different BSH levels [29]. USA300 is a highly virulent CA-MRSA strain, which produces many unique virulence factors encoded on prophages, pathogenicity islands and other mobile genetic elements [93]. In addition, USA300 has a higher level of BSH compared to COL. Thus, the biosensor response of USA300 could be lower under diamide stress resulting in a lower dynamic range of fully reduced *versus* oxidized probes. In addition, strain USA300 could be less permeable or more resistant to diamide compared to COL, leading only to partial biosensor oxidation. Future studies should involve other strong oxidants, such as cumene hydroperoxide or redox cycling agents for full oxidation of the biosensor to increase the dynamic range in USA300.

Treatment of *S. aureus* COL with different oxidants resulted in a fast biosensor response, but at different oxidation degrees. While doses of 50–100 μM NaOCl stress lead to the fully oxidation of the biosensor, exposure of *S. aureus* to 1–10 mM H_2O_2 revealed only a slightly increased oxidation degree with rapid regeneration of the reduced state. This lower biosensor response under H_2O_2 stress might be due to the high H_2O_2 resistance of *S. aureus* which is able to survive up to 300 mM H_2O_2 [94]. We further measured the changes in BSH redox potential

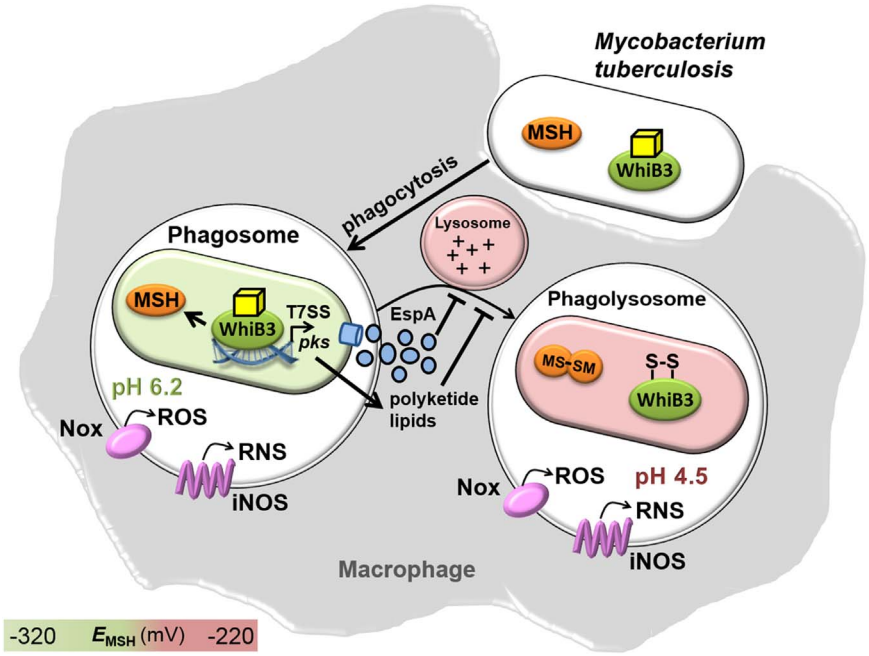

Fig. 5. The role of E_{MSH} and the WhiB3 transcription factor in *M. tuberculosis* persistence under acidic conditions during infection of macrophages as shown by the Mrx1-roGFP2 biosensor. *M. tuberculosis* is an intracellular pathogen that replicates inside the acidic phagosome of macrophages (pH ~ 6.2) preventing phagosomal maturation to phagolysosomes as survival mechanism. During immune activation of macrophages, phagosomes are fused with lysosomes resulting in further pH decrease to pH 4.5. The mild acidification in phagosomes causes a highly reduced E_{MSH} inside *M. tuberculosis*, while strong acidification leads to oxidized E_{MSH} as measured in phagolysosomes [96]. The WhiB3 transcription factor senses acidic conditions in the phagosome and activates transcription of WhiB3 regulon genes, such as type-VII-secretion system effectors (EspA) and polyketide lipids that inhibit phagosomal maturation. WhiB3 causes up-regulation of antioxidant systems (MSH, Trx) to restore the redox balance and to promote survival and persistence of *M. tuberculosis* inside the phagosome.
This figure is adapted from Ref. [96].

inside *S. aureus* COL after infection of THP-1 macrophages using flow cytometry. The Brx-roGFP2 biosensor was 87% oxidized in *S. aureus* COL inside macrophages indicating that *S. aureus* experiences oxidative stress after internalization. In future studies, the redox dynamics of persister cells inside macrophages should be investigated to reveal the BSH redox dynamics during internalization, which is often the cause of chronic *S. aureus* infections.

The biosensor response was also measured in *S. aureus* COL and USA300 *bshA* mutants and in RN4220, which is a natural *bshC* mutant of the NCTC8325-4 lineage. Brx-roGFP2 was fully oxidized in the BSH-deficient mutants indicating an impaired redox balance in the absence of BSH. In previous studies, a lower NADPH level was found in the *bshA* mutant perhaps explaining its impaired redox balance [29]. To clarify whether ROS generation contributes to the killing mode of antibiotics, *S. aureus* was exposed to sub-lethal doses of different antibiotics classes, including rifampicin, fosfomycin, ampicillin, oxacillin, vancomycin, aminoglycosides and fluoroquinolones. However, no increased oxidation degree of the Brx-roGFP2 biosensor was measured under antibiotics treatment, which confirms the findings in *S.* Typhimurium [86]. However, the biosensor responds fast to oxidants and could be a valuable tool in drug-research to screen for new ROS-generating antibiotics that affect the BSH redox potential in *S. aureus.* Future studies should be directed to measure the ROS detoxification capacity in mutants lacking antioxidant systems and in MRSA-isolates of various genetic lineages to unravel the link between ROS resistance and the BSH redox potential in *S. aureus*.

2.3. Dynamic measurements of the MSH redox potential (E_{MSH}) in *Mycobacterium tuberculosis* using the Mrx1-roGFP2 biosensor

In *Mtb,* an analogous Mrx1-roGFP2 biosensor was developed for dynamic measurements of the MSH redox potential (E_{MSH}) in drug-resistant isolates and inside the acidic phagosomes of macrophages [74,95,96]. The increasing prevalence of persistent and chronic relapsing *Mtb* infections as well as multiple and extreme drug-resistant (MDR/XDR) *Mtb* isolates are a major health burden. Thus, the development of new drugs against severe tuberculosis infections is an urgent need. The new biosensor was successfully applied to screen for ROS-generating anti-TB drugs and combination therapies (*e.g.* augmentin or isoniazid combinations) that affected E_{MSH} to study drug actions linked to the E_{MSH} to combat life-threatening TB infections [95,97–99]. It was revealed that the E_{MSH} inside infected macrophages is heterogeneous with sub-populations that have reduced, oxidized and basal levels of E_{MSH}. This redox heterogeneity depends on sub-vacuolar compartments inside macrophages and the cytoplasmic acidification that requires WhiB3 as central redox regulator [95,96]. These results using the Mrx1-roGFP2 biosensor have advanced the understanding how this major pathogen copes with anti-TB drug and persists inside macrophages. The major results obtained with Mrx1-roGFP2 are summarized in this part of the review.

After construction of the Mrx1-roGFP2 biosensor, it was demonstrated that the Mrx1-roGFP2 fusion is specific to measure MSSM, but does not respond to other LMW thiol-disulfides [95]. It was further controlled that overexpression of Mrx1-roGFP2 does not affect cellular metabolism, stress resistance and the basal level of E_{MSH} in *Mtb* [95]. Importantly, differences were observed in the biosensor response between slow growing *Mtb* strains and fast growing *M. smegmatis* resulting in a delayed response to H_2O_2 in *Mtb* and a rapid H_2O_2 response in *M. smegmatis* [95]. However, there was only little variation between the basal E_{MSH} in various drug-resistant (MDR/XDR) and drug-sensitive clinical *Mtb* isolates during laboratory growth, where the intracellular E_{MSH} was calculated as highly reduced with values of − 273 mV to − 280 mV [95]. However, in slow growing *Mtb* strains the E_{MSH} is more oxidizing compared to fast growing *M. smegmatis*. In *M. smegmatis*, a basal E_{MSH} of − 300 mV was calculated which is consistent with the higher MSH/MSSM ratio (200:1) in *M. smegmatis* compared to that in *Mtb* (50:1) [100].

2.3.1. E_{MSH} redox heterogeneity in Mtb sub-populations depends on specific vacuole compartments

In general, different *Mtb* strains did not show strong variations in their intracellular E_{MSH} when grown under *in vitro* conditions in growth media. However, this was completely different under *in vivo* infection conditions. Different *Mtb* sub-populations with reduced (− 300 mV), oxidized (− 240 mV) and basal E_{MSH} (− 270 mV) could be observed and quantified by flow cytometry under infection conditions inside THP-1 macrophages [95]. It was further shown that the reduced E_{MSH} sub-population is decreased and the oxidized E_{MSH} sub-population is increased at later time points of macrophage infections which correlates with a decreased MSH/MSSM ratio [95]. Thus, the intramacrophage

environment induces redox heterogeneity with different E_{MSH} sub-populations in *Mtb*. Of note, the sub-populations with reduced, oxidized and basal E_{MSH} were different during the time course of infections and also between various MDR/XDR *Mtb* isolates indicating a strongly varying redox balance between *Mtb* isolates. Immune activation further leads to an oxidative shift of *Mtb* sub-populations, which resulted from NO stress as part of host innate immune defense [95].

Mtb is an intracellular pathogen, that is engulfed by macrophages and trapped in an organelle, called the phagosome **(**Fig. 5**)**. Phagosomal maturation occurs by the interaction of phagosomes with endosomes and fusion with lysosomes to phagolysosomes, a highly acidic and microbicidal compartment that finally degrades invading bacteria [101]. However, *Mtb* successfully restricts phagosomal maturation by preventing fusion of phagosomes with lysosomes. This enables *Mtb* to persist and replicate inside the phagosome to cause chronic and relapsing *Mtb* infections [102,103]. It was suggested, that the different sub-vacuolar compartments might induce this E_{MSH} redox heterogeneity in *Mtb* [95]. The *Mtb* sub-populations were investigated in different vacuolar compartments including early endosomes, autophagosomes and lysosomes. Interestingly, the *Mtb* sub-population located in autophagosome showed almost oxidized E_{MSH}, while those residing in lysosomes were 58% oxidized and the sub-population in early endosomes showed mostly (54%) reduced E_{MSH}. Thus, the biosensor identified the sources of redox heterogeneity as the specific compartments in which *Mtb* resides inside macrophages.

2.3.2. Mechanisms of antibiotics-mediated ROS generation as strategy to combat drug resistance in Mtb

Due to the controversial debate about the role of ROS in antibiotic-mediated bacterial killing, the changes in intramycobacterial E_{MSH} were investigated after exposure to anti-TB drugs. In agreement with the biosensor responses under antibiotics stress in *S*. Typhimurium and *S. aureus* [86,92], no oxidative shift in E_{MSH} was reported in shake-flask experiments with *Mtb* populations that were exposed to sub-lethal anti-TB-drugs, *e.g.* isoniazide, ethambutol and rifampicin [95]. The only exception was the redox-cycling drug clofazimine, which caused an oxidative shift in E_{MSH} in *Mtb* shake-flask cultures. However, under macrophage infections, different antibiotics classes caused oxidative stress as shown by an oxidative shift in the E_{MSH} sub-populations, which was accompanied by increased killing of bacteria. Moreover, the redox heterogeneous sub-populations vary in their susceptibilities to antibiotics. The more oxidized population in autophagosomes and lysosomes was more susceptible to antibiotics killing, while the reduced population in endosomes displayed resistance to anti-TB drugs. Thus, immune activation inside macrophages potentiates drug killing while populations with reduced E_{MSH} promote antibiotics tolerance. Together these results showed important novel insights into the redox heterogeneity of *Mtb* sub-populations in different macrophage compartments, their susceptibility to antibiotics and the mechanisms of persistence [95].

In subsequent studies, several efforts were undertaken to understand the mechanisms of drug resistance and to develop new ROS-producing anti-TB drugs. These ROS-generating drug were used alone and in combination therapies as promising strategy to counteract the increasing problem of antimicrobial resistance and to combat XDR/MDR *Mtb* isolates [97–99]. First, hydroquinone-based antibiotics were synthesized, including ATD-3169 which was shown to cause superoxide production in *Mtb* isolates and increases the irreversible oxidized *Mtb* sub-population [99]. Next, combination therapies of isoniazid (INH) and inhibitors of antioxidant responses were found as promising strategy to threat drug resistant *Mtb* isolates [98]. Such inhibitors of antioxidant responses were ebselen, vancomycin and phenylarsine oxide that were highly effective in combination with INH to kill drug resistant Mtb isolates.

INH is a pro-drug that is activated by the catalase KatG and converted to a NAD-INH-adduct, that subsequently inhibits the enoyl-ACP reductase (InhA) in the mycolic acid biosynthesis pathway [98]. To identify the mechanisms of drug resistant *Mtb* strains, isoniazid resistance was studied in more detail in laboratory evolved INH-resistant *M. smegmatis* strains [98]. Genome sequencing revealed that INH resistant strains carried point mutations in genes for NADH dehydrogenase (*ndh*), catalase (*katG*) or the 3-dehydroquinate synthase (*aroB*). Transcriptomics identified antioxidant responses as dominating in the differentially transcribed genes in the INH resistant *M. smegmatis* strains. Moreover, the INH resistant strain was more sensitive to compounds that block antioxidant responses and disturb E_{MSH}. In agreement with this finding, the Mrx1-roGFP2 biosensor measurements revealed an oxidized shift in basal E_{MSH} and a higher sensitivity to oxidative stress by H_2O_2 in the INH-resistant *M. smegmatis* strain [98]. This higher ROS-sensitivity was not only observed in the INH-resistant *M. smegmatis* strain, but also in clinical MDR and XDR *Mtb* patient isolates. Thus, the evolution of drug resistance is associated with changes in the basal E_{MSH} and shifted to the oxidized redox state in multiple resistant *Mtb* isolates. Finally, it was shown that antibiotics that produce ROS or block antioxidant responses are in combination with INH more potent to induce oxidative shift in E_{MSH} during infections. These drugs should be promising strategies to tackle tuberculosis disease and to combat drug resistant isolates [98].

2.3.3. E_{MSH} regulates the redox state of WhiB4 mediating augmentin resistance and tolerance

In another study, the mode of action for combination therapy of β-lactam antibiotics (amoxicillin) with β-lactamase inhibitors (clavulanate), termed as augmentin, has been studied. The Mrx1-roGFP2 biosensor revealed a role of E_{MSH} and the WhiB4 redox sensor in augmentin resistance **(**Fig. 6**)** [97]. To study the mode of action of augmentin, a transcriptomics approach was used and identified cell wall and oxidative stress responses, respiration and carbon metabolism induced under augmentin treatment. Using biosensor measurements, an increase in the oxidized E_{MSH} sub-population was observed by augmentin over time during *Mtb* infections inside macrophages. Thus, augmentin effects the redox balance in *Mtb*, which potentiates its mycobactericidal effect and contributes to augmentin killing [97]. Furthermore, MSH was shown to protect *Mtb* from toxicity under augmentin treatment in survival assays. In further analysis, the FeS-cluster redox sensor WhiB4 was identified which regulates the shift to the oxidized E_{MSH} sub-population after augmentin treatment. Moreover, this oxidized shift modulates expression of the β-lactamase BlaC, which is regulated by WhiB4 in a redox-dependent manner. Specifically, BlaC is overexpressed in the *whiB4* mutant which increases resistance to β-lactam antibiotics **(**Fig. 6**)**. In contrast, overexpression of oxidized WhiB4 under augmentin treatment resulted in strong *blaC* repression and increased killing by β-lactams potentiating drug action. Thus, WhiB4 was identified as central regulator of β-lactam antibiotics resistance and the oxidative shift in E_{MSH} after augmentin combination therapy [97].

2.3.4. E_{MSH} regulates the redox state of WhiB3 mediating acid resistance and inhibition of phagosomal maturation

WhiB3 is another FeS cluster redox sensor that is also regulated by E_{MSH} and is essential for acid resistance of *Mtb* which allows survival of *Mtb* inside the acidic phagosome upon immune-stimulation [60,104,105]. WhiB3 was shown to play a protective role together with MSH under acidic stress conditions inside the phagosome of activated macrophages **(**Fig. 5**)** [96]. WhiB3 mediates acid resistance and inhibits phagosomal maturation, which is linked to changes in E_{MSH} under infection conditions. WhiB3 controls genes for lipid biosynthesis, secretion of the type-VII-secretion effectors as well as MSH biosynthesis and recycling under acidic stress. The limited decreased pH upon acidification of the phagosome (pH ~ 6.2) results in a reductive shift of E_{MSH} sub-populations and WhiB3 as well as MSH were found as key regulators for this reductive shift in E_{MSH}. WhiB3 was further required

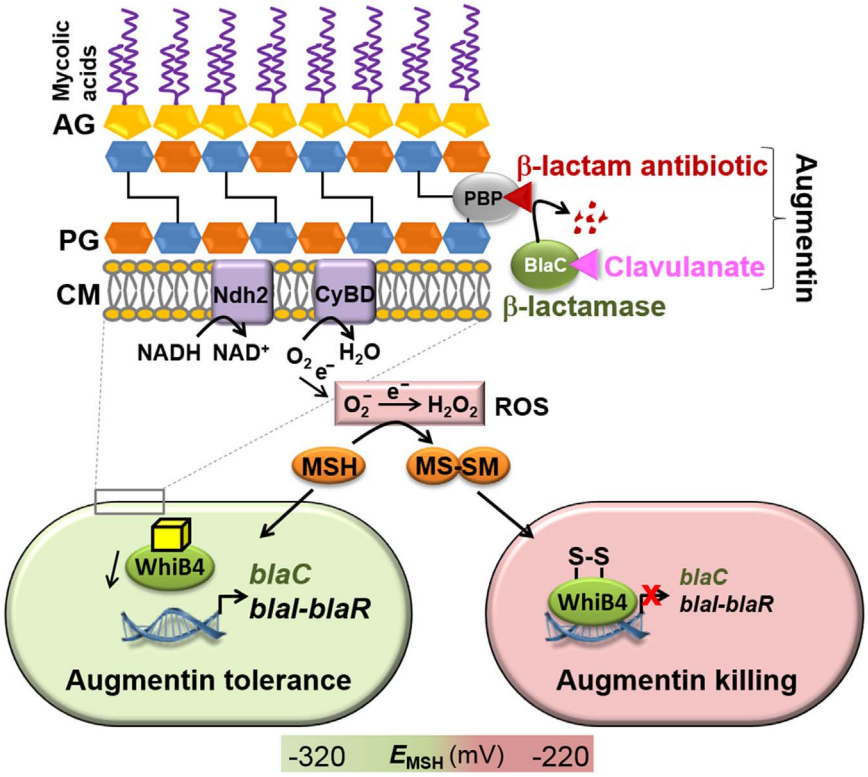

Fig. 6. The augmentin combination therapy of β-lactam antibiotics and β-lactamase inhibitor (clavulanate) causes ROS formation and changes in E_{MSH} in *Mtb* that affect WhiB4-mediated expression of β-lactamase expression. β-lactam antibiotics inhibit penicillin-binding proteins that cross-link the peptide side chains of the peptidoglycan (PG). Clavulanate inhibits the β-lactamase BlaC in *Mtb* that is controlled by the BlaI repressor and WhiB4. The combination therapy of β-lactam and Clavulanate (Augmentin) causes cell wall stress and ROS production in *Mtb* due to the re-direction of aerobic respiration *via* the Ndh2 and CyBD routes [97]. Increased ROS leads to the oxidative shift of E_{MSH} and oxidation of WhiB4 that represses transcription of *blaC* and the *blaI-blaR* operon resulting in down-regulation of the β-lactamase BlaC and killing by augmentin [97]. Tolerance to augmentin is induced by down-regulation or reduction of WhiB4 presumable in the reduced E_{MSH} sub-population resulting in derepression of the β-lactamase-encoding *blaC* gene directly or indirectly *via* derepression of the *blaIR* operon and proteolytic degradation of the BlaI repressor by the protease BlaR. This figure is adapted from Ref. [97]. Abbreviations: CM: cytoplasmic membrane, PG: peptidoglycan, Ndh2: NADH dehydrogenase 2, CyBD: cytochrome BD oxidase, PBP: penicillin-binding protein.

for survival under acidic conditions and protects *Mtb* from acid stress by controlling genes that restrict phagosomal maturation to subvert acidification and by down-regulation of the innate immune response. The *whiB3* mutant was also attenuated in the lung of guinea pigs. These results revealed a link between phagosome acidification, the reductive shift in E_{MSH} and virulence of *Mtb* that is controlled by WhiB3 mediating acid resistance and inhibiting phagosomal maturation as mechanism of persistent and chronic *Mtb* infections [96].

2.3.5. E_{MSH} is controlled by the sulfur assimilation pathway, the membrane SodA/DoxX/SseA complex and macrophage GSH production that are required for survival of Mtb

For the treatment of persistent *Mtb* infections, the sulfur assimilation pathway was selected as promising target that is required for biosynthesis of sulfur-containing amino acids and thiol-cofactors, such as cysteine and MSH [106]. The sulfur assimilation pathway, including the enzyme 5' adenosine phosphosulfate (APS) reductase (CysH), was especially important for virulence and survival of *Mtb* during chronic and persistent infections in mice and macrophage models [107,108]. Thus, a high-throughput drug screening approach was used to identify three inhibitors of the APS reductase as potent anti-TB compounds that decreased the levels of sulfur-containing metabolites, including MSH [106]. Using the Mrx1-roGFP2 biosensor, an oxidative shift in E_{MSH} was measured in response to these APS reductase inhibitors indicating the link between persistence, antibiotic tolerance and the sulfate assimilation pathway in *Mtb*.

In another study, the Mrx1-roGFP2 biosensor was used to identify the link between a novel membrane-associated oxidoreductase complex (MRC) and the MSH redox potential [109]. Using a Tn-seq approach, the authors screened for interactions of pathways required in *Mtb* for detoxification of radicals from the phagocyte oxidative burst. The superoxide dismutase (SodA), an integral membrane protein (DoxX) and the conserved thiol oxidoreductase SseA were identified as functionally linked MRC and the electron transfer was verified *in vivo*. Single mutants in each MRC component are similar sensitive to radical stress and exhibited an oxidized E_{MSH} as revealed by Mrx1-roGFP2 biosensor measurements. This study established a link between a novel oxidative stress resistance network with the E_{MSH} in *Mtb* to overcome the oxidative burst during infections [109].

An interaction between macrophage-derived GSH and E_{MSH} during *Mtb* infection has been revealed using the Mrx1-roGFP2 biosensor in a mice model of tuberculosis [110]. The GSH pool of macrophages depends on the xCT cystine-glutamate transporter, which is induced during *Mtb* infection. The deletion of xCT resulted in protection against TB and decreased pulmonary pathology in the mice lung. Mrx1-roGFP2 biosensor measurement revealed an oxidized E_{MSH} of *Mtb* in the infected mice xCT mutant. The increased E_{MSH} is caused by a decreased GSH production in the macrophages indicating a link between host GSH and bacterial MSH redox homeostasis. This study has further identified inhibitors of the xCT transporter as host-directed drugs for TB treatment [110].

Finally, the Mrx1-roGFP2 biosensor was applied in a mycobacterial biofilms under hypoxic conditions [111]. In the absence of oxygen as terminal electron acceptor, novel polyketide quinones were produced as alternative electron carriers in the respiratory chain to maintain bioenergetics and the membrane potential. About 70% of mycobacterial cells showed alterations in E_{MSH} under hypoxic biofilm conditions compared to planktonic cells, including 53% of cells with more reduced E_{MSH} and 16% with oxidative shift in E_{MSH}. Thus, the different oxygen levels across the biofilm affect the membrane potential and the MSH redox balance [111].

In summary, the Mrx1-roGFP2 biosensor was approved as valuable tool to study the mechanisms of redox heterogeneity, persistence and survival of *Mtb* under acidic conditions inside macrophage vacuolar compartments and the evolution and changes in E_{MSH} in drug resistant *Mtb* isolates. The biosensor has further contributed to elucidate novel ROS defense mechanisms in *Mtb*, such as the radical scavenging membrane MRC complex and the role of host GSH to regulate the MSH redox balance of *Mtb* inside macrophages. In drug research, the biosensor was used to study the regulation and mode of action of combination therapies (INH and augmentin) involving ROS-generating antibiotics as well as novel inhibitors of the sulfate-assimilation pathway as

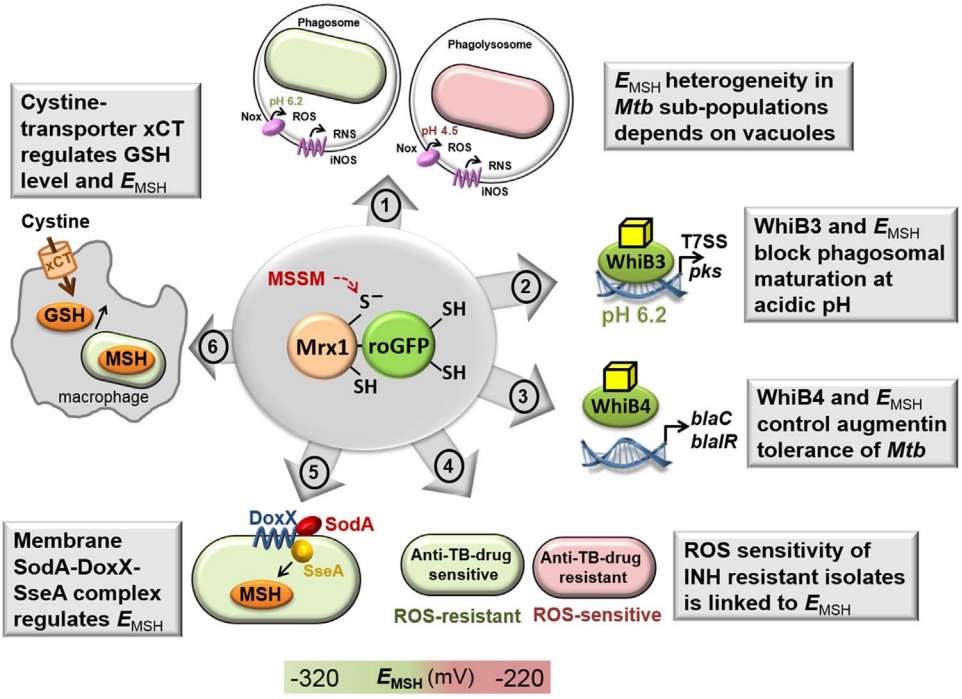

Fig. 7. Summary of the E_{MSH} changes in *Mtb* as measured using the Mrx1-roGFP2 biosensor. The genetically encoded Mrx1-roGFP2 biosensor contributed to a deeper understanding of pathogenicity, survival and anti-tuberculosis drug resistance mechanisms as follows: (1) E_{MSH} redox heterogeneity was shown in *Mtb* sub-populations that depends on the location in specific vacuole compartments [95]. (2) The WhiB3 sensor and E_{MSH} control induction of type-VII secretion systems and polyketide lipids under acid conditions in the phagosome to inhibit phagosomal maturation [96]. (3) The WhiB4 redox sensor and E_{MSH} control expression of β-lactamase to induce augmentin tolerance in the reduced *Mtb* population and augmentin killing in the oxidized *Mtb* population [97]. (4) Isoniazid (INH) resistant *Mtb* isolates have an oxidative E_{MSH} and are highly ROS-sensitive, while INH-sensitive strains are more resistant to ROS due to a more reduced E_{MSH} [98]. (5) The membrane-associated oxidoreductase complex (SodA-DoxX-SseA) regulates radical detoxification and MSH redox balance under infection conditions [109]. (6) The cystine-glutamate transporter xCT regulates cystine import into macrophages, resulting in increased host-GSH biosynthesis and a reduced E_{MSH} which contributes to TB disease in a mice infection model [110].

promising future anti-TB drugs to treat MDR/XDR, persistent and chronic *Mtb* infections. These main results revealed thus far using Mrx1-roGFP2 biosensor measurements in *Mtb* are summarized in the schematics of Fig. 7. Similar mechanisms might be relevant for other intracellular pathogens and persistent bacterial infections. As revealed in *Mtb* using the Mrx1-roGFP2 biosensor, redox heterogeneity of the intracellular pathogen *S*. Typhimurium could be also dependent on subvacuolar compartments. Inside the SCV, *S*. Typhimurium could be more tolerant to antibiotics due to a more reduced intrabacterial redox potential, which facilitates the persistent state. In contrast, cytosolic bacteria should have a more oxidized redox state and should be susceptible to clinical relevant antibiotics. The mechanisms of persistence and antibiotics resistance as result of redox heterogeneity remain interesting subject for future studies in redox infection biology.

Acknowledgements

This work was supported by grants from the Deutsche Forschungsgemeinschaft (AN746/4-1 and AN746/4-2) within the SPP1710 on “Thiol-based Redox switches” and by the DFG Project C08 within the SFB973 to H.A. Further funding was provided by the DFG Research Training Group GRK1947, project (C1) and by an ERC Consolidator Grant (GA 615585) MYCOTHIOLOME to H.A.

Author disclosure statement

No competing financial interests exist.

References

[1] K. Van Laer, C.J. Hamilton, J. Messens, Low-molecular-weight thiols in thiol-disulfide exchange, Antioxid. Redox Signal. 18 (2013) 1642–1653.
[2] R.C. Fahey, Glutathione analogs in prokaryotes, Biochim. Biophys. Acta 1830 (2013) 3182–3198.
[3] A.J. Potter, C. Trappetti, J.C. Paton, *Streptococcus pneumoniae* uses glutathione to defend against oxidative stress and metal ion toxicity, J. Bacteriol. 194 (2012) 6248–6254.
[4] B. Vergauwen, K. Verstraete, D.B. Senadheera, A. Dansercoer, D.G. Cvitkovitch, E. Guedon, S.N. Savvides, Molecular and structural basis of glutathione import in Gram-positive bacteria via GshT and the cystine ABC importer TcyBC of *Streptococcus mutans*, Mol. Microbiol. 89 (2013) 288–303.
[5] L. Masip, K. Veeravalli, G. Georgiou, The many faces of glutathione in bacteria, Antioxid. Redox Signal. 8 (2006) 753–762.
[6] C. Hwang, H.F. Lodish, A.J. Sinskey, Measurement of glutathione redox state in cytosol and secretory pathway of cultured cells, Methods Enzymol. 251 (1995) 212–221.
[7] I.R. Booth, G.P. Ferguson, S. Miller, C. Li, B. Gunasekera, S. Kinghorn, Bacterial production of methylglyoxal: a survival strategy or death by misadventure? Biochem. Soc. Trans. 31 (2003) 1406–1408.
[8] G.P. Ferguson, I.R. Booth, Importance of glutathione for growth and survival of *Escherichia coli* cells: detoxification of methylglyoxal and maintenance of intracellular K^+, J. Bacteriol. 180 (1998) 4314–4318.
[9] G.P. Ferguson, S. Totemeyer, M.J. MacLean, I.R. Booth, Methylglyoxal production in bacteria: suicide or survival? Arch. Microbiol. 170 (1998) 209–218.
[10] M.J. MacLean, L.S. Ness, G.P. Ferguson, I.R. Booth, The role of glyoxalase I in the detoxification of methylglyoxal and in the activation of the KefB K^+ efflux system in *Escherichia coli*, Mol. Microbiol. 27 (1998) 563–571.
[11] M. Song, M. Husain, J. Jones-Carson, L. Liu, C.A. Henard, A. Vazquez-Torres, Low-molecular-weight thiol-dependent antioxidant and antinitrosative defences in *Salmonella* pathogenesis, Mol. Microbiol. 87 (2013) 609–622.
[12] J. van der Heijden, E.S. Bosman, L.A. Reynolds, B.B. Finlay, Direct measurement of oxidative and nitrosative stress dynamics in *Salmonella* inside macrophages, Proc. Natl. Acad. Sci. USA 112 (2015) 560–565.
[13] M. Hall, C. Grundstrom, A. Begum, M.J. Lindberg, U.H. Sauer, F. Almqvist, J. Johansson, A.E. Sauer-Eriksson, Structural basis for glutathione-mediated activation of the virulence regulatory protein PrfA in *Listeria*, Proc. Natl. Acad. Sci. USA 113 (2016) 14733–14738.
[14] M.L. Reniere, A.T. Whiteley, K.L. Hamilton, S.M. John, P. Lauer, R.G. Brennan, D.A. Portnoy, Glutathione activates virulence gene expression of an intracellular pathogen, Nature 517 (2015) 170–173.
[15] N.E. Freitag, G.C. Port, M.D. Miner, *Listeria monocytogenes* – from saprophyte to intracellular pathogen, Nat. Rev. Microbiol. 7 (2009) 623–628.
[16] Y. Wang, H. Feng, Y. Zhu, P. Gao, Structural insights into glutathione-mediated activation of the master regulator PrfA in *Listeria monocytogenes*, Protein Cell 8 (2017) 308–312.
[17] J.L. Portman, S.B. Dubensky, B.N. Peterson, A.T. Whiteley, D.A. Portnoy, Activation of the *Listeria monocytogenes* virulence program by a reducing environment, mBio 8 (2017) e01595-17.
[18] J.L. Portman, Q. Huang, M.L. Reniere, A.T. Iavarone, D.A. Portnoy, Activity of the pore-forming virulence factor listeriolysin O is reversibly inhibited by naturally occurring *S*-glutathionylation, Infect. Immun. 85 (2017) e00959-16.
[19] K. McGourty, T.L. Thurston, S.A. Matthews, L. Pinaud, L.J. Mota, D.W. Holden, *Salmonella* inhibits retrograde trafficking of mannose-6-phosphate receptors and lysosome function, Science 338 (2012) 963–967.
[20] K. Uchiya, M.A. Barbieri, K. Funato, A.H. Shah, P.D. Stahl, E.A. Groisman, A *Salmonella* virulence protein that inhibits cellular trafficking, EMBO J. 18 (1999) 3924–3933.
[21] A. Vazquez-Torres, Y. Xu, J. Jones-Carson, D.W. Holden, S.M. Lucia, M.C. Dinauer, P. Mastroeni, F.C. Fang, *Salmonella* pathogenicity island 2-dependent evasion of the phagocyte NADPH oxidase, Science 287 (2000) 1655–1658.
[22] M.M. Marketon, R.W. DePaolo, K.L. DeBord, B. Jabri, O. Schneewind, Plague bacteria target immune cells during infection, Science 309 (2005) 1739–1741.

[23] C.A. Mueller, P. Broz, S.A. Muller, P. Ringler, F. Erne-Brand, I. Sorg, M. Kuhn, A. Engel, G.R. Cornelis, The V-antigen of *Yersinia* forms a distinct structure at the tip of injectisome needles, Science 310 (2005) 674–676.
[24] V.T. Lee, C. Tam, O. Schneewind, LcrV, a substrate for *Yersinia enterocolitica* type III secretion, is required for toxin targeting into the cytosol of HeLa cells, J. Biol. Chem. 275 (2000) 36869–36875.
[25] A. Mitchell, C. Tam, D. Elli, T. Charlton, P. Osei-Owusu, F. Fazlollahi, K.F. Faull, O. Schneewind, Glutathionylation of *Yersinia pestis* LcrV and its effects on plague pathogenesis, mBio 8 (2017).
[26] A. Gaballa, G.L. Newton, H. Antelmann, D. Parsonage, H. Upton, M. Rawat, A. Claiborne, R.C. Fahey, J.D. Helmann, Biosynthesis and functions of bacillithiol, a major low-molecular-weight thiol in Bacilli, Proc. Natl. Acad. Sci. USA 107 (2010) 6482–6486.
[27] G.L. Newton, M. Rawat, J.J. La Clair, V.K. Jothivasan, T. Budiarto, C.J. Hamilton, A. Claiborne, J.D. Helmann, R.C. Fahey, Bacillithiol is an antioxidant thiol produced in bacilli, Nat. Chem. Biol. 5 (2009) 625–627.
[28] V.V. Loi, M. Rossius, H. Antelmann, Redox regulation by reversible protein *S*-thiolation in bacteria, Front. Microbiol. 6 (2015) 187.
[29] A.C. Posada, S.L. Kolar, R.G. Dusi, P. Francois, A.A. Roberts, C.J. Hamilton, G.Y. Liu, A. Cheung, Importance of bacillithiol in the oxidative stress response of *Staphylococcus aureus*, Infect. Immun. 82 (2014) 316–332.
[30] D.C. Pöther, P. Gierok, M. Harms, J. Mostertz, F. Hochgräfe, H. Antelmann, C.J. Hamilton, I. Borovok, M. Lalk, Y. Aharonowitz, M. Hecker, Distribution and infection-related functions of bacillithiol in *Staphylococcus aureus*, Int. J. Med. Microbiol. 303 (2013) 114–123.
[31] P. Chandrangsu, R. Dusi, C.J. Hamilton, J.D. Helmann, Methylglyoxal resistance in *Bacillus subtilis*: contributions of bacillithiol-dependent and independent pathways, Mol. Microbiol. 91 (2014) 706–715.
[32] Z. Rosario-Cruz, J.M. Boyd, Physiological roles of bacillithiol in intracellular metal processing, Curr. Genet. 62 (2016) 59–65.
[33] Z. Fang, P.C. Dos Santos, Protective role of bacillithiol in superoxide stress and Fe-S metabolism in *Bacillus subtilis*, MicrobiologyOpen 4 (2015) 616–631.
[34] Z. Rosario-Cruz, H.K. Chahal, L.A. Mike, E.P. Skaar, J.M. Boyd, Bacillithiol has a role in Fe-S cluster biogenesis in *Staphylococcus aureus*, Mol. Microbiol. 98 (2015) 218–242.
[35] P. Chandrangsu, V.V. Loi, H. Antelmann, J.D. Helmann, The Role of Bacillithiol in Gram-Positive *Firmicutes*, Antioxid. Redox Signal. 28 (2018,) 445–462.
[36] S.V. Sharma, M. Arbach, A.A. Roberts, C.J. Macdonald, M. Groom, C.J. Hamilton, Biophysical features of bacillithiol, the glutathione surrogate of *Bacillus subtilis* and other *Firmicutes*, Chembiochem 14 (2013) 2160–2168.
[37] V.R. Perera, G.L. Newton, K. Pogliano, Bacillithiol: a key protective thiol in *Staphylococcus aureus*, Exp. Rev. Anti-Infect. Ther. 13 (2015) 1089–1107.
[38] B.K. Chi, A.A. Roberts, T.T. Huyen, K. Bäsell, D. Becher, D. Albrecht, C.J. Hamilton, H. Antelmann, *S*-bacillithiolation protects conserved and essential proteins against hypochlorite stress in firmicutes bacteria, Antioxid. Redox Signal. 18 (2013) 1273–1295.
[39] G.L. Newton, R.C. Fahey, M. Rawat, Detoxification of toxins by bacillithiol in *Staphylococcus aureus*, Microbiology 158 (2012) 1117–1126.
[40] C.C. Winterbourn, A.J. Kettle, Redox reactions and microbial killing in the neutrophil phagosome, Antioxid. Redox Signal. 18 (2013) 642–660.
[41] C.C. Winterbourn, A.J. Kettle, M.B. Hampton, Reactive oxygen species and neutrophil function, Annu. Rev. Biochem. 85 (2016) 765–792.
[42] J.N. Green, A.L.P. Chapman, C.J. Bishop, C.C. Winterbourn, A.J. Kettle, Neutrophil granule proteins generate bactericidal ammonia chloramine on reaction with hydrogen peroxide, Free Radic. Biol. Med. 113 (2017) 363–371.
[43] M. Imber, N.T.T. Huyen, A.J. Pietrzyk-Brzezinska, V.V. Loi, M. Hillion, J. Bernhardt, L. Thärichen, K. Kolsek, M. Saleh, C.J. Hamilton, L. Adrian, F. Gräter, M.C. Wahl, H. Antelmann, Protein *S*-bacillithiolation functions in thiol protection and redox regulation of the glyceraldehyde-3-phosphate dehydrogenase gap in *Staphylococcus aureus* under hypochlorite stress, Antioxid. Redox Signal. 28 (2018,) 410–430.
[44] N. Brandes, S. Schmitt, U. Jakob, Thiol-based redox switches in eukaryotic proteins, Antioxid. Redox Signal. 11 (2009) 997–1014.
[45] M. Ralser, M.M. Wamelink, A. Kowald, B. Gerisch, G. Heeren, E.A. Struys, E. Klipp, C. Jakobs, M. Breitenbach, H. Lehrach, S. Krobitsch, Dynamic rerouting of the carbohydrate flux is key to counteracting oxidative stress, J. Biol. 6 (2007) 10.
[46] Y. Tsuchiya, S.Y. Peak-Chew, C. Newell, S. Miller-Aidoo, S. Mangal, A. Zhyvoloup, J. Bakovic, O. Malanchuk, G.C. Pereira, V. Kotiadis, G. Szabadkai, M.R. Duchen, M. Campbell, S.R. Cuenca, A. Vidal-Puig, A.M. James, M.P. Murphy, V. Filonenko, M. Skehel, I. Gout, Protein CoAlation: a redox-regulated protein modification by coenzyme A in mammalian cells, Biochem. J. 474 (2017) 2489–2508.
[47] A. Gaballa, B.K. Chi, A.A. Roberts, D. Becher, C.J. Hamilton, H. Antelmann, J.D. Helmann, Redox regulation in *Bacillus subtilis*: the bacilliredoxins BrxA(YphP) and BrxB(YqiW) function in de-bacillithiolation of *S*-bacillithiolated OhrR and MetE, Antioxid. Redox Signal. 21 (2014) 357–367.
[48] G.L. Newton, N. Buchmeier, R.C. Fahey, Biosynthesis and functions of mycothiol, the unique protective thiol of Actinobacteria, Microbiol. Mol. Biol. Rev. 72 (2008) 471–494.
[49] V.K. Jothivasan, C.J. Hamilton, Mycothiol: synthesis, biosynthesis and biological functions of the major low molecular weight thiol in actinomycetes, Nat. Prod. Rep. 25 (2008) 1091–1117.
[50] N.A. Buchmeier, G.L. Newton, R.C. Fahey, A mycothiol synthase mutant of *Mycobacterium tuberculosis* has an altered thiol-disulfide content and limited tolerance to stress, J. Bacteriol. 188 (2006) 6245–6252.
[51] N.A. Buchmeier, G.L. Newton, T. Koledin, R.C. Fahey, Association of mycothiol with protection of *Mycobacterium tuberculosis* from toxic oxidants and antibiotics, Mol. Microbiol. 47 (2003) 1723–1732.
[52] M. Rawat, C. Johnson, V. Cadiz, Y. Av-Gay, Comparative analysis of mutants in the mycothiol biosynthesis pathway in *Mycobacterium smegmatis*, Biochem. Biophys. Res. Commun. 363 (2007) 71–76.
[53] Y.B. Liu, M.X. Long, Y.J. Yin, M.R. Si, L. Zhang, Z.Q. Lu, Y. Wang, X.H. Shen, Physiological roles of mycothiol in detoxification and tolerance to multiple poisonous chemicals in *Corynebacterium glutamicum*, Arch. Microbiol. 195 (2013) 419–429.
[54] Q. Zhao, M. Wang, D. Xu, Q. Zhang, W. Liu, Metabolic coupling of two small-molecule thiols programs the biosynthesis of lincomycin A, Nature 518 (2015) 115–119.
[55] A.M. Reyes, B. Pedre, M.I. De Armas, M.A. Tossounian, R. Radi, J. Messens, M. Trujillo, Chemistry and redox biology of mycothiol, Antioxid. Redox Signal. 28 (2018,) 487–504.
[56] B.K. Chi, T. Busche, K. Van Laer, K. Basell, D. Becher, L. Clermont, G.M. Seibold, M. Persicke, J. Kalinowski, J. Messens, H. Antelmann, Protein S-mycothiolation functions as redox-switch and thiol protection mechanism in *Corynebacterium glutamicum* under hypochlorite stress, Antioxid. Redox Signal. 20 (2014) 589–605.
[57] M. Hillion, J. Bernhardt, T. Busche, M. Rossius, S. Maaß, D. Becher, M. Rawat, M. Wirtz, R. Hell, C. Rückert, J. Kalinowski, H. Antelmann, Monitoring global protein thiol-oxidation and S-mycothiolation in *Mycobacterium smegmatis* under hypochlorite stress using Voronoi redox treemaps, Sci. Rep. (2017).
[58] M. Hillion, M. Imber, B. Pedre, J. Bernhardt, M. Saleh, V.V. Loi, S. Maass, D. Becher, L. Astolfi Rosado, L. Adrian, C. Weise, R. Hell, M. Wirtz, J. Messens, H. Antelmann, The glyceraldehyde-3-phosphate dehydrogenase GapDH of *Corynebacterium diphtheriae* is redox-controlled by protein S-mycothiolation under oxidative stress, Sci. Rep. 7 (2017) 5020.
[59] G.L. Newton, K. Arnold, M.S. Price, C. Sherrill, S.B. Delcardayre, Y. Aharonowitz, G. Cohen, J. Davies, R.C. Fahey, C. Davis, Distribution of thiols in microorganisms: mycothiol is a major thiol in most actinomycetes, J. Bacteriol. 178 (1996) 1990–1995.
[60] V. Saini, B.M. Cumming, L. Guidry, D.A. Lamprecht, J.H. Adamson, V.P. Reddy, K.C. Chinta, J.H. Mazorodze, J.N. Glasgow, M. Richard-Greenblatt, A. Gomez-Velasco, H. Bach, Y. Av-Gay, H. Eoh, K. Rhee, A.J.C. Steyn, Ergothioneine maintains redox and bioenergetic homeostasis essential for drug susceptibility and virulence of *Mycobacterium tuberculosis*, Cell Rep. 14 (2016) 572–585.
[61] C.M. Sassetti, E.J. Rubin, Genetic requirements for mycobacterial survival during infection, Proc. Natl. Acad. Sci. USA 100 (2003) 12989–12994.
[62] C. Sao Emani, M.J. Williams, I.J. Wiid, N.F. Hiten, A.J. Viljoen, R.D. Pietersen, P.D. van Helden, B. Baker, Ergothioneine is a secreted antioxidant in *Mycobacterium smegmatis*, Antimicrob. Agents Chemother. 57 (2013) 3202–3207.
[63] P. Ta, N. Buchmeier, G.L. Newton, M. Rawat, R.C. Fahey, Organic hydroperoxide resistance protein and ergothioneine compensate for loss of mycothiol in *Mycobacterium smegmatis* mutants, J. Bacteriol. 193 (2011) 1981–1990.
[64] M.A. Tossounian, B. Pedre, K. Wahni, H. Erdogan, D. Vertommen, I. Van Molle, J. Messens, *Corynebacterium diphtheriae* methionine sulfoxide reductase a exploits a unique mycothiol redox relay mechanism, J. Biol. Chem. 290 (2015) 11365–11375.
[65] B. Pedre, I. Van Molle, A.F. Villadangos, K. Wahni, D. Vertommen, L. Turell, H. Erdogan, L.M. Mateos, J. Messens, The *Corynebacterium glutamicum* mycothiol peroxidase is a reactive oxygen species-scavenging enzyme that shows promiscuity in thiol redox control, Mol. Microbiol. 96 (2015) 1176–1191.
[66] M. Hugo, K. Van Laer, A.M. Reyes, D. Vertommen, J. Messens, R. Radi, M. Trujillo, Mycothiol/mycoredoxin 1-dependent reduction of the peroxiredoxin AhpE from *Mycobacterium tuberculosis*, J. Biol. Chem. 289 (2014) 5228–5239.
[67] Y. Liu, X. Yang, Y. Yin, J. Lin, C. Chen, J. Pan, M. Si, X. Shen, Mycothiol protects *Corynebacterium glutamicum* against acid stress via maintaining intracellular pH homeostasis, scavenging ROS, and S-mycothiolating MetE, J. Gen. Appl. Microbiol. 62 (2016) 144–153.
[68] D. Sareen, G.L. Newton, R.C. Fahey, N.A. Buchmeier, Mycothiol is essential for growth of *Mycobacterium tuberculosis* Erdman, J. Bacteriol. 185 (2003) 6736–6740.
[69] Z. Ma, C. Lienhardt, H. McIlleron, A.J. Nunn, X. Wang, Global tuberculosis drug development pipeline: the need and the reality, Lancet 375 (2010) 2100–2109.
[70] M.H. Hazbon, M. Brimacombe, M. Bobadilla del Valle, M. Cavatore, M.I. Guerrero, M. Varma-Basil, H. Billman-Jacobe, C. Lavender, J. Fyfe, L. Garcia-Garcia, C.I. Leon, M. Bose, F. Chaves, M. Murray, K.D. Eisenach, J. Sifuentes-Osornio, M.D. Cave, A. Ponce de Leon, D. Alland, Population genetics study of isoniazid resistance mutations and evolution of multidrug-resistant *Mycobacterium tuberculosis*, Antimicrob. Agents Chemother. 50 (2006) 2640–2649.
[71] R. Rawat, A. Whitty, P.J. Tonge, The isoniazid-NAD adduct is a slow, tight-binding inhibitor of InhA, the *Mycobacterium tuberculosis* enoyl reductase: adduct affinity and drug resistance, Proc. Natl. Acad. Sci. USA 100 (2003) 13881–13886.
[72] S.S. Nilewar, M.K. Kathiravan, Mycothiol: a promising antitubercular target, Bioorg. Chem. 52 (2014) 62–68.
[73] M. Schwarzlander, T.P. Dick, A.J. Meyer, B. Morgan, Dissecting redox biology using fluorescent protein sensors, Antioxid. Redox Signal. 24 (2016) 680–712.
[74] A.J. Meyer, T.P. Dick, Fluorescent protein-based redox probes, Antioxid. Redox Signal. 13 (2010) 621–650.
[75] M. Gutscher, A.L. Pauleau, L. Marty, T. Brach, G.H. Wabnitz, Y. Samstag, A.J. Meyer, T.P. Dick, Real-time imaging of the intracellular glutathione redox potential, Nat. Methods 5 (2008) 553–559.
[76] D.S. Bilan, V.V. Belousov, New tools for redox biology: from imaging to manipulation, Free Radic. Biol. Med. 109 (2017) 167–188.
[77] B. Morgan, M.C. Sobotta, T.P. Dick, Measuring E(GSH) and H_2O_2 with roGFP2-based redox probes, Free Radic. Biol. Med. 51 (2011) 1943–1951.
[78] A.J. Meyer, T. Brach, L. Marty, S. Kreye, N. Rouhier, J.P. Jacquot, R. Hell,

Redox-sensitive GFP in *Arabidopsis thaliana* is a quantitative biosensor for the redox potential of the cellular glutathione redox buffer, Plant J. 52 (2007) 973–986.
[79] P. Back, W.H. De Vos, G.G. Depuydt, F. Matthijssens, J.R. Vanfleteren, B.P. Braeckman, Exploring real-time in vivo redox biology of developing and aging *Caenorhabditis elegans*, Free Radic. Biol. Med. 52 (2012) 850–859.
[80] D. Kasozi, F. Mohring, S. Rahlfs, A.J. Meyer, K. Becker, Real-time imaging of the intracellular glutathione redox potential in the malaria parasite *Plasmodium falciparum*, PLoS Pathog. 9 (2013) e1003782.
[81] C.R. Arias-Barreiro, K. Okazaki, A. Koutsaftis, S.H. Inayat-Hussain, A. Tani, M. Katsuhara, K. Kimbara, I.C. Mori, A bacterial biosensor for oxidative stress using the constitutively expressed redox-sensitive protein roGFP2, Sensors 10 (2010) 6290–6306.
[82] G.T. Hanson, R. Aggeler, D. Oglesbee, M. Cannon, R.A. Capaldi, R.Y. Tsien, S.J. Remington, Investigating mitochondrial redox potential with redox-sensitive green fluorescent protein indicators, J. Biol. Chem. 279 (2004) 13044–13053.
[83] L. Ooi, L.Y. Heng, I.C. Mori, A high-throughput oxidative stress biosensor based on *Escherichia coli* roGFP2 cells immobilized in a k-carrageenan matrix, Sensors 15 (2015) 2354–2368.
[84] J.A. Imlay, The molecular mechanisms and physiological consequences of oxidative stress: lessons from a model bacterium, Nat. Rev. Microbiol. 11 (2013) 443–454.
[85] S. Mishra, J. Imlay, Why do bacteria use so many enzymes to scavenge hydrogen peroxide? Arch. Biochem. Biophys. 525 (2012) 145–160.
[86] J. van der Heijden, S.L. Vogt, L.A. Reynolds, J. Pena-Diaz, A. Tupin, L. Aussel, B.B. Finlay, Exploring the redox balance inside gram-negative bacteria with redox-sensitive GFP, Free Radic. Biol. Med. 91 (2016) 34–44.
[87] M.A. Kohanski, D.J. Dwyer, B. Hayete, C.A. Lawrence, J.J. Collins, A common mechanism of cellular death induced by bactericidal antibiotics, Cell 130 (2007) 797–810.
[88] Y. Liu, J.A. Imlay, Cell death from antibiotics without the involvement of reactive oxygen species, Science 339 (2013) 1210–1213.
[89] I. Keren, Y. Wu, J. Inocencio, L.R. Mulcahy, K. Lewis, Killing by bactericidal antibiotics does not depend on reactive oxygen species, Science 339 (2013) 1213–1216.
[90] P. Shukla, V.S. Khodade, M. SharathChandra, P. Chauhan, S. Mishra, S. Siddaramappa, B.E. Pradeep, A. Singh, H. Chakrapani, "On demand" redox buffering by H2S contributes to antibiotic resistance revealed by a bacteria-specific H_2S donor, Chem. Sci. 8 (2017) 4967–4972.
[91] J. van der Heijden, L.A. Reynolds, W. Deng, A. Mills, R. Scholz, K. Imami, L.J. Foster, F. Duong, B.B. Finlay, *Salmonella* rapidly regulates membrane permeability to survive oxidative stress, mBio 7 (2016) e01238–01216.
[92] V.V. Loi, M. Harms, M. Müller, N.T.T. Huyen, C.J. Hamilton, F. Hochgräfe, J. Pane-Farre, H. Antelmann, Real-time imaging of the bacillithiol redox potential in the human pathogen *Staphylococcus aureus* using a genetically encoded bacilliredoxin-fused redox biosensor, Antioxid. Redox Signal. 26 (2017) 835–848.
[93] B.A. Diep, S.R. Gill, R.F. Chang, T.H. Phan, J.H. Chen, M.G. Davidson, F. Lin, J. Lin, H.A. Carleton, E.F. Mongodin, G.F. Sensabaugh, F. Perdreau-Remington, Complete genome sequence of USA300, an epidemic clone of community-acquired meticillin-resistant *Staphylococcus aureus*, Lancet 367 (2006) 731–739.
[94] H. Weber, S. Engelmann, D. Becher, M. Hecker, Oxidative stress triggers thiol oxidation in the glyceraldehyde-3-phosphate dehydrogenase of *Staphylococcus aureus*, Mol. Microbiol. 52 (2004) 133–140.
[95] A. Bhaskar, M. Chawla, M. Mehta, P. Parikh, P. Chandra, D. Bhave, D. Kumar, K.S. Carroll, A. Singh, Reengineering redox sensitive GFP to measure mycothiol redox potential of *Mycobacterium tuberculosis* during infection, PLoS Pathog. 10 (2014) e1003902.
[96] M. Mehta, R.S. Rajmani, A. Singh, *Mycobacterium tuberculosis* WhiB3 responds to vacuolar pH-induced changes in mycothiol redox potential to modulate phagosomal maturation and virulence, J. Biol. Chem. 291 (2016) 2888–2903.
[97] S. Mishra, P. Shukla, A. Bhaskar, K. Anand, P. Baloni, R.K. Jha, A. Mohan, R.S. Rajmani, V. Nagaraja, N. Chandra, A. Singh, Efficacy of beta-lactam/beta-lactamase inhibitor combination is linked to WhiB4-mediated changes in redox physiology of *Mycobacterium tuberculosis*, Elife 6 (2017) e25624.
[98] J. Padiadpu, P. Baloni, K. Anand, M. Munshi, C. Thakur, A. Mohan, A. Singh, N. Chandra, Identifying and tackling emergent vulnerability in drug-resistant mycobacteria, ACS Infect. Dis. 2 (2016), pp. 592–607.
[99] P. Tyagi, A.T. Dharmaraja, A. Bhaskar, H. Chakrapani, A. Singh, *Mycobacterium tuberculosis* has diminished capacity to counteract redox stress induced by elevated levels of endogenous superoxide, Free Radic. Biol. Med. 84 (2015) 344–354.
[100] K.S. Ung, Y. Av-Gay, Mycothiol-dependent mycobacterial response to oxidative stress, FEBS Lett. 580 (2006) 2712–2716.
[101] V. Poirier, Y. Av-Gay, Intracellular growth of bacterial pathogens: the role of secreted effector proteins in the control of phagocytosed microorganisms, Microbiol. Spectr. 3 (2015).
[102] S. Ehrt, D. Schnappinger, Mycobacterial survival strategies in the phagosome: defence against host stresses, Cell Microbiol. 11 (2009) 1170–1178.
[103] D. Schnappinger, S. Ehrt, M.I. Voskuil, Y. Liu, J.A. Mangan, I.M. Monahan, G. Dolganov, B. Efron, P.D. Butcher, C. Nathan, G.K. Schoolnik, Transcriptional adaptation of *Mycobacterium tuberculosis* within macrophages: insights into the phagosomal environment, J. Exp. Med. 198 (2003) 693–704.
[104] G.B. Coulson, B.K. Johnson, H. Zheng, C.J. Colvin, R.J. Fillinger, E.R. Haiderer, N.D. Hammer, R.B. Abramovitch, Targeting *Mycobacterium tuberculosis* sensitivity to thiol stress at acidic pH kills the bacterium and potentiates antibiotics, Cell Chem. Biol. 24 (2017) 993–1004 (e1004).
[105] A. Singh, L. Guidry, K.V. Narasimhulu, D. Mai, J. Trombley, K.E. Redding, G.I. Giles, J.R. Lancaster Jr, A.J. Steyn, *Mycobacterium tuberculosis* WhiB3 responds to O2 and nitric oxide via its [4Fe-4S] cluster and is essential for nutrient starvation survival, Proc. Natl. Acad. Sci. USA 104 (2007) 11562–11567.
[106] P.B. Palde, A. Bhaskar, L.E. Pedro Rosa, F. Madoux, P. Chase, V. Gupta, T. Spicer, L. Scampavia, A. Singh, K.S. Carroll, First-in-class inhibitors of sulfur metabolism with bactericidal activity against non-replicating *M. tuberculosis*, ACS Chem. Biol. 11 (2016) 172–184.
[107] J. Rengarajan, B.R. Bloom, E.J. Rubin, Genome-wide requirements for *Mycobacterium tuberculosis* adaptation and survival in macrophages, Proc. Natl. Acad. Sci. USA 102 (2005) 8327–8332.
[108] R.H. Senaratne, A.D. De Silva, S.J. Williams, J.D. Mougous, J.R. Reader, T. Zhang, S. Chan, B. Sidders, D.H. Lee, J. Chan, C.R. Bertozzi, L.W. Riley, 5'-Adenosinephosphosulphate reductase (CysH) protects *Mycobacterium tuberculosis* against free radicals during chronic infection phase in mice, Mol. Microbiol. 59 (2006) 1744–1753.
[109] S. Nambi, J.E. Long, B.B. Mishra, R. Baker, K.C. Murphy, A.J. Olive, H.P. Nguyen, S.A. Shaffer, C.M. Sassetti, The oxidative stress network of *Mycobacterium tuberculosis* reveals coordination between radical detoxification systems, Cell Host Microbe 17 (2015) 829–837.
[110] Y. Cai, Q. Yang, M. Liao, H. Wang, C. Zhang, S. Nambi, W. Wang, M. Zhang, J. Wu, G. Deng, Q. Deng, H. Liu, B. Zhou, Q. Jin, C.G. Feng, C.M. Sassetti, F. Wang, X. Chen, xCT increases tuberculosis susceptibility by regulating antimicrobial function and inflammation, Oncotarget 7 (2016) 31001–31013.
[111] A. Anand, P. Verma, A.K. Singh, S. Kaushik, R. Pandey, C. Shi, H. Kaur, M. Chawla, C.K. Elechalawar, D. Kumar, Y. Yang, N.S. Bhavesh, R. Banerjee, D. Dash, A. Singh, V.T. Natarajan, A.K. Ojha, C.C. Aldrich, R.S. Gokhale, Polyketide quinones are alternate intermediate electron carriers during mycobacterial respiration in oxygen-deficient niches, Mol. Cell 60 (2015) 637–650.

Chapter 3

Staphylococcus aureus uses the bacilliredoxin (BrxAB)/ bacillithiol disulfide reductase (YpdA) redox pathway to defend against oxidative stress under infections

Nico Linzner[1], Vu Van Loi[1], Verena Nadin Fritsch[1], Quach Ngoc Tung[1], Saskia Stenzel[1], Markus Wirtz[2], Rüdiger Hell[2], Chris Hamilton[3], Karsten Tedin[4], Marcus Fulde[4] and Haike Antelmann[1*]

[1]Freie Universität Berlin, Institute for Biology-Microbiology, D-14195 Berlin, Germany
[2]Plant Molecular Biology, Centre for Organismal Studies Heidelberg, University of Heidelberg, Heidelberg, Germany
[3]School of Pharmacy, University of East Anglia, Norwich Research Park, Norwich, NR4 7TJ, UK
[4]Freie Universität Berlin, Institute of Microbiology and Epizootics, Centre for Infection Medicine, D-14163 Berlin, Germany

*Corresponding author: haike.antelmann@fu-berlin.de

Published in: Frontiers in Microbiology 10: 1355. (2019)
DOI: https://doi.org/10.3389/fmicb.2019.01355

Personal contribution:

I contributed to the concept of the paper and performed most experiments for this study. I prepared the samples for quantifications of LMW thiols and disulfides by HPLC **(Fig. 3, S3)**. I measured all kinetics of Brx- and Tpx-roGFP2 biosensor oxidations in comparative studies and among the growth curves *in vivo* and calculated the BSH redox potentials of the different *S. aureus* strains **(Fig. 4, S4-5, S6B, D, S8A, B, and Tab. S4-6)**. I performed the anti-BSH Western blot analyses **(Fig. 5)**. Furthermore, I was involved in performance of the phenotype analyses after NaOCl and H_2O_2 stress **(Fig. 6, 7)** and contributed with the infection assay of the complemented strains **(Fig. 8B, D)** to this study. I conducted the multiple alignments of BrxA, BrxB and YpdA proteins **(Fig. S1)**. I drafted most of the figures and wrote the paper together with Haike Antelmann.

frontiers in Microbiology

ORIGINAL RESEARCH
published: 18 June 2019
doi: 10.3389/fmicb.2019.01355

Staphylococcus aureus Uses the Bacilliredoxin (BrxAB)/Bacillithiol Disulfide Reductase (YpdA) Redox Pathway to Defend Against Oxidative Stress Under Infections

*Nico Linzner[1], Vu Van Loi[1], Verena Nadin Fritsch[1], Quach Ngoc Tung[1], Saskia Stenzel[1], Markus Wirtz[2], Rüdiger Hell[2], Chris J. Hamilton[3], Karsten Tedin[4], Marcus Fulde[4] and Haike Antelmann[1]**

[1] Institute for Biology – Microbiology, Freie Universität Berlin, Berlin, Germany, [2] Plant Molecular Biology, Centre for Organismal Studies Heidelberg, Heidelberg University, Heidelberg, Germany, [3] School of Pharmacy, University of East Anglia, Norwich, United Kingdom, [4] Institute of Microbiology and Epizootics, Centre for Infection Medicine, Freie Universität Berlin, Berlin, Germany

OPEN ACCESS

Edited by:
Boris Macek,
University of Tübingen, Germany

Reviewed by:
Alberto A. Iglesias,
National University of the Littoral, Argentina
Ivan Mijakovic,
Chalmers University of Technology, Sweden
Bruno Manta,
New England Biolabs, United States

***Correspondence:**
Haike Antelmann
haike.antelmann@fu-berlin.de

Specialty section:
This article was submitted to Microbial Physiology and Metabolism, a section of the journal Frontiers in Microbiology

Received: 03 February 2019
Accepted: 31 May 2019
Published: 18 June 2019

Citation:
Linzner N, Loi VV, Fritsch VN, Tung QN, Stenzel S, Wirtz M, Hell R, Hamilton CJ, Tedin K, Fulde M and Antelmann H (2019) Staphylococcus aureus Uses the Bacilliredoxin (BrxAB)/Bacillithiol Disulfide Reductase (YpdA) Redox Pathway to Defend Against Oxidative Stress Under Infections. Front. Microbiol. 10:1355. doi: 10.3389/fmicb.2019.01355

Staphylococcus aureus is a major human pathogen and has to cope with reactive oxygen and chlorine species (ROS, RCS) during infections. The low molecular weight thiol bacillithiol (BSH) is an important defense mechanism of *S. aureus* for detoxification of ROS and HOCl stress to maintain the reduced state of the cytoplasm. Under HOCl stress, BSH forms mixed disulfides with proteins, termed as *S*-bacillithiolations, which are reduced by bacilliredoxins (BrxA and BrxB). The NADPH-dependent flavin disulfide reductase YpdA is phylogenetically associated with the BSH synthesis and BrxA/B enzymes and was recently suggested to function as BSSB reductase (Mikheyeva et al., 2019). Here, we investigated the role of the complete bacilliredoxin BrxAB/BSH/YpdA pathway in *S. aureus* COL under oxidative stress and macrophage infection conditions *in vivo* and in biochemical assays *in vitro*. Using HPLC thiol metabolomics, a strongly enhanced BSSB level and a decreased BSH/BSSB ratio were measured in the *S. aureus* COL Δ*ypdA* deletion mutant under control and NaOCl stress. Monitoring the oxidation degree (OxD) of the Brx-roGFP2 biosensor revealed that YpdA is required for regeneration of the reduced BSH redox potential (E_{BSH}) upon recovery from oxidative stress. In addition, the Δ*ypdA* mutant was impaired in H_2O_2 detoxification as measured with the novel H_2O_2-specific Tpx-roGFP2 biosensor. Phenotype analyses further showed that BrxA and YpdA are required for survival under NaOCl and H_2O_2 stress *in vitro* and inside murine J-774A.1 macrophages in infection assays *in vivo*. Finally, NADPH-coupled electron transfer assays provide evidence for the function of YpdA in BSSB reduction, which depends on the conserved Cys14 residue. YpdA acts together with BrxA and BSH in de-bacillithiolation of *S*-bacillithiolated GapDH. In conclusion, our results point to a major role of the BrxA/BSH/YpdA pathway in BSH redox homeostasis in *S. aureus* during recovery from oxidative stress and under infections.

Keywords: *Staphylococcus aureus*, oxidative stress, bacillithiol, bacilliredoxin, bacillithiol disulfide reductase, YpdA, roGFP2

INTRODUCTION

Staphylococcus aureus is an important human pathogen, which can cause many diseases, ranging from local soft-tissue and wound infections to life-threatening systemic and chronic infections, such as endocarditis, septicaemia, bacteraemia, pneumonia or osteomyelitis (Archer, 1998; Lowy, 1998; Boucher and Corey, 2008). Due to the prevalence of methicillin-resistant *S. aureus* isolates, which are often resistant to multiple antibiotics, treatment options are limited to combat *S. aureus* infections (Livermore, 2000). Therefore, the "European Center of Disease Prevention and Control" has classified *S. aureus* as one out of six ESKAPE pathogens which are the leading causes of nosocomial infections worldwide (Pendleton et al., 2013). During infections, activated macrophages and neutrophils produce reactive oxygen and chlorine species (ROS, RCS) in large quantities, including H_2O_2 and HOCl with the aim to kill invading pathogens (Winterbourn and Kettle, 2013; Hillion and Antelmann, 2015; Beavers and Skaar, 2016; Winterbourn et al., 2016).

Low molecular weight thiols play important roles in the defense against ROS and HOCl in bacterial pathogens and are required for survival, host colonization, and pathogenicity (Loi et al., 2015; Tung et al., 2018). Gram-negative bacteria produce GSH as major LMW thiol, which is absent in most Gram-positive bacteria (Fahey, 2013). Instead, many firmicutes utilize BSH as alternative LMW thiol (**Figure 1A**), which is essential for virulence of *S. aureus* in macrophage infection assays (Newton et al., 2012; Pöther et al., 2013; Posada et al., 2014; Chandrangsu et al., 2018). A recent study identified a BSH derivative with an *N*-methylated cysteine as *N*-methyl-BSH in anaerobic phototrophic *Chlorobiaceae*, suggesting that BSH derivatives are more widely distributed and not restricted to Gram-positive firmicutes (Hiras et al., 2018). In *S. aureus* and *Bacillus subtilis*, BSH was characterized as cofactor of thiol-*S*-transferases (e.g., FosB), glyoxalases, peroxidases, and other redox enzymes that are involved in detoxification of ROS, HOCl, methylglyoxal, toxins, and antibiotics (Chandrangsu et al., 2018). In addition, BSH participates in post-translational thiol-modifications under HOCl stress by formation of BSH mixed protein disulfides, termed as protein *S*-bacillithiolations (Chi et al., 2011, 2013; Imber et al., 2018a,c).

Protein *S*-bacillithiolation functions in thiol-protection and redox regulation of redox-sensing regulators, metabolic enzymes and antioxidant enzymes (Chi et al., 2011, 2013; Loi et al., 2015; Imber et al., 2018a,b,c). In *S. aureus*, the glycolytic glyceraldehyde-3-phosphate dehydrogenase (GapDH) and the aldehyde dehydrogenase AldA were identified as most abundant *S*-bacillithiolated proteins that are inactivated under HOCl stress (Imber et al., 2018a,b). In *B. subtilis*, the methionine synthase MetE and the OhrR repressor are *S*-bacillithiolated under HOCl stress leading to methionine auxotrophy and derepression of the OhrR-controlled *ohrA* peroxiredoxin gene, respectively (Fuangthong et al., 2001; Lee et al., 2007; Chi et al., 2011).

Reduction of *S*-bacillithiolated OhrR, MetE, and GapDH proteins is catalyzed by the bacilliredoxins (BrxA/B) in *B. subtilis* and *S. aureus in vitro* (Gaballa et al., 2014; Chandrangsu et al., 2018). BrxA (YphP) and BrxB (YqiW) are paralogous thioredoxin-fold proteins of the UPF0403 family with an unusual CGC active site that are conserved in BSH-producing firmicutes (**Supplementary Figure S1**). Upon de-bacillithiolation, the BSH moiety is transferred to the Brx active site, resulting in BrxA-SSB formation (**Figure 1B**). However, the Brx associated thiol-disulfide reductase involved in regeneration of Brx activity is not known. In GSH-producing bacteria, Grx catalyze the reduction of *S*-glutathionylated proteins, which requires GSH for regeneration of Grx, resulting in GSSG formation (Lillig et al., 2008; Allen and Mieyal, 2012). The regeneration of GSH is catalyzed by the flavoenzyme Gor, which belongs to the pyridine nucleotide disulfide reductases and recycles GSSG on expense of NADPH (Argyrou and Blanchard, 2004; Deponte, 2013).

Phylogenomic profiling of protein interaction networks using EMBL STRING search has suggested the flavoenzyme YpdA (SACOL1520) as putative NADPH-dependent BSSB reductase (**Supplementary Figure S1**), since YpdA co-occurs together with BrxA/B and the BSH biosynthesis enzymes (BshA/B/C) only in BSH-producing bacteria, such as *B. subtilis* and *S. aureus* (**Supplementary Figure S2**; Gaballa et al., 2010). While our work was in progress, a recent study provides first evidence for the function of YpdA as putative BSSB reductase in *S. aureus in vivo* since an increased BSSB level and a decreased BSH/BSSB ratio was measured in the Δ*ypdA* mutant under control and H_2O_2 stress conditions (Mikheyeva et al., 2019). YpdA overproduction was shown to increase the BSH level and contributes to

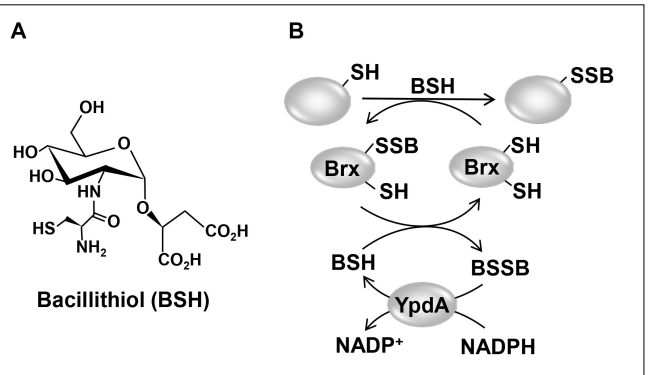

FIGURE 1 | Structure of the LMW thiol bacillithiol (BSH) **(A)** and mechanism of the bacilliredoxin (Brx)/BSH/YpdA de-bacillithiolation pathway **(B)**. **(A)** Bacillithiol is composed of glucosamine, malate, and cysteine. **(B)** Under HOCl stress, BSH leads to *S*-bacillithiolation of proteins which are reduced by bacilliredoxins (BrxA/B), resulting in the transfer of BSH to the Brx active site (Brx-SSB). BSH functions in Brx-SSB reduction to restore Brx activity, leading to BSSB formation. The BSSB reductase YpdA (SACOL1520) regenerates BSH on expense of NADPH.

Abbreviations: BSH, bacillithiol; BSSB, bacillithiol disulfide; BrxA/B, bacilliredoxin A (YphP)/bacilliredoxin B (YqiW); CFUs, colony forming units; DTT, dithiothreitol; E_{BSH}, bacillithiol redox potential; GapDH, glyceraldehyde 3-phosphate dehydrogenase; GSH, glutathione; GSSG, glutathione disulfide; Gor, glutathione disulfide reductase; Grx, glutaredoxins; HOCl, hypochlorous acid; LMW, low molecular weight; Mtr, mycothiol disulfide reductase; NaOCl, sodium hypochlorite; OD_{500}, optical density at 500 nm; rdw, raw dry weight; RCS, reactive chlorine species; ROS, reactive oxygen species; YpdA, bacillithiol disulfide reductase.

oxidative stress resistance, fitness, and virulence of *S. aureus* (Mikheyeva et al., 2019). However, biochemical evidence for the function of YpdA as BSSB reductase and the association of YpdA to the BrxA/B enzymes have not been demonstrated in *B. subtilis* or *S. aureus*.

In this work, we aimed to investigate the role of the complete BrxAB/BSH/YpdA pathway in *S. aureus in vivo* and *in vitro*. We used phenotype and biochemical analyses, HPLC metabolomics and redox biosensor measurements to study the physiological role of the Brx/BSH/YpdA redox pathway in *S. aureus* under oxidative stress and macrophage infection assays. Our data point to important roles of both BrxA and YpdA in the oxidative stress defense for regeneration of reduced E_{BSH} and de-bacillithiolation upon recovery from oxidative stress. Biochemical assays further provide evidence for the function of YpdA as BSSB reductase *in vitro*, which acts in the BrxA/BSH/YpdA electron pathway in de-bacillithiolation of GapDH-SSB.

MATERIALS AND METHODS

Bacterial Strains, Growth, and Survival Assays

Bacterial strains, plasmids and primers used in this study are listed in **Supplementary Tables S1, S2, S3**. For cloning and genetic manipulation, *Escherichia coli* was cultivated in LB medium. For stress experiments, *S. aureus* COL wild type and mutant strains were cultivated in LB, RPMI, or Belitsky minimal medium and exposed to the different compounds during the exponential growth as described previously (Loi et al., 2017, 2018b). NaOCl, methylglyoxal, diamide, methylhydroquinone, DTT, cumene hydroperoxide (80% w/v), H_2O_2 (35% w/v), and monobromobimane were purchased from Sigma Aldrich.

Cloning, Expression, and Purification of His-Tagged Brx-roGFP2, Tpx-roGFP2, GapDH, BrxA, YpdA, and YpdAC14A Proteins in *E. coli*

Construction of plasmids pET11b-*brx-roGFP2* for expression of the Brx-roGFP2 biosensor was described previously (Loi et al., 2017). The pET11b-derived plasmids for overexpression of the His-tagged GapDH and BrxA (SACOL1321) proteins were generated previously (Imber et al., 2018a). The plasmid pET11b-*brx-roGFP2* was used as a template for construction of the Tpx-roGFP2 biosensor to replace *brx* by the *tpx* gene of *S. aureus*. The *tpx* gene (*SACOL1762*) was PCR-amplified from chromosomal DNA of *S. aureus* COL using primers pET-tpx-for-NheI and pET-tpx-rev-SpeI (**Supplementary Table S3**), digested with *Nhe*I and *Bam*HI and cloned into plasmid pET11b-*brx-roGFP2* to generate pET11b-*tpx-roGFP2*. To construct plasmids pET11b-*ypdA* or pET11b-*ypdAC14A*, the *ypdA* gene (*SACOL1520*) was PCR-amplified from chromosomal DNA of *S. aureus* COL with pET-ypdA-for-NdeI or pET-ypdAC14A-for-NdeI as forward primers and pET-ypdA-rev-BamHI as reverse primer (**Supplementary Table S3**), digested with *Nde*I and *Bam*HI and inserted into plasmid pET11b (Novagen). For expression of His-tagged proteins (GapDH, BrxA, YpdA, YpdAC14A, Tpx-roGFP2), *E. coli* BL21(DE3) *plys*S carrying plasmids pET11b-*gap,* pET11b-*brxA,* pET11b-*ypdA*, pET11b-*ypdAC14A* and pET11b-*tpx-roGFP2* was cultivated in 1 l LB medium until an OD_{600} of 0.8 followed by addition of 1 mM IPTG (isopropyl-β-D-thiogalactopyranoside) for 16 h at 25°C. His_6-tagged GapDH, BrxA, YpdA, YpdAC14A, and Tpx-roGFP2 proteins were purified using His Trap™ HP Ni-NTA columns (5 ml; GE Healthcare, Chalfont St Giles, United Kingdom) and the ÄKTA purifier liquid chromatography system (GE Healthcare) as described (Loi et al., 2018b).

Construction of *S. aureus* COL Δ*ypdA,* Δ*brxAB* and Δ*brxAB*Δ*ypdA* Clean Deletion Mutants and Complemented Mutant Strains

Staphylococcus aureus COL Δ*ypdA* (*SACOL1520*), Δ*brxA* (*SACOL1464*), and Δ*brxB* (*SACOL1558*) single deletion mutants as well as the Δ*brxAB* double and Δ*brxAB*Δ*ypdA* triple mutants were constructed using pMAD as described (Arnaud et al., 2004; Loi et al., 2018b). Briefly, the 500 bp up- and downstream regions of *ypdA*, *brxA,* and *brxB* were amplified using gene-specific primers (**Supplementary Table S3**), fused by overlap extension PCR and ligated into the *Bgl*II and *Sal*I sites of plasmid pMAD. The pMAD constructs were electroporated into *S. aureus* RN4220 and further transduced into *S. aureus* COL using phage 81 (Rosenblum and Tyrone, 1964). The clean marker-less deletions of *ypdA*, *brxA,* or *brxB* were selected after plasmid excision as described (Loi et al., 2018b). All mutants were clean deletions of internal gene regions with no genetic changes in the up- and downstream encoding genes. The deletions of the internal gene regions were verified by PCR and DNA sequencing. The Δ*brxAB* and Δ*brxAB*Δ*ypdA* double and triple mutants were obtained by transduction and excision of pMAD-Δ*brxB* into the Δ*brxA* mutant, leading to the Δ*brxAB* deletion and of plasmid pMAD-Δ*ypdA* into the Δ*brxAB* mutant, resulting in the Δ*brxAB*Δ*ypdA* knockout. For construction of *ypdA, brxA,* and *brxB* complemented strains, the xylose-inducible ectopic *E. coli/S. aureus* shuttle vector pRB473 was applied (Brückner et al., 1993). Primers pRB-ypdA, pRB-brxA, and pRB-brxB (**Supplementary Table S3**) were used for amplification of the genes, which were cloned into pRB473 after digestion with *Bam*HI and *Kpn*I to generate plasmids pRB473-*ypdA*, pRB473-*brxA,* and pRB473-*brxB,* respectively. The pRB473 constructs were confirmed by PCR and DNA sequencing and transduced into the Δ*ypdA* and Δ*brxAB* deletion mutants as described (Loi et al., 2017).

Construction of Tpx-roGFP2 and Brx-roGFP2 Biosensor Fusions in *S. aureus* COL

The *tpx-roGFP2* fusion was amplified from plasmid pET11b-*tpx-roGFP2* with primers pRB-tpx-roGFP2-for-BamHI and pRB-tpx-roGFP2-rev-SacI and digested with *Bam*HI and *Sac*I (**Supplementary Table S3**). The PCR product was cloned into

pRB473 generating plasmid pRB473-*tpx-roGFP2*, which was confirmed by DNA sequencing. The biosensor plasmids pRB473-*tpx-roGFP2* and pRB473-*brx-roGFP2* were electroporated into *S. aureus* RN4220 and further transferred to the *S. aureus* COL Δ*ypdA*, Δ*brxAB* and Δ*brxAB*Δ*ypdA* mutants by phage transduction as described (Loi et al., 2017).

Northern Blot Experiments

Northern blot analyses were performed using RNA isolated from *S. aureus* COL before and 15 min after exposure to 0.5 mM methylglyoxal, 0.75 mM formaldehyde, 1 mM NaOCl, 10 mM H_2O_2, 2 mM diamide, and 45 μM methylhydroquinone as described (Wetzstein et al., 1992). Hybridizations were conducted using digoxigenin-labeled antisense RNA probes for *ypdA, brxA,* and *brxB* that were synthesized *in vitro* using T7 RNA polymerase and primers ypdA-NB-for/rev, brxA-NB-for/rev, or brxB-NB-for/rev (**Supplementary Table S3**) as in previous studies (Tam le et al., 2006).

HPLC Thiol Metabolomics for Quantification of LMW Thiols and Disulfides

For preparation of thiol metabolomics samples, *S. aureus* COL WT, Δ*ypdA* and Δ*brxAB* mutants as well as the *ypdA* complemented strains were grown in RPMI medium to an OD_{500} of 0.9 and exposed to 2 mM NaOCl stress for 30 min. The intracellular amounts of reduced and oxidized LMW thiols and disulfides (BSH, BSSB, cysteine and cystine) were extracted from the *S. aureus* cells, labeled with monobromobimane and measured by HPLC thiol metabolomics as described (Chi et al., 2013).

Western Blot Analysis

Staphylococcus aureus strains were grown in LB until an OD_{540} of 2, transferred to Belitsky minimal medium and treated with 100 μM NaOCl for 60 and 90 min. Cytoplasmic proteins were prepared and subjected to non-reducing BSH-specific Western blot analysis using the polyclonal rabbit anti-BSH antiserum as described previously (Chi et al., 2013). The de-bacillithiolation reactions with purified GapDH-SSB and the BrxA/BSH/YpdA/NADPH pathway were also subjected to non-reducing BSH-specific Western blots.

Brx-roGFP2 and Tpx-roGFP2 Biosensor Measurements

Staphylococcus aureus COL, Δ*ypdA* and Δ*brxAB* mutant strains expressing the Brx-roGFP2 and Tpx-roGFP2 biosensor plasmids were grown in LB and used for measurements of the biosensor oxidation degree (OxD) along the growth curves and after injection of the oxidants H_2O_2 and NaOCl as described previously (Loi et al., 2017). The fully reduced and oxidized control samples of Tpx-roGFP2 expression strains were treated with 15 mM DTT and 20 mM cumene hydroperoxide, respectively. The Brx-roGFP2 and Tpx-roGFP2 biosensor fluorescence emission was measured at 510 nm after excitation at 405 and 488 nm using the CLARIOstar microplate reader (BMG Labtech). The OxD of the Brx-roGFP2 and Tpx-roGFP2 biosensors was determined for each sample and normalized to fully reduced and oxidized controls as described (Loi et al., 2017) according to the Eq. (1):

$$O{\times}D = \frac{I405_{sample} \times I488_{red} - I405_{red} \times I488_{sample}}{I405_{sample} \times I488_{red} - I405_{sample} \times I488_{ox} + I405_{ox} \times I488_{sample} - I405_{red} \times I488_{sample}} \quad (1)$$

The values of $I405_{sample}$ and $I488_{sample}$ are the observed fluorescence excitation intensities at 405 and 488 nm, respectively. The values of $I405_{red}$, $I488_{red}$, $I405_{ox}$, and $I488_{ox}$ represent the fluorescence intensities of fully reduced and oxidized controls, respectively.

Based on the OxD values and the previously determined $E^{o'}_{roGFP2} = -280$ mV (Dooley et al., 2004), the BSH redox potential (E_{BSH}) can be calculated using to the Nernst equation (2):

$$E_{BSH} = E_{roGFP2} = E^{o'}_{roGFP2} - \left(\frac{RT}{2F}\right) \times \ln\left(\frac{1 - OxD}{OxD}\right) \quad (2)$$

Biochemical Assays for NADPH-Dependent BSSB Reduction by YpdA and De-Bacillithiolation of GapDH-SSB Using the BrxA/BSH/YpdA Electron Pathway *in vitro*

Before the activity assays, the purified BrxA, YpdA, and YpdAC14A proteins were prereduced with 10 mM DTT followed by DTT removal with Micro Biospin 6 columns (Biorad). For the biochemical activity assays of the specific BSSB reductase activity, 12.5 μM of purified YpdA and YpdAC14A proteins were incubated with 40 μM BSSB, 40 μM GSSG, or 40 μM coenzyme A disulfide and 500 μM NADPH in 20 mM Tris, 1.25 mM EDTA, pH 8.0. NADPH consumption of YpdA and YpdAC14A was measured immediately after the start of the reaction as absorbance change at 340 nm using the Clariostar microplate reader. The NADPH-dependent BrxA/BSH/YpdA electron pathway was reconstituted *in vitro* for de-bacillithiolation of GapDH-SSB. About 60 μM of purified GapDH was *S*-bacillithiolated with 600 μM BSH in the presence of 6 mM H_2O_2 for 5 min. Excess of BSH and H_2O_2 were removed with Micro Biospin 6 columns, which were equilibrated with 20 mM Tris, 1.25 mM EDTA, pH 8.0. Before starting the de-bacillithiolation assay using the BrxA/BSH/YpdA electron pathway, 2.5 μM GapDH-SSB was incubated with 12.5 μM BrxA, 40 μM BSH, and 500 μM NADPH in 20 mM Tris, 1.25 mM EDTA, pH 8.0 at room temperature for 30 min. Next, 12.5 μM YpdA or YpdAC14A proteins were added to the reaction mix at 30°C for 8 min and NADPH consumption was measured at 340 mm. The biochemical activity assays were performed in four replicate experiments.

Infection Assays With Murine Macrophage Cell Line J-774A.1

The murine cell line J774A.1 was cultivated in Iscove's modified Dulbecco MEM medium (Biochrom) with 10% heat inactivated

fetal bovine serum (FBS) and used for *S. aureus* infection assays as described (Loi et al., 2018b). Macrophages were infected with *S. aureus* cells at a multiplicity of infection (MOI) of 1:25. One hour after infection, the cell culture medium was replaced and 150 μg/ml gentamycin was added for 1 h to kill extracellular bacteria and to stop the uptake of *S. aureus*. The *S. aureus* cells were harvested at 2, 4, and 24 h post infection. To determine the percentage of surviving *S. aureus* cells, infected macrophages were lysed with 0.1% Triton X-100 and the supernatant of internalized bacteria was plated on brain heart infusion (BHI) agar plates. The CFUs were counted after incubation for 24–36 h at 37°C (Loi et al., 2018b).

Statistical Analyses

Statistical analysis of growth and survival assays was performed using the Student's unpaired two-tailed *t*-test by the graph prism software. The statistics of the J-774.1 macrophage infection assays was calculated using the one-way ANOVA and Tukey's multiple comparisons *post hoc* test by the graph prism software. The results of the statistical tests are included in the figure legends.

RESULTS

Transcription of *ypdA*, *brxA,* and *brxB* Is Induced Under Disulfide Stress by Diamide and NaOCl in *S. aureus* COL

The bacilliredoxins BrxA (SACOL1464) and BrxB (SACOL1558) of *S. aureus* share an unusual CGC active site and are highly conserved in BSH-producing firmicutes (**Supplementary Figure S1**; Gaballa et al., 2014). The pyridine nucleotide disulfide oxidoreductase YpdA (SACOL1520) belongs to the FAD/NAD(P)-binding domain superfamily (IPR036188) and was annotated as putative BSSB reductase due to its phylogenetic co-occurence with the BSH biosynthesis enzymes and BrxA/B in BSH-producing firmicutes (**Supplementary Figure S2**; Gaballa et al., 2010). We used Northern blot analysis to investigate whether transcription of *brxA*, *brxB,* and *ypdA* is co-regulated and up-regulated under thiol-specific stress conditions, such as 0.5 mM methylglyoxal, 0.75 mM formaldehyde, 1 mM NaOCl, 10 mM H_2O_2, 2 mM diamide and 45 μM methylhydroquinone (**Figure 2**). The *brxA* gene is co-transcribed with *SACOL1465-66-67* in a 2 kb operon and *brxB* is located in the 1.6 kb *SACOL1557-brxB-SACOL1559* operon. The genes co-transcribed together with *brxA* and *brxB* encode proteins of unknown functions. The Northern blot results revealed significant basal transcription of the *brxA, brxB,* and *ypdA* genes and operons in the control, and strong induction under disulfide stress provoked by NaOCl and diamide. Of note, the *brxB* operon was stronger induced under disulfide stress compared to the *brxA* operon (**Figure 2**). No up-regulation of the *brxA, brxB,* and *ypdA* specific mRNAs was detected upon H_2O_2, aldehyde and quinone stress. The co-regulation of BrxA/B and YpdA under disulfide stress suggests that they act in the same pathway to regenerate

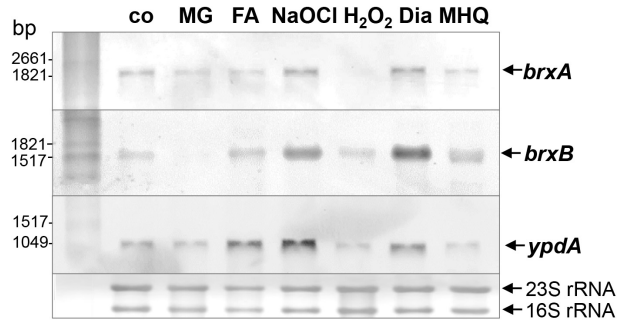

FIGURE 2 | Transcription of *brxA*, *brxB,* and *ypdA* is induced by disulfide stress in *S. aureus*. Northern blot analysis was used to analyze transcription of *brxA*, *brxB,* and *ypdA* in *S. aureus* COL wild type before (co) and 15 min after exposure to 0.5 mM methylglyoxal (MG), 0.75 mM formaldehyde (FA), 1 mM NaOCl, 10 mM H_2O_2, 2 mM diamide (Dia), and 45 μM methylhydroquinone (MHQ) stress at an OD_{500} of 0.5. The arrows point toward the transcript sizes of the *brxA*, *brxB,* and *ypdA* specific genes and operons. The methylene blue-stained bands of the 16S and 23S rRNAs are shown as RNA loading control at the bottom.

S-bacillithiolated proteins under NaOCl stress upon recovery from oxidative stress.

The BSSB Level Is Significantly Increased and the BSH/BSSB Ratio Is Decreased in the *S. aureus* Δ*ypdA* Mutant

To investigate the physiological role of BrxA/B and YpdA under oxidative stress and in BSH redox homeostasis, we constructed Δ*brxAB* and Δ*ypdA* deletion mutants. Using HPLC thiol metabolomics, the intracellular levels of BSH and BSSB were determined in the Δ*brxAB* and Δ*ypdA* mutants under control and NaOCl stress after monobromobimane derivatisation of LMW thiols and disulfides. In the *S. aureus* COL wild type, a BSH level of 1.6–1.9 μmol/g rdw was determined, which was not significantly different in the Δ*ypdA* and Δ*brxAB* mutants (**Figure 3A**). Exposure of *S. aureus* to 2 mM NaOCl stress caused a five to sixfold decreased intracellular BSH level in the wild type, Δ*ypdA* and Δ*brxAB* mutants (**Figure 3A**). The level of BSSB was similar in control and NaOCl-treated cells of the wild type and Δ*brxAB* mutant (∼0.05 μmol/g rdw) (**Figure 3B**). Most interestingly, the Δ*ypdA* mutant showed a significantly twofold increased BSSB level under control and NaOCl stress compared to the wild type (**Figure 3B**), confirming previous data (Mikheyeva et al., 2019). Thus, the BSH/BSSB ratio is ∼2–3-fold decreased in the Δ*ypdA* mutant under control and NaOCl relative to the parent (**Figure 3C**). The increased BSSB levels and the decreased BSH/BSSB redox ratio in the Δ*ypdA* mutant could be restored to wild type levels in the *ypdA* complemented strain. In addition, a significantly 1.5-fold increased cysteine level was measured in the Δ*ypdA* mutant under NaOCl stress, but no changes in the level of cystine (**Supplementary Figures S3A–C**). The cysteine levels could be also restored to wild type level in the *ypdA* complemented

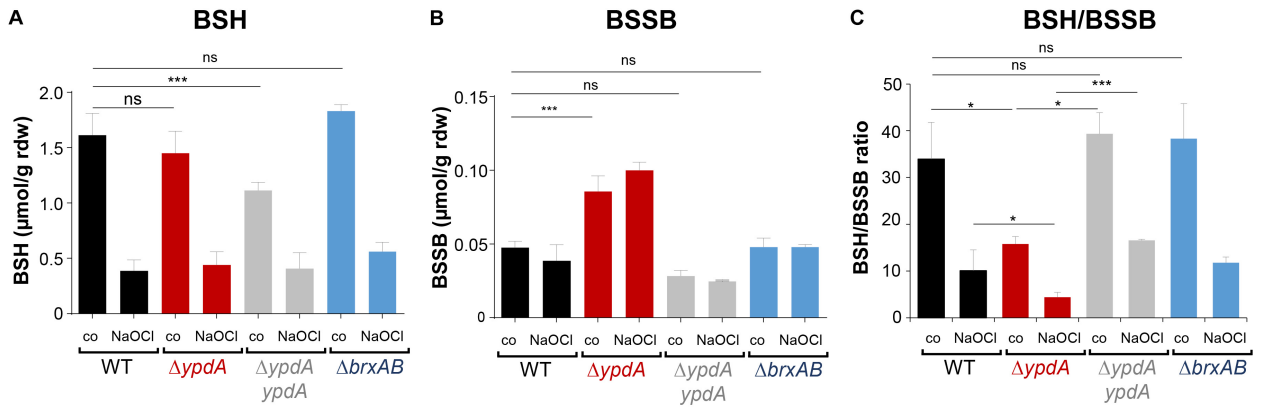

FIGURE 3 | The BSSB level is strongly increased and the BSH/BSSB redox ratio is decreased in the *S. aureus* COL Δ*ypdA* mutant under control and NaOCl stress. The levels of BSH **(A)**, BSSB **(B)** and the BSH/BSSB redox ratio **(C)** were determined in *S. aureus* COL wild type (WT), the Δ*ypdA* and Δ*brxAB* mutants as well as in the *ypdA* complemented strain before (co) and 30 min after treatment with 2 mM NaOCl stress. LMW thiols and disulfides were labeled with monobromobimane and measured using HPLC-thiol-metabolomics. Mean values and standard deviations (SD) of four biological replicates are shown. $^{ns}p > 0.05$; $^{*}p \leq 0.01$, and $^{***}p \leq 0.001$.

strain. These results indicate that YpdA is important to maintain the reduced level of BSH under control and NaOCl stress, supporting previous results (Mikheyeva et al., 2019), while the bacilliredoxins BrxA/B are dispensible for the cellular BSH/BSSB redox balance during the growth and under oxidative stress in *S. aureus*.

The *S. aureus* Δ*ypdA* Mutant Is Impaired to Regenerate the Reduced BSH Redox Potential and to Detoxify H_2O_2 Under Oxidative Stress

Next, we applied the Brx-roGFP2 biosensor to monitor the changes of its OxD in *S. aureus* COL wild type, the Δ*ypdA* and Δ*brxAB* mutants during the growth and under oxidative stress (Loi et al., 2017). Using the Nernst equation the OxD values were used to calculate the changes in the BSH redox potential (E_{BSH}) in wild type and mutant strains (see section "Materials and Methods" for details). Measurements of the Brx-roGFP2 OxD in LB medium along the growth did not reveal notable differences in the basal level of E_{BSH} between wild type, Δ*ypdA* and Δ*brxAB* mutant strains (**Supplementary Figures S4A,B, S5A,B** and **Supplementary Table S4**). The basal level of E_{BSH} varied from −282 to −295 mV in the wild type and from −286 to −299 mV in the Δ*ypdA* and Δ*brxAB* mutants in different growth phases (**Supplementary Figures S5A,B** and **Supplementary Table S4**). Thus, we monitored the biosensor OxD and calculated the E_{BSH} changes in Δ*ypdA* and Δ*brxAB* mutants after exposure to sub-lethal doses of 100 µM NaOCl and 100 mM H_2O_2 to identify functions for BrxAB or YpdA under oxidative stress. The Brx-roGFP2 biosensor was strongly oxidized under NaOCl and H_2O_2 stress in the wild type, the Δ*ypdA* and Δ*brxAB* mutants (**Figures 4A–D**). The calculated E_{BSH} increased upon NaOCl stress from −286 to −254 mV in the wild type, from −285 to −247 mV in the Δ*ypdA* mutant and from −288 to −259 mV in the Δ*brxAB* mutant (**Supplementary Figures S5C,D** and **Supplementary Table S5**). This indicates a stronger increase of E_{BSH} by NaOCl stress in the Δ*ypdA* mutant compared to the wild type. Regeneration of the reduced basal level E_{BSH} occurred already after 2 h reaching values of −269 mV in the wild type and −274 mV in the Δ*brxAB* mutant (**Figure 4B**, **Supplementary Figure S5D**, and **Supplementary Table S5**). However, the Δ*ypdA* mutant was significantly impaired to recover the reduced state and E_{BSH} values remained high with −252 mV after 2 h of NaOCl stress (**Figure 4A**, **Supplementary Figure S5C**, and **Supplementary Table S5**). Of note, the defect of the Δ*ypdA* mutant to restore the reduced state of E_{BSH} was reproducible with both oxidants, H_2O_2 and NaOCl (**Figures 4A,C**, **Supplementary Figures S5C,E**, and **Supplementary Table S6**). While recovery of reduced E_{BSH} after H_2O_2 stress was fast in the wild type and Δ*brxAB* mutant reaching E_{BSH} values of −280 and −283 mV already after 60 min, the Δ*ypdA* mutant was still oxidized after 2 h with high E_{BSH} values of −264 mV (**Supplementary Figures S5E,F** and **Supplementary Table S6**). These Brx-roGFP2 measurements document the important role of YpdA to reduce BSSB and to regenerate the reduced E_{BSH} during the recovery phase of cells from oxidative stress.

We further hypothesized that the Δ*ypdA* mutant is defective in H_2O_2 detoxification due to its increased BSSB levels. To analyse the kinetics of H_2O_2 detoxification in the Δ*ypdA* mutant, we constructed a genetically encoded H_2O_2-specific Tpx-roGFP2 biosensor. First, we verified that Tpx-roGFP2 showed the same ratiometric changes of the excitation spectrum in the fully reduced and oxidized state *in vitro* and *in vivo* as previously measured for Brx-roGFP2 (**Supplementary Figures S6A,B**). Tpx-roGFP2 was shown to respond strongly to low levels of 0.5–1 µM H_2O_2 *in vitro* and was fully oxidized with 100 mM H_2O_2 inside *S. aureus* COL wild type cells indicating the utility of the probe to measure H_2O_2 detoxification kinetics in *S. aureus* (**Supplementary Figures S6C,D**). Measurements of Tpx-roGFP2 oxidation along the growth in LB medium

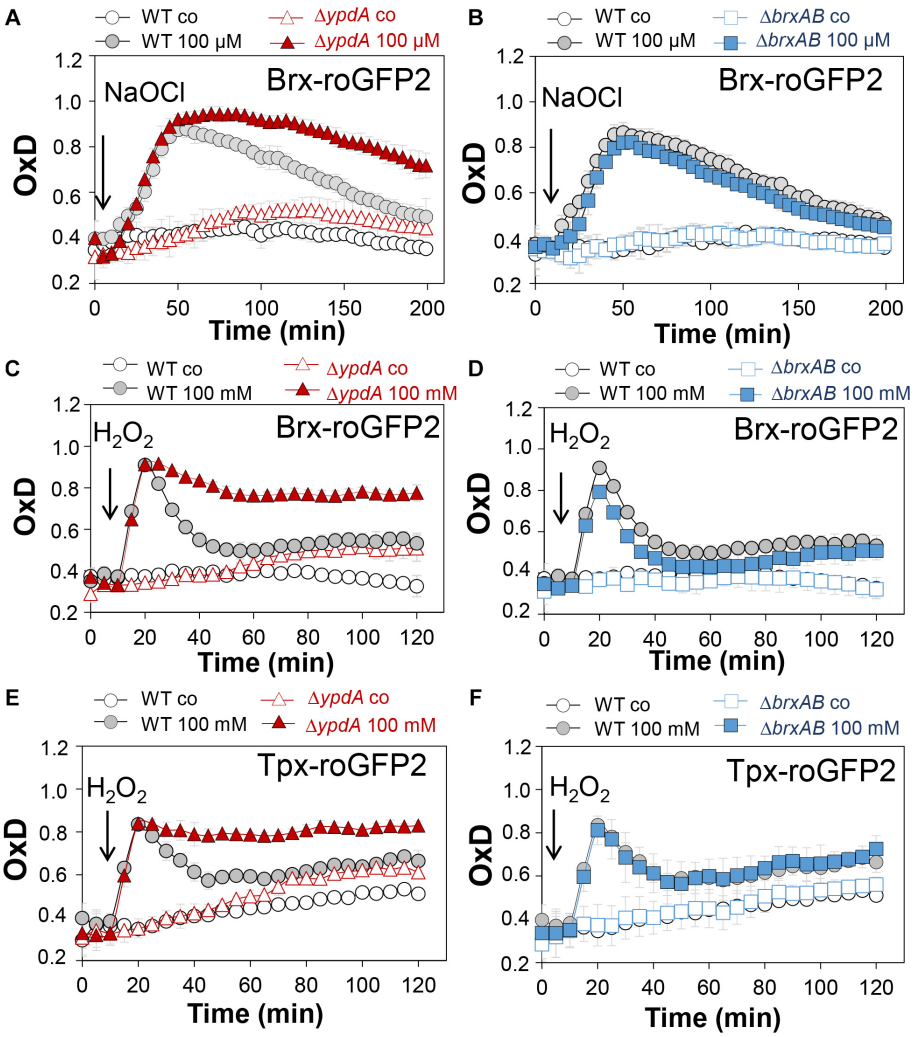

FIGURE 4 | Brx-roGFP2 and Tpx-roGFP2 biosensors measurements of the OxD indicate that the *S. aureus* Δ*ypdA* mutant is impaired to regenerate the reduced state of E_{BSH} and to detoxify H_2O_2 during recovery from oxidative stress. **(A–D)** Response of the Brx-roGFP2 biosensor to 100 µM NaOCl and 100 mM H_2O_2 stress in *S. aureus* COL WT, the Δ*ypdA* **(A,C)** and Δ*brxAB* **(B,D)** mutants. **(E,F)** Response of the Tpx-roGFP2 biosensor under 100 mM H_2O_2 stress in the *S. aureus* COL WT, the Δ*ypdA* and Δ*brxAB* mutants. The Brx-roGFP2 biosensor responses are shown as OxD values and the corresponding E_{BSH} changes were calculated using the Nernst equation and presented in **Supplementary Figure S5** and **Supplementary Tables S5, S6**. Mean values and SD of three biological replicates are shown.

revealed a similar high OxD of ∼0.5–0.6 in the wild type, Δ*brxAB* and Δ*ypdA* mutant strains (**Supplementary Figures S4C,D**). The absence of BrxA/B or YpdA did not affect the biosensor OxD under non-stress conditions, which further provides evidence for roles under oxidative stress. Thus, we monitored the H_2O_2 response of Tpx-roGFP2 and the kinetics of H_2O_2 detoxification in the Δ*ypdA* and Δ*brxAB* mutants. Interestingly, Tpx-roGFP2 showed a similar response to 100 mM H_2O_2 in all strains, but the Δ*ypdA* mutant was significantly impaired in H_2O_2 detoxification compared to the wild type (**Figures 4E,F**). These results clearly confirmed that the Δ*ypdA* mutant is defective to recover from oxidative stress due to its higher BSSB level resulting in an oxidized E_{BSH} as revealed using Brx-roGFP2 and thiol-metabolomics studies.

S-Bacillithiolation of GapDH Is Not Affected in Δ*ypdA* and Δ*brxAB* Mutants or in *ypdA*, *brxA*, and *brxB* Complemented Strains

In *S. aureus*, the glyceraldehyde-3 phosphate dehydrogenase GapDH was previously identified as most abundant *S*-bacillithiolated protein under NaOCl stress that is visible as major band in BSH-specific non-reducing Western blots (Imber et al., 2018a). Since GapDH activity could be recovered with purified BrxA *in vitro* previously (Imber et al., 2018a), we analyzed the pattern of GapDH *S*-bacillithiolation in the Δ*brxAB* and Δ*ypdA* mutants as well as in *ypdA*, *brxA* and *brxB* complemented strains *in vivo*. However, the amount of *S*-bacillithiolated GapDH was similar after

100 μM NaOCl stress between wild type, Δ*brxAB* and Δ*ypdA* mutants and complemented strains (**Figures 5A,B**). This indicates that the absence of the BrxAB/YpdA pathway does not affect the level of *S*-bacillithiolation of GapDH under NaOCl stress.

The Bacilliredoxins BrxA/B and the Putative BSSB Reductase YpdA Are Important for Growth and Survival Under Oxidative Stress and Macrophage Infections

Next, we analyzed the physiological role of the BrxA/B/YpdA pathway for growth and survival of *S. aureus* under H_2O_2 and NaOCl stress. The growth of the Δ*ypdA* and Δ*brxAB* mutants in RPMI medium without stress exposure was comparable to the wild type (**Figures 6A,C**). Interestingly, both Δ*brxAB* and Δ*ypdA* mutants displayed a small, but statistically significant growth delay after exposure to sub-lethal amounts of 1.5 mM NaOCl compared to the wild type, while no growth delay was observed with sub-lethal 10 mM H_2O_2 (**Figures 6A,C**, **7A,B**). This might indicate that BrxAB and YpdA function in the same pathway as already suggested by phylogenomic profiling using STRING search (**Supplementary Figure S2**). Determination of viable counts revealed significantly ∼2-fold decreased survival rates of both Δ*brxAB* and Δ*ypdA* mutants after exposure to lethal doses of 3.5 mM NaOCl and 40 mM H_2O_2 relative to the wild type (**Figures 6F,G**, **7C,D**). These oxidant sensitive growth and survival phenotypes of the Δ*brxAB* and Δ*ypdA* mutants could be restored back to wild type levels by complementation with *brxA* and *ypdA,* respectively (**Figures 6B,D,F,G**, **7C,D**). However, complementation of the Δ*brxAB* mutant with *brxB* did not restore the growth and viability of the wild type under NaOCl stress (**Figures 6E,G**), although xylose-inducible *brxB* expression of plasmid pRB473-*brxB* could be verified in Northern blots (**Supplementary Figure S7**). Moreover, the Δ*brxAB*Δ*ypdA* triple mutant displayed the same sensitivity as the Δ*brxAB* mutant to 40 mM H_2O_2 and 3 mM NaOCl indicating that BrxA and YpdA function in the same pathway for reduction of *S*-bacillithiolated proteins (**Figures 7D** and **Supplementary Figure S8C**).

To investigate the function of the BrxA/B/YpdA pathway under infection-relevant conditions, we measured the intracellular survival of the Δ*brxAB* and Δ*ypdA* mutants in phagocytosis assays inside murine macrophages of the cell line J-774A.1, as previously (Loi et al., 2018b). The viable counts (CFUs) of internalized *S. aureus* cells were determined at 2, 4, and 24 h post infection of the macrophages. The number of surviving cells decreased to 21.3% at 24 h post infection for the *S. aureus* COL wild type, but more strongly to 11.4 and 10.2% for the Δ*ypdA* and Δ*brxAB* mutants (**Figures 8A,C**). Thus, the number of viable counts was significantly ∼2-fold lower for both Δ*brxAB* and Δ*ypdA* mutants at 24 h post infection compared to the wild type. These sensitive phenotypes of the Δ*ypdA* and Δ*brxAB* mutants under macrophage infections could be restored to 80% of wild type levels after complementation with plasmid-encoded *ypdA* or *brxA*, respectively (**Figures 8B,D**). However, complementation with *brxB* did not restore the survival defect of the Δ*brxAB* mutant, pointing again to the major role of BrxA in this pathway.

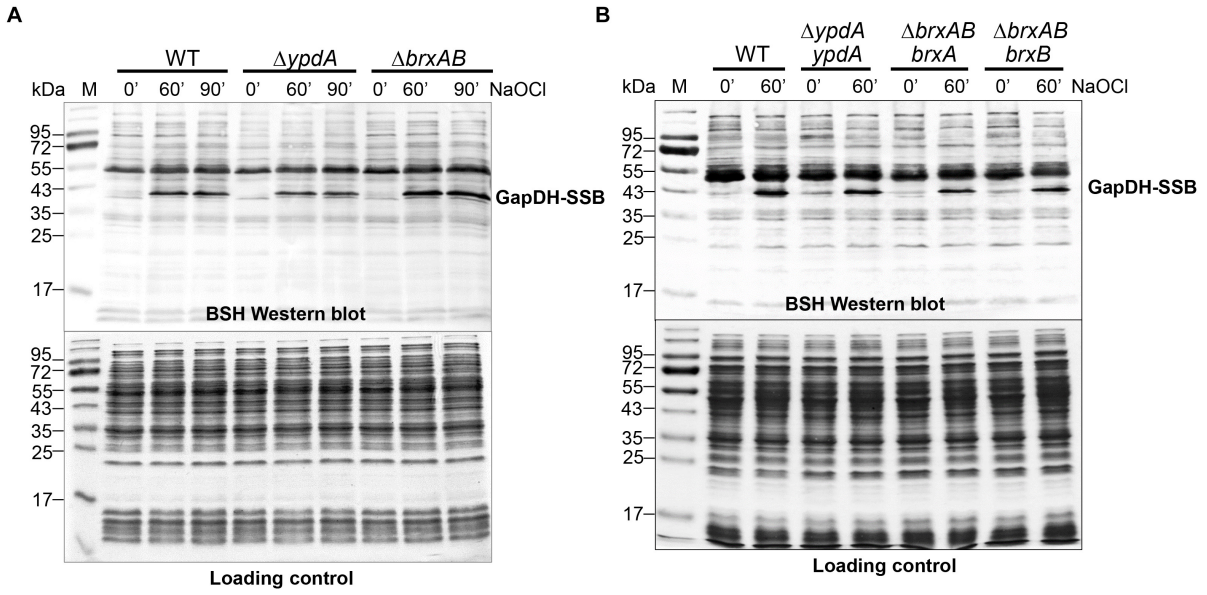

FIGURE 5 | Protein *S*-bacillithiolation of GapDH is not affected in the Δ*ypdA* and Δ*brxAB* mutants **(A)** or in the *ypdA*, *brxA,* and *brxB* complemented strains **(B)** as revealed by non-reducing BSH Western blots. The prominent GapDH-SSB band is visible in the cell extracts of NaOCl-treated *S. aureus* cells using non-reducing BSH Western blots. Other bands visible under control and stress conditions are proteins cross-reactive with the polyclonal rabbit anti-BSH antibodies. The amount of GapDH-SSB is similar in the WT, Δ*ypdA* and Δ*brxAB* mutants **(A)** as well as in the *ypdA*, *brxA,* and *brxB* complemented strains **(B)**. The SDS PAGE loading control is shown at the bottom for comparison.

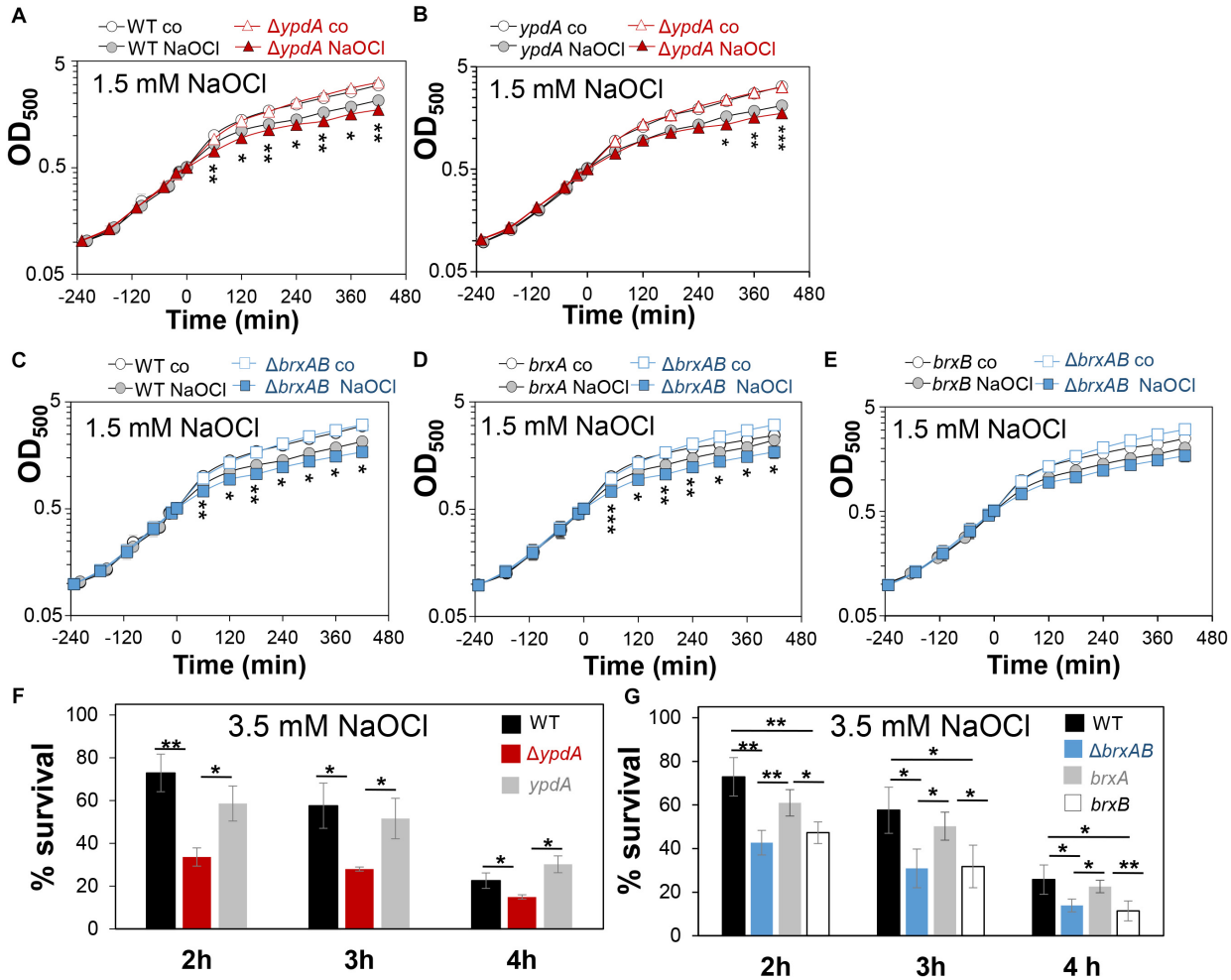

FIGURE 6 | The *S. aureus* Δ*ypdA* and Δ*brxAB* mutants are more sensitive under NaOCl stress. **(A–E)** Growth curves of *S. aureus* COL WT, Δ*ypdA* and Δ*brxAB* mutants as well as *ypdA*, *brxA,* and *brxB* complemented strains in RPMI medium after exposure to 1.5 mM NaOCl stress at an OD_{500} of 0.5. **(F,G)** Survival rates were determined as CFUs for *S. aureus* COL WT, Δ*ypdA* and Δ*brxAB* mutants as well as *ypdA*, *brxA,* and *brxB* complemented strains at 2, 3, and 4 h after treatment with 3.5 mM NaOCl. Survival of the untreated control was set to 100%. Mean values and SD of 3–4 biological replicates are presented. The statistics was calculated using a Student's unpaired two-tailed *t*-test by the graph prism software. Symbols are: $^{ns}p > 0.05$, $^{*}p \leq 0.05$, and $^{**}p \leq 0.01$.

Taken together, our results revealed that the bacilliredoxin BrxA and the putative BSSB reductase YpdA are required for improved survival of *S. aureus* inside macrophages to resist the oxidative burst. Our data suggest that BrxA and YpdA act together in the BrxA/BSH/YpdA pathway to regenerate *S*-bacillithiolated proteins and to restore the BSH redox potential upon recovery from oxidative stress during infections.

The Flavin Disulfide Reductase YpdA Functions in BSSB Reduction and De-Bacillithiolation of GapDH-SSB in the BrxA/BSH/YpdA Electron Transfer Assay *in vitro*

Next, we aimed to analyze the catalytic activity of purified YpdA in a NADPH-coupled assay with BSSB as substrate *in vitro,* since biochemical evidence for the function of YpdA as BSSB reductase activity *in vitro* is still missing (Mikheyeva et al., 2019). The His-tagged YpdA protein was purified as yellow colored enzyme and the UV-visible spectrum revealed the presence of the FAD co-factor indicated by the two absorbance peaks at 375 and 450 nm (**Supplementary Figure S9**). Incubation of YpdA protein with BSSB resulted in significant and fast consumption of NADPH as measured by a rapid absorbance decrease at 340 nm (**Figure 9A**). Only little NADPH consumption was measured with YpdA alone in the absence of the BSSB substrate supporting previous finding that YpdA consumes NADPH alone (Mikheyeva et al., 2019). However, in our assays, BSSB significantly enhanced NADPH consumption by YpdA compared to the control reaction without BSSB. No increased NADPH consumption was measured with coenzyme A disulphide ($CoAS_2$) or GSSG as substrate indicating the specificity of YpdA for BSSB (**Figure 9A**). In addition, we investigated the role of the conserved Cys14 of YpdA for the BSSB reductase activity in the NADPH-coupled assay.

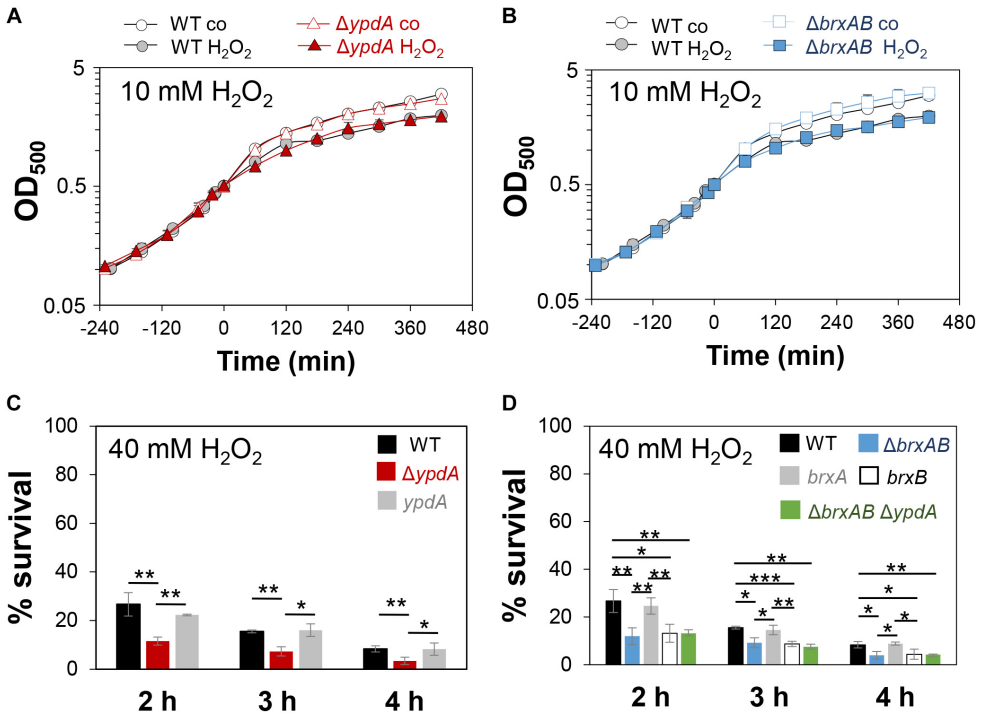

FIGURE 7 | The *S. aureus* Δ*ypdA* and Δ*brxAB* mutants show increased sensitivities to H_2O_2 stress. **(A,B)** Growth curves of *S. aureus* COL WT, the Δ*ypdA* and Δ*brxAB* mutants in RPMI after exposure to 10 mM H_2O_2 stress at an OD_{500} of 0.5. **(C,D)** Survival rates were determined as CFUs for *S. aureus* COL WT, Δ*ypdA*, Δ*brxAB* and Δ*brxAB*Δ*ypdA* mutants as well as *ypdA*, *brxA*, *brxB* complemented strains at 2, 3, and 4 h after treatment with 40 mM H_2O_2. Survival of the untreated control was set to 100%. Mean values and SD of 3–5 biological replicates are presented. The statistics was calculated using a Student's unpaired two-tailed *t*-test by the graph prism software. Symbols are: $^{ns}p > 0.05$, $^{*}p \leq 0.05$, and $^{**}p \leq 0.01$.

NADPH-consumption of YpdAC14A upon BSSB reduction was much slower and similar to the control reaction of YpdA and YpdAC14A without BSSB (**Figure 9B**).

Our *in vivo* data support that YpdA and BrxA act together in the BrxA/BSH/YpdA de-bacillithiolation pathway. Thus, we analyzed NADPH-consumption by the BrxA/BSH/YpdA electron pathway in de-bacillithiolation of GapDH-SSB *in vitro*. The de-bacillithiolation assays revealed fast NADPH consumption in the complete BrxA/BSH/YpdA coupled assays (**Figure 9C**). NADPH consumption by YpdA was slower in the absence of BrxA and might be caused by residual BSSB in the BSH samples. The control reaction of GapDH-SSB with BrxA did not consume NADPH and only little NADPH consumption was measured with BrxA, BSH and the YpdAC14A mutant protein in de-bacillithiolation of GapDH-SSB (**Figure 9D**).

In addition, BSH-specific non-reducing Western blots were used to investigate if BrxA and the complete BrxA/BSH/YpdA pathway catalyze de-bacillithiolation of GapDH-SSB (**Figure 9E**). The BSH-blots showed that BrxA is sufficient for de-bacillithiolation of GapDH-SSB, since all reactions of GapDH-SSB with BrxA lead to complete de-bacillithiolation with and without YpdA or YpdAC14A plus NADPH. However, the reactions of GapDH-SSB with YpdA/NADPH alone did not lead to reduction of GapDH-SSB, indicating the main role of BrxA in de-bacillithiolation while YpdA functions in regeneration of BSH in the BrxA/BSH/YpdA/NADPH redox cycle.

In conclusion, our biochemical assays revealed that YpdA functions as BSSB reductase in an NADPH coupled assay. Cys14 of YpdA is important for the BSSB reductase activity *in vitro*. Thus, YpdA facilitates together with BrxA the reduction of *S*-bacillithiolated GapDH in the BrxA/BSH/YpdA redox pathway upon recovery from oxidative stress.

DISCUSSION

The putative disulfide reductase YpdA was previously shown to be phylogenetically associated with the BSH biosynthesis enzymes and bacilliredoxins (**Supplementary Figure S2**), providing evidence for a functional Brx/BSH/YpdA pathway in BSH-producing bacteria (Gaballa et al., 2010). Recent work confirmed the importance of YpdA for the BSH/BSSB redox balance and survival under oxidative stress and neutrophil infections in *S. aureus in vivo* (Mikheyeva et al., 2019). Here, we have studied the role of the bacilliredoxins BrxA/B and the BSSB reductase YpdA in the defense of *S. aureus* against oxidative stress *in vivo* and their biochemical function in the de-bacillithiolation pathway *in vitro*. Transcription of *brxA*, *brxB* and *ypdA* is strongly upregulated under disulfide stress, provoked by diamide and NaOCl. About two to fourfold increased transcription of *ypdA*, *brxA*, and *brxB* was previously found under H_2O_2, diamide and NaOCl stress, by the antimicrobial surface coating

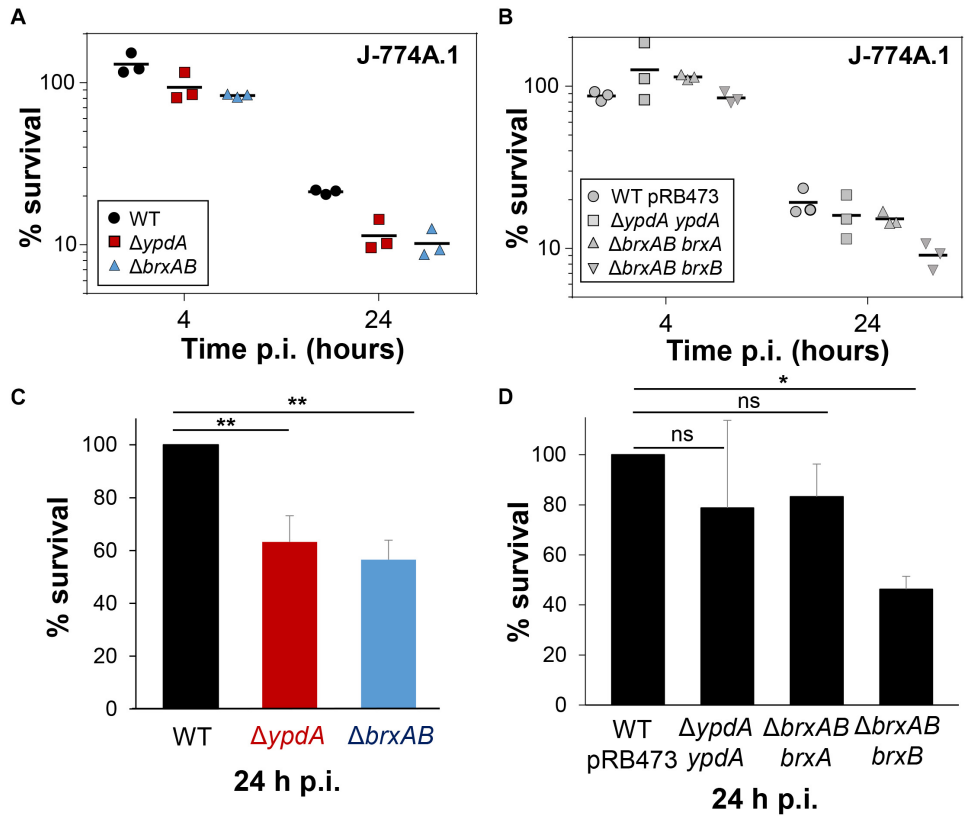

FIGURE 8 | YpdA and BrxA/B promote the intracellular survival of *S. aureus* inside murine macrophages during infections. **(A,B)** The survival of *S. aureus* WT, Δ*ypdA* and Δ*brxAB* mutants and complemented strains was analyzed 2, 4 and 24 h post infection (p.i.) of the murine macrophage cell line J-774A.1 by CFU counting. The percentages in survival of the Δ*ypdA* and Δ*brxAB* mutants and complemented strains were calculated after 4 and 24 h in relation to the 2 h time point, which was set to 100%. **(C,D)** The average percentage in survival was calculated for Δ*ypdA* and Δ*brxAB* mutants **(C)** and complemented strain **(D)** in relation to the WT and WT with empty plasmid pRB473, which were set to 100%. Error bars represent the SEM and the statistics were calculated using one-way ANOVA and Tukey's multiple comparisons *post hoc* test using the graph prism software ($p = 0.0050$ for WT/Δ*ypdA*, $p = 0.0022$ for WT/Δ*brxAB* and $p = 0.026$ for WT pRB473/Δ*brxAB brxB*). Symbols: $^{ns}p > 0.05$; $^{*}p \leq 0.05$, and $^{**}p \leq 0.01$.

composed of Ag^{+} and Ru^{+} (AGXX®) and after exposure to azurophilic granule proteins in *S. aureus* (Palazzolo-Ballance et al., 2008; Posada et al., 2014; Mäder et al., 2016; Loi et al., 2018a,b; Mikheyeva et al., 2019). The elevated transcription of *brxA, brxB,* and *ypdA* under disulfide stress correlated with the up-regulation of the *bshA*, *bshB,* and *bshC* genes for BSH biosynthesis in *S. aureus* and *B. subtilis* (Chi et al., 2011; Nicolas et al., 2012; Loi et al., 2018a,b). The *bshA, bshB,* and *bshC* genes and operons are under control of the disulfide stress-specific Spx regulator in *B. subtilis,* which controls a large regulon for thiol-redox homeostasis (Gaballa et al., 2013). Thus, genes for BSH biosynthesis and the BrxA/B/YpdA pathway might be also regulated by Spx in *S. aureus*.

The co-regulation of BrxA/B and YpdA under disulfide stress points to their function in the same pathway in *S. aureus*. HOCl, diamide and AGXX® were shown to cause a strong disulfide stress response in the transcriptome and protein *S*-bacillithiolation in the proteome of *S. aureus* (Imber et al., 2018a; Loi et al., 2018a,b). Thus, the BrxA/B and YpdA redox enzymes are up-regulated under conditions of protein *S*-bacillithiolations, connecting their functions to the de-bacillithiolation pathway. We could show here that NaOCl stress leads to five to sixfold depletion of the cellular pool of reduced BSH in the *S. aureus* COL wild type, which was not accompanied by an enhanced BSSB level. In the previous study, 20 mM H_2O_2 resulted in twofold reduction of BSH and threefold increase of BSSB in the *S. aureus* wild type (Mikheyeva et al., 2019). Most probably, the increased BSSB level under NaOCl stress was used for protein *S*-bacillithiolation in our study (Imber et al., 2018a), while sub-lethal 20 mM H_2O_2 might not lead to an increase in *S*-bacillithiolation in the previous study (Mikheyeva et al., 2019).

The BSH/BSSB redox ratio of *S. aureus* wild type cells was determined as ∼35:1 under control conditions and decreased threefold to 10:1 under NaOCl. Of note, this basal BSH/BSSB ratio in *S. aureus* COL wild type was higher compared to the basal BSH/BSSB ratio of ∼17:1 as determined previously in the *bshC* repaired SH1000 strain (Mikheyeva et al., 2019). In *E. coli*, the GSH/GSSG redox ratio was determined in the range between 30:1 and 100:1 (Hwang et al., 1995; Van Laer et al., 2013), which is similar as measured for the basal BSH/BSSB ratio in *S. aureus* COL. The differences in the BSH/BSSB ratios might be related to different *S. aureus* strain

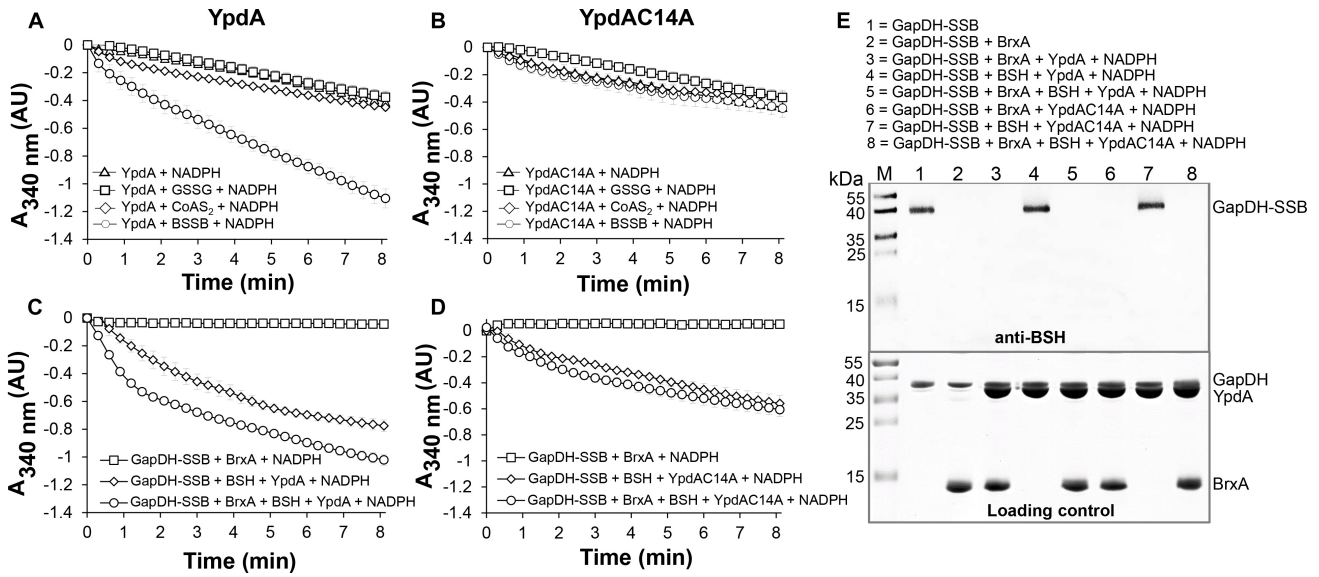

FIGURE 9 | YpdA functions as BSSB reductase in the NADPH-coupled BrxA/BSH/YpdA electron pathway for de-bacillithiolation of GapDH-SSB *in vitro*. **(A)** Purified YpdA is able to reduce BSSB back to BSH with electrons from NADPH as measured by the absorbance change at 340 nm. Only little NADPH consumption was measured with YpdA alone in the absence of BSSB, with coenzymeA disulfide (CoAS2) or glutathione disulfide (GSSG) **(A)** and in the YpdAC14A mutant **(B)** indicating the function of the conserved Cys14 as active site of YpdA for BSSB reduction. **(C)** NADPH consumption of YpdA was measured in the coupled BrxA/BSH/YpdA de-bacillithiolation assay for reduction of GapDH-SSB. While fast NADPH consumption was measured upon de-bacillithiolation of GapDH-SSB with purified YpdA **(C)**, the reaction was much slower with the YpdAC14A mutant **(D)**. The coupled assays were conducted with 2.5 μM Gap-SSB, 12.5 μM BrxA, 40 μM BSH, 500 μM NADPH in 20 mM Tris, 1.25 mM EDTA, pH 8.0. After 30-min incubation, 12.5 μM YpdA or YpdAC14A proteins were added to the reaction mix and NADPH consumption was monitored at 340 nm as a function of time. Mean values and SEM of four independent experiments are shown. **(E)** The de-bacillithiolation of GapDH-SSB is catalyzed by BrxA or the complete BrxA/BSH/YpdA pathway, but not by YpdA alone as shown by non-reducing BSH-specific Western blots. The loading controls are shown below as Coomassie-stained SDS-PAGE with the same de-bacillithiolation reactions of GapDH-SSB as in the BSH-blot.

backgrounds or growth conditions. Nevertheless, NaOCl and H_2O_2 decreased the BSH/BSSB ratio in our and the previous study (Mikheyeva et al., 2019). In the *S. aureus* Δ*brxAB* mutant, we also measured a threefold decrease of the BSH/BSSB ratio from control conditions (38:1) to NaOCl (12:1). However, the Δ*ypdA* mutant showed a twofold enhanced BSSB level in control and NaOCl-treated cells, leading to a significantly decreased BSH/BSSB ratio under control (17:1) and NaOCl stress (5:1). These results support previous results of the *bshC* repaired SH1000, showing a decreased BSH/BSSB ratio under control (6:1) to H_2O_2 stress (2:1) (Mikheyeva et al., 2019), although both ratios were again much lower as in our study. Taken together, our data indicate that BrxAB are dispensable for the BSH redox homeostasis, while YpdA is essential for BSSB reduction to maintain the reduced pool of BSH and a high BSH/BSSB ratio in *S. aureus*.

Brx-roGFP2 biosensor measurements provide further support that YpdA is the candidate BSSB reductase. The Δ*ypdA* mutant was significantly impaired to restore reduced E_{BSH} during recovery from NaOCl and H_2O_2 stress as calculated using the Nernst equation based on the OxD values of the Brx-roGFP2 biosensor measurements (**Supplementary Tables S5, S6**). Moreover, application of the Tpx-roGFP2 biosensor revealed a delay in H_2O_2 detoxification in Δ*ypdA* mutant cells during the recovery phase. These results clearly support the important role of YpdA as BSSB reductase particularly under oxidative stress to recover reduced E_{BSH} required for detoxification of ROS.

These *in vivo* data were further corroborated by biochemical activity assays of YpdA for BSSB reduction in a NADPH-coupled assay. While little NADPH consumption was measured in the presence of YpdA alone, BSSB significantly enhanced NADPH consumption, supporting the crucial role of YpdA as BSSB reductase *in vitro*. Further electron transfer assays revealed that YpdA functions together with BrxA and BSH in reduction of GapDH-SSB *in vitro*. Previous de-bacillithiolation assays have revealed regeneration of GapDH activity by BrxA *in vitro* (Imber et al., 2018a). Here, we confirmed that BrxA activity is sufficient for complete de-bacillithiolation of GapDH-SSB *in vitro*, while YpdA alone had no effect on the GapDH-SSB reduction. Thus, BrxA catalyzes reduction of *S*-bacillithiolated proteins and YpdA is involved in BSH regeneration in the complete BrxA/BSH/YpdA redox cycle.

The BSSB reductase activity of YpdA was shown to be dependent on the conserved Cys14, which is located in the glycine-rich Rossmann-fold NAD(P)H binding domain ($GGGPC_{14}G$) (Bragg et al., 1997; Mikheyeva et al., 2019). Cys14 might be *S*-bacillithiolated by BSSB and reduced by electron transfer from NADPH via the FAD co-factor. Cys14 was previously identified as oxidized under NaOCl stress in the *S. aureus* redox proteome using the OxICAT method, further supporting its role as active site Cys and its *S*-bacillithiolation

during the BrxA/BSH/YpdA catalytic cycle (Imber et al., 2018a). The catalytic mechanism of BSSB reduction via Cys14 of YpdA is an interesting subject of future studies.

Previous phenotype results of the Δ*ypdA* mutant revealed that YpdA is important for survival of *S. aureus* in infection assays with human neutrophils (Mikheyeva et al., 2019). Our phenotype analyses further showed protective functions of the complete BrxA/BSH/YpdA redox pathway for growth and survival of *S. aureus* under oxidative stress *in vitro* and in macrophage infections *in vivo*. The Δ*ypdA* and Δ*brxAB* mutants were significantly impaired in growth and survival after exposure to sub-lethal and lethal doses of NaOCl and displayed survival defects under lethal H_2O_2. Moreover, the H_2O_2 and NaOCl-sensitivity and the defect to recover reduced E_{BSH} in the Δ*brxAB*Δ*ypdA* triple mutant was comparable with that of the Δ*ypdA* mutant (**Figure 7D** and **Supplementary Figure S8**). These results clearly indicate that BrxA/B and YpdA function in the same de-bacillithiolation pathway, which is an important defense mechanism of *S. aureus* against oxidative stress.

Based on previous bacilliredoxin activity assays *in vitro*, both BrxA and BrxB should use a monothiol mechanism to reduce *S*-bacillithiolated client proteins, such as OhrR, GapDH and MetE in *B. subtilis* and *S. aureus* (Gaballa et al., 2014; Imber et al., 2018a). Most di-thiol Grx of *E. coli* (Grx1, Grx2, and Grx3) use the monothiol mechanism for de-glutathionylation of proteins (Lillig et al., 2008; Allen and Mieyal, 2012; Loi et al., 2015). In the monothiol mechanism, the nucleophilic thiolate of the Brx CGC motif attacks the *S*-bacillithiolated protein, resulting in reduction of the protein substrate and Brx-SSB formation. Brx-SSB is then recycled by BSH, leading to increased BSSB formation. YpdA reduces BSSB back to BSH with electrons from NADPH (**Figure 1B**). The oxidation-sensitive phenotypes of Δ*ypdA* and Δ*brxAB* mutants could be complemented by plasmid-encoded *ypdA* and *brxA*, but not *brxB*, respectively. These results provide evidence for the function of the BrxA/BSH/YpdA de-bacillithiolation pathway using the monothiol-Brx mechanism in *S. aureus*.

Similar phenotypes were found for mutants lacking related redox enzymes of the GSH and mycothiol pathways in other bacteria. In *E. coli*, strains lacking the Gor and Grx are more sensitive under diamide and cumene hydroperoxide stress (Alonso-Moraga et al., 1987; Vlamis-Gardikas et al., 2002; Lillig et al., 2008). In *Mycobacterium smegmatis*, the mycoredoxin-1 mutant displayed an oxidative stress-sensitive phenotype (Van Laer et al., 2012). In *Corynebacterium glutamicum*, deficiency of the Mtr resulted in an oxidized mycothiol redox potential (Tung et al., 2019), and Mtr overexpression contributed to improved oxidative stress resistance (Si et al., 2016). Taken together, our results revealed that not only BSH, but also BrxA and YpdA are required for virulence and promote survival in infection assays inside murine macrophages.

In several human pathogens, such as *Streptococcus pneumoniae, Listeria monocytogenes, Salmonella Typhimurium*, and *Pseudomonas aeruginosa*, LMW thiols or the Gor are required for virulence, colonization and to resist host-derived oxidative or nitrosative stress (Potter et al., 2012; Song et al., 2013; Reniere et al., 2015; Tung et al., 2018; Wongsaroj et al., 2018). *S. aureus* BSH deficient mutants showed decreased survival in murine macrophages and in human whole blood infections (Pöther et al., 2013; Posada et al., 2014). The virulence mechanisms might be related to a lack of BSH regeneration and decreased recovery of inactivated *S*-bacillithiolated proteins inside macrophages. Future studies should elucidate the targets for *S*-bacillithiolations that are reduced by the BrxA/BSH/YpdA pathway inside macrophages, increasing survival, metabolism or persistence under infections.

In summary, our results showed the importance of the BrxA/BSH/YpdA redox pathway to resist oxidative stress and macrophage infection in *S. aureus*. Through measurements of the BSH/BSSB redox ratio and E_{BSH}, we provide evidence that the NADPH-dependent disulfide reductase YpdA regenerates BSH and restores reduced E_{BSH} upon recovery from oxidative stress in *S. aureus*. Finally, biochemical evidence for YpdA as BSSB reductase and for the role of BrxA/BSH/YpdA pathway in de-bacillithiolation was provided *in vitro*. The detailed biochemical mechanism of YpdA and the cross-talk of the Trx and Brx systems in de-bacillithiolation under oxidative stress and infections are subject of our future studies.

AUTHOR CONTRIBUTIONS

HA and NL designed the experiments of this study. NL, VVL, VNF, QNT and SS constructed the mutants, performed the experiments and analyzed the data of this manuscript. MW and RH performed the HPLC thiol metabolomics analyses and analyzed the data. KT and MF contributed with the infection assays to this work. CH synthesized BSH and BSSB for the biochemical assays of the manuscript. NL and HA wrote the manuscript. All authors contributed with corrections of the manuscript.

FUNDING

In this work, HA was supported by an ERC Consolidator Grant (GA 615585) MYCOTHIOLOME and grants from the Deutsche Forschungsgemeinschaft (AN746/4-1 and AN746/4-2) within the SPP1710, by the SFB973 project C08N, and by the SFB/TR84 project B06. We further thank funding by the SPP1710 grants HE1848/16-1 and WI3560/2-1 to RH and MW.

ACKNOWLEDGMENTS

We acknowledge support by the Open Access Publication Initiative of Freie Universität Berlin.

SUPPLEMENTARY MATERIAL

The Supplementary Material for this article can be found online at: https://www.frontiersin.org/articles/10.3389/fmicb.2019.01355/full#supplementary-material

REFERENCES

Allen, E. M., and Mieyal, J. J. (2012). Protein-thiol oxidation and cell death: regulatory role of glutaredoxins. *Antioxid. Redox Signal.* 17, 1748–1763. doi: 10.1089/ars.2012.4644

Alonso-Moraga, A., Bocanegra, A., Torres, J. M., Lopez-Barea, J., and Pueyo, C. (1987). Glutathione status and sensitivity to GSH-reacting compounds of *Escherichia coli* strains deficient in glutathione metabolism and/or catalase activity. *Mol. Cell Biochem.* 73, 61–68.

Archer, G. L. (1998). *Staphylococcus aureus*: a well-armed pathogen. *Clin. Infect. Dis.* 26, 1179–1181. doi: 10.1086/520289

Argyrou, A., and Blanchard, J. S. (2004). Flavoprotein disulfide reductases: advances in chemistry and function. *Progr. Nucleic Acid Res. Mol. Biol.* 78, 89–142. doi: 10.1016/s0079-6603(04)78003-4

Arnaud, M., Chastanet, A., and Débarbouillé, M. (2004). New vector for efficient allelic replacement in naturally nontransformable, low-GC-content, gram-positive bacteria. *Appl. Environ. Microbiol.* 70, 6887–6891. doi: 10.1128/aem.70.11.6887-6891.2004

Beavers, W. N., and Skaar, E. P. (2016). Neutrophil-generated oxidative stress and protein damage in *Staphylococcus aureus*. *Pathog. Dis.* 74:ftw060. doi: 10.1093/femspd/ftw060

Boucher, H. W., and Corey, G. R. (2008). Epidemiology of methicillin-resistant *Staphylococcus aureus*. *Clin. Infect Dis.* 46(Suppl. 5), S344–S349. doi: 10.1086/533590

Bragg, P. D., Glavas, N. A., and Hou, C. (1997). Mutation of conserved residues in the NADP(H)-binding domain of the proton translocating pyridine nucleotide transhydrogenase of *Escherichia coli*. *Arch. Biochem. Biophys.* 338, 57–66. doi: 10.1006/abbi.1996.9797

Brückner, R., Wagner, E., and Götz, F. (1993). Characterization of a sucrase gene from *Staphylococcus xylosus*. *J. Bacteriol.* 175, 851–857. doi: 10.1128/jb.175.3.851-857.1993

Chandrangsu, P., Loi, V. V., Antelmann, H., and Helmann, J. D. (2018). The role of bacillithiol in Gram-positive *Firmicutes*. *Antioxid. Redox Signal.* 28, 445–462. doi: 10.1089/ars.2017.7057

Chi, B. K., Gronau, K., Mäder, U., Hessling, B., Becher, D., and Antelmann, H. (2011). *S*-bacillithiolation protects against hypochlorite stress in *Bacillus subtilis* as revealed by transcriptomics and redox proteomics. *Mol. Cell Proteo.* 10:M111009506. doi: 10.1074/mcp.M111.009506

Chi, B. K., Roberts, A. A., Huyen, T. T., Bäsell, K., Becher, D., Albrecht, D., et al. (2013). *S*-bacillithiolation protects conserved and essential proteins against hypochlorite stress in *Firmicutes* bacteria. *Antioxid. Redox Signal.* 18, 1273–1295. doi: 10.1089/ars.2012.4686

Deponte, M. (2013). Glutathione catalysis and the reaction mechanisms of glutathione-dependent enzymes. *Biochim. Biophys. Acta* 1830, 3217–3266. doi: 10.1016/j.bbagen.2012.09.018

Dooley, C. T., Dore, T. M., Hanson, G. T., Jackson, W. C., Remington, S. J., and Tsien, R. Y. (2004). Imaging dynamic redox changes in mammalian cells with green fluorescent protein indicators. *J. Biol. Chem.* 279, 22284–22293. doi: 10.1074/jbc.m312847200

Fahey, R. C. (2013). Glutathione analogs in prokaryotes. *Biochim. Biophys. Acta* 1830, 3182–3198. doi: 10.1016/j.bbagen.2012.10.006

Fuangthong, M., Atichartpongkul, S., Mongkolsuk, S., and Helmann, J. D. (2001). OhrR is a repressor of *ohrA*, a key organic hydroperoxide resistance determinant in *Bacillus subtilis*. *J. Bacteriol.* 183, 4134–4141. doi: 10.1128/jb.183.14.4134-4141.2001

Gaballa, A., Antelmann, H., Hamilton, C. J., and Helmann, J. D. (2013). Regulation of *Bacillus subtilis* bacillithiol biosynthesis operons by Spx. *Microbiology* 159, 2025–2035. doi: 10.1099/mic.0.070482-0

Gaballa, A., Chi, B. K., Roberts, A. A., Becher, D., Hamilton, C. J., Antelmann, H., et al. (2014). Redox regulation in *Bacillus subtilis*: The bacilliredoxins BrxA(YphP) and BrxB(YqiW) function in de-bacillithiolation of S-bacillithiolated OhrR and MetE. *Antioxid. Redox Signal.* 21, 357–367. doi: 10.1089/ars.2013.5327

Gaballa, A., Newton, G. L., Antelmann, H., Parsonage, D., Upton, H., Rawat, M., et al. (2010). Biosynthesis and functions of bacillithiol, a major low-molecular-weight thiol in Bacilli. *Proc. Natl. Acad. Sci. U.S.A.* 107, 6482–6486. doi: 10.1073/pnas.1000928107

Hillion, M., and Antelmann, H. (2015). Thiol-based redox switches in prokaryotes. *Biol. Chem.* 396, 415–444. doi: 10.1515/hsz-2015-0102

Hiras, J., Sharma, S. V., Raman, V., Tinson, R. A. J., Arbach, M., Rodrigues, D. F., et al. (2018). Physiological studies of *Chlorobiaceae* suggest that bacillithiol derivatives are the most widespread thiols in bacteria. *MBio* 9:e01603-18. doi: 10.1128/mBio.01603-18

Hwang, C., Lodish, H. F., and Sinskey, A. J. (1995). Measurement of glutathione redox state in cytosol and secretory pathway of cultured cells. *Methods Enzymol.* 251, 212–221. doi: 10.1016/0076-6879(95)51123-7

Imber, M., Huyen, N. T. T., Pietrzyk-Brzezinska, A. J., Loi, V. V., Hillion, M., Bernhardt, J., et al. (2018a). Protein *S*-bacillithiolation functions in thiol protection and redox regulation of the glyceraldehyde-3-phosphate dehydrogenase Gap in *Staphylococcus aureus* under hypochlorite stress. *Antioxid. Redox Signal.* 28, 410–430. doi: 10.1089/ars.2016.6897

Imber, M., Loi, V. V., Reznikov, S., Fritsch, V. N., Pietrzyk-Brzezinska, A. J., Prehn, J., et al. (2018b). The aldehyde dehydrogenase AldA contributes to the hypochlorite defense and is redox-controlled by protein *S*-bacillithiolation in *Staphylococcus aureus*. *Redox. Biol.* 15, 557–568. doi: 10.1016/j.redox.2018.02.001

Imber, M., Pietrzyk-Brzezinska, A. J., and Antelmann, H. (2018c). Redox regulation by reversible protein *S*-thiolation in Gram-positive bacteria. *Redox. Biol.* 20, 130–145. doi: 10.1016/j.redox.2018.08.017

Lee, J. W., Soonsanga, S., and Helmann, J. D. (2007). A complex thiolate switch regulates the *Bacillus subtilis* organic peroxide sensor OhrR. *Proc. Natl. Acad. Sci. U.S.A.* 104, 8743–8748. doi: 10.1073/pnas.0702081104

Lillig, C. H., Berndt, C., and Holmgren, A. (2008). Glutaredoxin systems. *Biochim. Biophys. Acta* 1780, 1304–1317. doi: 10.1016/j.bbagen.2008.06.003

Livermore, D. M. (2000). Antibiotic resistance in staphylococci. *Int. J. Antimicrob. Agents* 16(Suppl. 1), S3–S10.

Loi, V. V., Busche, T., Preuss, T., Kalinowski, J., Bernhardt, J., and Antelmann, H. (2018a). The AGXX antimicrobial coating causes a thiol-specific oxidative stress response and protein S-bacillithiolation in *Staphylococcus aureus*. *Front. Microbiol.* 9:3037. doi: 10.3389/fmicb.2018.03037

Loi, V. V., Busche, T., Tedin, K., Bernhardt, J., Wollenhaupt, J., Huyen, N. T. T., et al. (2018b). Redox-sensing under hypochlorite stress and infection conditions by the Rrf2-family repressor HypR in *Staphylococcus aureus*. *Antioxid. Redox Signal.* 29, 615–636. doi: 10.1089/ars.2017.7354

Loi, V. V., Harms, M., Müller, M., Huyen, N. T. T., Hamilton, C. J., Hochgräfe, F., et al. (2017). Real-time imaging of the bacillithiol redox potential in the human pathogen *Staphylococcus aureus* using a genetically encoded bacilliredoxin-fused redox biosensor. *Antioxid. Redox Signal.* 26, 835–848. doi: 10.1089/ars.2016.6733

Loi, V. V., Rossius, M., and Antelmann, H. (2015). Redox regulation by reversible protein *S*-thiolation in bacteria. *Front. Microbiol.* 6:187. doi: 10.3389/fmicb.2015.00187

Lowy, F. D. (1998). *Staphylococcus aureus* infections. *N. Engl. J. Med.* 339, 520–532.

Mäder, U., Nicolas, P., Depke, M., Pane-Farre, J., Debarbouille, M., Van Der Kooi-Pol, M. M., et al. (2016). *Staphylococcus aureus* transcriptome architecture: from laboratory to infection-mimicking conditions. *PLoS Genet.* 12:e1005962. doi: 10.1371/journal.pgen.1005962

Mikheyeva, I. V., Thomas, J. M., Kolar, S. L., Corvaglia, A. R., Gaiotaa, N., Leo, S., et al. (2019). YpdA, a putative bacillithiol disulfide reductase, contributes to cellular redox homeostasis and virulence in *Staphylococcus aureus*. *Mol. Microbiol.* 111, 1039–1056. doi: 10.1111/mmi.14207

Newton, G. L., Fahey, R. C., and Rawat, M. (2012). Detoxification of toxins by bacillithiol in *Staphylococcus aureus*. *Microbiology* 158, 1117–1126. doi: 10.1099/mic.0.055715-0

Nicolas, P., Mäder, U., Dervyn, E., Rochat, T., Leduc, A., Pigeonneau, N., et al. (2012). Condition-dependent transcriptome reveals high-level regulatory architecture in *Bacillus subtilis*. *Science* 335, 1103–1106. doi: 10.1126/science.1206848

Palazzolo-Ballance, A. M., Reniere, M. L., Braughton, K. R., Sturdevant, D. E., Otto, M., Kreiswirth, B. N., et al. (2008). Neutrophil microbicides induce a pathogen survival response in community-associated methicillin-resistant *Staphylococcus aureus*. *J. Immunol.* 180, 500–509. doi: 10.4049/jimmunol.180.1.500

Pendleton, J. N., Gorman, S. P., and Gilmore, B. F. (2013). Clinical relevance of the ESKAPE pathogens. *Expert Rev. Anti. Infect. Ther.* 11, 297–308. doi: 10.1586/eri.13.12

Posada, A. C., Kolar, S. L., Dusi, R. G., Francois, P., Roberts, A. A., Hamilton, C. J., et al. (2014). Importance of bacillithiol in the oxidative stress response of *Staphylococcus aureus*. *Infect. Immun.* 82, 316–332. doi: 10.1128/IAI.01074-13

Pöther, D. C., Gierok, P., Harms, M., Mostertz, J., Hochgräfe, F., Antelmann, H., et al. (2013). Distribution and infection-related functions of bacillithiol in *Staphylococcus aureus*. *Int. J. Med. Microbiol.* 303, 114–123. doi: 10.1016/j.ijmm.2013.01.003

Potter, A. J., Trappetti, C., and Paton, J. C. (2012). *Streptococcus pneumoniae* uses glutathione to defend against oxidative stress and metal ion toxicity. *J. Bacteriol.* 194, 6248–6254. doi: 10.1128/JB.01393-12

Reniere, M. L., Whiteley, A. T., Hamilton, K. L., John, S. M., Lauer, P., Brennan, R. G., et al. (2015). Glutathione activates virulence gene expression of an intracellular pathogen. *Nature* 517, 170–173. doi: 10.1038/nature14029

Rosenblum, E. D., and Tyrone, S. (1964). Serology, density, and morphology of staphylococcal phages. *J. Bacteriol.* 88, 1737–1742.

Si, M., Zhao, C., Zhang, B., Wei, D., Chen, K., Yang, X., et al. (2016). Overexpression of mycothiol disulfide reductase enhances *Corynebacterium glutamicum* robustness by modulating cellular redox homeostasis and antioxidant proteins under oxidative stress. *Sci. Rep.* 6:29491. doi: 10.1038/srep29491

Song, M., Husain, M., Jones-Carson, J., Liu, L., Henard, C. A., and Vazquez-Torres, A. (2013). Low-molecular-weight thiol-dependent antioxidant and antinitrosative defences in *Salmonella* pathogenesis. *Mol. Microbiol.* 87, 609–622. doi: 10.1111/mmi.12119

Tam le, T., Eymann, C., Albrecht, D., Sietmann, R., Schauer, F., Hecker, M., et al. (2006). Differential gene expression in response to phenol and catechol reveals different metabolic activities for the degradation of aromatic compounds in *Bacillus subtilis*. *Environ. Microbiol.* 8, 1408–1427. doi: 10.1111/j.1462-2920.2006.01034.x

Tung, Q. N., Linzner, N., Loi, V. V., and Antelmann, H. (2018). Application of genetically encoded redox biosensors to measure dynamic changes in the glutathione, bacillithiol and mycothiol redox potentials in pathogenic bacteria. *Free Radic. Biol. Med.* 128, 84–96. doi: 10.1016/j.freeradbiomed.2018.02.018

Tung, Q. N., Loi, V. V., Busche, T., Nerlich, A., Mieth, M., Milse, J., et al. (2019). Stable integration of the Mrx1-roGFP2 biosensor to monitor dynamic changes of the mycothiol redox potential in *Corynebacterium glutamicum*. *Redox. Biol.* 20, 514–525. doi: 10.1016/j.redox.2018.11.012

Van Laer, K., Buts, L., Foloppe, N., Vertommen, D., Van Belle, K., Wahni, K., et al. (2012). Mycoredoxin-1 is one of the missing links in the oxidative stress defence mechanism of Mycobacteria. *Mol. Microbiol.* 86, 787–804. doi: 10.1111/mmi.12030

Van Laer, K., Hamilton, C. J., and Messens, J. (2013). Low-molecular-weight thiols in thiol-disulfide exchange. *Antioxid. Redox Signal.* 18, 1642–1653. doi: 10.1089/ars.2012.4964

Vlamis-Gardikas, A., Potamitou, A., Zarivach, R., Hochman, A., and Holmgren, A. (2002). Characterization of *Escherichia coli* null mutants for glutaredoxin 2. *J. Biol. Chem.* 277, 10861–10868.

Wetzstein, M., Völker, U., Dedio, J., Löbau, S., Zuber, U., Schiesswohl, M., et al. (1992). Cloning, sequencing, and molecular analysis of the *dnaK* locus from *Bacillus subtilis*. *J. Bacteriol.* 174, 3300–3310. doi: 10.1128/jb.174.10.3300-3310.1992

Winterbourn, C. C., and Kettle, A. J. (2013). Redox reactions and microbial killing in the neutrophil phagosome. *Antioxid. Redox Signal.* 18, 642–660. doi: 10.1089/ars.2012.4827

Winterbourn, C. C., Kettle, A. J., and Hampton, M. B. (2016). Reactive oxygen species and neutrophil function. *Annu. Rev. Biochem.* 85, 765–792. doi: 10.1146/annurev-biochem-060815-014442

Wongsaroj, L., Saninjuk, K., Romsang, A., Duang-Nkern, J., Trinachartvanit, W., Vattanaviboon, P., et al. (2018). *Pseudomonas aeruginosa* glutathione biosynthesis genes play multiple roles in stress protection, bacterial virulence and biofilm formation. *PLoS One* 13:e0205815. doi: 10.1371/journal.pone.0205815

Conflict of Interest Statement: The authors declare that the research was conducted in the absence of any commercial or financial relationships that could be construed as a potential conflict of interest.

Figure S1

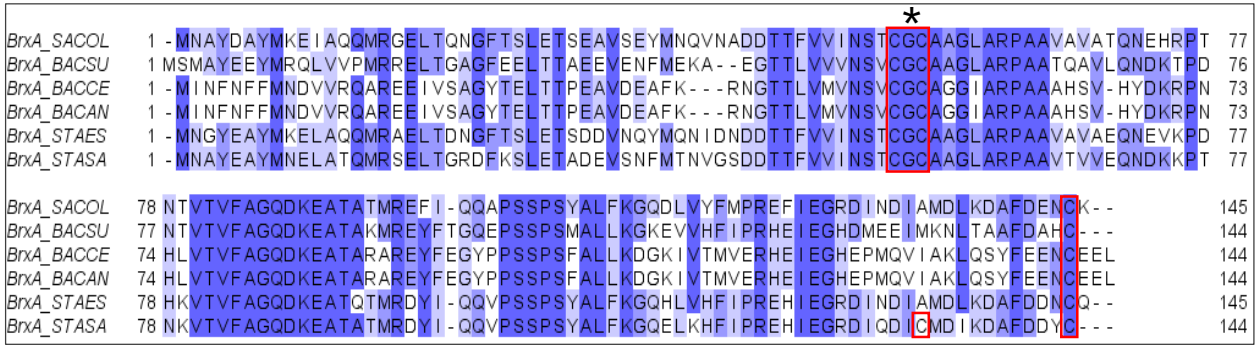

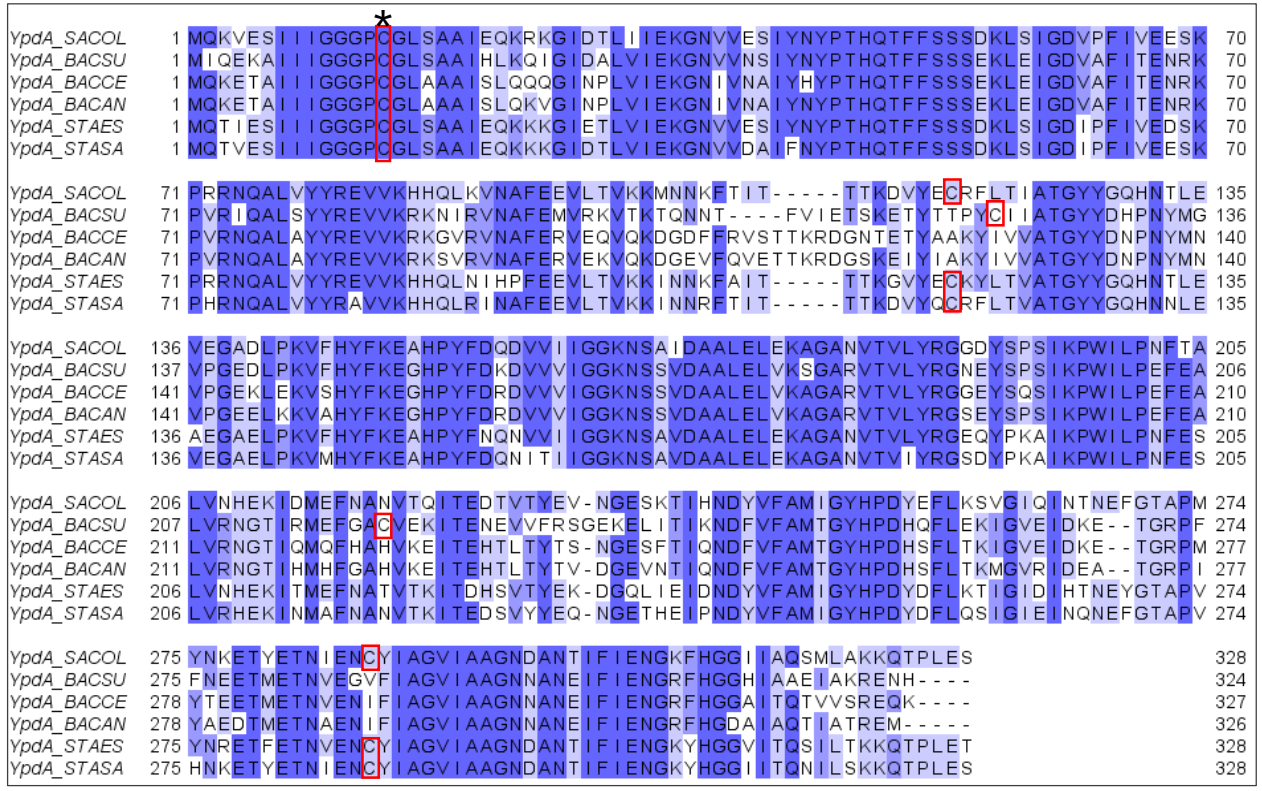

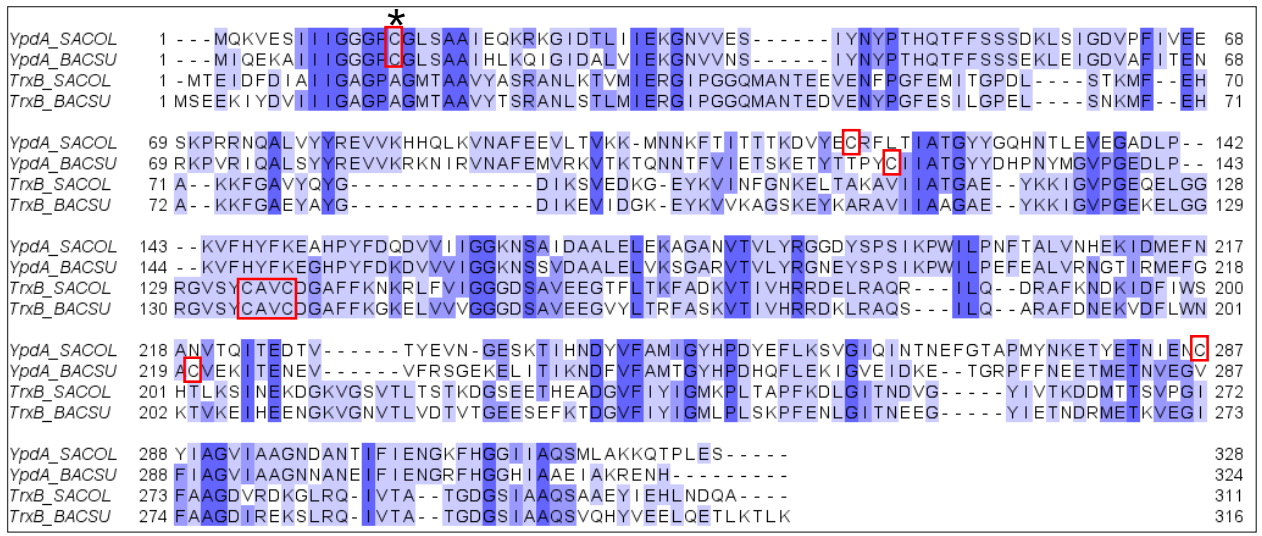

Fig. S1. ClustalΩ2 protein sequence alignments of BrxA/B and YpdA homologs across firmicutes. The % identities of the homologs to *S. aureus* BrxA, BrxB and YpdA are given in parenthesis.

BrxA (SACOL1464) of *S. aureus* COL was aligned with BrxA homologs of *Staphylococcus epidermidis* (BrxA_STAES, 79.3%), *Staphylococcus saprophyticus* (BrxA_STASA, 73.1%), *B. subtilis* (BrxA_BACSU, 55.1%), *Bacillus cereus* (BrxA_BACCE, 43.2%) and *Bacillus anthracis* (BrxA_BACAN, 43.2%).

BrxB (SACOL1558) of *S. aureus* COL was aligned with BrxB homologs of *S. epidermidis* (BrxB_STAES, 87.6%), *S. saprophyticus* (BrxB_STASA, 84.1%), *B. subtilis* (BrxB_BACSU, 68.3%), *B. cereus* (BrxB_BACCE, 68.3%) and *B. anthracis* (BrxB_BACAN, 46.3%).

YpdA (SACOL1520) of *S. aureus* COL was aligned with YpdA homologs of *S. saprophyticus* ((YpdA_STASA, 84.1%), *S. epidermidis* (YpdA_STAES, 82.3%), *B. subtilis* (YpdA_BACSU, 62.8%), *B. cereus* (YpdA_BACCE, 61.3%) and *B. anthracis* (YpdA_BACAN, 60.1%). In the lower panel, YpdA of *S. aureus* (SACOL1520) and *B. subtilis* (BSU22950) were aligned with TrxB of *S. aureus* (SACOL0829) and *B. subtilis* (BSU34790). The conserved CGC motif of BrxA/B and the conserved Cys14 residue of YpdA are labeled in red with asterisks (*).

Figure S2

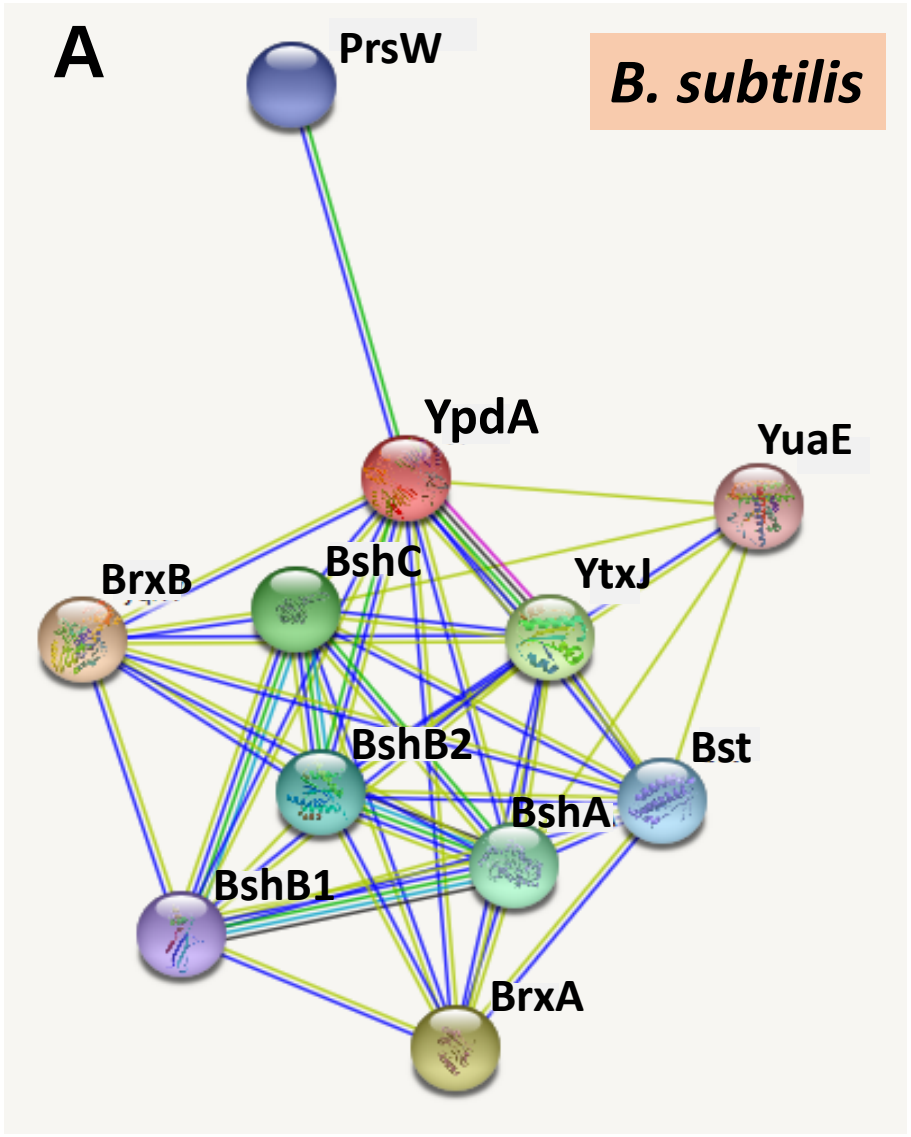

https://string-db.org/cgi/network.pl?taskId=nLwfWwHpDe6G

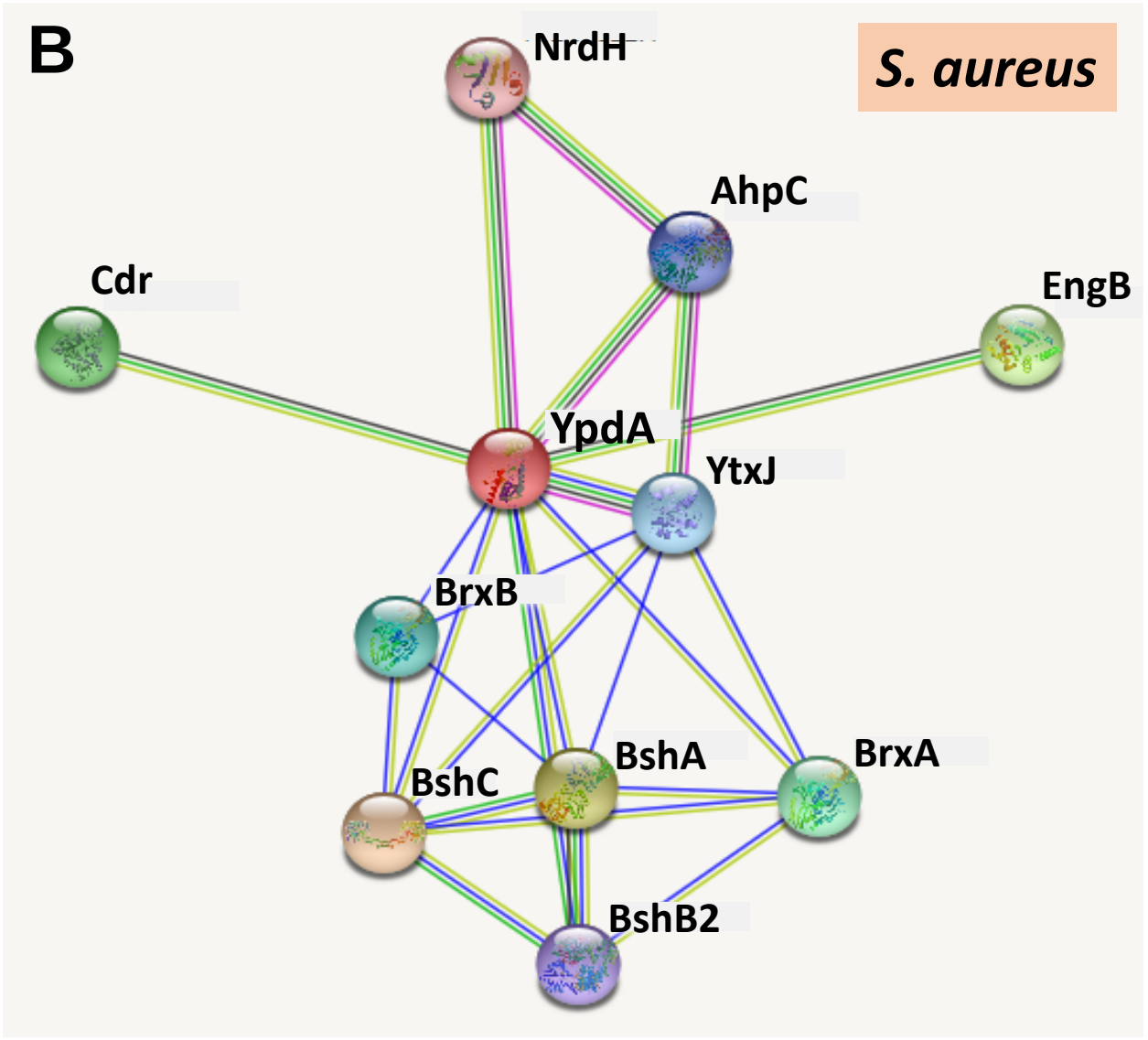

https://string-db.org/cgi/network.pl?taskId=EAbilN4U7gOB

Fig. S2. Phylogenomic profiling of YpdA interaction networks with the BSH biosynthesis enzymes (BshA, BshB1/2, BshC) and bacilliredoxins BrxA/B (YphP/YqiW) in *Bacillus subtilis* (A) and *Staphylococcus aureus* NCTC 8325 as revealed by EMBL STRING search (https://string-db.org). The green and blue lines denote co-localization and co-occurrence of genes in genomes, respectively.

Figure S3

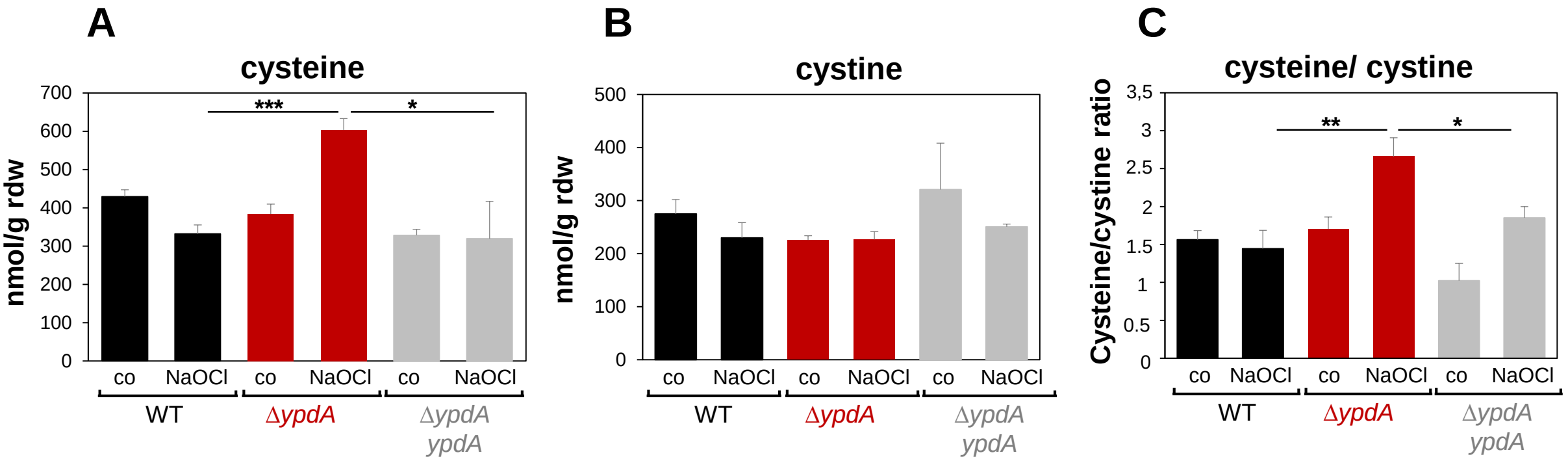

Fig. S3. Levels of cysteine (A) and cystine (B) and the cysteine/cysteine ratio (C) under control and NaOCl stress in *S. aureus* COL WT, the Δ*ypdA* mutant and *ypdA* complemented strain. *S. aureus* strains were grown in RPMI and exposed to 2 mM NaOCl stress for 30 min at an OD_{500} of 0.9. mBBr-labeled LMW thiols and disulfides were measured by HPLC thiol metabolomics. Mean values and SD of 3 biological replicates are shown. $^{ns}p > 0.05$; *p ≤ 0.05 **p ≤ 0.01 and ***p ≤ 0.001.

Figure S4

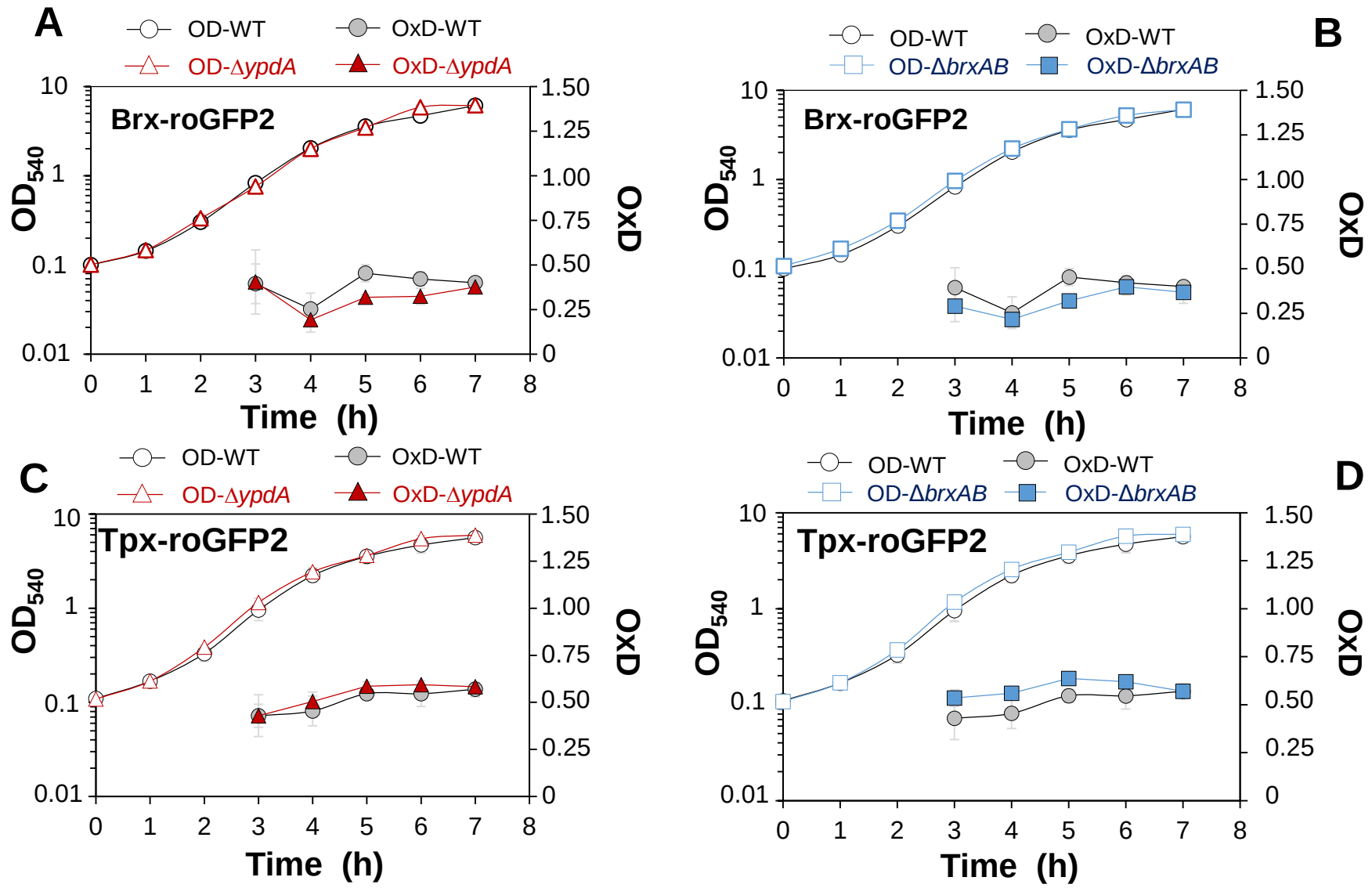

Fig. S4. The basal level OxD of the Brx-roGFP2 and Tpx-roGFP2 biosensors is not affected in Δ*ypdA* and Δ*brxAB* mutants during the growth. *S. aureus* COL WT, Δ*ypdA* and Δ*brxAB* mutants expressing Brx-roGFP2 **(A,B)** and Tpx-roGFP2 **(C,D)** were grown in LB medium and the OxD values were determined along the growth curve. Mean values and SD of 3 biological replicates are shown. The corresponding E_{BSH} changes for S4AB were calculated using the Nernst equation in Fig. S5AB.

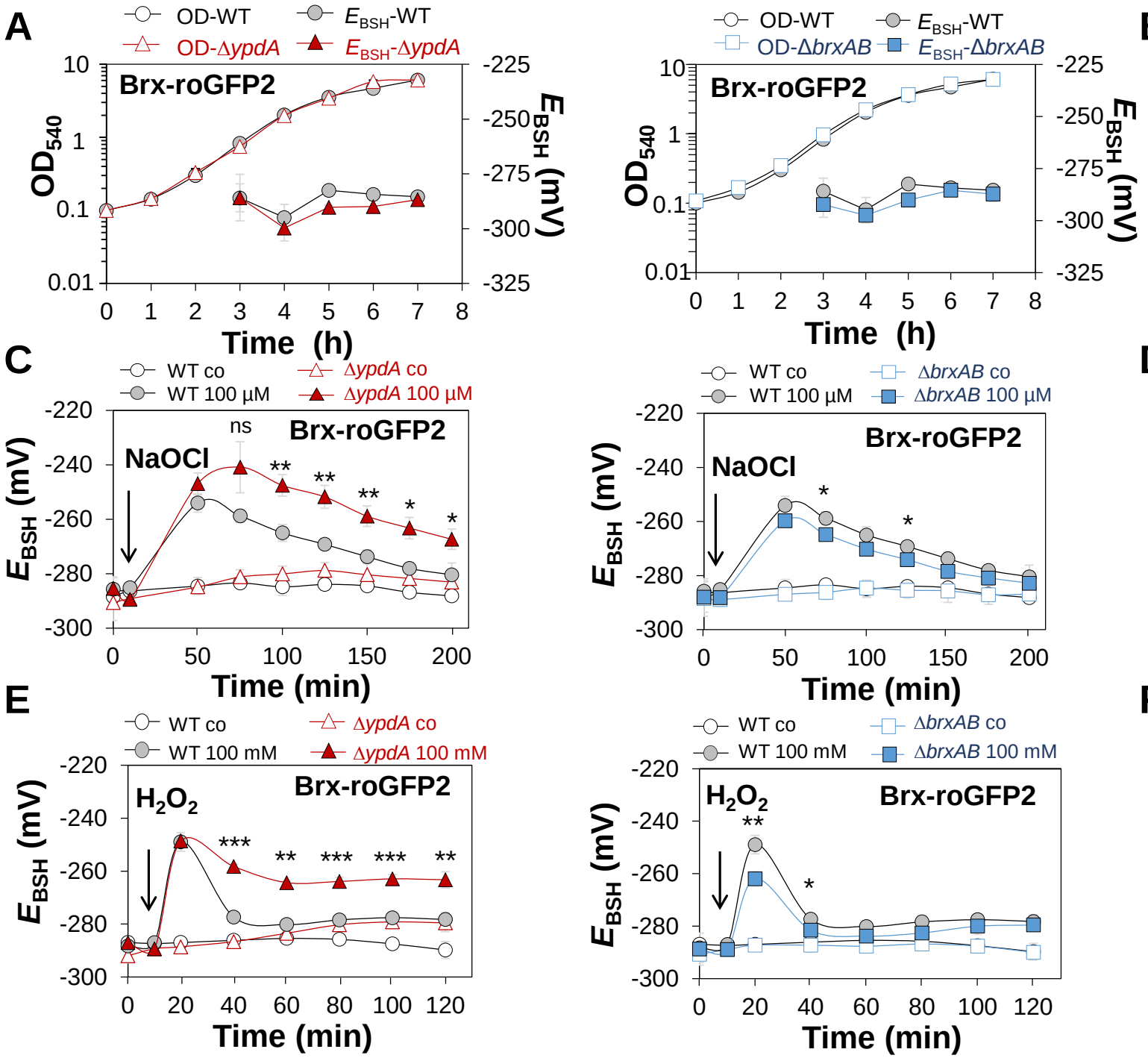

Fig. S5. YpdA and BrxAB do not affect the basal E_{BSH} level during the growth (A, B), but the Δ*ypdA* mutant is impaired to regenerate the reduced E_{BSH} during recovery from oxidative stress (C, E).

The E_{BSH} changes were measured in *S. aureus* COL WT, Δ*ypdA* and Δ*brxAB* mutants expressing Brx-roGFP2 along the growth curve in LB **(A, B)** and after exposure to 100 µM NaOCl **(C, D)** or 100 mM H_2O_2 stress **(E, F)** in Belitsky minimal medium (BMM). The E_{BSH} values were calculated using the Nernst equation based on the OxD values of Fig. S4AB and Fig. 4A-D.

Figure S6

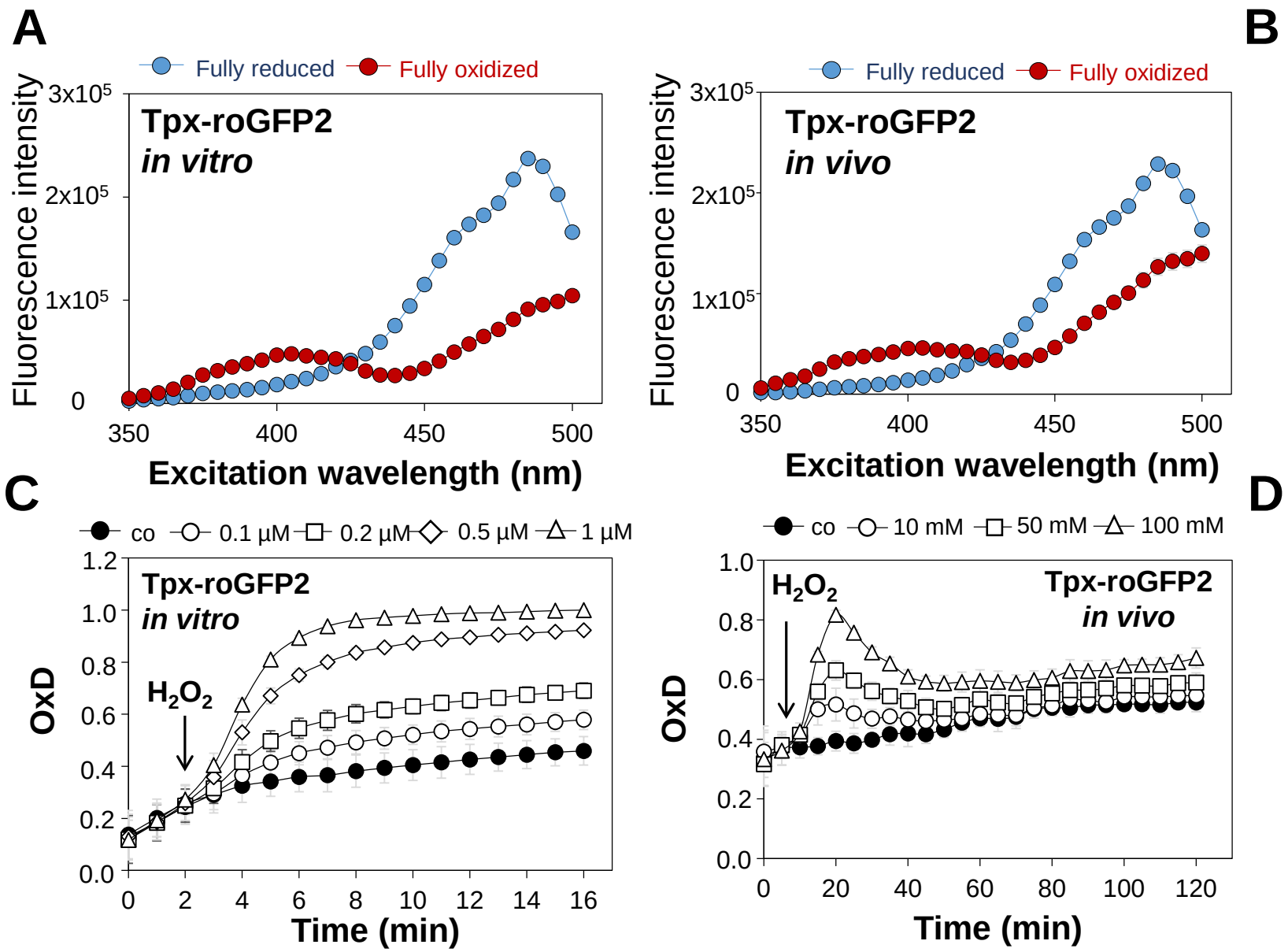

Fig. S6. Responses of Tpx-roGFP2 *in vitro* (A,C) and *in vivo* inside *S. aureus* COL after exposure to H_2O_2 (B,D). (A, B) The ratiometric Tpx-roGFP2 response in the DTT-treated fully reduced and diamide-treated fully oxidized state *in vitro* **(A)** and inside *S. aureus* COL *in vivo* **(B)**. **(C)** Purified Tpx-roGFP2 (1 µM) responds specifically to low levels H_2O_2 (0.1-1 µM H_2O_2) *in vitro*. **(D)** Tpx-roGFP2 inside *S. aureus* COL is rapidly and reversible oxidized by sub-lethal 1-100 mM H_2O_2 *in vivo*. Mean values and SD of 3-5 replicates are shown.

Figure S7

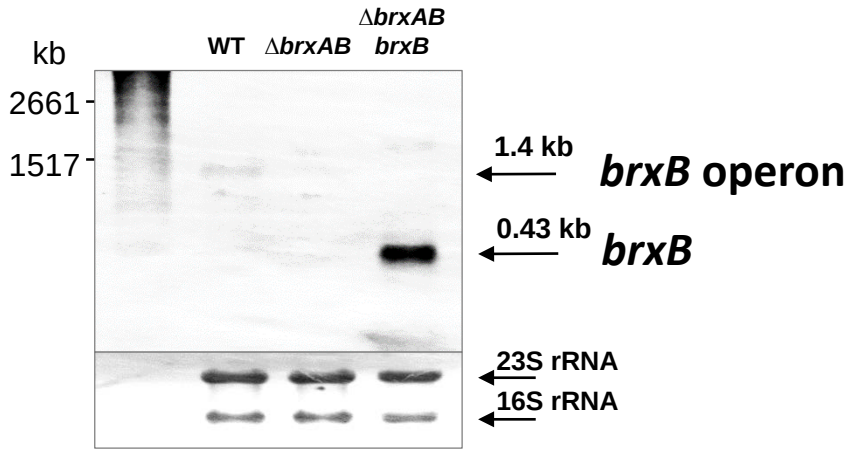

Fig. S7. Northern blot analysis of *brxB* transcription in the *S. aureus* COL WT, Δ*brxAB* mutant and in the *brxB* complemented strain using a *brxB*-specific RNA probe. RNA was isolated of *S. aureus* cells grown in LB to an OD_{540} of 2.0 with 1% xylose to induce *brxB* expression in the pRB473-*brxB* complemented Δ*brxAB* mutant strain. *brxB* transcription in the *brxB* complemented strain is shown by the 0.43 kb band on the Northern blot. Methylene blue stained bands for 16S and 23S rRNAs indicate the RNA loading controls below the Northern blot image.

Figure S8

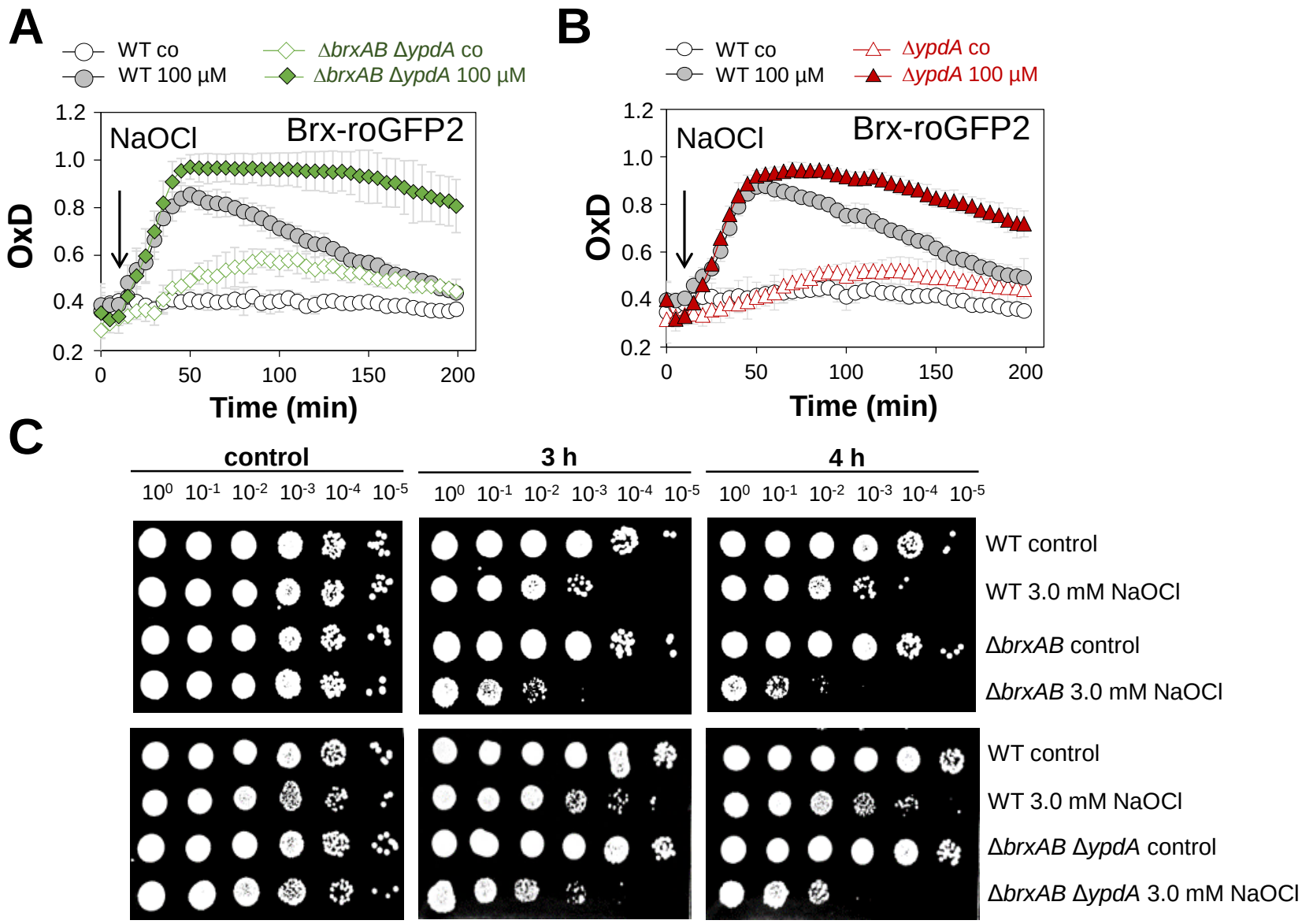

Fig. S8. Brx-roGFP2 measurements and survival assays indicate that the *S. aureus* Δ*brxAB* Δ*ypdA* triple mutant is similar defective to rescue E_{BSH} as the Δ*ypdA* mutant and similar sensitive to NaOCl stress as the Δ*brxAB* mutant. (A, B) Brx-roGFP2 response in the *S. aureus* COL WT, Δ*ypdA* and Δ*brxAB* Δ*ypdA* mutants under 100 µM NaOCl stress**. (C)** Survival assays of the *S. aureus* COL WT, Δ*brxAB* and Δ*brxAB* Δ*ypdA* mutants at 3-4 hours after exposure to 3.0 mM NaOCl.

Figure S9

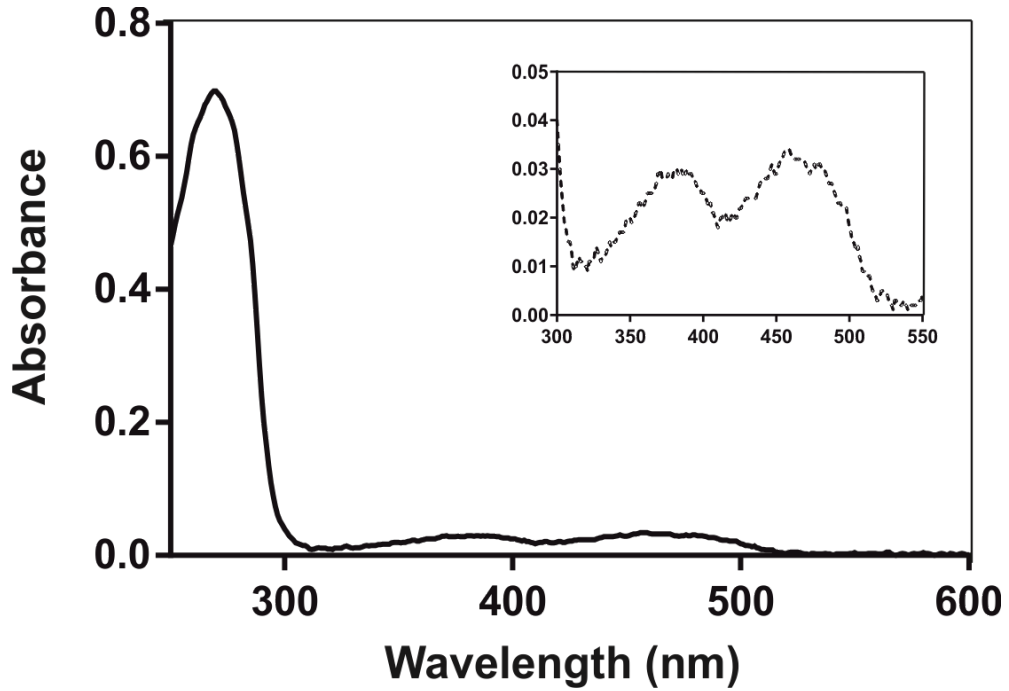

Fig. S9. The UV-visible absorption spectrum of purified yellow coloured YpdA protein indicates that YpdA is a flavoprotein containing the FAD co-factor with absorbance peaks at 375 and 450 nm (insert).

Table S1. Bacterial strains

Strain	Description	Reference
Escherichia coli		
DH5α	F-φ80dlacZ Δ(lacZYA-argF) U169 deoRsupE44ΔlacU169 (f80lacZDM15) hsdR17 recA1 endA1 (rk- mk+) supE44gyrA96 thi-1 gyrA69 relA1	[1]
BL21(DE3)*plys*S	F- ompT hsdS gal (rb- mb+) DE3(Sam7 Δnin5 lacUV5-T7 Gen1)	[1]
Staphylococcus aureus		
RN4220	restriction negative strain/MSSA cloning intermediate derived from 8325-4	[2]
COL	Archaic HA-MRSA strain	[3]
COL-Δ*ypdA*	COL *ypdA* deletion mutant	This study
COL-Δ*brxA*	COL *brxA* deletion mutant	This study
COL-Δ*brxAB*	COL *brxAB* double mutant	This study
COL-Δ*brxAB* Δ*ypdA*	COL *brxAB ypdA* triple mutant	This study
COL pRB473		[4]
COL pRB473-*brx-roGFP2*		[4]
COL Δ*ypdA::*pRB473-*brx-roGFP2*		This study
COL Δ*brxAB::*pRB473-*brx-roGFP2*		This study
COL Δ*brxAB* Δ*ypdA::*pRB473-*brx-roGFP2*		This study
COL pRB473-*tpx-roGFP2*		This study
COL Δ*ypdA::*pRB473-*tpx-roGFP2*		This study
COL Δ*brxAB::*pRB473-*tpx-roGFP2*		This study
COL-Δ*ypdA::*pRB473-*ypdA*		This study
COL-Δ*brxAB::*pRB473-*brxA*		This study
COL-Δ*brxAB::*pRB473-*brxB*		This study
Staphylococcus phage 81		[5]

Table S2. Plasmids

Plasmid	Description	Reference
pET11b	*E. coli* expression plasmid	Novagen
pET11b-*ypdA*	pET11b-derivative for overexpression of His-tagged YpdA	This work
pET11b-*ypdAC14A*	pET11b-derivative for overexpression of His-tagged YpdAC14A	This work
pET11b-*brxA*	pET11b-derivative for overexpression of His-tagged BrxA	[6]
pET11b-*gapDH*	pET11b-derivative for overexpression of His-tagged GapDH	[6]
pET11b-*brx-roGFP2*	pET11b-derivative for overexpression of His-tagged Brx-roGFP2	[4]
pET11b-*tpx-roGFP2*	pET11b-derivative for overexpression of His-tagged Tpx-roGFP2	This study
pRB473	pRB373-derivative, *E. coli/ S. aureus* shuttle vector, containing xylose-inducible P_{Xyl} promoter, Amp^r, Cm^r Amp^r, Cm^r	[7, 8]
pRB473-*brx-roGFP2*	pRB473-derivative expressing *brx-roGFP2* under P_{Xyl}	[4]
pRB473-*tpx-roGFP2*	pRB473-derivative expressing *tpx-roGFP2* under P_{Xyl}	This study
pRB473-*ypdA*	pRB473-derivative expressing *ypdA* under P_{Xyl}	This study
pRB473-*brxA*	pRB473-derivative expressing *brxA* under P_{Xyl}	This study
pRB473-*brxB*	pRB473-derivative expressing *brxB* under P_{Xyl}	This study

Table S3. Oligonucleotide primers

Primer name	Sequence (5' to 3')
pET-tpx-for-NheI	CTAGCTAGCATGACTGAAATAACATTCAAAGG
pET-tpx-rev-SpeI	GCGACTAGTAATATTTTTGTATGCAGCTAAAGC
pET-ypdA-for-NdeI	GGAATTCCATATGCAAAAAGTTGAAAGTATCATA
pET-ypdAC14A-for-NdeI	GGAATTCCATATGCAAAAAGTTGAAAGTATCATAATTGGTGGAGGGCCA**GCG**G GATT
pET-ypdA-rev-BamHI	CGCGGATCCTTAGTGATGGTGATGGTGATGTGATTCTAAGGGCGTTTGTTTC
pRB-tpx-roGFP2-for-BamHI	CGCGGATCCTTAGTGATGGTGATGGTGATGTGATTCTAAGGGCGTTTGTTTC
pRB-tpx-roGFP2-rev-SacI	CGCGAGCTCTTACTTGTACAGCTCGTCCATGC
pMAD-ypdA-for-BglII	CGCAGATCTGACATACAGTGAATGGTCAAG
pMAD-ypdA-f1-rev	GTTATTTAGTACATAGACCTTTATTTCATTGTTTCGGCCTCCTTTAATC
pMAD-ypdA-f2-for	GATTAAAGGAGGCCGAAACAATGAAATAAAGGTCTATGTACTAAATAAC
pMAD-ypdA-rev-SalI	CCAGTCGACTGTATTGACAAAGGATCGTGTG
pMAD-brxA-for-BglII	CGCAGATCTCGATCATTTCGTGTATTTCCTA
pMAD-brxA-f1-rev	TAAATATGAATGCATATGATGCTCCTTTGACGAAAATTGTAAATAGT
pMAD-brxA-f2-for	ACTATTTACAATTTTCGTCAAAGGAGCATCATATGCATTCATATTTA
pMAD-brxA-rev-SalI	CCAGTCGACTGGAAGACTCGATTACGAATG
pMAD-brxB-for-BglII	CGCAGATCTCAATCGCAATGGTATCTTCATA
pMAD-brxB-f1-rev	GGATAGGTGATTGAACTTATGGATTGTGAAGAAAGATAAGAGGC
pMAD-brxB-f2-for	GCCTCTTATCTTTCTTCACAATCCATAAGTTCAATCACCTATCC
pMAD-brxB-rev-SalI	CCAGTCGACTGATATGATTGCAATTCGTAAC
pRB-ypdA-for-BamHI	TAGGGATCCTTAAAGGAGGCCGAAACAATGCAAAAAGTTGAAAGTATCA
pRB-ypdA-rev-KpnI	CTCGGTACCTTATGATTCTAAGGGCGTTTG
pRB-brxA-for-BamHI	TAGGGATCCTAATTGGAGGAATTAAATATGAAT
pRB-brxA-rev-KpnI	CTCGGTACCCTATTTACAATTTTCGTCAAAGG
pRB-brxB-for-BamHI	TAGGGATCCGGATAGGTGATTGAACTTATGG
pRB-brxB-rev-KpnI	CTCGGTACCTTATCTTTCTTCACAATATTTATTG
ypdA-NB-for	GGGCCATGCGGATTAAGTG
ypdA-NB-rev	CTAATACGACTCACTATAGGGAGACGTTCCCTGCAGCAATTACA
brxA-NB-for	GCTTATATGAAAGAAATTGCGC
brxA-NB-rev	CTAATACGACTCACTATAGGGAGAAATTTTCGTCAAAGGCATCCTT
brxB-NB-for	TTATACATGAACGGTGTTGTAG
brxB-NB-rev	CTAATACGACTCACTATAGGGAGAATTACGTTCATCACATCATGAC

Restriction sites are underlined.

Table S4. The basal BSH redox potential (E_{BSH}) of *S aureus* COL wild type (WT), Δ*ypdA* and Δ*brxAB* mutants at different time points during the growth curve in LB medium

Time (h)	WT		Δ*ypdA*		Δ*brxAB*	
	OD_{540}	E_{BSH} (mV)	OD_{540}	E_{BSH} (mV)	OD_{540}	E_{BSH} (mV)
3	0.83	-285.93 ± 6.36	0.76	-292.36 ± 6.00	0.97	-285.79 ± 10.63
4	2.04	-294.90 ± 6.04	1.99	-297.44 ± 3.58	2.22	-299.73 ± 5.82
5	3.57	-282.51 ± 2.60	3.46	-290.10 ± 0.94	3.66	-290.16 ± 0.98
6	4.69	-284.26 ± 2.14	5.83	-285.51 ± 2.62	5.22	-289.88 ± 2.71
7	6.10	-285.45 ± 0.93	6.13	-288.31 ± 3.53	6.07	-286.75 ± 0.31

Table S5. Effect of 100 µM NaOCl on E_{BSH} changes in *S aureus* COL WT, Δ*ypdA* and Δ*brxAB* mutants

Time (min)	E_{BSH} (mV)		
	WT	Δ*ypdA*	Δ*brxAB*
0	-285.73 ± 4.57	-285.48 ± 3.95	-287.92 ± 5.60
10	-285.18 ± 1.22	-289.49 ± 0.27	-288.12 ± 2.95
50	-254.04 ± 3.33	-247.00 ± 3.96	-258.69 ± 2.47
75	-258.80 ± 2.40	-240.87 ± 9.39	-264.83 ± 1.03
100	-265.00 ± 3.09	-247.58 ± 3.92	-270.21 ± 0.55
125	-269.22 ± 1.91	-251.82 ± 4.21	-274.14 ± 1.10
150	-273.76 ± 2.56	-258.88 ± 3.81	-278.43 ± 1.26
175	-278.06 ± 1.91	-263.24 ± 3.95	-280.87 ± 1.35
200	-280.43 ± 4.33	-267.35 ± 3.74	-282.80 ± 1.36

Table S6: Effect of 100 mM H_2O_2 on E_{BSH} changes in *S aureus* COL WT, Δ*ypdA* and Δ*brxAB* mutants

Time (min)	E_{BSH} (mV)		
	WT	Δ*ypdA*	Δ*brxAB*
0	-288.25 ± 1.72	-287.04 ± 2.04	-288.77 ± 6.09
10	-287.00 ± 1.78	-289.33 ± 1.13	-288.96 ± 1.38
20	-248.94 ± 3.54	-248.62 ± 0.98	-261.96 ± 2.63
40	-277.32 ± 1.91	-258.26 ± 0.93	-281.54 ± 1.36
60	-280.16 ± 2.00	-264.35 ± 0.63	-283.82 ± 1.36
80	-278.40 ± 1.69	-263.89 ± 1.50	-282.60 ± 3.31
100	-277.58 ± 1.93	-262.93 ± 1.60	-280.03 ± 3.15
120	-278.25 ± 2.64	-263.27 ± 3.09	-279.60 ± 2.38

Supplementary References

[1] F.W. Studier, B.A. Moffatt, Use of bacteriophage-T7 RNA-polymerase to direct selective high-level expression of cloned genes, J Mol Biol 189(1) (1986) 113-130.

[2] B.N. Kreiswirth, S. Lofdahl, M.J. Betley, M. O'Reilly, P.M. Schlievert, M.S. Bergdoll, R.P. Novick, The toxic shock syndrome exotoxin structural gene is not detectably transmitted by a prophage, Nature 305(5936) (1983) 709-12.

[3] W.M. Shafer, J.J. Iandolo, Genetics of staphylococcal enterotoxin B in methicillin-resistant isolates of *Staphylococcus aureus*, Infect Immun 25(3) (1979) 902-11.

[4] V.V. Loi, M. Harms, M. Müller, N.T.T. Huyen, C.J. Hamilton, F. Hochgräfe, J. Pane-Farre, H. Antelmann, Real-time imaging of the bacillithiol redox potential in the human pathogen *Staphylococcus aureus* using a genetically encoded bacilliredoxin-fused redox biosensor, Antioxid Redox Signal 26(15) (2017) 835-848.

[5] E.D. Rosenblum, S. Tyrone, Serology, density, and morphology of staphylococcal phages, J Bacteriol 88 (1964) 1737-42.

[6] M. Imber, N.T.T. Huyen, A.J. Pietrzyk-Brzezinska, V.V. Loi, M. Hillion, J. Bernhardt, L. Thärichen, K. Kolsek, M. Saleh, C.J. Hamilton, L. Adrian, F. Gräter, M.C. Wahl, H. Antelmann, Protein S-Bacillithiolation functions in thiol protection and redox regulation of the glyceraldehyde-3-phosphate dehydrogenase Gap in *Staphylococcus aureus* under hypochlorite stress, Antioxid Redox Signal 28(6) (2018) 410-430.

[7] D.C. Pöther, P. Gierok, M. Harms, J. Mostertz, F. Hochgräfe, H. Antelmann, C.J. Hamilton, I. Borovok, M. Lalk, Y. Aharonowitz, M. Hecker, Distribution and infection-related functions of bacillithiol in *Staphylococcus aureus*, Int J Med Microbiol 303(3) (2013) 114-23.

[8] R. Brückner, E. Wagner, F. Götz, Characterization of a sucrase gene from *Staphylococcus xylosus*, J Bacteriol 175(3) (1993) 851-7.

Chapter 4

The plant-derived naphthoquinone lapachol causes an oxidative stress response in *Staphylococcus aureus*

Nico Linzner[1#], Verena Nadin Fritsch[1#], Tobias Busche[1,2], Quach Ngoc Tung[1], Vu Van Loi[1], Jörg Bernhardt[3], Jörn Kalinowski[2], and Haike Antelmann[1*]

[1]*Freie Universität Berlin, Institute of Biology-Microbiology, 14195 Berlin, Germany*

[2]*Center for Biotechnology, University Bielefeld, 33615 Bielefeld, Germany*

[3]*Institute for Microbiology, University of Greifswald, 17489 Greifswald, Germany*

#Both authors contributed equally to this work.

*Corresponding author: haike.antelmann@fu-berlin.de

Revision re-submitted to Free Radical Biology and Medicine on 28th June 2020

Personal contribution:

My contribution included the analyses of the antimicrobial effect of lapachol on *S. aureus* **(Fig. 1)** and the determination of the MIC **(Tab. S4)**. I conducted the measurements of the Brx- and Tpx-roGFP2 biosensors **(Fig. 4A, B)**. Furthermore, I performed the anti-BSH Western blots **(Fig. 6)** and the analyses of GapDH aggregation *in vitro* after lapachol stress **(Fig. S1A)**. I drafted most of the figures and wrote the manuscript together with Haike Antelmann.

Graphical abstract

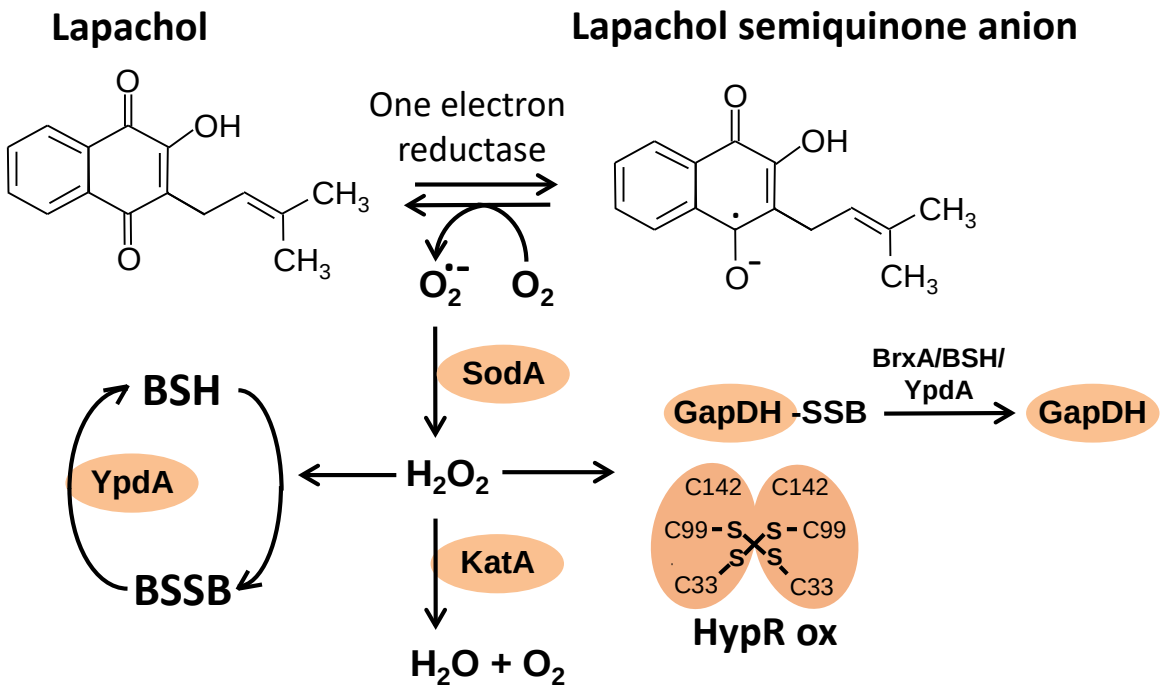

The plant-derived naphthoquinone lapachol causes an oxidative stress response in *Staphylococcus aureus*

Authors:

Nico Linzner[1#], Verena Nadin Fritsch[1#], Tobias Busche[1,2], Quach Ngoc Tung[1], Vu Van Loi[1], Jörg Bernhardt[3], Jörn Kalinowski[2], and Haike Antelmann[1*]

Departments & Institutions:

[1]*Freie Universität Berlin, Institute of Biology-Microbiology, 14195 Berlin, Germany*

[2]*Center for Biotechnology, University Bielefeld, 33615 Bielefeld, Germany*

[3]*Institute for Microbiology, University of Greifswald, 17489 Greifswald, Germany*

# Both authors contributed equally to this work.

Abbreviated title: Lapachol induces an oxidative stress response

***Corresponding author:**

Haike Antelmann, Institute of Biology-Microbiology, Freie Universität Berlin,

Königin-Luise-Strasse 12-16, D-14195 Berlin, Germany,

Tel: +49-(0)30-838-51221, Fax: +49-(0)30-838-451221

E-mail: haike.antelmann@fu-berlin.de

Keywords: *Staphylococcus aureus*, lapachol, quinone, ROS, bacillithiol, bacilliredoxin, YpdA

Abstract

Staphylococcus aureus is a major human pathogen, which causes life-threatening systemic and chronic infections and rapidly acquires resistance to multiple antibiotics. Thus, new antimicrobial compounds are required to combat infections with drug resistant *S. aureus* isolates. The 2-hydroxy-3-(3-methyl-2-butenyl)-1,4-naphthoquinone lapachol was previously shown to exert antimicrobial effects. In this study, we investigated the antimicrobial mode of action of lapachol in *S. aureus* using RNAseq transcriptomics, redox biosensor measurements, *S*-bacillithiolation assays and phenotype analyses of mutants. In the RNA-seq transcriptome, lapachol caused an oxidative and quinone stress response as well as protein damage as revealed by induction of the PerR, HypR, QsrR, MhqR, CtsR and HrcA regulons. Lapachol treatment further resulted in up-regulation of the SigB and GraRS regulons, which is indicative for cell wall and general stress responses. The redox-cycling mode of action of lapachol was supported by an elevated bacillithiol (BSH) redox potential (E_{BSH}), higher endogenous ROS levels, a faster H_2O_2 detoxification capacity and increased thiol-oxidation of GapDH and the HypR repressor *in vivo*. The ROS scavenger N-acetyl cysteine and microaerophilic growth conditions improved the survival of lapachol-treated *S. aureus* cells. Phenotype analyses revealed an involvement of the catalase KatA and the Brx/BSH/YpdA pathway in protection against lapachol-induced ROS-formation in *S. aureus*. However, no evidence for irreversible protein alkylation and aggregation was found in lapachol-treated *S. aureus* cells. Thus, the antimicrobial mode of action of lapachol in *S. aureus* is mainly caused by ROS formation resulting in an oxidative stress response, an oxidative shift of the E_{BSH} and increased protein thiol-oxidation. As ROS-generating compound, lapachol is an attractive alternative antimicrobial to combat multi-resistant *S. aureus* isolates.

Introduction

Staphylococcus aureus is an important human pathogen, which can cause acute skin and soft tissue infections, but also life-threatening systemic and chronic diseases, such as sepsis, endocarditis, pneumonia and osteomyelitis [1-4]. Moreover, the prevalence of multiple antibiotic resistant strains, such as methicillin-resistant *S. aureus* (MRSA) imposes a major health burden [5, 6]. Thus, the discovery of new antimicrobial compounds from natural sources is an urgent need to combat infections with multi-resistant *S. aureus* isolates.

Many natural antimicrobial compounds contain quinone-like structures, such as the fungal 6-brom-2-vinyl-chroman-4-on [7]. Recently, two novel quinone compounds with cytostatic properties were discovered from the fungus *Septofusidium berolinense,* including 3,6-dihydroxy-2-propylbenzaldehyde (GE-1) and 2-hydroxymethyl-3-propylcyclohexa-2,5-diene-1,4-dione (GE-2), which act as topoisomerase-II inhibitors [8, 9]. In addition, the 2-hydroxy-3-(3-methyl-2-butenyl)-1,4-naphthoquinone lapachol of the lapacho tree *Tabebuia impetiginosa* was shown to exert antimicrobial, antiparasitic and cytostatic effects [10-15]. Lapachol showed strong killing effects against various Gram-positive bacteria, such as *Bacillus subtilis*, *Enterococcus faecalis*, *Clostridium perfringens* and *S. aureus*, but was less effective against Gram-negative *Escherichia coli*, *Pseudomonas aeruginosa* and *Salmonella* Typhimurium [16-20]. Furthermore, lapachol was antiproliferative in WHCO1 oesophageal and promyelocytic leukemia HL-60 cancer cell lines with 50% growth inhibition at concentrations of 24.1 µM and 3.18 µM, respectively [21, 22]. Cytotoxic lapachol concentrations were determined as 185 µg/ml, which kill 50% Balb/c murine peritoneal macrophages [23]. While ROS formation has been demonstrated by lapachol *in vitro* [24, 25], its antimicrobial mode of action in pathogenic bacteria has not been studied in detail.

The antimicrobial and toxic effect of quinones can be attributed to their mode of actions as electrophiles and oxidants [26-31]. In the electrophilic mode, quinones lead to alkylation and aggregation of thiols via the irreversible *S*-alkylation chemistry, resulting in thiol depletion in the proteome and thiol-metabolome [29, 31]. As oxidants, quinones can be reduced to semiquinone anion radicals that transfer electrons to molecular oxygen, leading to ROS

formation, such as superoxide anion [24, 25, 27, 28, 32, 33]. The mode of action of quinones is dependent on the physicochemical features, the chemical structure and the availability of oxygen [34-36]. In general, the toxicity and thiol-alkylation ability of quinones increases when the positions adjacent to the keto groups are unsubstituted in the quinone ring (e.g. benzoquinone) [27, 34]. Fully substituted quinone rings cannot alkylate protein thiols, but retain redox-cycling activity, including ubiquinone and tetramethyl-*p*-benzoquinone [36]. Since the quinone ring is fully substituted, lapachol may act mainly via the oxidative mode as antimicrobial in *S. aureus*, which was subject of this study [27, 34].

We have previously investigated the transcriptome signature in response to 2-methylhydroquinone (MHQ) in *S. aureus* [26]. MHQ was shown to induce a strong thiol-specific oxidative and quinone stress response in the *S. aureus* transcriptome [26]. The quinone-responsive QsrR and MhqR regulons were most strongly induced by MHQ and conferred independent resistance to quinones and quinone-like antimicrobials, including ciprofloxacin pyocyanin, norfloxacin and rifampicin [26, 37]. The MhqR repressor controls the *mhqRED* operon, which encodes for the predicted phospholipase/ carboxylesterase MhqD and ring-cleavage dioxygenase MhqE involved in quinone detoxification [26]. The redox-sensing QsrR repressor senses quinones by thiol-*S*-alkylation and regulates paralogous dioxygenases and quinone reductases in *S. aureus* [37].

The oxidative mode of action of MHQ was revealed by induction of the peroxide-specific PerR regulon, which controls antioxidant enzymes, such as catalase and peroxidases (KatA, Tpx, Bcp), Fe-binding miniferritin (Dps) and the FeS-cluster machinery (Suf) [38-40]. Moreover, the disulfide-stress-specific HypR regulon was upregulated by MHQ, including the NADPH-dependent flavin disulfide reductase MerA [41]. In addition to ROS detoxification enzymes, *S. aureus* uses the low molecular weight thiol bacillithiol (BSH) for protection against ROS [42]. BSH is an important thiol cofactor that functions in detoxification of various redox-active compounds, electrophiles and antibiotics and contributes to survival of *S. aureus* in macrophage infection assays [42-45]. BSH also participates in redox modifications of proteins and forms protein *S*-bacillithiolation under disulfide stress, such as HOCl and the ROS-

producing antimicrobial surface coating AGXX® [46-48]. Protein *S*-bacillithiolations are involved in thiol-protection and regulate protein activities as shown for the glycolytic glyceraldehyde-3-phosphate dehydrogenase (GapDH) in *S. aureus* [31, 46-50]. The removal of protein *S*-bacillithiolation is controlled by bacilliredoxins (Brx), which are regenerated by BSH and the bacillithiol disulfide (BSSB) reductase YpdA [48, 51-53]. Moreover, the Brx/BSH/YpdA pathway is important for protection of *S. aureus* under oxidative stress and infection conditions [51, 52].

In this study, we analyzed the molecular stress responses and mode of action of lapachol in *S. aureus*. Using RNA-seq transcriptomics, lapachol induced an oxidative and quinone stress response as well as strong protein damage in *S. aureus*. This signature was revealed by the induction of the QsrR, MhqR, PerR, HypR, CtsR and HrcA regulons and of the enzymes of the Brx/BSH/YpdA redox pathway. The oxidative mode of action of lapachol was demonstrated by an oxidative shift of the BSH redox potential, elevated ROS formation and faster H_2O_2 detoxification capacity, increased protein *S*-bacillithiolation of GapDH and thiol-oxidation of the HypR repressor *in vivo*. However, no evidence for protein alkylation and aggregation was revealed. In support of the oxidative mode, the ROS scavenger N-acetyl cysteine and microaerophilic growth conditions improved the survival of *S. aureus* under lapachol stress. Phenotype analyses revealed that KatA and the Brx/BSH/YpdA pathway are important for the defense of *S. aureus* against lapachol-induced ROS. Overall, our results indicate that the antimicrobial effect of lapachol is mainly caused by ROS-formation, resulting in an impaired redox homeostasis and increased protein thiol-oxidation in *S. aureus*.

Experimental procedures

Bacterial strains, growth and survival assays. For cloning and genetic manipulation, *E. coli* was cultivated in Luria broth (LB) medium. The His-tagged GapDH protein of *S. aureus* was expressed and purified in *E. coli* BL21(DE3) *plys*S with plasmid pET11b-*gapDH* as previously described [48]. For lapachol stress experiments, we used *S. aureus* COL *katA*, *bshA*, *brxAB* and *ypdA* deletion mutants and the *katA, bshA*, *ypdA, brxA* and *brxB* complemented strains as

described in **Tables S1 and S2** [51]. *S. aureus* strains were cultivated in LB, RPMI or Belitsky minimal medium (BMM) depending on the specific experiments and treated with lapachol during the exponential growth as described [41, 54]. Specifically, biosensor experiments, *S*-bacillithiolation and HypR oxidation assays were performed in BMM medium due to high expression of the biosensor and low ROS quenching effects as described [54, 55]. All growth and survival assays as well as RNAseq experiments were performed in rich RPMI medium, which resembles infection conditions and allows fast growth. Survival assays were performed by plating 100 µl of serial dilutions of *S. aureus* onto LB agar plates and determination of colony forming units (CFUs). Statistical analysis was performed using Student's unpaired two-tailed t-test by the graph prism software. Lapachol, diamide, sodium hypochlorite (NaOCl), N-acetyl cysteine, dithiothreitol (DTT) and cumene hydroperoxide (CHP, 80% w/v) were purchased from Sigma Aldrich.

Determination of the minimal inhibitory concentration (MIC) of lapachol. MIC assays were performed in 96-well plates with 200 µl of serial two-fold dilutions of the 40 mM lapachol stock in RPMI medium. The *S. aureus* overnight culture was inoculated to an OD_{500} of 0.03 into the microplate wells. After 24 h shaking at 37°C, the OD_{500} was measured using the CLARIOstar microplate reader (BMG Labtech).

Construction of *S. aureus* COL *katA* and *bshA* mutants as well as complemented strains. The construction of the *S. aureus katA* and *bshA* deletion mutants were performed using the pMAD *E. coli S. aureus* shuttle vector as described [41, 56]. Briefly, the 500 bp up- and downstream regions of *katA* and *bshA* were amplified using primers pMAD-katA-for-BglII, pMAD-katA-f1-rev, pMAD-katA-f2-for, pMAD-katA-rev-SalI for *katA* and pMAD-bshA-f1-rev, pMAD-bshA-for-BglII, pMAD-bshA-rev-SalI, pMAD-bshA-f2-for for *bshA* **(Table S3)**, fused by overlap extension PCR and ligated into the *Bgl*II and *Sal*I sites of plasmid pMAD. The pMAD constructs were electroporated into *S. aureus* RN4220 and further transduced into *S. aureus* COL using phage 81 [57]. The clean deletions of *katA* and *bshA* were selected after plasmid excision as described [41].

For construction of the *katA* and *bshA* complemented strains, the xylose-inducible ectopic *E. coli/ S. aureus* shuttle vector pRB473 was applied [58]. Primer pairs pRB-katA-for-*Bam*HI and pRB-katA-rev-*Kpn*I as well as pRB bshA-for-*Bam*HI and pRB bshA-rev-*Kpn*I **(Table S3)** were used for amplification of *katA* and *bshA*, respectively. The PCR products were cloned into pRB473 after digestion with *Bam*HI and *Kpn*I to generate plasmids pRB473-*katA* and pRB473-*bshA*. The pRB473-*katA* and pRB473-*bshA* plasmids were transduced into the *katA* and *bshA* deletion mutants, respectively, to construct the complemented strains as described [54].

For construction of *S. aureus* COL WT expressing His-tagged HypR, *hypR*-His was amplified from the *S. aureus* COL genome by PCR using primer pRB-hypR-for-BamHI and primer pRB-hypR-His-rev-KpnI **(Table S3)**, which included the codons for 6 His residues at the C-terminus. The PCR product was cloned into plasmid pRB473 after digestion with *Bam*HI and *Kpn*I to generate plasmid pRB473-*hypR*-His, which was introduced into *S. aureus* COL WT via phage transduction as described [41].

Live/Dead viability assay. The viability assay of *S. aureus* COL WT was conducted after treatment with sub-lethal and lethal concentrations of 0.3-1 mM lapachol at an OD_{500} of 0.5 using the LIVE/DEAD™ BacLight™ bacterial viability kit (Thermo Fisher) as described [59]. In brief, *S. aureus* COL was stained with SYTO9 or propidium iodide for live or dead cells, respectively. Fluorescence was analyzed after excitation at 488 and 555 nm using a fluorescence microscope (Nikon, Eclipse, T*i*2) (SYTO9 Ex: 488 nm, propidium iodide Ex: 555 nm). Live and dead cells were false-colored in green and red, respectively.

RNA isolation, library preparation, next generation cDNA sequencing and differential gene expression analysis after lapachol stress. RNA-seq transcriptomics was performed using RNA of *S. aureus* COL, which was grown in RPMI medium and subjected to 0.3 mM lapachol for 30 min as described [59]. Differential gene expression analysis of 3 biological replicates was performed using DESeq2 [60] with ReadXplorer v2.2 [61] using an adjusted p-value cut-off of $P \leq 0.05$ and a signal intensity ratio (M-value) cut-off of ≥1 or ≤-1 (fold-change

of +/- 2) as described previously [59]. The RNA-seq raw data files for the whole transcriptome are available in the ArrayExpress database (www.ebi.ac.uk/arrayexpress) under E-MTAB-8691.

Construction of the Voronoi transcriptome treemap. The lapachol transcriptome treemap was constructed using the Paver software (DECODON GmbH, Greifswald, Germany) as described [59]. The red-blue color gradient indicates log2-fold changes (M-values) of selected genes, operons and regulons that are up- or down-regulated under lapachol stress. The cell sizes denote absolute log2-fold changes in the transcriptome under lapachol versus the control.

Brx-roGFP2 and Tpx-roGFP2 biosensor measurements. *S. aureus* COL expressing the biosensor plasmids pRB473-*tpx-roGFP2* and pRB473-*brx-roGFP2* were grown in LB overnight and used for measurements of the biosensor oxidation degree (OxD) after treatment with 100 µM lapachol as described [51, 54]. The fully reduced and oxidized controls of *S. aureus* cells expressing Tpx-roGFP2 were treated with 15 mM DTT and 20 mM cumene hydroperoxide, respectively. The Brx-roGFP2 and Tpx-roGFP2 biosensor fluorescence emission was measured at 510 nm after excitation at 405 and 488 nm using the CLARIOstar microplate reader (BMG Labtech). The OxD of the Brx-roGFP2 and Tpx-roGFP2 biosensors was determined for each sample and normalized to fully reduced and oxidized controls as described [51, 54].

Analyses of GapDH *S*-bacillithiolation and thiol-oxidation of the HypR repressor after lapachol stress. For GapDH *S*-bacillithiolation assay *in vivo*, *S. aureus* cells were grown in LB until an OD_{540} of 2, harvested by centrifugation and transferred to Belitsky minimal medium (BMM) as described [47]. The cells were treated with 100 µM lapachol and harvested after 30, 60, 120 and 180 min in TE buffer (pH 8.0) with 50 mM N-ethylmaleimide (NEM). Protein extracts were prepared and analyzed by BSH-specific Western blot analysis for *S*-bacillithiolated proteins using polyclonal rabbit anti-BSH antiserum as described [47]. To analyze *S*-bacillithiolation of purified GapDH with lapachol *in vitro*, 60 µM of GapDH was *S*-

bacillithiolated with 600 µM BSH in the presence of 10-fold excess of 6 mM lapachol for 5 min. As control, GapDH was incubated with BSH in absence of lapachol. Excess of BSH and lapachol were removed with Micro Biospin 6 columns (Biorad). *S*-bacillithiolation of GapDH was analyzed using non-reducing BSH-specific Western blots. To study thiol-oxidation of the HypR repressor *in vivo*, *S. aureus* COL WT strain expressing His-tagged HypR **(Table S1)** was cultivated as described for the *in vivo S*-bacillithiolation assay above. Cell extracts were alkylated with 50 mM NEM and HypR oxidation analyzed using non-reducing SDS-PAGE and Western blot analysis with His-tag specific monoclonal antibodies (Thermo Fisher).

Analysis of H_2O_2 detoxification capacity in cell extracts by the FOX assay. The FOX assay was performed with cytoplasmic cell extracts as described previously [62]. FOX reagent was prepared by adding 100 ml FOX I (100 mM sorbitol, 125 µM xylenol orange) to 1ml FOX II (25 mM ammonium ferrous(II)sulfate in 2.5 M H_2SO_4). To prepare cytoplasmic extracts, *S. aureus* COL WT was cultivated in RPMI to an OD_{500} of 0.5, exposed to 0.3 mM lapachol and harvested after 1 h and 2 h. Cells were washed in 83 mM phosphate buffer (pH 7.05), disrupted using the ribolyzer and 100 µl cell lysate was added to 500 µl of 10 mM H_2O_2 solution. After different times (1-5 min), 2 µl of the samples were added to 200 µl FOX reagent and incubated for 30 min at room temperature. The absorbance was measured at 560 nm using the CLARIOstar microplate reader (BMG Labtech). H_2O_2 standard curves were measured with 20 µl H_2O_2 (0-18 µM final concentrations) and 200 µl FOX reagent as above.

Protein aggregation assays after lapachol stress *in vitro* and *in vivo*. For *in vitro* aggregation analyses, purified GapDH was pre-reduced with 10 mM DTT for 30 min at RT and DTT removed with spin columns. Subsequently, 5 µM GapDH was incubated with different concentrations of lapachol for 30 min at RT and subjected to SDS-PAGE. For isolation of insoluble protein aggregates of cell extracts *in vivo*, *S. aureus* COL WT was cultivated in RPMI to an OD_{500} of 0.5 and treated with 0.3 and 1.0 mM lapachol for 30 min. Cell extracts were harvested and protein aggregates isolated as insoluble protein fraction as described previously [59, 63, 64].

Results

Lapachol has a strong antimicrobial and killing effect on *S. aureus* COL. To determine the growth-inhibitory and lethal lapachol concentrations, *S. aureus* COL was grown in RPMI medium and exposed to increasing doses 0.3-1 mM lapachol during the exponential growth **(Fig. 1AB)**. Cell viability was analyzed using CFU counting and the LIVE/DEAD™ Bacterial Viability Kit **(Fig. 1BC)**. Sub-lethal doses of 0.3 mM lapachol resulted in a decreased growth rate, but cells were able to recover in growth and the survival rate was not affected **(Fig. 1AB)**. This result was confirmed using live/dead staining since only few red cells were observed after treatment with sub-lethal 0.3 mM lapachol similar as in the untreated control **(Fig. 1C).**

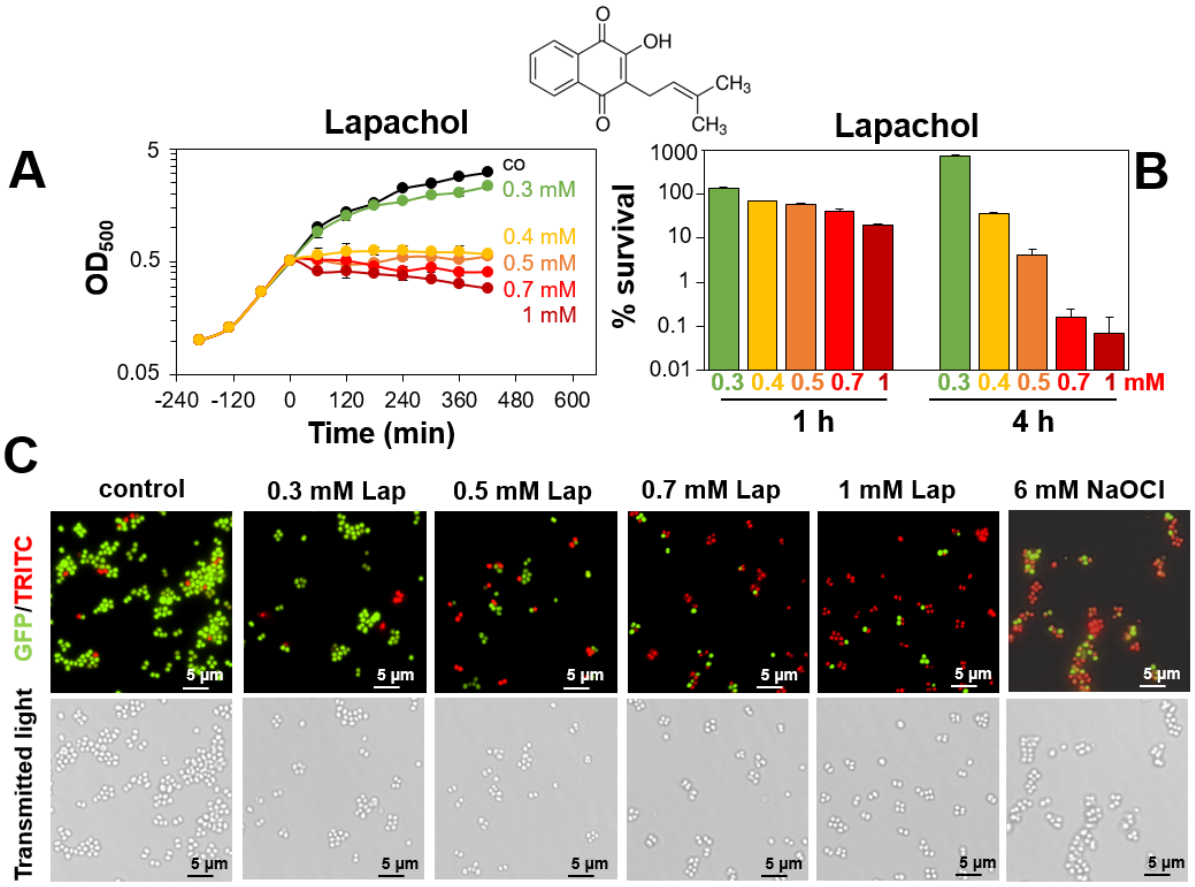

Fig. 1. Lapachol has a strong antimicrobial effect in *S. aureus*. (A-C) The structure of the 2-hydroxy-3-(3-methyl-2-butenyl)-1,4-naphthoquinone lapachol is shown above the figures **(A)** and **(B)**. *S. aureus* COL was grown in RPMI medium to an OD_{500} of 0.5 and exposed to sub-lethal (300 µM) and lethal (0.4, 0.5, 0.7 and 1 mM) doses lapachol. **(A)** Growth curves and **(B)** survival assays were performed to determine sub-lethal and lethal lapachol concentrations. The cells were plated for CFUs after 1 and 4 h of lapachol stress. **(C)** Cell viability was also analyzed after 1 h of lapachol stress using the Live/Dead™ BacLight™ Bacterial Viability Kit and visualized with a fluorescence microscope (Nikon, Eclipse, T*i*2). Live and dead cells show green and red fluorescence, respectively. As control for dead cells, the toxic concentration of 6 mM NaOCl was applied.

Increasing concentrations of 0.4-1 mM lapachol were lethal for *S. aureus* COL as shown by decreased growth and viability rates **(Fig. 1AB)**. Only few SYTO9-labelled cells could be observed using the LIVE/DEAD™ assay after exposure to 0.7-1 mM lapachol, indicating that lapachol exerts a strong antimicrobial and killing effect in *S. aureus* **(Fig. 1C)**. However, the MIC of lapachol was determined as 1.25 mM in *S. aureus* **(Table S4)**, which was higher compared to the growth-inhibitory amount. The higher MIC is probably caused by inactivation of lapachol over the long time of incubation for 24 h in the microplate assay.

Lapachol induces a quinone and oxidative stress response in the *S. aureus* COL transcriptome. In previous transcriptome studies, we monitored physiological stress responses by treatment of *S. aureus* with sub-lethal doses of antimicrobial compounds [41, 59, 65]. Thus, the changes in the transcriptome were analysed after exposure of *S. aureus* COL to sub-lethal 0.3 mM lapachol stress for 30 min in 3 biological replicates using the RNA-seq method as described earlier [41]. Significant differential gene expression is indicated by the M-value cut-off (log2-fold change lapachol/ control) of ≥1 and ≤-1 (fold-change of +/- 2, P≤0.05) which includes most known redox regulons upregulated under lapachol stress **(Fig. 2)**. In total, 564 genes were significantly >2-fold up-regulated and 515 genes were <-2-fold down-regulated in the lapachol transcriptome of *S. aureus* COL **(Fig. 2, Tables S5 and S6)**. Overall, the significantly and most strongly induced regulons in the lapachol transcriptome include the CtsR, HrcA, PerR, HypR, NsrR, MhqR, QsrR, CymR, SaeRS, GraRS and SigB regulons. These regulons indicate that lapachol causes an oxidative and quinone stress transcriptome signature and protein damage. Up-regulated genes and regulons are labelled with different color codes in the ratio/intensity scatter plot (M/A-plot) and are also displayed in the Voronoi transcriptomics treemap **(Fig. 2 and 3, Tables S5 and S6)**.

Lapachol stress leads to strong induction of the CtsR and HrcA regulons, which control the protein quality control machinery, including Clp proteases and the DnaK-GrpE, GroESL chaperones [66, 67]. The heat-shock specific CtsR controlled *ctsR-mcsA-mcsB-clpC* operon and the HrcA-regulated *hrcA-grpE-dnaKJ* operon are 46-62-fold and 44-50-fold up-regulated, respectively, under lapachol stress **(Fig. 2 and 3, Tables S5 and S6)**.

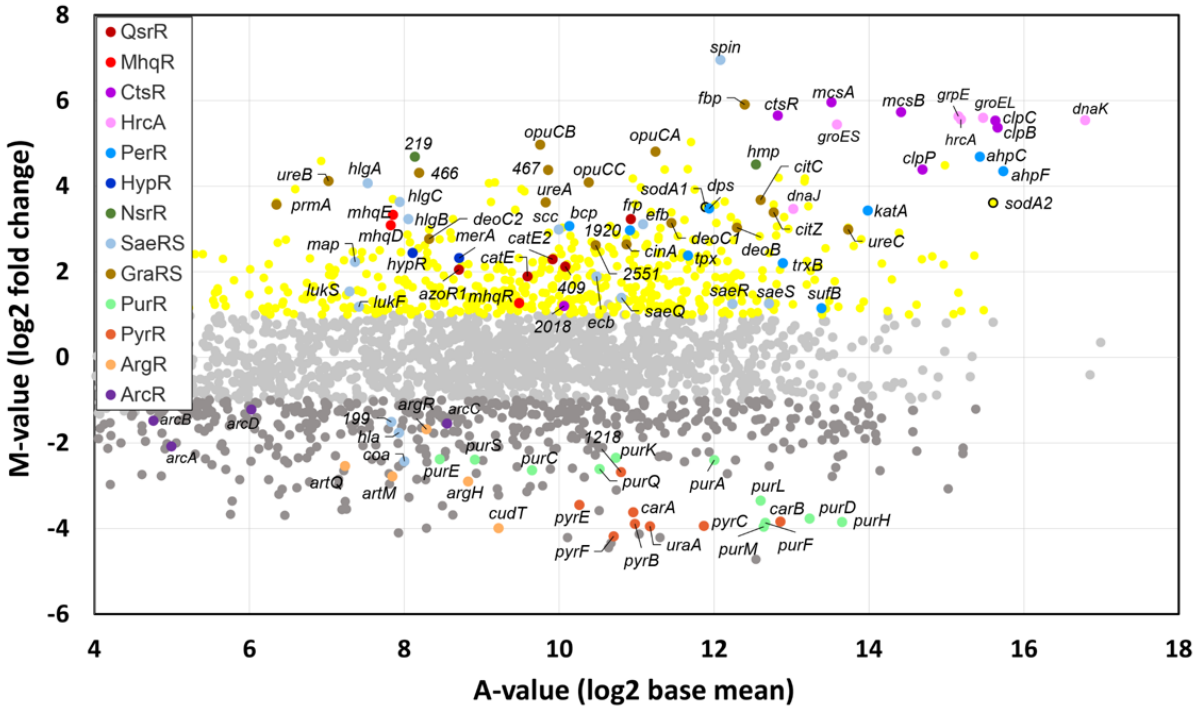

Fig. 2. RNA-seq transcriptomics after lapachol stress in *S. aureus* COL. For RNA-seq transcriptomics, *S. aureus* COL was grown in RPMI medium and treated with 300 µM lapachol for 30 min. The gene expression profile is shown as ratio/intensity scatter plot (M/A-plot) which is based on differential gene expression analysis using DeSeq2. Colored symbols indicate subsets of the significantly induced regulons QsrR, MhqR, CtsR, HrcA, PerR, HypR, SaeRS, NsrR (red, dark red, magenta, light magenta, dark blue, blue, light blue, green). The significantly down-regulated regulons PurR, PyrR, ArgR, ArcR are labelled in light green, orange, light orange and dark violet. All other significantly induced (yellow) or repressed (dark grey) transcripts were defined with an M-value≥1 or ≤-1; P-value ≤0.05. Light grey symbols denote transcripts with no fold-changes after lapachol stress (P>0.05). The transcriptome analysis was performed from three biological replicates. The RNA-seq expression data of all genes after lapachol stress and their regulon classifications are listed in **Tables S5 and S6**.

Thus, lapachol induces strong protein damage, which might be caused by oxidative or electrophilic protein modifications, such as thiol-oxidation or *S*-alkylations. Among the top scorers was further the peroxide specific PerR regulon with fold-changes of 5-26. The PerR-regulon genes encode for peroxidases *ahpCF* (20-26-fold), *bcp* (11-fold), *tpx* (5-fold), the catalase *katA* (11-fold), the miniferritin *dps* (11-fold) and the thioredoxin reductase *trxB* (5-fold) **(Fig. 2 and 3, Tables S5 and S6)**. The induction of the PerR-regulon confirms that lapachol acts via the oxidative mode leading to ROS formation, such as H_2O_2 inside *S. aureus*. Furthermore, both genes encoding superoxide dismutases (*sodA1* and *sodA2*) were highly expressed (11-12-fold) under lapachol stress **(Fig. 2, Tables S5 and S6)**. This supports the generation of superoxide anions in the oxidative mode of lapachol as has been measured previously *in vitro* [24].

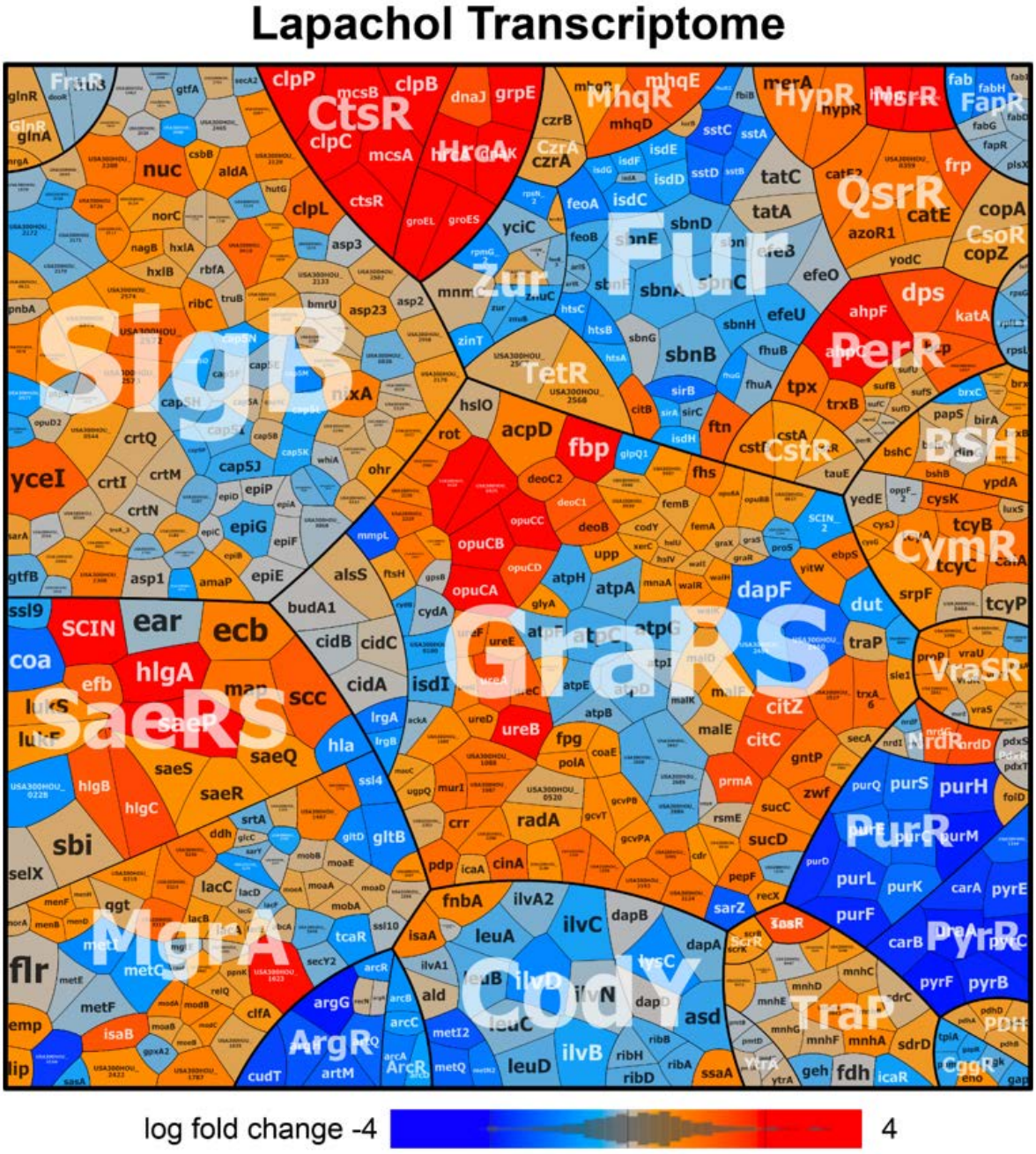

Fig. 3. The transcriptome treemap after lapachol indicates an oxidative and quinone stress response in *S. aureus* COL. The treemap shows the log2-fold changes (m-values) using the red-blue color code where red indicates log2-fold induction and blue repression of selected regulons after exposure to 300 µM lapachol in the RNA-seq transcriptome of *S. aureus* COL. The genes, operons and regulons are based on RegPrecise (http://regprecise.lbl.gov/RegPrecise/index.jsp) and previous classifications. Lapachol caused a strong quinone and oxidative stress response as well as protein damage as revealed by induction of the PerR, HypR, QsrR, MhqR, CtsR, HrcA regulons in *S. aureus*. The induction of the SigmaB and GraRS regulons further indicates cell wall and general stress responses in *S. aureus*. The detailed transcriptome data of all genes differentially expressed in response to lapachol are presented in **Tables S5 and S6**.

In addition, lapachol resulted in 23-26-fold induction of the NsrR-controlled *hmp* gene encoding a flavohemoglobin, which is predominantly involved in nitric oxide detoxification [68]. Interestingly, Hmp of *S. aureus* was shown to function in quinone and nitrocompound

detoxification using mixed one- and two electron reduction mechanisms [69]. Hmp exhibits a strong substrate preference for 2-methyl-1,4-naphthoquinones [69], which are related to lapachol. Thus, Hmp might be involved in lapachol detoxification in *S. aureus*. Furthermore, the HypR regulon, including the disulfide reductase encoding *merA* gene was 5-fold induced by lapachol, which is indicative for disulfide stress caused by lapachol [41].

The RNA-seq transcriptome data further suggest an electrophilic mode of action of lapachol, as revealed by the significant induction of both quinone-specific MhqR and QsrR regulons. The MhqR-regulated *mhqRED* operon was 10-fold induced under lapachol treatment. The QsrR regulon genes encoding quinone reductases and dioxygenases are 3.7-9-fold up-regulated by lapachol, including *catE, catE2*, *azoR1*, *frp* and *yodC* **(Fig. 2 and 3, Tables S5 and S6)**. Thus, the main transcriptome signature suggests that lapachol exerts its toxicity as oxidant and electrophile in *S. aureus*. In addition, lapachol leads to strong up-regulation of the SaeRS, GraRS and SigB regulons. Among the virulence factor controlling SaeRS regulon, the myeloperoxidase inhibitor SPIN was most strongly 123-fold induced, while the γ-hemolysin operon *hlgABC* was 8-10-fold up-regulated by lapachol. Several GraRS regulon members were 3-60-fold up-regulated. The large GraRS regulon responds to cell wall-active antibiotics and is involved in the oxidative stress defense in *S. aureus* [70]. Finally, the genes encoding enzymes for biosynthesis of BSH and the Brx/YpdA pathway, such as *bshA*, *bshB*, *bshC, brxB* and *ypdA* were 2-4-fold up-regulated by lapachol in *S. aureus*. This further points to the generation of ROS in the oxidative mode of lapachol resulting in an impaired redox homeostasis in *S. aureus*.

Among the down-regulated regulons, the CodY and ArgR regulons involved in the biosynthesis of branched chain amino acids (lysine, isoleucine and leucine) and arginine, respectively, were strongly repressed in the lapachol transcriptome. The PyrR and PurR regulons, which control purine and pyrimidine biosynthesis operons were further down-regulated under lapachol. The shut-down of amino acid and nucleotide biosynthesis enzymes might be caused by decreased ATP levels since the ATP synthase operon was further down-regulated under lapachol stress **(Fig. 2 and 3, Tables S5 and S6).**

Altogether, the RNA-seq transcriptome signature indicates that lapachol causes an oxidative, quinone and cell wall stress response as well as protein damage, suggesting its mode of action as oxidant and electrophile.

Lapachol stress leads to an increased BSH redox potential, elevated endogenous ROS levels and enhanced H_2O_2 detoxification in *S. aureus*. Previous studies revealed that lapachol is reduced to its semiquinone anion radical, leading to reduction of O_2 and formation of reactive oxygen species (ROS), such as superoxide anions and hydroxyperoxyl radicals [24, 25]. Our transcriptome data further support the oxidative mode of lapachol and an impaired redox balance **(Fig. 2 and 3)**. Thus, we applied the recently constructed genetically encoded Brx-roGFP2 and Tpx-roGFP2 biosensors to measure intracellular redox changes in *S. aureus* after sub-lethal doses of 100 µM lapachol [51, 54]. The coupled Brx-roGFP2 biosensor is specific for BSSB leading to *S*-bacillithiolation of the Brx active site Cys and transfer of BSH to the roGFP2 moiety, which finally rearranges to the roGFP2 disulfide [54]. Oxidation of roGFP2 results in a ratiometric change of the 405 and 488 nm excitation maxima. The 405/488 nm excitation ratio of Brx-roGFP2 after lapachol stress reflects the oxidation degree (OxD) of the biosensor and the changes in the BSH redox potential (E_{BSH}) in *S. aureus* [54]. The Brx-roGFP2 biosensor showed an increased OxD of 0.65 after 100 µM lapachol stress compared to the untreated control (OxD ~ 0.3) **(Fig. 4A)**. However, cells were unable to regenerate the reduced basal level of E_{BSH} within 3 h of lapachol stress. These results indicate that lapachol causes a constant oxidative shift in E_{BSH} in *S. aureus* probably due to its redox-cycling action.

Next, we monitored endogenous H_2O_2 levels using the Tpx-roGFP2 biosensor in *S. aureus* after lapachol stress [51]. The Tpx-roGFP2 biosensor is specific for low levels of H_2O_2 [51]. H_2O_2 reacts with the Tpx active site to Cys sulfenic acid (SOH), which is transferred to roGFP2 leading to roGFP2 disulfide formation and the ratiometric changes in the roGFP2 excitation spectrum. The Tpx-roGFP2 biosensor was shown to respond very fast to 100 µM lapachol leading to an increased OxD of ~0.7 **(Fig. 4B)**. These results confirm that lapachol treatment leads to increased endogenous H_2O_2 levels resulting in an increased E_{BSH} supporting the oxidative mode of action. In addition, the FOX assay was performed to investigate the H_2O_2

detoxification capacity of cellular extracts of *S. aureus* after lapachol stress. H_2O_2 detoxification occurred much faster in lapachol-treated cell extracts, compared to that of untreated control cells **(Fig. 4C)**. Thus, *S. aureus* has an enhanced H_2O_2 detoxification capacity after lapachol stress due to a higher catalase activity, which is consistent with the increased expression of the PerR controlled *katA* and *ahpCF* antioxidant genes.

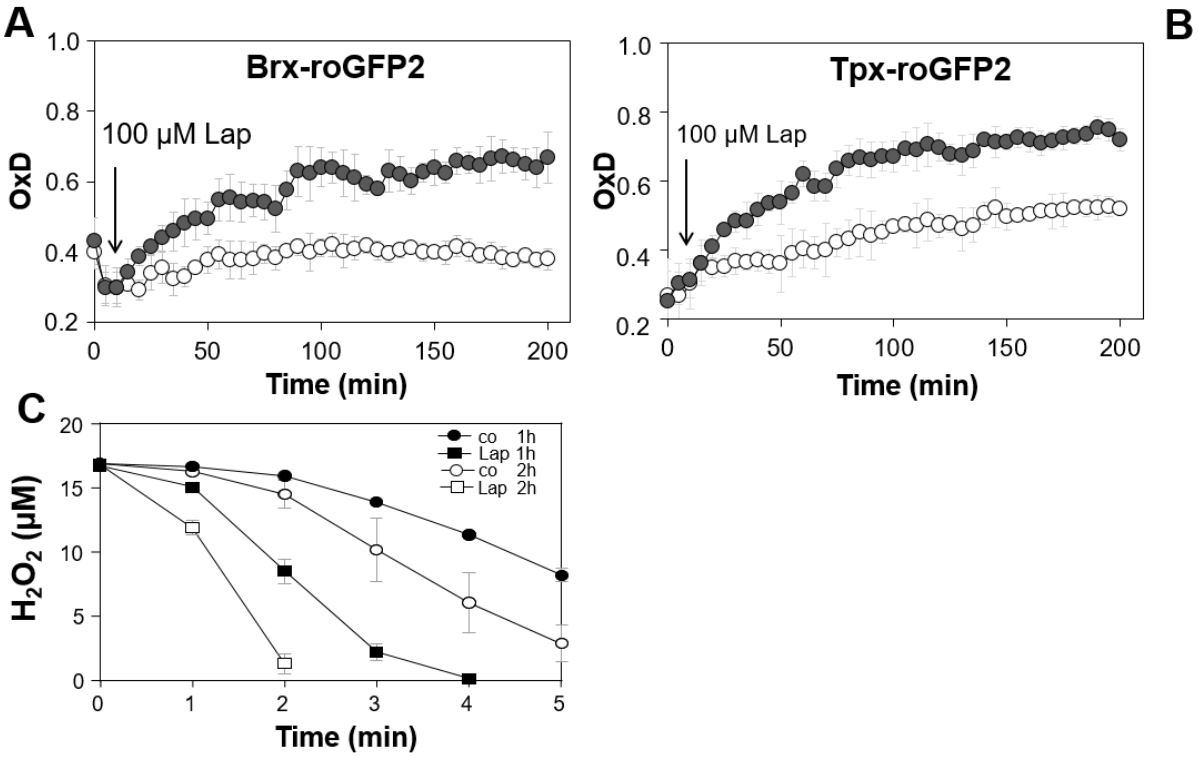

Fig. 4. Lapachol causes an increased BSH redox potential, elevated endogenous H_2O_2 levels and faster H_2O_2 detoxification in *S. aureus* COL. Responses of the Brx-roGFP2 **(A)** and Tpx-roGFP2 **(B)** biosensors to 100 µM lapachol stress in *S. aureus* COL. The oxidation degrees (OxD) of the Brx-roGFP2 and Tpx-roGFP2 biosensors were calculated for untreated control cells (white symbols) and after lapachol stress (grey symbols). OxD values were calibrated to fully reduced and oxidized controls. **(C)** Lapachol-treated *S. aureus* cells showed faster H_2O_2 detoxification in the FOX assay indicating higher catalase activity. *S. aureus* was exposed to 0.3 mM lapachol for 1-2 h and cell extracts were analyzed for H_2O_2 decomposition using the FOX-Assay. Mean values and SD of 3-4 biological replicates are shown.

The ROS scavenger N-acetyl cysteine and microaerophilic growth conditions improve the survival of *S. aureus* under lapachol stress. Since ROS generation by lapachol depends on oxygen availability, we compared the survival of *S. aureus* under aerobic and microaerophilic growth conditions. The results showed that the survival of *S. aureus* was strongly improved after 0.4 and 1 mM lapachol stress under microaerophilic conditions **(Fig. 5A)**. Both concentrations were lethal under aerobic conditions **(Fig. 1B; Fig. 5A)**. While

microaerophilic growth resulted in ~80% survival of cells exposed to 1 mM lapachol, only less than 1% of cells survived with 1 mM lapachol under aerobic conditions **(Fig. 5A)**. This result was supported by the ROS scavenger N-acetyl cysteine, which was added to the aerobic culture before the exposure to 0.4 mM lapachol **(Fig. 5B)**. The aerobic *S. aureus* culture treated with N-acetyl cysteine showed significantly improved survival after 0.4 mM lapachol stress **(Fig. 5B)**. Together, our results revealed that the antimicrobial effect of lapachol is based on ROS formation, since decreased ROS levels lead to an enhanced survival of lapachol-treated cells.

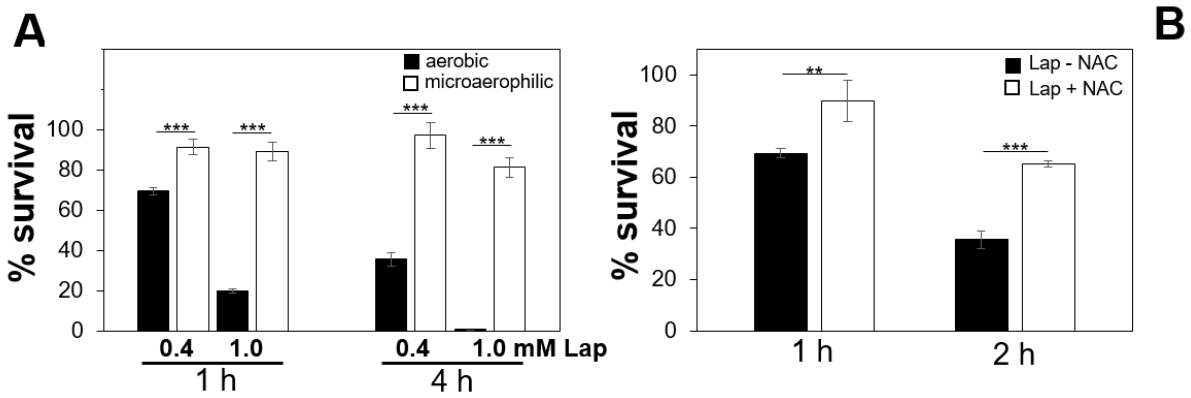

Fig. 5. Microaerophilic growth and the ROS-scavenger N-acetyl cysteine improve survival of *S. aureus* under lapachol stress. (A) Survival assays were performed of *S. aureus* COL WT grown in RPMI under aerobic or microaerophilic conditions after exposure to 0.4 and 1 mM lapachol at an OD_{500} of 0.5. The aerobic survival rates are the same shown in Fig.1B. **(B)** Survival rates were determined under aerobic growth conditions after 0.4 mM lapachol stress in the absence or presence of 1.25 mM N-acetyl cysteine (NAC). CFUs were determined after 1 or 4 h of stress exposure and the survival of the untreated control was set to 100%. Mean values and SD of three to four biological replicates are presented. The statistics was calculated using a Student's unpaired two-tailed t-test by the graph prism software. Symbols are: **p ≤ 0.01 and ***p ≤ 0.001.

Lapachol causes increased *S*-bacillithiolation of GapDH and thiol-oxidation of the HypR repressor in *S. aureus*. Previously, we used BSH-specific Western blots to analyze the extent of protein *S*-bacillithiolation in *S. aureus* under HOCl stress [48]. The glyceraldehyde-3-phosphate dehydrogenase GapDH was the most abundant *S*-bacillithiolated protein under HOCl stress that could be visualized as major band in non-reducing BSH-specific Western blots [48]. Thus, we investigated the oxidative mode of action of lapachol by analysis of the pattern of *S*-bacillithiolation in *S. aureus*. The BSH specific Western blots revealed an increased *S*-bacillithiolation of the GapDH band after 30-120 min of lapachol stress, which was

absent in the *bshA* mutant **(Fig. 6A)**. These results confirm the oxidative mode of action to induce thiol-oxidation of GapDH in *S. aureus in vivo*.

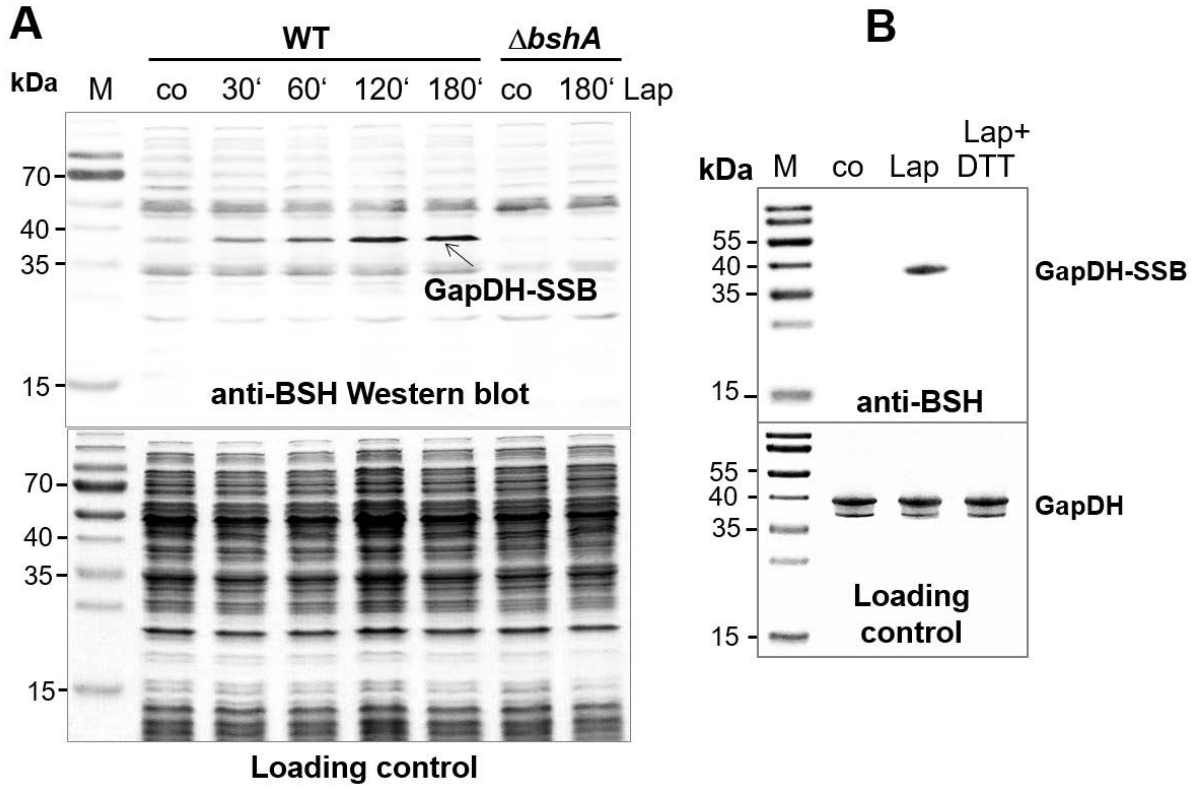

Fig. 6. Lapachol leads to *S*-bacillithiolation of GapDH *in vivo* and *in vitro*. (A) *S. aureus* COL WT and the *bshA* mutant were exposed to 100 µM lapachol for different times and the *S*-bacillithiolated GapDH (GapDH-SSB) is visualized in BSH-specific Western blot as most abundant *S*-bacillithiolated protein as shown previously under NaOCl stress [48]. **(B)** Purified GapDH is treated with 6 mM lapachol in the presence of 600 µM BSH resulting in *S*-bacillithiolation of GapDH *in vitro* as revealed in BSH-specific Western blots. As control, GapDH was treated with BSH alone (co). The Coomassie-stained SDS-PAGE loading controls are shown below the BSH Western blots.

Next, we used BSH-specific non-reducing Western blots to investigate whether lapachol-induced ROS can also lead to *S*-bacillithiolation of purified GapDH *in vitro*. Pre-reduced GapDH was treated with lapachol in the presence of BSH. While no *S*-bacillithiolated GapDH band was visible in the control reaction of GapDH with BSH alone, the presence of lapachol strongly induced *S*-bacillithiolation of GapDH *in vitro* **(Fig. 6B)**. However, we did not find evidence for protein alkylation or aggregation of purified GapDH after treatment with increasing doses 0.5-7.5 mM lapachol alone as revealed by SDS-PAGE **(Fig. S1A)**. In addition, we isolated the insoluble protein fraction of protein aggregates from lapachol-treated cells using the protocol as established previously [63, 64]. However, the results did not reveal increased protein aggregates after lapachol stress **(Fig. S1B)**.

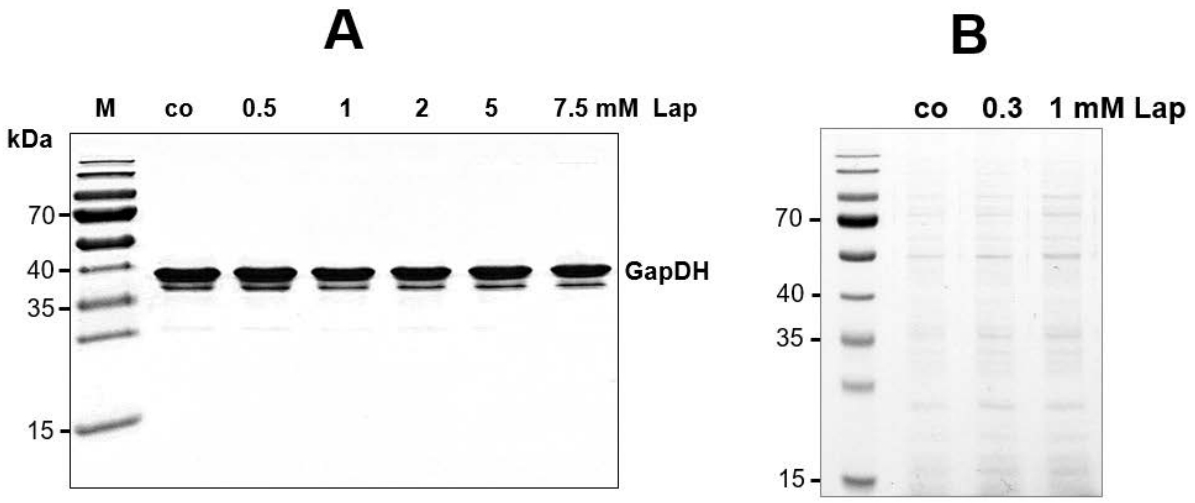

Fig. S1. Lapachol does not induce protein aggregation in purified GapDH *in vitro* (A) or in cellular protein extracts *in vivo* (B). (A) Purified GapDH was exposed to 0.5-7.5 mM lapachol (Lap) for 30 min and analyzed by SDS-PAGE. **(B)** *S. aureus* COL cells were grown in RPMI medium to OD_{500} of 0.5 and exposed to 0.3 and 1 mM lapachol for 30 min to analyze the insoluble protein fraction of protein aggregates by SDS-PAGE.

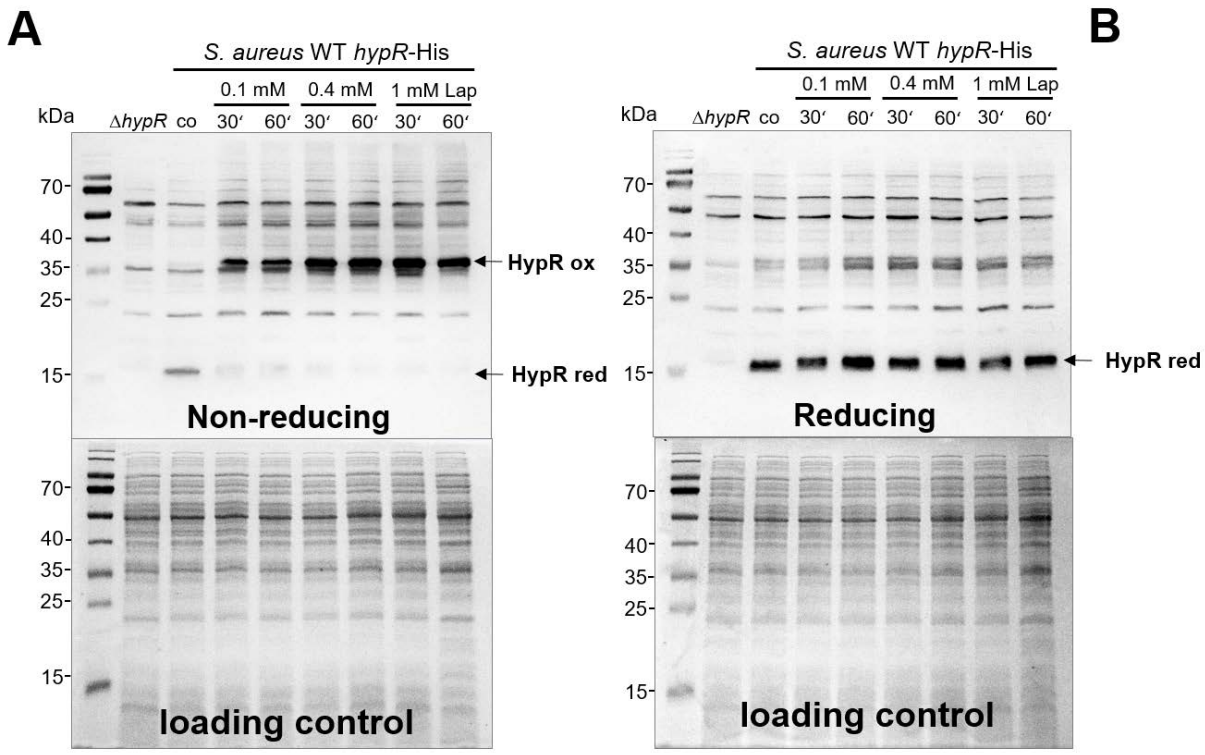

Fig. S2. The oxidative mode of lapachol is revealed by HypR oxidation *in vivo.* *S. aureus* WT expressing His-tagged HypR was exposed to 0.1, 0.4 and 1 mM lapachol for 30 and 60 min. The protein extracts were subjected to non-reducing Western blots with anti-His-tag antibodies to visualize reduced HypR (HypR red) and the oxidized HypR intersubunit disulfide-linked dimer (HypR ox). As HypR negative control, the *hypR* mutant (Δ*hypR*) was separated under control conditions **(A)**. The HypR disulfide can be reduced by DTT as shown by reducing Western blot analysis **(B)**. The loading controls are shown as Coomassie-stained SDS PAGE below the anti-His-tag Western blots.

To further support the oxidative mode of lapachol, we investigated the redox state of the redox-sensing HypR repressor, which senses disulfide stress by intersubunit disulfide formation in *S.*

aureus [41]. *S. aureus* cells expressing His-tagged HypR protein were subjected to different concentrations of 0.1-1 mM lapachol stress. The redox state of HypR was analyzed using non-reducing Western blots with anti-His-tag specific monoclonal antibodies. The results revealed that lapachol leads to oxidation of HypR to the intermolecular disulfide-linked dimer after lapachol stress **(Fig. S2AB)**. Thiol-oxidation of HypR was reversible with DTT, supporting the oxidative mode of lapachol. However, we could not detect irreversible protein alkylation and aggregation of proteins in the Western blot or SDS PAGE loading control. Together, our results support the oxidative mode of lapachol to induce protein *S*-bacillithiolation of GapDH *in vitro* and *in vivo* as well as reversible thiol-oxidation of the redox-sensing HypR repressor in *S. aureus*.

The catalase KatA and the Brx/BSH/YpdA pathway confer tolerance of *S. aureus* towards lapachol treatment. To confirm the oxidative mode of lapachol by ROS generation, we analyzed the phenotype of the *katA* mutant deficient for major catalase. The *katA* mutant displayed a growth delay under lapachol stress and was strongly impaired in survival compared to the parent **(Fig. 7AB)**. These results clearly confirm the production of H_2O_2 and increased catalase activity by lapachol as shown with the Tpx-roGFP2 biosensor and FOX assay, since the *katA* mutant is very sensitive to oxidative stress. In addition, we showed previously that the BrxA/BSH/YpdA redox pathway is important for de-bacillithiolation of proteins during recovery from oxidative stress and infection conditions [51]. Here, we have shown that lapachol causes an oxidative shift in E_{BSH} and increased *S*-bacillithiolation of GapDH **(Fig. 4 and 6)**. Thus, we investigated the phenotypes of the *bshA*, *brxAB* and *ypdA* deletion mutants during growth and survival of *S. aureus* under lapachol stress. The growth of mutants deficient for BSH, bacilliredoxins BrxA/B and the BSSB reductase YpdA was significantly impaired after exposure to sub-lethal 0.3 mM lapachol **(Fig. 7CEG)**. Furthermore, all mutants showed a significantly decreased survival after lethal 0.4 mM lapachol stress **(Fig. 7DFH)**. These lapachol-sensitive phenotypes could be restored back to WT level after complementation with *katA*, *bshA*, *brxA* and *ypdA*, respectively **(Fig. 7BDFH; Fig. S3ABCE)**. However, the complementation of the

brxAB mutant with *brxB* did not restore the phenotype back to wild type level **(Fig. 7H; Fig.S3D)**. Taken together, these results revealed that the catalase KatA and the BrxA/BSH/YpdA redox pathway provide protection against lapachol-induced ROS formation in *S. aureus*.

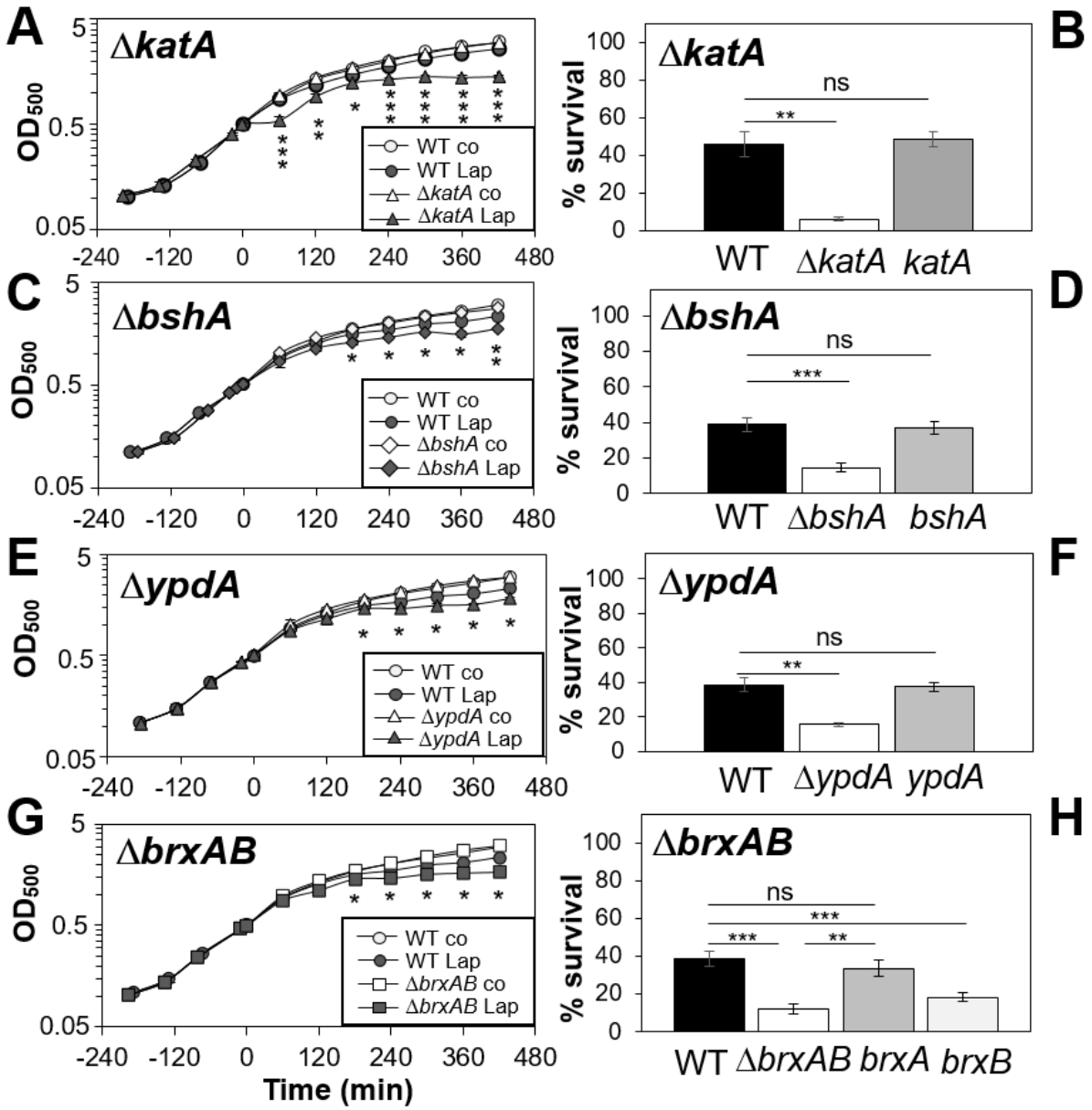

Fig. 7. The *S. aureus katA, bshA*, *ypdA* and *brxAB* deletion mutants are more sensitive under lapachol stress as shown in growth and survival assays. (A-H) Growth curves **(A, C, E, G)** and survival assays **(B,D,F,H)** were performed of *S. aureus* COL WT, *katA*, *bshA*, *brxAB*, and *ypdA* mutants and complemented strains (*katA*, *bshA, ypdA, brxA, brxB*) in RPMI medium after exposure to lapachol stress at an OD_{500} of 0.5. Growth phenotypes were determined after 300 µM lapachol and survival rates were calculated 4 h after exposure to 400 µM lapachol and determination of CFUs. Growth curves of the *bshA, katA, ypdA, brxA* and *brxB* complemented strains are shown in Fig. S3. Survival of the untreated control was set to 100%. Mean values and SD of four biological replicates are presented. The statistics was calculated using a Student's unpaired two-tailed t-test by the graph prism software. Symbols are: $^{ns}p > 0.05$, $^{*}p \leq 0.05$, $^{**}p \leq 0.01$ and $^{***}p \leq 0.001$.

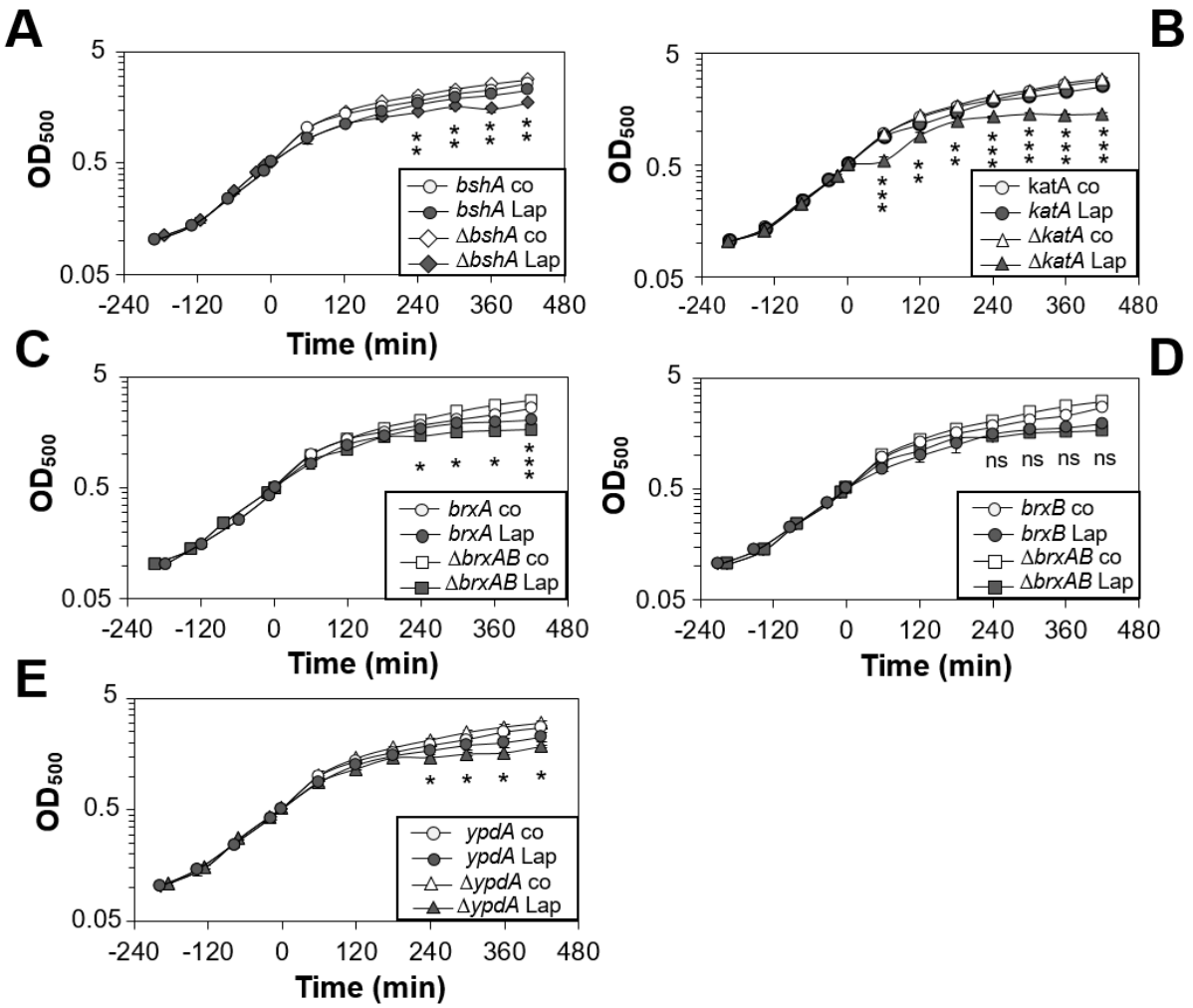

Fig. S3. The *S. aureus bshA*, *katA*, *ypdA* and *brxA* complemented strains restore the lapachol sensitive phenotypes of the mutants in growth assays. (A-E) Growth curves were performed of *S. aureus* COL WT, *bshA*, *katA, brxAB*, and *ypdA* mutants and the *bshA, katA, ypdA, brxA, brxB* complemented strains in RPMI medium after exposure to 300 µM lapachol stress at an OD_{500} of 0.5. Mean values and SD of four biological replicates are presented. The statistics was calculated using a Student's unpaired two-tailed t-test by the graph prism software. Symbols are: $^{ns}p > 0.05$, $^{*}p \leq 0.05$, $^{**}p \leq 0.01$ and $^{***}p \leq 0.001$.

Discussion

In this study, we have analyzed the antimicrobial mode of action of the naphthoquinone lapachol in the major pathogen *S. aureus*. Using growth and survival assays, the sub-lethal lapachol concentration was determined as 0.3 mM, while higher doses of 0.4-1.0 mM were toxic for *S. aureus* and strongly decreased the survival. Previously, the MIC of lapachol in *S. aureus* has been determined as 128-256 µg/ml (~0.53-1.06 mM) [71], which is in agreement with the MIC determined in this work. Since low doses of 0.4 mM lapachol are toxic for exponentially growing *S. aureus* cells, lapachol could be suited as redox-active antimicrobial to treat MRSA strains in wound infections.

In this work, we combined RNA-seq transcriptomics, redox biosensor measurements, protein thiol-oxidation assays and phenotype analyses of mutants to investigate the antimicrobial mode of action and stress responses caused by lapachol in *S. aureus*. The transcriptome results showed that lapachol caused an oxidative and quinone stress response and protein damage in *S. aureus*. The oxidative stress-specific PerR and HypR regulons, which control catalases, peroxidases and disulfide reductases, and the superoxide dismutases *sodA1* and *sodA2* are most strongly up-regulated by lapachol, which are indicative for the oxidative mode of action of lapachol. This antioxidant response induced by lapachol supports the generation of ROS by the redox cycling action of lapachol, such as superoxide anions, which are converted to H_2O_2 by SodA1/2.

Thus, our results are in agreement with previous studies of the bioactivation of lapachol using NADPH-dependent cytochrome P450 reductase and the interaction of lapachol with oxygen *in vitro* [24, 25]. The naphthoquinone lapachol was shown to be bioactivated via reduction by P450 reductase to semiquinone anion radical, which leads to electron transfer to molecular oxygen, resulting in superoxide anion generation [25]. In an electrochemical study, the semiquinone anion radical was demonstrated to interact with oxygen in an electron-chain mechanism, resulting in the deprotonated lapachol and hydroxyperoxyl radicals [24].

To investigate the oxidative stress response caused by lapachol-induced ROS, we studied the changes of the BSH redox potential and endogenous H_2O_2 formation by lapachol using the Brx-roGFP2 and Tpx-roGFP2 biosensors in *S. aureus*. Our results showed an oxidative shift of E_{BSH} after lapachol stress in *S. aureus*. Increased H_2O_2 production was measured in *S. aureus* with the Tpx-roGFP2 biosensor after lapachol exposure. However, both biosensors could not be regenerated after 3 h of stress, which is probably caused by the constant redox-cyclic action of lapachol in *S. aureus*. In addition, we used the FOX assay to demonstrate an enhanced H_2O_2 detoxification capacity of *S. aureus* cells after lapachol stress, which supports an increased catalase activity in lapachol-treated cells. Survival assays under aerobic and microaerophilic conditions could further link lapachol toxicity to increased ROS formation under aerobic conditions in *S. aureus*. The survival of lapachol-treated *S. aureus*

cells was strongly increased under microaerophilic conditions, while the aerobic culture was protected against lapachol toxicity by the ROS scavenger N-acetyl cysteine. These combined results of an oxidative shift in E_{BSH}, elevated H_2O_2 levels with the Tpx-roGFP2 biosensor, faster H_2O_2 detoxification and increased survival with decreased ROS levels indicate that the redox-cycling mode is the main antimicrobial mode of action of lapachol in *S. aureus* cells.

In agreement with the oxidative mode, growth and survival assays revealed an increased sensitivity of the *katA* mutant to lapachol, which is compromised in H_2O_2 detoxification [72]. Apart from *katA*, the peroxidase *ahpCF* operon is very strongly 20-26-fold induced by lapachol. Both KatA and AhpCF have compensatory roles in peroxide detoxification, since the absence of KatA resulted in elevated AhpCF expression and *vice versa* [72]. Our transcriptome results indicate that both KatA and AhpCF are highly induced by lapachol to remove H_2O_2. The increased catalase activity was confirmed using the FOX assay in extracts of lapachol-treated cells. In the *katA* mutant, the *ahpCF* operon might compensate for H_2O_2 detoxification produced by lapachol.

In addition, we analyzed the thiol-oxidation of GapDH and the HypR repressor in the proteome of *S. aureus*. Lapachol induced *S*-bacillithiolation of GapDH both *in vivo* and *in vitro*, supporting further ROS generation. *S*-bacillithiolation of GapDH was previously observed in response to strong oxidants, such as HOCl and by the antimicrobial coating AGXX®, which causes hydroxyl anion formation [48, 59]. Thus, the previously measured hydroxyperxoxyl radicals under lapachol stress might provoke *S*-bacillithiolation of GapDH [24]. Regeneration of *S*-bacillithiolated proteins and BSSB was shown to require the BrxA/BSH/YpdA pathway in *S. aureus*, which is important under oxidative stress and infections [48, 51, 52]. Consistent with these results, the *bshA*, *brxAB* and *ypdA* mutants showed significant growth and survival defects under lapachol stress. This confirms the importance of the BrxA/BSH/YpdA pathway for recovery of *S. aureus* from lapachol stress by reduction of oxidized proteins and BSSB.

The HypR repressor was previously shown to sense strong disulfide stress, such as HOCl, AGXX® and allicin [41, 59, 65]. The redox-sensing mechanism of HypR involves intermolecular disulfide formation under HOCl stress. Here, we confirmed that HypR is

oxidized to the HypR disulfide-linked dimer leading to its inactivation and derepression of transcription of the disulfide reductase-encoding *merA* gene. Consistent with these results, the *hypR-merA* operon was 5-fold induced in the transcriptome under lapachol stress. The increased protein thiol-oxidation by lapachol is further in agreement with the strong induction of the CtsR and HrcA regulons, controlling Clp proteases and the DnaK-GrpE, GroESL chaperones to degrade and refold oxidatively damaged proteins. Altogether, our results indicate that lapachol provokes mainly an oxidative stress response in the transcriptome, which was confirmed by an oxidized E_{BSH}, elevated H_2O_2 levels, increased catalase activity and protein thiol-oxidation during aerobic growth in *S. aureus*.

However, quinones have been described to exert their cytotoxicity via oxidative and electrophilic mechanisms [13, 27, 28]. In the electrophilic mode, quinones lead to *S*-alkylation of nucleophilic Cys residues, resulting in irreversible protein aggregation and depletion of Cys proteins in the proteome [29]. Thus, the question arises whether the naphthoquinone lapachol could lead to thiol-*S*-alkylation and aggregation of protein thiols. Previous studies on diesel exhaust phenanthraquinone revealed the oxidation of proximal protein thiols and oxidative modification of Cu,Zn superoxide dismutase through the redox cycling mode of action [33, 73]. Our transcriptome signature revealed the induction of the quinone-specific MhqR and QsrR regulons under lapachol stress, which could point to the alkylation mode. However, these quinone-specific regulons were induced at lower levels (~10-fold) compared to the oxidant-induced PerR-regulated *ahpCF* and *katA* genes. This might indicate that the naphthoquinone lapachol does not lead to alkylation and aggregation of protein thiols as shown for benzoquinones previously [29]. In contrast, the MhqR and QsrR regulons responded much stronger to the hydroquinone MHQ in previous transcriptome studies [26]. Specifically, MHQ leads to 34-67-fold induction of the MhqR regulon and up-to 280-fold induction of the QsrR regulon in *S. aureus* [26]. The *S*-alkylation and oxidation modes of action were both previously demonstrated for benzoquinones in *B. subtilis* [29].

To exclude the alkylation mode of lapachol, we treated the GapDH protein with increasing concentrations of lapachol up-to 7.5 mM *in vitro*, but did not observe any

aggregation in the higher molecular range **(Fig. S1A)** compared to previous studies with benzoquinones [29]. The isolation of the insoluble protein fraction in cell extracts *in vivo* did not reveal increased protein aggregates after treatment of cells with 0.3 and 1 mM lapachol **(Fig. S1B)**. In addition, no irreversible protein aggregation could be observed for the HypR repressor, which was oxidized to the reversible HypR intermolecular disulfides indicative for the oxidative mode **(Fig. S2AB)**. We did not find any evidence for protein alkylation and aggregation since cellular proteins could be well separated using SDS-PAGE. No alkylated aggregates migrated in the upper range of the SDS gel or remained in the stacking gel (see loading controls of **Fig. 6A** and **Fig. S2AB**) as observed previously for benzoquinones [29]. These results were expected since the quinone ring is fully substituted in lapachol, which prevents thiol-*S*-alkylation and aggregation of protein thiols [27, 34]. In general, the toxicity and alkylation activity increases with the number of unsubstituted positions adjacent to the keto groups of the quinone rings [27, 34]. In conclusion, our results demonstrate that lapachol leads to ROS formation and acts mainly via its redox-cycling oxidative mode as antimicrobial mechanism in *S. aureus*.

Finally, the question arises if *S. aureus* is able to detoxify lapachol. Lapachol metabolic pathways have been studied in fungi and streptomycetes, which involve monooxygenases or dioxygenases [74, 75]. Our transcriptome data identified the flavohemoglobin *hmp* as strongly induced under lapachol stress in *S. aureus*. Hmp was characterized as NO dioxygenase, which converts NO and O_2 to NO_3^- via the haem-Fe^{2+} active center using NADPH and FAD as cofactors for electron transfer [68]. Recently, *S. aureus* Hmp was revealed to function in detoxification of quinones by mixed single and two-electron reduction mechanisms with preference for 1,4-naphthoquinones as best electron acceptors [69]. Quinone reduction required electrons from NADH and reduced FAD, but not from haem-$Fe^{2+}O_2$, indicating that quinones are subverse substrates for Hmp using different mechanisms for detoxification compared to NO [69]. These results indicate that lapachol detoxification could involve various NADPH-dependent flavoenzymes in *S. aureus*, which are upregulated in the transcriptome under lapachol stress and remain to be subjects of future studies.

References

[1] F.D. Lowy, *Staphylococcus aureus* infections, N Engl J Med 339(8) (1998) 520-32.

[2] H.W. Boucher, G.R. Corey, Epidemiology of methicillin-resistant *Staphylococcus aureus*, Clin Infect Dis 46 Suppl 5 (2008) S344-9.

[3] G.L. Archer, *Staphylococcus aureus*: a well-armed pathogen, Clin Infect Dis 26(5) (1998) 1179-81.

[4] S.Y. Tong, J.S. Davis, E. Eichenberger, T.L. Holland, V.G. Fowler, Jr., *Staphylococcus aureus* infections: epidemiology, pathophysiology, clinical manifestations, and management, Clin Microbiol Rev 28(3) (2015) 603-61.

[5] D.M. Livermore, Antibiotic resistance in staphylococci, Int J Antimicrob Agents 16 Suppl 1 (2000) S3-10.

[6] S. Lakhundi, K. Zhang, Methicillin-Resistant *Staphylococcus aureus*: Molecular characterization, evolution, and epidemiology, Clin Microbiol Rev 31(4) (2018).

[7] V.D. Nguyen, C. Wolf, U. Mäder, M. Lalk, P. Langer, U. Lindequist, M. Hecker, H. Antelmann, Transcriptome and proteome analyses in response to 2-methylhydroquinone and 6-brom-2-vinyl-chroman-4-on reveal different degradation systems involved in the catabolism of aromatic compounds in *Bacillus subtilis*, Proteomics 7(9) (2007) 1391-408.

[8] K.R. Vann, G. Ekiz, S. Zencir, E. Bedir, Z. Topcu, N. Osheroff, Effects of secondary metabolites from the fungus *Septofusidium berolinense* on DNA cleavage mediated by human topoisomerase II alpha, Chem Res Toxicol 29(3) (2016) 415-20.

[9] G. Ekiz, E.E. Hames, A. Nalbantsoy, E. Bedir, Two rare quinone-type metabolites from the fungus *Septofusidium berolinense* and their biological activities, J Antibiot (Tokyo) 69(2) (2016) 111-3.

[10] H. Hussain, I.R. Green, Lapachol and lapachone analogs: a journey of two decades of patent research(1997-2016), Expert Opinion Therapeut Path 27(10) (2017) 1111-1121.

[11] C.A. Colwell, M. McCall, Studies on the mechanism of antibacterial action of 2-methyl-1,4-naphthoquinone, Science 101(2632) (1945) 592-4.

[12] H. Schildknecht, Die Wehrchemie von Land-und Wasserkäfern, Angew Chem 82(1) (1970) 17-25.

[13] R.A. Morton, Biochemistry of quinones, Academic Press1965.

[14] Á. Ravelo, A. Estévez-Braun, E. Pérez-Sacau, The chemistry and biology of lapachol and related natural products α and β-lapachones, Studies in Natural Products Chemistry, Elsevier2003, pp. 719-760.

[15] F. Epifano, S. Genovese, S. Fiorito, V. Mathieu, R. Kiss, Lapachol and its congeners as anticancer agents: a review, Phytochem Rev 13(1) (2014) 37-49.

[16] O.A. Binutu, K.E. Adesogan, J.I. Okogun, Antibacterial and antifungal compounds from *Kigelia pinnata*, Planta Med 62(4) (1996) 352-3.

[17] R.M. Ali, P.J. Houghton, A. Raman, J.R.S. Hoult, Antimicrobial and antiinflammatory activities of extracts and constituents of *Oroxylum indicum* (L.) Vent, Phytomedicine 5(5) (1998) 375-381.

[18] B.S. Park, J.R. Kim, S.E. Lee, K.S. Kim, G.R. Takeoka, Y.J. Ahn, J.H. Kim, Selective growth-inhibiting effects of compounds identified in *Tabebuia impetiginosa* inner bark on human intestinal bacteria, J Agric Food Chem 53(4) (2005) 1152-7.

[19] E.M. Pereira, B. Machado Tde, I.C. Leal, D.M. Jesus, C.R. Damaso, A.V. Pinto, M. Giambiagi-deMarval, R.M. Kuster, K.R. Santos, *Tabebuia avellanedae* naphthoquinones: activity against methicillin-resistant staphylococcal strains, cytotoxic activity and *in vivo* dermal irritability analysis, Ann Clin Microbiol Antimicrob 5 (2006) 5.

[20] M.A. Souza, S. Johann, L.A. Lima, F.F. Campos, I.C. Mendes, H. Beraldo, E.M. Souza-Fagundes, P.S. Cisalpino, C.A. Rosa, T.M. Alves, N.P. de Sa, C.L. Zani, The antimicrobial activity of lapachol and its thiosemicarbazone and semicarbazone derivatives, Mem Inst Oswaldo Cruz 108(3) (2013).

[21] E. Perez-Sacau, R.G. Diaz-Penate, A. Estevez-Braun, A.G. Ravelo, J.M. Garcia-Castellano, L. Pardo, M. Campillo, Synthesis and pharmacophore modeling of naphthoquinone derivatives with cytotoxic activity in human promyelocytic leukemia HL-60 cell line, J Med Chem 50(4) (2007) 696-706.

[22] S.N. Sunassee, C.G. Veale, N. Shunmoogam-Gounden, O. Osoniyi, D.T. Hendricks, M.R. Caira, J.A. de la Mare, A.L. Edkins, A.V. Pinto, E.N. da Silva Junior, M.T. Davies-Coleman, Cytotoxicity of lapachol, beta-lapachone and related synthetic 1,4-naphthoquinones against oesophageal cancer cells, Eur J Med Chem 62 (2013) 98-110.

[23] M.N. Rocha, P.M. Nogueira, C. Demicheli, L.G. de Oliveira, M.M. da Silva, F. Frezard, M.N. Melo, R.P. Soares, Cytotoxicity and *in vitro* antileishmanial activity of antimony (V), bismuth (V), and tin (IV) complexes of lapachol, Bioinorg Chem Appl 2013 (2013) 961783.

[24] M.O. Goulart, P. Falkowski, T. Ossowski, A. Liwo, Electrochemical study of oxygen interaction with lapachol and its radical anions, Bioelectrochem 59(1-2) (2003) 85-7.

[25] Y. Kumagai, Y. Tsurutani, M. Shinyashiki, S. Homma-Takeda, Y. Nakai, T. Yoshikawa, N. Shimojo, Bioactivation of lapachol responsible for DNA scission by NADPH-cytochrome P450 reductase, Environ Toxicol Pharmacol 3(4) (1997) 245-50.

[26] V.N. Fritsch, V.V. Loi, T. Busche, A. Sommer, K. Tedin, D.J. Nürnberg, J. Kalinowski, J. Bernhardt, M. Fulde, H. Antelmann, The MarR-type repressor MhqR confers quinone and antimicrobial resistance in *Staphylococcus aureus*, Antioxid Redox Signal 31(16) (2019) 1235-1252.

[27] P.J. O'Brien, Molecular mechanisms of quinone cytotoxicity, Chem Biol Interact 80(1) (1991) 1-41.

[28] T.J. Monks, R.P. Hanzlik, G.M. Cohen, D. Ross, D.G. Graham, Quinone chemistry and toxicity, Toxicol Appl Pharmacol 112(1) (1992) 2-16.

[29] M. Liebeke, D.C. Pöther, N. van Duy, D. Albrecht, D. Becher, F. Hochgräfe, M. Lalk, M. Hecker, H. Antelmann, Depletion of thiol-containing proteins in response to quinones in *Bacillus subtilis*, Mol Microbiol 69(6) (2008) 1513-29.

[30] H. Antelmann, J.D. Helmann, Thiol-based redox switches and gene regulation, Antioxid Redox Signal 14(6) (2011) 1049-63.

[31] V.V. Loi, M. Rossius, H. Antelmann, Redox regulation by reversible protein *S*-thiolation in bacteria, Front Microbiol 6 (2015) 187.

[32] S. Bittner, When quinones meet amino acids: chemical, physical and biological consequences, Amino Acids 30(3) (2006) 205-24.

[33] Y. Kumagai, S. Koide, K. Taguchi, A. Endo, Y. Nakai, T. Yoshikawa, N. Shimojo, Oxidation of proximal protein sulfhydryls by phenanthraquinone, a component of diesel exhaust particles, Chem Res Toxicol 15(4) (2002) 483-9.

[34] M.T. Smith, Quinones as mutagens, carcinogens, and anticancer agents: introduction and overview, J Toxicol Environ Health 16(5) (1985) 665-72.

[35] T.W. Schultz, G.D. Sinks, M.T.D. Cronin, Quinone-induced toxicity to *Tetrahymena*: structure-activity relationships, Aquatic Toxicology 39(3-4) (1997) 267-278.

[36] A. Brunmark, E. Cadenas, Redox and addition chemistry of quinoid compounds and its biological implications, Free Rad Biol Med 7(4) (1989) 435-477.

[37] Q. Ji, L. Zhang, M.B. Jones, F. Sun, X. Deng, H. Liang, H. Cho, P. Brugarolas, Y.N. Gao, S.N. Peterson, Molecular mechanism of quinone signaling mediated through S-quinonization of a YodB family repressor QsrR, Proc Natl Acad Sci 110(13) (2013) 5010-5015.

[38] C.J. Ji, J.H. Kim, Y.B. Won, Y.E. Lee, T.W. Choi, S.Y. Ju, H. Youn, J.D. Helmann, J.W. Lee, *Staphylococcus aureus* PerR is a hypersensitive hydrogen peroxide sensor using iron-mediated histidine oxidation, J Biol Chem 290(33) (2015) 20374-86.

[39] A. Pinochet-Barros, J.D. Helmann, Redox sensing by Fe(2+) in bacterial Fur family metalloregulators, Antioxid Redox Signal 29(18) (2018) 1858-1871.

[40] M.J. Horsburgh, M.O. Clements, H. Crossley, E. Ingham, S.J. Foster, PerR controls oxidative stress resistance and iron storage proteins and is required for virulence in *Staphylococcus aureus*, Infect Immun 69(6) (2001) 3744-54.

[41] V.V. Loi, T. Busche, K. Tedin, J. Bernhardt, J. Wollenhaupt, N.T.T. Huyen, C. Weise, J. Kalinowski, M.C. Wahl, M. Fulde, H. Antelmann, Redox-sensing under hypochlorite stress and infection conditions by the Rrf2-family repressor HypR in *Staphylococcus aureus*, Antioxid Redox Signal 29(7) (2018) 615-636.

[42] P. Chandrangsu, V.V. Loi, H. Antelmann, J.D. Helmann, The role of bacillithiol in Gram-positive firmicutes, Antioxid Redox Signal 28(6) (2018) 445-462.

[43] G.L. Newton, R.C. Fahey, M. Rawat, Detoxification of toxins by bacillithiol in *Staphylococcus aureus*, Microbiology 158(Pt 4) (2012) 1117-26.

[44] D.C. Pöther, P. Gierok, M. Harms, J. Mostertz, F. Hochgräfe, H. Antelmann, C.J. Hamilton, I. Borovok, M. Lalk, Y. Aharonowitz, M. Hecker, Distribution and infection-related functions of bacillithiol in *Staphylococcus aureus*, Int J Med Microbiol 303(3) (2013) 114-23.

[45] A.C. Posada, S.L. Kolar, R.G. Dusi, P. Francois, A.A. Roberts, C.J. Hamilton, G.Y. Liu, A. Cheung, Importance of bacillithiol in the oxidative stress response of *Staphylococcus aureus*, Infect Immun 82(1) (2014) 316-32.

[46] B.K. Chi, K. Gronau, U. Mäder, B. Hessling, D. Becher, H. Antelmann, *S*-bacillithiolation protects against hypochlorite stress in *Bacillus subtilis* as revealed by transcriptomics and redox proteomics, Mol Cell Proteomics 10(11) (2011) M111 009506.

[47] B.K. Chi, A.A. Roberts, N.T.T. Huyen, K. Bäsell, D. Becher, D. Albrecht, C.J. Hamilton, H. Antelmann, *S*-bacillithiolation protects conserved and essential proteins against hypochlorite stress in firmicutes bacteria, Antioxid Redox Signal 18(11) (2013) 1273-95.

[48] M. Imber, N.T.T. Huyen, A.J. Pietrzyk-Brzezinska, V.V. Loi, M. Hillion, J. Bernhardt, L. Tharichen, K. Kolsek, M. Saleh, C.J. Hamilton, L. Adrian, F. Grater, M.C. Wahl, H. Antelmann, Protein *S*-bacillithiolation functions in thiol protection and redox regulation of the glyceraldehyde-3-phosphate dehydrogenase Gap in *Staphylococcus aureus* under hypochlorite stress, Antioxid Redox Signal 28(6) (2018) 410-430.

[49] M. Imber, V.V. Loi, S. Reznikov, V.N. Fritsch, A.J. Pietrzyk-Brzezinska, J. Prehn, C. Hamilton, M.C. Wahl, A.K. Bronowska, H. Antelmann, The aldehyde dehydrogenase AldA contributes to the hypochlorite defense and is redox-controlled by protein S-bacillithiolation in *Staphylococcus aureus*, Redox Biol 15 (2018) 557-568.

[50] M. Imber, A.J. Pietrzyk-Brzezinska, H. Antelmann, Redox regulation by reversible protein S-thiolation in Gram-positive bacteria, Redox Biol 20 (2018) 130-145.

[51] N. Linzner, V.V. Loi, V.N. Fritsch, Q.N. Tung, S. Stenzel, M. Wirtz, R. Hell, C.J. Hamilton, K. Tedin, M. Fulde, H. Antelmann, *Staphylococcus aureus* uses the bacilliredoxin (BrxAB)/bacillithiol disulfide reductase (YpdA) redox pathway to defend against oxidative stress under infections, Front Microbiol 10 (2019) 1355.

[52] I.V. Mikheyeva, J.M. Thomas, S.L. Kolar, A.R. Corvaglia, N. Gaiotaa, S. Leo, P. Francois, G.Y. Liu, M. Rawat, A.L. Cheung, YpdA, a putative bacillithiol disulfide reductase, contributes to cellular redox homeostasis and virulence in *Staphylococcus aureus*, Mol Microbiol 111(4) (2019) 1039-1056.

[53] A. Gaballa, B.K. Chi, A.A. Roberts, D. Becher, C.J. Hamilton, H. Antelmann, J.D. Helmann, Redox regulation in Bacillus subtilis: The bacilliredoxins BrxA(YphP) and BrxB(YqiW) function in de-bacillithiolation of *S*-bacillithiolated OhrR and MetE, Antioxid Redox Signal 21(3) (2014) 357-67.

[54] V.V. Loi, M. Harms, M. Müller, N.T.T. Huyen, C.J. Hamilton, F. Hochgräfe, J. Pane-Farre, H. Antelmann, Real-time imaging of the bacillithiol redox potential in the human pathogen *Staphylococcus aureus* using a genetically encoded bacilliredoxin-fused redox biosensor, Antioxid Redox Signal 26(15) (2017) 835-848.

[55] V. Van Loi, H. Antelmann, Method for measurement of bacillithiol redox potential changes using the Brx-roGFP2 redox biosensor in *Staphylococcus aureus*, MethodsX 7 (2020) 100900.

[56] M. Arnaud, A. Chastanet, M. Debarbouille, New vector for efficient allelic replacement in naturally nontransformable, low-GC-content, gram-positive bacteria, Appl Environ Microbiol 70(11) (2004) 6887-91.

[57] E.D. Rosenblum, S. Tyrone, Serology, density, and morphology of staphylococcal phages, J Bacteriol 88(6) (1964) 1737-42.

[58] R. Brückner, E. Wagner, F. Götz, Characterization of a sucrase gene from *Staphylococcus xylosus*, J Bacteriol 175(3) (1993) 851-857.

[59] V.V. Loi, T. Busche, T. Preuss, J. Kalinowski, J. Bernhardt, H. Antelmann, The AGXX® antimicrobial coating causes a thiol-specific oxidative stress response and protein *S*-bacillithiolation in *Staphylococcus aureus*, Front Microbiol 9 (2018) 3037.

[60] M.I. Love, W. Huber, S. Anders, Moderated estimation of fold change and dispersion for RNA-seq data with DESeq2, Genome Biol 15(12) (2014) 550.

[61] R. Hilker, K.B. Stadermann, O. Schwengers, E. Anisiforov, S. Jaenicke, B. Weisshaar, T. Zimmermann, A. Goesmann, ReadXplorer 2-detailed read mapping analysis and visualization from one single source, Bioinformatics 32(24) (2016) 3702-3708.

[62] J. Nourooz-Zadeh, J. Tajaddini-Sarmadi, S.P. Wolff, Measurement of plasma hydroperoxide concentrations by the ferrous oxidation-xylenol orange assay in conjunction with triphenylphosphine, Anal Biochem 220(2) (1994) 403-9.

[63] B. Groitl, J.U. Dahl, J.W. Schroeder, U. Jakob, *Pseudomonas aeruginosa* defense systems against microbicidal oxidants, Mol Microbiol 106(3) (2017) 335-350.

[64] T. Tomoyasu, F. Arsene, T. Ogura, B. Bukau, The C terminus of sigma(32) is not essential for degradation by FtsH, J Bacteriol 183(20) (2001) 5911-7.

[65] V.V. Loi, N.T.T. Huyen, T. Busche, Q.N. Tung, M.C.H. Gruhlke, J. Kalinowski, J. Bernhardt, A.J. Slusarenko, H. Antelmann, *Staphylococcus aureus* responds to allicin by global S-thioallylation - Role of the Brx/BSH/YpdA pathway and the disulfide reductase MerA to overcome allicin stress, Free Radic Biol Med 139 (2019) 55-69.

[66] D. Frees, U. Gerth, H. Ingmer, Clp chaperones and proteases are central in stress survival, virulence and antibiotic resistance of *Staphylococcus aureus*, Int J Med Microbiol 304(2) (2014) 142-9.

[67] D. Frees, K. Savijoki, P. Varmanen, H. Ingmer, Clp ATPases and ClpP proteolytic complexes regulate vital biological processes in low GC, Gram-positive bacteria, Mol Microbiol 63(5) (2007) 1285-95.

[68] R.K. Poole, Flavohaemoglobin: the pre-eminent nitric oxide-detoxifying machine of microorganisms, F1000Res 9 (2020).

[69] M. Moussaoui, L. Miseviciene, Z. Anusevicius, A. Maroziene, F. Lederer, L. Baciou, N. Cenas, Quinones and nitroaromatic compounds as subversive substrates of *Staphylococcus aureus* flavohemoglobin, Free Rad Biol Med 123 (2018) 107-115.

[70] M. Falord, U. Mäder, A. Hiron, M. Debarbouille, T. Msadek, Investigation of the *Staphylococcus aureus* GraSR regulon reveals novel links to virulence, stress response and cell wall signal transduction pathways, PLoS One 6(7) (2011) e21323.

[71] C.G. Oliveira, F.F. Miranda, V.F. Ferreira, C.C. Freitas, R.F. Rabello, J.M. Carballido, L.C. Corrêa, Synthesis and antimicrobial evaluation of 3-hydrazino-naphthoquinones as analogs of lapachol., J Braz Chem Soc 12(3) (2001) 339-345.

[72] K. Cosgrove, G. Coutts, I.M. Jonsson, A. Tarkowski, J.F. Kokai-Kun, J.J. Mond, S.J. Foster, Catalase (KatA) and alkyl hydroperoxide reductase (AhpC) have compensatory roles in peroxide stress resistance and are required for survival, persistence, and nasal colonization in Staphylococcus aureus, J Bacteriol 189(3) (2007) 1025-35.

[73] R. Koizumi, K. Taguchi, M. Hisamori, Y. Kumagai, Interaction of 9,10-phenanthraquinone with dithiol causes oxidative modification of Cu,Zn-superoxide dismutase (SOD) through redox cycling, J Toxicol Sci 38(3) (2013) 317-24.

[74] S. Otten, J.P. Rosazza, Microbial transformations of natural antitumor agents: oxidation of lapachol by *Penicillium notatum*, Appl Environ Microbiol 35(3) (1978) 554-7.

[75] S.L. Otten, J.P. Rosazza, Oxidative ring fission of the naphthoquinones lapachol and dichloroallyl lawsone by *Penicillium notatum*, J Biol Chem 258(3) (1983) 1610-3.

Table S1. Bacterial strains

Bacterial strains	Description	Reference
Escherichia coli		
DH5α	F-φ80dlacZ Δ(lacZYA-argF) U169 deoRsupE44ΔlacU169 (f80lacZDM15) hsdR17 recA1 endA1 (rk- mk+) supE44gyrA96 thi-1 gyrA69 relA1	[1]
BL21(DE3)*plys*S	F- ompT hsdS gal (rb- mb+) DE3(Sam7 Δnin5 lacUV5-T7 Gen1)	[1]
Staphylococcus aureus		
RN4220	restriction negative strain/MSSA cloning intermediate derived from 8325-4	[2]
COL	Archaic HA-MRSA strain	[3]
COL-Δ*bshA*	COL *bshA* deletion mutant	This study
COL-Δ*ypdA*	COL *ypdA* deletion mutant	[4]
COL-Δ*brxAB*	COL *brxAB* double mutant	[4]
COL-Δ*hypR*	COL *hypR* deletion mutant	[5]
COL-Δ*katA*	COL *katA* deletion mutant	This study
COL pRB473-*brx-roGFP2*		[6]
COL pRB473-*tpx-roGFP2*		[4]
COL-Δ*bshA*::pRB473-*bshA*	COL *bshA* mutant complemented with pRB473-*bshA*	This study
COL-Δ*ypdA::*pRB473-*ypdA*	COL *ypdA* mutant complemented with pRB473-*ypdA*	[4]
COL-Δ*brxAB::*pRB473-*brxA*	COL *brxAB* mutant complemented with pRB473-*brxA*	[4]
COL-Δ*brxAB::*pRB473-*brxB*	COL *brxAB* mutant complemented with pRB473-*brxB*	[4]
COL-Δ*katA::*pRB473-*katA*	COL *katA* mutant complemented with pRB473-*katA*	This study
COL::pRB473-*hypR-His*	COL wild type complemented with pRB473-*hypR-His*	This study
Staphylococcus phage 81		[7]

Table S2. Plasmids

Plasmid	Description	Reference
pET11b	*E. coli* expression plasmid	Novagen
pET11b-*gapDH*	pET11b-derivative for overexpression of His-tagged YpdA	[4]
pRB473	pRB373-derivative, *E. coli/ S. aureus* shuttle vector, containing xylose-inducible P_{Xyl} promoter, Amp^r, Cm^r Amp^r, Cm^r	[8, 9]
pRB473-*brx-roGFP2*	pRB473-derivative expressing *brx-roGFP2* under P_{Xyl}	[6]
pRB473-*tpx-roGFP2*	pRB473-derivative expressing *tpx-roGFP2* under P_{Xyl}	[4]
pRB473-*bshA*	pRB473-derivative expressing *bshA* under P_{Xyl}	This study
pRB473-*katA*	pRB473-derivative expressing *katA* under P_{Xyl}	This study
pRB473-*hypR-His*	pRB473-derivative expressing *hypR-His* under P_{Xyl}	This study

Table S3. Oligonucleotide primers

Primer name	Sequence (5' to 3')
pMAD-bshA-f1-rev	TTACTCGCCTTTACTTTTGTTATATCCTTTCTTTCTATTTCTCTCT
pMAD-bshA-for-BglII	CGCAGATCTGACAATTTAAAACAGGATATTTTT
pMAD-bshA-rev-SalI	CCAGTCGACGGAACCTTAAACATCGAATCAT
pMAD-bshA-f2-for	AGAGAGAAATAGAAAGAAAGGATATAACAAAAGTAAAGGCGAGTA
pRB-bshA-for-BamHI	TAGGGATCCAGAGAGAAATAGAAAGAAAGGAT
pRB-bshA-rev-KpnI	CTCGGTACCTTACTCGCCTTTACTTTTGTTAT
pMAD-katA-for-BglII	CGCAGATCTCCACAATGCCCAATACAACC
pMAD-katA-f1-rev	CAAAGTTTTCGTATGTTTCATCAGTCTTGTTGTGACATAGTCATC
pMAD-katA-f2-for	GATGACTATGTCACAACAAGACTGATGAAACATACGAAAACTTTG
pMAD-katA-rev-SalI	CCAGTCGACCTACTATATTAAATACTCTTTCAAG
pRB-katA-for-BamHI	TAGGGATCCTAAATTGTGGAGGGATGACTAT
pRB-katA-rev-KpnI	CTCGGTACCTTATTTTTCAAAGTTTTCGTATGTT
pRB-hypR-for-BamH	TAGGGATCCGTTACAATTATGAGGTGAGAAACATTGAATTTAGAAT TAACA
pRB-hypR-His-rev-KpnI	CTCGGTACCTTAGTGATGGTGATGGTGATGTATGTTTTCATGACAT AATCCTC

Restriction sites are underlined.

Table S4. Determination of the minimal inhibitory concentration of lapachol in *S. aureus* COL

Lapachol (mM)	OD_{500} after 24 h
20	0.110 ± 0.221
10	0.040 ± 0.079
5	0.271 ± 0.441
2.5	0.682 ± 0.122
1.25	0.592 ± 0.366
0.625	1.993 ± 0.259
0.313	2.145 ± 0.064
0.157	2.057 ± 0.065
0.078	2.037 ± 0.080
0.039	2.087 ± 0.078
0.020	2.096 ± 0.070
control	2.147 ± 0.059

Supplementary References

[1] Studier, F. W.; Moffatt, B. A. Use of bacteriophage-T7 RNA-polymerase to direct selective high-level expression of cloned genes. *J Mol Biol* **189:**113-130; 1986.

[2] Kreiswirth, B. N.; Lofdahl, S.; Betley, M. J.; O'Reilly, M.; Schlievert, P. M.; Bergdoll, M. S.; Novick, R. P. The toxic shock syndrome exotoxin structural gene is not detectably transmitted by a prophage. *Nature* **305:**709-712; 1983.

[3] Shafer, W. M.; Iandolo, J. J. Genetics of staphylococcal enterotoxin B in methicillin-resistant isolates of *Staphylococcus aureus*. *Infect Immun* **25:**902-911; 1979.

[4] Linzner, N.; Loi, V. V.; Fritsch, V. N.; Tung, Q. N.; Stenzel, S.; Wirtz, M.; Hell, R.; Hamilton, C. J.; Tedin, K.; Fulde, M.; Antelmann, H. *Staphylococcus aureus* uses the bacilliredoxin (BrxAB)/bacillithiol disulfide reductase (YpdA) redox pathway to defend against oxidative stress under infections. *Front Microbiol* **10:**1355; 2019.

[5] Loi, V. V.; Busche, T.; Tedin, K.; Bernhardt, J.; Wollenhaupt, J.; Huyen, N. T. T.; Weise, C.; Kalinowski, J.; Wahl, M. C.; Fulde, M.; Antelmann, H. Redox-sensing under hypochlorite stress and infection conditions by the Rrf2-family repressor HypR in *Staphylococcus aureus*. *Antioxid Redox Signal* **29:**615-636; 2018.

[6] Loi, V. V.; Harms, M.; Muller, M.; Huyen, N. T. T.; Hamilton, C. J.; Hochgrafe, F.; Pane-Farre, J.; Antelmann, H. Real-time imaging of the bacillithiol redox potential in the human pathogen *Staphylococcus aureus* using a genetically encoded bacilliredoxin-fused redox biosensor. *Antioxid Redox Signal* **26:**835-848; 2017.

[7] Rosenblum, E. D.; Tyrone, S. Serology, density, and morphology of staphylococcal phages. *J Bacteriol* **88:**1737-1742; 1964.

[8] Pöther, D. C.; Gierok, P.; Harms, M.; Mostertz, J.; Hochgräfe, F.; Antelmann, H.; Hamilton, C. J.; Borovok, I.; Lalk, M.; Aharonowitz, Y.; Hecker, M. Distribution and infection-related functions of bacillithiol in *Staphylococcus aureus*. *Int J Med Microbiol* **303:**114-123; 2013.

[9] Brückner, R.; Wagner, E.; Götz, F. Characterization of a sucrase gene from *Staphylococcus xylosus*. *J Bacteriol* **175:**851-857; 1993.

Curriculum vitae

”For reasons of data protection, the curriculum vitae is not published in the electronic version.”

”For reasons of data protection, the curriculum vitae is not published in the electronic version.”

Acknowledgement

Firstly, I would like to express my sincere gratitude to my supervisor Prof. Dr. Haike Antelmann for giving me the great opportunity to work on these interesting projects in her Lab, to learn many new methods and to do my doctorate! Especially, I thank her for the continuous support, the many scientific discussions and her patience with me! I am deeply grateful that she believed in me and that she extended my knowledge about redox biology and bacterial physiology due to her immense knowledge and experiences!

I would like to thank Prof. Dr. Markus Wahl (Laboratory of Structural Biochemistry, Freie Universität Berlin) for the friendly acquisition of the second review!

I thank a lot all cooperation partners, who greatly supported the projects with their excellent work and experience! Especially, I would like to thank Dr. Karsten Tedin and Prof. Dr. Marcus Fulde (Institute of Microbiology and Epizootics, Freie Universität Berlin) for their support with the infection assays and the opportunity to perform the experiments in their lab. Moreover, I thank Dr. Markus Wirtz and Prof. Dr. Rüdiger Hell (Centre for Organismal Studies, University of Heidelberg) for the great support and performance of the HPLC measurements of the thiol metabolomics. I also thank Dr. Tobias Busche, Prof. Dr. Jörn Kalinowski (Center for Biotechnology, University Bielefeld) and Dr. Jörg Bernhardt (Insitute for Microbiology, University of Greifswald) for the RNA-seq analyses and for making the treemap of the lapachol transcriptome!

My special thanks go to all colleagues and Lab members of the Antelmann Group! Each one was always extremely helpful and friendly and it was fun to work with them! Without them, this work would be impossible! I am very grateful to Dr. Eberhard Klauck, Dr. Vu Van Loi and Dr. Quach Ngoc Tung for their great support in any form, in particular for their help with experiments, the introduction in the biosensor measurements and our scientific discussions. I would like to express my deep gratitude to Verena Fritsch for her constant immense support and help during the last years! She always had time for many brilliant scientific discussions and also supported me mentally a lot! I would also like to thank my Bachelor student Saskia Stenzel for her support and good work! I thank Melanie Skibbe and Franziska Kiele for their excellent technical assistance! For the future, I wish you all the best!

I thank the Deutsche Forschungsgemeinschaft (AN746/4-1 and AN746/4-2) within the SPP1710 on “Thiol-based Redox switches” for the financial support of this work!

Finally, I would like to express my deepest gratitude to my family and all my friends for their support, encouragement, mental motivation and belief in me! Their support has given me a lot of strength and motivation to accomplish my PhD degree. I am very happy and thankful to know that you are always stand behind me!

Declaration

Hereby, I certify that this thesis has not been submitted for a degree or any other qualification at Freie Universität Berlin or any other institution. I declare that I have written this thesis by myself under the guidance and supervision of Prof. Dr. Haike Antelmann, Institute for Biology-Microbiology, Freie Universität Berlin. Furthermore, I did not take any text sections of a third person without identification.

Berlin, 09th July 2020

_____

Nico Linzner